Prediction of Geotechnical Parameters from DMT, CPT and PMT Tests and Formation of Design Chart

Thesis submitted by

SAPTARSHI NANDI

Doctor of Philosophy (Engineering)

Department of Construction Engineering

Faculty Council of Engineering & Technology

Jadavpur University

Kolkata, India

2024

JADAVPUR UNIVERSITY

KOLKATA – 700032 INDIA

FACULTY OF ENGINEERING AND TECHNOLOGY

DEPARTMENT OF CONSTRUCTION ENGINEERING

CERTIFICATE FROM THE SUPERVISOR

This is to certify that the thesis entitled "**Prediction of Geotechnical Parameters from DMT, CPT and PMT Tests and Formation of Design Chart**" submitted by Saptarshi Nandi, who got his name registered on 28th August, 2017 (Reg. no. 1011705001) for the award of Ph.D. (Engineering) degree of Jadavpur University is absolutely based upon his own work under the supervision of Dr. Kaushik Bandyopadhyay and Dr. Dipanjan Basu and that neither his thesis nor any part of the thesis has been submitted for any degree/diploma or any other academic award anywhere before.

Kaushik Bandyopadhyay

(Dr. Kaushik Bandyopadhyay)

Dipanjan Basu

(Dr. Dipanjan Basu)

PROFORMA – 1

"Statement of Originality"

I Saptarshi Nandi registered on 28th August, 2017 (Reg. no. 1011705001) do hereby declare that this thesis entitled"**Prediction of Geotechnical Parameters from DMT, CPT and PMT Tests and Formation of Design Chart**"contains literature survey and original research work done by the undersigned candidate as part of Doctoral studies.

All information in this thesis have been obtained and presented in accordance with existing academic rules and ethical conduct. I declare that, as required by these rules and conduct, I have fully cited and referred all materials and results that are not original to this work.

I also declare that I have checked this thesis as per the "Policy on Anti Plagiarism, Jadavpur University, 2019", and the level of similarity as checked by iThenticate software is **4%.**

Saptarshi Nandi

Signature of Candidate:-
Date:-

Certified by Supervisor(s):
(Signature with date, seal)

1. Kaushik Bandyopadhyay

Dr. K. Bandyopadhyay
Professor
Department of Construction Engg.
Jadavpur University

2. Dipanjan Basu

JADAVPUR UNIVERSITY
KOLKATA-700032, INDIA

Index No. 203 / 17/ E

1. Title of the thesis:

Prediction of Geotechnical Parameters from DMT, CPT and PMT Tests and Formation of Design Chart

2. Name, Designation and Institution of supervisor

Prof. (Dr.) Kaushik Bandyopadhyay

Professor,

Department of Construction Engineering,

Jadavpur University,

Kolkata-700032, India

Prof. (Dr.) Dipanjan Basu

Professor,

Department of Civil & Environmental Engineering,

University of Waterloo

Waterloo, ON Canada

3. List of Publication (Related to thesis)

Journal Papers:

1) **Nandi, S.**, Bandyopadhyay, K., Basu, D., & Shiuly, A. (2024). Correlation of Pressuremeter Test Results with SPT N Values and Liquidity Index for Cohesive Soil of Normal Calcutta Deposit. Indian Geotechnical Journal, 1–15. https://doi.org/10.1007/s40098-023-00842-0
2) Bandyopadhyay, K., Das, K., **Nandi, S.**, & Halder, A. (2022). Dilatometer—an in-Situ Soil Exploration Tool for Problematic Ground Conditions vis-à-vis for Economizing Construction Activities. Indian

Geotechnical Journal, 52(5), 1155–1170. https://doi.org/10.1007/s40098-022-00655-7

Conference Proceedings (International):

1) **Nandi, S.**, Bandyopadhyay, Kaushik, & Das, K. (2023, December 14). Equivalent Approach for the prediction of Consistency of Cohesive Sub-Soil Using DMT Test. INDIAN GEOTECHNICAL CONFERENCE, ROORKEE on Geotechnical Advances in Sustainable Infrastructure Development and Risk Reduction.
2) Das, K., **Nandi, S.**, Chattaraj, S., Halder, A., & Sadhukhan, W. (2022). Estimation of subsoil parameters and settlement of foundation for a project in Kolkata based on CPT, DMT. Journal of Physics: Conference Series, 2286(1), 012026. https://doi.org/10.1088/1742-6596/2286/1/012026
3) Bandyopadhyay, K., **Nandi, S.**, Scholer, P., Babu, S., & Professor, G. (2020). Prediction of settlement of high court building, Kolkata using flat dilatometer-a case study. In A. M. and E. K. Tamás Huszák (Ed.), 6th International Conference on Geotechnical and Geophysical Site Characterization. ISSMGE.

Book Chapter:

1) Bandyopadhyay, K., Halder, A., **Nandi, S.**, Koley, B., & Saraswati, S. (2021). West Bengal. In Geotechnical Characteristics of Soils and Rocks of India (pp. 695–718). CRC Press. https://doi.org/10.1201/9781003177159-37

Conference Proceedings (National): NIL

List of Patents: NIL

List of Presentation in National/International:

1) **Nandi, S.,** Bandyopadhyay K., Halder A., & Basu D. (2022). Equivalent CPT Method for estimation of shear strength parameters for a project site in Kolkata using combination of SPT, DMT and CPT- a case study. In Rahman & Jaksa (Eds.), Proceedings of the 20th International Conference on Soil Mechanics and Geotechnical Engineering (pp. 483–487). © 2022 Australian Geomechanics Society, ISBN 978-0-9946261-4-1
2) **Nandi, S.**, Singh, R., & Bandyopadhyay, K. (2023). Estimation of Undrained Cohesion of Cohesive Sub-Soil in Kolkata Region using Pressuremeter Test. In J. J. Regin, Suhasini A., I. Jessy Mol, D. Judson, Shiny D. Smiline, & Illanthalir A. (Eds.), INTERNATIONAL CONFERENCE ON ADVANCES IN SUSTAINABILITY OF MATERIALS AND ENVIRONMENT (ICASME'23). St. Xavier 's Catholic College of Engineering

Dedicated to

My beloved Parents

ACKNOWLEDGEMENT

It is with great pleasure and proud privilege that I express my profound and heartfelt gratitude to my research supervisors, Prof. Kaushik Bandyopadhyay & Prof. Dipanjan Basu, without whose constant source of inspiration throughout my study, it would not have been possible to complete this thesis. I am grateful to them for their patience, detailed and constructive comments, continuous encouragement, and invaluable guidance throughout my research work.

I would like to offer thank to Prof. S.Saraswati, Prof. P.P.Biswas, Prof. G.N.Bhandari, Prof. P. Ghosh for their valuable support and guidance for my research work. They were not only members of my Doctoral committee but also mentors of my research work.

I also sincerely convey my immense gratitude to all my professors, the laboratory officials and my research colleagues of the Construction Engineering Department, Jadavpur University, for their constant encouragement and co-operation.

I am very much grateful to Constell Consultants Pvt. Ltd, R.V.N.L, L&T Infrastructure Engineering Ltd., M.N.Consultants, Public Works Department (Govt. of West Bengal) and Bentley Education for providing necessary data. I gratefully acknowledge the Studio Prof. Marchettis.r.l., Rome, Italy, and Pagani Geotechnical Equipment, Calendasco, Italy for providing the necessary supports related to the instruments used for the study.

Further, I would like to offer thank to Mr. B.N.Basak, Director, Constell Consultants Pvt. Ltd. and Prof. A.Shiuly, Associate Professor, Civil Engineering Department, Jadavpur University, for their guidance and providing all kinds of facilities for my research work.

Acknowledgement

I would like to thank my senior colleagues in Constell Consultants Pvt. Ltd.: Mr. Soumitra Bhattacharjee, Mr. Subrata Ray, Mr. Santanu Ballav, Mr. Mrityunjoy Poddar, Mr.Mrityunjoy Das and others for their constant help, support and encouragement till the end.

I am extremely thankful to my friend and colleague Mr. Kaustav Das and Mr. Prasanta Sardar for their continuous encouragement and support during the time of my research work.

My deepest gratitude goes to my parents, my sister and Ms. Swati Ghosh for their love and support throughout my life. They have always been there for me during the ups and downs, sharing my excitement and frustration. Their love and understanding have allowed me to make it successfully.

Finally, I bow down before the Almighty who had made everything possible.

Place: Jadavpur University

Saptarshi Nandi

ABSTRACT

In the recent past, our country India has witnessed rapid growth in urbanization. Due to this rapid urbanization, an inclination towards in situ testing is observed in the geotechnical field. In this study, focus is given to the geotechnical parameters obtained directly from the in-situ tests and compare with the results obtained from the most widely used in-situ test (i.e., standard penetration tests, SPT) and laboratory tests (conducted on collected undisturbed samples from conventional boreholes). Based on the comparison, also an effort has been made to establish a relationship among them, so that one can predict the sub-soil profile along with the required geotechnical parameters (for design purpose) by carrying out only the in-situ tests instead of conventional laboratory and in-situ tests.

In this context, three numbers of in-situ tests, which are rarely used for the geotechnical investigation work in India, are chosen for this study. These tests are Marchetti Flat Dilatometer Test (DMT), Cone Penetration Test (CPT) and Pressuremeter Test (PMT). The DMT, CPT and PMT tests are carried out adjacent to the conventional bore-hole (BH) accompanied with SPT test, at various project sites located in the states of West Bengal (WB) and Odisha (OR).

Based on the laboratory test results (conducted on collected samples from the adjacent conventional boreholes), the site wise sub-soil profile has been predicted. Also, the site wise variation of SPT N values (estimated from the adjacent boreholes) and shear strength parameters of sub-soil have been plotted along depth.

In each site, for DMT tests, the variation of shear strength parameters (undrained cohesion, C_u and angle of internal friction ϕ), vertical drained constrained modulus (M_{DMT}), Dilatometer Modulus (E_D) and Material Index (I_D) have been plotted along depth. Also the sub-soil profile has been predicted based on the value of I_D.

Besides, for the CPT test, site- wise variation of shear strength parameters (C_u and ϕ), vertical drained constrained modulus (M_{CPT}), Cone penetration resistance (q_c), Sleeve friction (f_s) and Soil behavior type index (I_C) estimated from CPT tests, have been plotted along depth. Also, the sub-soil profile has been predicted based on the value of I_C. Apart from this, for the PMT tests, the variation of limit pressure (P_L) and pressuremeter modulus (E_{PMT}) have been plotted along depth and sub-soil profile has been predicted based on the adjacent boreholes and by visual inspection during the progress of PMT test in the borehole.

The first objective of this study is to compare the sub-soil profile obtained from the conventional boreholes, with the predicted profile from DMT and CPT tests by virtue of material index (I_D) and (I_C) respectively.

The shear parameters i.e., undrained cohesion (C_u) and angle of internal friction (ϕ) obtained from the laboratory tests (conducted on collected undisturbed samples) has been compared with the values empirically estimated from the DMT and CPT tests.

Another attempt has been made to predict the range of E_D, M_{DMT} for the cohesive sub-soil (silty clay/ clayey silt) with different consistency (SPT based consistency) by establishing a relationship between E_D and M_{DMT} with the SPT N values. In this regard, a chart has been suggested to predict the SPT based consistency from DMT test. Besides, probable value of the plastic limit (W_P) and plasticity index (PI) have been suggested from the estimated values of E_D and M_{DMT} by establishing relations between E_D/PI and E_D/W_P with the M_{DMT}.

In addition to this, in CPT test, an attempt has been made to predict the range of q_c, f_s and M_{CPT} for the cohesive sub-soil (silty clay/ clayey silt) with different SPT based consistency by establishing a relation between q_c, f_s and M_{CPT} with the SPT N values. In this regard, a chart has been prepared to predict probable value of the plastic limit

(W_P) and plasticity index (PI) from the estimated values of q_c and M_{CPT} by establishing relations between q_c/PI and q_c/W_P with the M_{CPT}.

In PMT test, a typical range of E_{PMT} and P_L, have been suggested for the cohesive sub-soil (silty clay/ clayey silt) with different SPT based consistency by establishing a relation between P_L and E_{PMT} with the SPT N. Simultaneously, another relation (relation between E_{PMT}/P_L with liquidity index, I_L) has been made to predict liquidity index (I_L) from the ratio of E_{PMT}/P_L.

In addition to the above, another study has been carried out on to predict the settlement of shallow foundation (placed on cohesive silty clay/ clayey silt soil) by CPT tests. In this context, it is worth mentioning that the settlement analysis has been calculated by using empirical equation based average cone resistance, C_{KD}. Then these values have been compared with the DMT based settlement along with the output of numerical model, (done on PLAXIS 2D software; based on Mohr Coulomb model).

It has also been observed that the undrained cohesion (C_u) estimated from DMT tests are more compatible with the laboratory triaxial (UU) test results than the CPT tests. However, it has been observed that the angle of internal friction (ϕ), estimated from both CPT and DMT tests, are well comparable with the laboratory direct shear test (DS) results. Besides, it has been observed that the vertical drained constrained modulus (M) of sub-soil, estimated from DMT and CPT tests are well tallying with each other.

It is concluded that the SPT based consistency of sub-soil (cohesive silty clay/ clayey silt) may be predicted from the DMT tests based on the value of E_D and M_{DMT}. The Liquid Limit (W_L), Plastic Limit (W_P) and plasticity index (PI) may also be predicted from the E_D and M_{DMT} values. Besides, SPT based consistency of silty clay/ clayey silt sub-soil may be predicted from the value of CPT based parameters i.e., q_c, f_s and M_{CPT}.

Also, the value of Liquid Limit (W_L), Plastic Limit (W_P) and plasticity index (PI) may be predicted from the value of q_c and M_{CPT}.

In PMT test, it is found that the nature of the variation of P_L along depth is similar with the SPT N values than the variation of E_{PMT} along depth. However, both the values of E_{PMT} and P_L depend on the consistency of soils. Therefore, a typical range of E_{PMT}, P_L alongwith the ratio of E_{PMT}/P_L for cohesive (silty clay/ clayey silt) sub-soil with different SPT based consistency has been suggested. Also, it is concluded that the liquidity index (I_L) may be predicted from the ratio of E_{PMT}/P_L.

On the study, for the prediction of settlement of shallow foundations (placed on cohesive soils) by CPT test, it is found that the predicted settlement based on C_{KD}, are well comparable with the other method. Lastly, it is concluded that the method to estimate settlement of shallow foundation based on the C_{KD}, may also be adopted for the shallow foundation placed on cohesive soil.

INDEX

Contents **Page No**

Contents **Page No**

Contents **Page No**

LIST OF TABLES

LIST OF FIGURES

LIST OF SYMBOLS

ENGLISH

a	net area ratio of CPT test
A	Area of foundation plate
A	Lift off "pressure reading of DMT
a	Slope intercept in volume calibration curve of pressure meter for PMT test
A_s	Surface area of sleeve
A_{sb}	Cross-section area of sleeve at base
A_{st}	Pressure reading of DMT tests on 1.1mm displacement of membrane
B	Cross-sectional area of sleeve at top
BH	Bore-Hole
B_q	Pore pressure ratio
BRE	Building Research Establishment
c	Constant of compressibility
C_{KD}	Average cone resistance
CPT	Cone penetration tests
CPTU	Cone penetration tests with pore water pressure measurement
C_u	Undrained cohesion
d_{eff}	Effective thickness of plate / foundation
D	Diameter of blade
D_{50}	Mean grain size
D_i	Inside diameter of the heavy duty steel casing
DMT	Marchetti Flat Dilatometer Tests
DS	Laboratory direct shear tests
DSS-CK_0U	CK0U Direct shear in consolidated undrained tests
E	Young's modulus / Modulus of elasticity any material
E_D	Dilatometer Modulus
E_{PMT}	Pressuremeter modulus
E_{pmt}	Pressuremeter modulus
E_s	Modulus of elasticity of the soil
E_{sBH}	modulus of elasticity of soil from SPT N values
F_r	Normalized friction ratio
f_t or f_s	Sleeve friction
G	Shear modulus
G_s	Average specific gravity of soil (ranges between 2.6-2.7)
H_t	Thickness of soil layer,
I	Moment of inertia of foundation plate
I_C	Soil behavior type index

I_D	Material Index
I_L	Liquidity index
I_P or PI	Plasticity index
I_r	Rigidity factor
K_D	Horizontal stress index from DMT
K_o	Coefficient of earth pressure at rest condition
L	Length of measuring cell of the probe
m	arbitrary factor
M	Vertical drained constrained modulus
M_{CPT}	Vertical drained constrained modulus by CPT
M_{DMT}	Vertical drained constrained modulus by DMT
Moed	Constrained modulus obtained from oedometer tests
m_v	Volume compressibility
N_{60}	SPT N value corresponding to the 60% energy ratio
N_c	Terzaghi bearing capacity factor
NC	Normally consolidated soil
N_{kt}	Cone factor
N_{ob}	Observed (field) SPT blow counts
NX	Size of borehole i.e., 76mm
$N_{\Delta u}$	Cone factor for excess pore pressure
OC	Over consolidated soil
OCR	Over consolidation ratio
OR	Odisha
p	Corrected pressure
P_0	Effective overburden stress
$\overline{P_0}$	Initial effective overburden pressure at mid height of the layer
p_0	Corrected fist reading of DMT Test
P_{0m}	Pressure corresponding the pressuremeter curve starts to be flat
p_a	Atmospheric pressure in same units as q_t
P_c	Pressure correction for pressuremeter tests
P_c	Preconsolidation stress
P-e	Pneumatic electric cable
P_f	Pressure at plastic state
P_L	Limit pressure
PLAXIS 2D	Two dimensional Plaxis software
P_{Ln} or P_L^*	Net limit pressure
PMT	Pressuremeter tests

P_r	Pressure increment
p_y	Yield pressure
q_c or q_t	Cone penetration resistance
Q_T	Total thrust
Q_t	Normalized cone resistance
R_f	Friction ratio
R_M	Non-dimension variable factor
R_{M0}	Non-dimension variable factor
R_p	First reading during penetration only the cone
R_p+R_L	Second reading during the penetration of cone alongwith the sleeve
R_T	Third reading during penetration of total assembly of cone
S_0	Displacement of membrane
SBP or SBPM or SBPT	Self-boring pressuremeter
SBT	Soil behavior type
SDMT	Software for interpretation of DMT raw data
sDMT- E lab	Seismic Dilatometer tests
SPT N	Blow count value from Standard penetration test
SPT	Standard Penetration test
S_t	Total settlement
$S_{t\,CPT}$	Settlement from CPT test
$S_{t\,DMT}$	DMT based settlement
S_u	Undrained shear strength
SX	Size of borehole i.e., 150mm
u_0	In-situ static pore water pressure
u_2	Position of porous filter on piezocone i.e., just behind the cone
u_3	Position of porous filter on piezocone i.e., above to the friction sleeve
UK	United Kingdom
UU	Unconsolidated undrained
V	Volume of the cavity
V	Volume
V_0	Initial volume of pressuremeter probe
v_0	Volume at pressure P_{0m}
V_c	Volume loss of pressuremeter instrument
V_i	Volume corresponding intercept of the slope with ordinate
v_m	Mean additional volume injected
V_m	Observed volume

V_r	Volume corresponding to each pressure increment
WB	West Bengal
W_L	Liquid Limit
W_P	Plastic limit
w_n	Natural moisture content
z	Thickness of compressible layers

latin

σ_v'	In-situ effective vertical overburden pressure
α	Roughness coefficient of cone / Significance level
β	Pressuremeter constant
α_M	Empirically derived dimensionless factor
ε	Vertical strain
Δu	Excess pore pressure
ΔV or Δv	Change of volume
ν	Poison's ratio
Π	Pi
σ_h	Horizontal stress
ϕ'	Effective stress friction angle
ϕ	Angle of internal friction
σ'_{vo}	In-situ effective vertical stress
σ_{vo}	In-situ total vertical stress,
ΔA	external suction pressure, applied to the DMT membrane for stiffness correction
ΔB	compression pressure, applied externally DMT membrane for stiffness correction
ΔP or $\Delta\sigma'_{vo}$	vertical stress increment,
Σ	Summation
χ^2	Chi square
β	Pressuremeter constant
γ	In-situ unit weight of soil
γ_t	Bulk density of soil
γ_d	Dry density of soil
γ_w	Unit weight of water
Δp	Change of pressure
$\Delta\sigma_v$	Vertical stress increment
Δz	Small thickness

UNIT	
cm	centimeter
gm	gram
kg	kilogram
km	kilo meter
kN	kilo Newton
kPa	kilo Pascal
kg / cm^2	kilogram per square centimeter
MPa	Mega Pascal
N/mm^2	Newton per square milli meter
°	Degree
kN/m^3	kilo Newton per cubic meter
%	Percentage
cc	cubic centimeter
m	meter
mm	millimeter
s	second

Chapter# 1
INTRODUCTION

1.1 GENERAL

The characteristics of sub-soil may be investigated by several methods. Amongst these, the conventional boring approach (such as wash boring, rotary drilling technique) is commonly adopted in India. Rather good to say, till date, in Eastern part of India, general practice of the sub-soil characterization is by laboratory test results conducted on "undisturbed samples" collected from conventional boreholes alongwith the Standard Penetration test (SPT) conducted at every 1.50 m depth interval on the same borehole. At first, it is an age-old technique which requires very careful handling of the undisturbed sample and also the disturbance of the collected samples might occur during transport to the laboratory for testing purpose. Secondly, the collection of undisturbed samples might not be possible every time from the subsoil when it comprises very soft or very stiff cohesive soil. On the other hand, collection of "undisturbed sample" of purely cohesionless soils is next to impossible or even if it is possible, the preparation and testing of the sample in laboratory is a very costly affair altogether. Moreover, this method is involved with many "ifs and buts" and requires thoughtful judgements and assumptions for the characterization of sub soil. Therefore, to overcome this situation, many engineers are leaning to the direct measurement of sub-soil formation in terms of shear parameters as well as compressibility characteristics by various in-situ tests. Besides, the prediction of total settlements (consolidation settlements and immediate settlement) of foundation placed on cohesive or cohesionless soil, using the parameters directly

obtained from this in-situ test is also becoming very popular. Hence, a new alternative approach should be thought of which is effective both in terms of time and cost and also depicts accurate properties of sub-soil without collecting the soil samples during investigation (Campbell and Hudson 1969; D. B. Campbell 1972; Johnston 1983). In this regard, the in-situ penetrometer tests have been introduced into the geotechnical engineering field. Unfortunately, these tests are not very much in vogue and rather unexplored in this part of the country (Sundaram et al. 2023). Purposefully for filling up this gap, three types of in-situ tests namely, Cone penetration test (CPT), Dilatometer test (DMT) and Pressuremeter test (PMT) are considered.

In general, the CPT and DMT tests are penetrometer tests which have been widely used in many western countries and corresponding results have been used for geotechnical design purpose. The Cone penetration Test (CPT) equipment was developed at the Dutch Laboratory in the 1950s to investigate directly the characteristics of sub-soil profile. On the other hand, Marchetti Flat Dilatometer (DMT) had been introduced in this family in very recent period. This instrument was developed by Prof. (Dr.) Silvano Marchetti in 1974 at the L'Aquila University in Italy.

Apart from this, the Pressuremeter test is conducted into the small size borehole. This test is widely used in France and a widely used tool in many parts of the world for the estimation of stiffness of soil and corresponding settlement of shallow or deep foundations (Clarke 1994). Initially, the concept of pressuremeter instrument was proposed by Kogler (1933) in Germany (Hughes et al. 1977). Based on this concept, the usable form of this instrument was first developed by a French engineer Louis Menard in the late 1950s and subsequently

this instrument was modified (Briaud 1992, 2019a; CLARKE 1996; Clarke 2022). This instrument was developed to apply pressure on sides of the borehole through a flexible membrane attached to the probe. The pressuremeter probe is built up by three cells namely "Measuring Cell", top "Guard Cell" and bottom "Guard Cell". The purpose of these two numbers of "Guard cell" is to isolate the expansion of the measuring cell from end effects (i.e., end of the probe) thus replicating the plane strain deformation conditions.

1.2 NEED FOR PRESENT STUDY

In Eastern part of India, the uses of CPT, DMT and PMT tests are very limited. Also, the available research on CPT, DMT and PMT tests are very scanty. In this regard, side by side comparison of various geotechnical parameters obtained from the DMT, CPT and PMT tests (conducted in several locations) need to be done with the conventional tests. Also, in order to bridge the gap between conventional laboratory and in situ test results, a design chart need to be predicted.

Besides, within the Indian context, there is a necessity to analyse the efficacy of average cone resistance from CPT test in predicting the settlement behavior of shallow foundation placed on cohesive soils.

1.3 OBJECTIVE AND SCOPE OF WORK

The objectives of the work are summarized below:

- To determine fundamental geotechnical parameters obtained from the cohesive subsoil in the coastal regions of West Bengal (WB) and Odisha (OR) using three distinct in-situ tests viz., DMT, CPT and PMT.

- To develop design charts based on parametric relations done by regression analyses of the outcomes of DMT, CPT, PMT, and SPT tests, particularly focusing on silty clay/clayey silt soil in the coastal regions of WB and OR.
- To determine the settlement of shallow foundation placed on cohesive soil within the coastal region of West Bengal and Odisha, using average cone resistance (C_{KD}) from the CPT test and comparing it with DMT-based settlement data along with a numerical analysis based settlement.

The scopes of the work are outlined below:

1) To carry out 29 numbers of DMT, 25 numbers of CPT tests adjacent to conventional boreholes at different project sites in WB and OR.
2) To carry out 48 numbers of PMT conducted into 12 numbers of NX size (diameter ≈ 76mm) bore-holes adjacent to conventional SX size (diameter ≈ 150mm) bore-hole.
3) To predict sub-soil profile from DMT and CPT tests and compare with the sub-soil profile predicted from the conventional adjacent boreholes.
4) To measure shear strength parameters e.g., undrained cohesion and angle of internal friction from DMT and CPT tests and compare with the results of undisturbed samples tested in the laboratory.
5) To estimate compressibility characteristics (in terms of vertical drained constrained modulus) from CPT test and compare the values with DMT predicted values.

6) To estimate basic parameters i.e., limit pressure (P_L) and pressure meter modulus (E_{PMT}) from PMT tests.

7) To develop relations based on the regression analysis between the Dilatometer modulus (E_D) and vertical drained constrained modulus (M_{DMT}) estimated from DMT tests with the observed standard penetration blow count (N_{ob}) for cohesive soil.

8) To create relations based on the regression analysis between E_D and M_{DMT} with the Plastic limit (W_P) and Plasticity index (PI) determined from laboratory tests on samples of soil obtained from adjacent boreholes.

9) To establish relations based on the regression analysis between the cone penetration resistance (q_c) and sleeve friction (f_s) and vertical drained constrained modulus (M_{CPT}) estimated from CPT tests with the observed standard penetration blow count (N_{ob}) for cohesive soil.

10) To establish relations based on the regression analysis between q_c and M_{CPT} with the Plastic limit (W_P) and Plasticity index (PI) determined from laboratory tests on samples of soil obtained from adjacent boreholes.

11) To develop relations based on the regression analysis between the limit pressure (P_L) and pressuremeter modulus (E_{PMT}) with the observed standard penetration blow count (N_{ob}) for cohesive soil.

12) To create relations based on the regression analysis between the ratio of (E_{PMT}/P_L) estimated from PMT tests with the liquidity index (I_L) derived from laboratory tests on samples of soil obtained from adjacent boreholes.

13) To predict reference range of E_D and M_{DMT} estimated from DMT tests for cohesive soil with different SPT based consistency.

14) To predict liquid limit and plastic limit from the value of E_D and M_{DMT} estimated from DMT tests.
15) To predict reference range of q_c, f_s and M_{CPT} estimated from CPT tests for cohesive (silty clay/clayey silt) sub-soil with different SPT based consistency.
16) To predict liquid limit and plastic limit from the value of q_c and M_{CPT} estimated from CPT tests.
17) To predict a reference range of limit pressure (P_L) and pressuremeter modulus (E_{PMT}) for cohesive sub-soil with different SPT based consistency.
18) To predict a reference range of E_{PMT}/P_L ratio for cohesive sub-soil with different liquidity index.
19) To estimate the settlement of shallow foundation placed on cohesive soil by two methods i.e., based on average cone penetration resistance (C_{KD}) from CPT tests and another based on M_{DMT} values from DMT test.
20) To determine settlement based on a numerical model using PLAXIS 2D software and to compare this with those obtained from DMT and CPT.

1.4 ORGANIZATION OF THESIS

The present thesis has been divided into eight chapters. The table and figures have been presented in a sequence as they appear in the text.

Chapter 1 an attempt has been made to introduce the problem along with need for present research, scope and objectives of the work and organization of thesis.

Chapter 2 furnishes a detailed literature review on the relevant topic like data interpretation from in-situ tests i.e., DMT, CPT and PMT, and assessment of geotechnical parameters from the DMT, CPT and PMT tests by using correlations, prediction of settlements etc. and site-specific correlations. The details of literature

review on characterization of sub-soil by in-situ tests and prediction of settlements from the data obtained from DMT and CPT tests also have been presented in this chapter.

Chapter 3 discusses the procedures for conducting DMT, CPT and PMT tests. The method for interpreting data from these tests has been presented here. This chapter also includes the procedure to prepare a design chart based on the comparative study. Furthermore, the methodology for finding out the suitability of CPT tests data to predict settlement of shallow foundations, placed on cohesive soil, are presented in this chapter.

Chapter 4 presents the detailed location plans of the study area along-with the description of individual site.

Chapter 5 describes a comparative overview of the subsoil characteristics, depicted from the conventional boreholes and DMT, CPT and PMT tests. It also includes the depth-wise variations of various key parameters such as vertical drained constrained modulus, dilatometer modulus, cone penetration resistance, sleeve friction, limit pressure, pressuremeter modulus etc. Besides, a comparative analysis between laboratory estimated shear strength parameters with the values predicted from DMT and CPT tests, has been presented. Furthermore, it also enumerates a comparison between the estimated values of q_c and f_s by two different methods viz. Robertson (Robertson 1990)(Lunne et al. 2002a)(Presti and Meisina 2019)(Pagani Geotechnical Equipment (manual) 2014) and IS 4968 (part III) (IS 4968 (Part-III) 1976).

Chapter 6 covers the comparison of basic parameters obtained from individual DMT, CPT and PMT tests with the observed standard penetration blow count (N_{ob}) obtained from adjacent boreholes. A design chart is also presented to predict those parameters for cohesive soil having different SPT based consistency. Additionally, an attempt has also been presented to predict index properties of cohesive soil by using the parameters derived from DMT, CPT and PMT tests.

Chapter 7 presents the prediction of settlement of shallow foundation with different shape and size (placed on cohesive soil) based on average cone penetration resistance (C_{KD}). The settlement has also been calculated by using M_{DMT} obtained from DMT tests. Besides, based on the geotechnical parameters estimated from DMT, CPT and conventional laboratory tests, numerical analysis has also been made using Plaxis 2D (ver.16) software. The estimated value of settlement from the average cone penetration resistance (C_{KD}) has been compared with the values obtained from other approaches. The detailed discussions on this comparison have also been presented.

Chapter 8 summarizes the study and presents important conclusions that have been arrived at based on the entire study. Limitations and future scope also have been discussed in this study.

A list of the **References** has been furnished at the end.

Appendix A. DMT Comparison: Comparison of DMT tests parameters with conventional Borehole

Appendix B. CPT Comparison: Comparison of CPT tests parameters with conventional Borehole

Appendix C. PMT Comparison: Comparison of PMT tests parameters with conventional Borehole

Appendix D. Sample calculation for the prediction of settlement

List of journals and conference papers (first page) are provided at the end.

Chapter# 2

LITERATURE REVIEW

2.1 THE FLAT DILATOMETER (DMT)

2.1.1 DESCRIPTION OF THE DMT APPARATUS

The flat dilatometer (DMT) is a push-in type in-situ soil testing instrument. It was developed by Prof. Marchetti in Italy on 1980 (Marchetti 1980) . In 1988, the Dilatometer is updated by installing seismic module above the DMT blade (Hepton 1989) referred as the seismic dilatometer (SDMT).

The DMT blade is made of by stainless steel, measured 15 mm thick and 96 mm in length with one sided circular membrane having 60 mm diameter (Figure 2.1)(Marchetti et al. 2001)(Powell and Uglow 1988; Lutenegger 1990a; Smith and Houlsby 1995). The blade is connected to a control unit by a nylon cable (i.e., P-e; pneumatic electric cable) through which gas pressure and electric circuit get connected and transmitted.

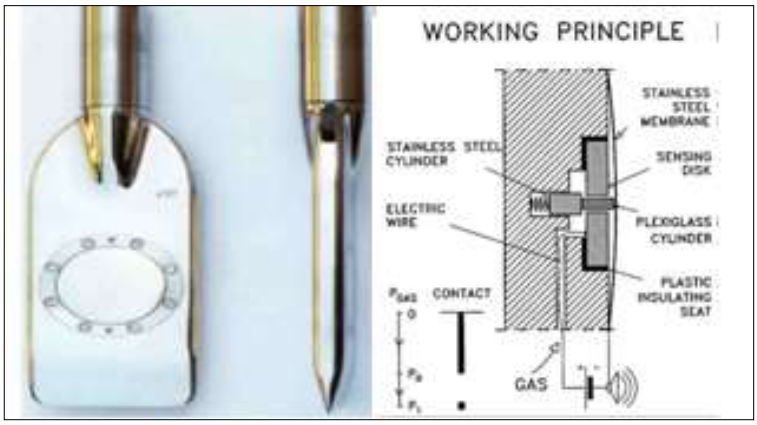

Figure: 2.1 DMT Blade along with working principle (Marchetti et al. 2001)

The circular membrane is flushed against the blade; in this seating position electrical circuit that runs along the single wire causes a buzzer to activate on the

control box. When the membrane is inflated, i.e., 'lift off' position, the circuit breaks and causing the buzzer to deactivate. When the membrane is inflated upto the limiting value of 1.1 mm displacement from the surface of the blade, again the internal circuit reconnects and the buzzer activates (Marchetti 1980)(Smith and Houlsby 1995) (Powell and Uglow 1988)(Marchetti et al. 2001)

The DMT blade is pushed into the ground by using an any penetrometer (such as CPT rig.) at 200 mm depth intervals. At desired test depth the penetration is stopped and the membrane is inflated by applying gas pressure (Schmertmann 1986a; Mayne and Martin 1998; Marchetti et al. 2001). When the membrane is inflated from the seating position, beeping sound from the buzzer goes off, the corresponding pressure reading is recorded from the dial gauge attached to the control box and noted as "A" (Marchetti 1980; Marchetti et al. 2001). After applying membrane correction to "A" reading, corresponding pressure reading is calculated and noted as corrected first pressure reading (p_0). Further, inflation of the membrane is allowed until the buzzer reactivates (deflection of membrane is reached to 1.1 mm). In this stage a pressure reading is taken; referred as "B" reading (Marchetti 1980; Powell and Uglow 1988; Smith and Houlsby 1995; Marchetti et al. 2001). This reading is corrected to the "p_1", termed as "corrected second pressure reading". On the next step gas pressure is released and the blade is drowned to the next 200 mm depth for further test and so on. The procedure is illustrated by schematic diagram (Figure 2.2).

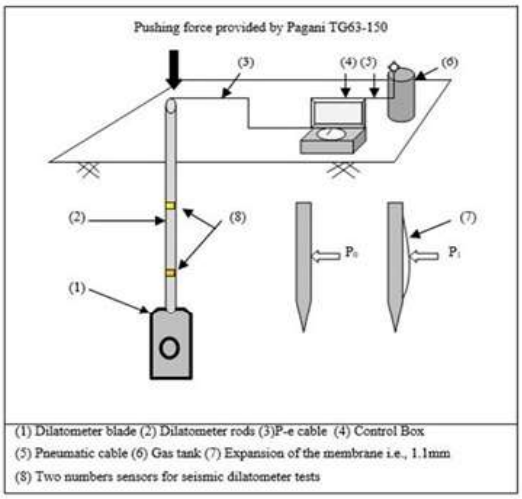

Figure: 2. 2 Schematic Diagram of DMT test and its components
(Bandyopadhyay et al. 2022)

This equipment is also used to determine the seismic properties by adding a seismic module with the DMT blade (Młynarek et al. 2006, 2010; Bihs et al. 2010) (Amoroso et al. 2013a). The seismic flat dilatometer test was initiated by P. Hepton on 1988 (Hepton 1989). Initially the mechanism of this test was adopted from Seismic Cone Penetration test (Hepton 1989) shown in Figure 2.3(a). The apparatus was developed by adding two numbers of geophone at 500mm distance apart (shown in Figure 2.3(b)) above to the DMT blade. The seismic test is carried out on every 500 mm depth interval (Marchetti et al. 2008a). The test procedure is presented schematically in Figure 5. A shear beam is kept on the ground surface. Next, this is struck with a hammer (weighing≈ 10 kg) to generate shear wave that propagates through the sub-soil(Mayne et al. 1999; McGillivray and Mayne 2004; Marchetti et al. 2008a; Amoroso et al. 2013a; Lanzano et al. 2020). The shear wave is then recognized by the geophones attached to the seismic module. The geophone signals are then recorded through sDMT- E lab software (previously installed on the computer kept on ground surface) as seismographs. Then seismographs are re-phased by to calculate a

true-interval of shear wave velocity (Marchetti et al. 2001, 2008a; McGillivray and Mayne 2004).

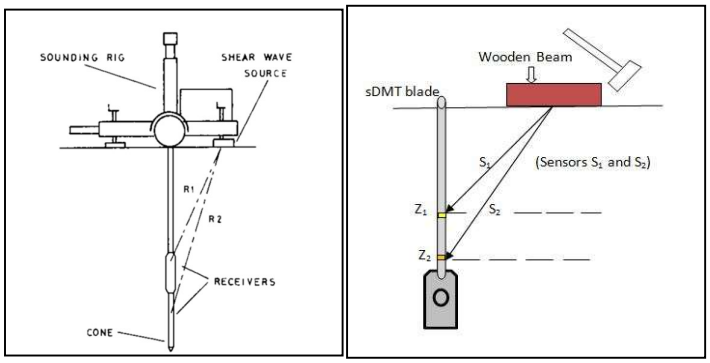

Figure: 2. 3(a) Schematic layout of seismic cone penetration test (Hepton 1989) (b) Schematic layout of SDMT test along with SDMT sensors

2.1.2 DEVELOPMENT OF THE DMT AND SDMT INSTRUMENT

The flat dilatometer (DMT) apparatus was first initiated to develop in the mid 1970's as a tool to investigate the values of geotechnical design modulus for laterally loaded driven piles. The concept of the instrument was originated from the technical behavior of the "Beach Umbrella" (Marchetti 2006) (Marchetti 2015). On 1974 the first version of this apparatus was fabricated(Marchetti 1975) (Marchetti 2006). Further modification work was undertaken to the Flat Dilatometer apparatus. The modification is illustrated in Figure 2.4.

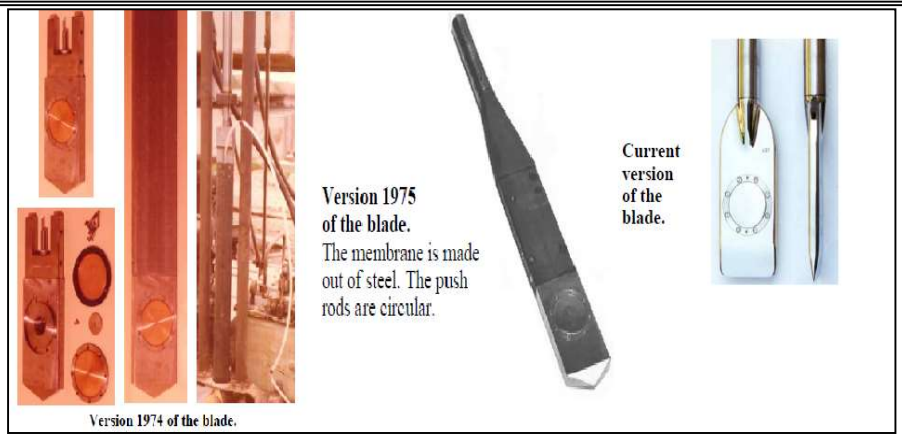

Figure: 2. 4 Development of DMT blade 1974-2015 (Marchetti 2006)

Further many experimental works were undertaken to determine other geotechnical parameters from the DMT tests (Marchetti and Crapps 1981; Schmertmann and Marchetti 1981; Davidson and Boghrat 1983; Motan and Gabr 1984; Motan and Khan 1988a, b; Su et al. 1993; Marchetti S. 1997; Redel et al. 1999) and the equipment was further modified. Since 1980, the mechanical Flat Dilatometer (DMT) equipment has been kept relatively unchanged.

The Flat Dilatometer apparatus was further developed (Hepton 1989) by adding a single triaxial geophone located just above to the Dilatometer blade for characterizing the seismicity of sub-soil profile and it was named as Seismic Dilatometer tests. (SDMT). Later on, a single horizontal velocity transducer was fitted with the SDMT apparatus. in 1996 (Kates 1996) (Holtrigter 2010). The Seismic Dilatometer Test apparatus was further improved at Georgia Tech, Atlanta, USA (Mayne and Martin 1998) (Mayne et al. 1999) shown in Figure 8. Again, an modification of SDMT apparatus was undertaken by Monaco on 2007 (Monaco et al. 2006a, b) in Italy. The "true interval" SDMT system was introduced by adding another geophone just above the DMT blade by keeping 0.5m gap from the other one (Marchetti et al. 2008a; Amoroso et al. 2013a;

Lanzano et al. 2020) (Marchetti et al. 2008b; Amoroso et al. 2013b, 2014; Marchetti and Monaco 2018) (Monaco and Marchetti 2007). This development was done to increase the accuracy of the test, shown in Figure 2.5.

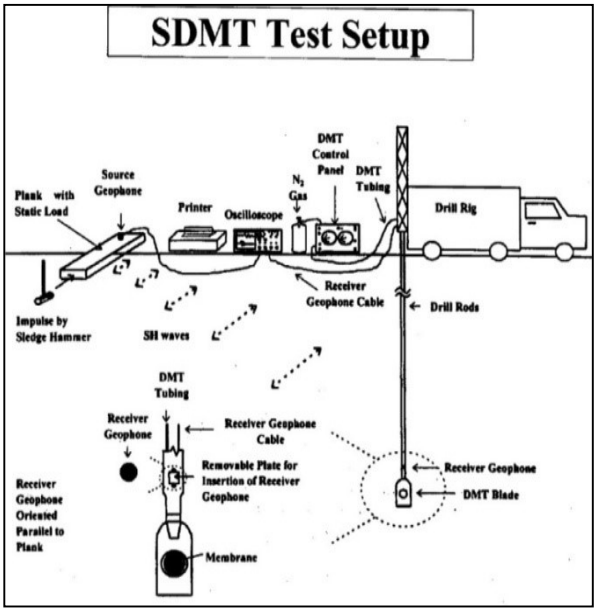

Figure: 2.5 Early SDMT Setup (Marchetti et al. 2008a)

2.1.3 INTERPRETATION OF DMT DATA

Two numbers of pressure readings are observed from the gauge attached to the control panel of DMT apparatus. Initially the first reading 'A' is noted when the membrane is lifted to its seating position. the second pressure reading (i.e.,'B') is taken when the membrane expands to the maximum limit of 1.1 mm (Marchetti 1980; Powell and Uglow 1988; Smith and Houlsby 1995; Marchetti et al. 2001). These pressure readings are then corrected for membrane stiffness to the pressure which is actually applied to the surrounding soils (p_0 and p_1 respectively) as given in following equations:

$$\mathbf{p_0} = \mathbf{A} + \Delta\mathbf{A} \quad (2.1)$$

$$\mathbf{p_1} = \mathbf{B} - \Delta\mathbf{B} \quad (2.2)$$

Where ΔA = the external suction pressure which is applied to the membrane in free air to keep it in contact with the sensing disc on the blade. ΔB = the compression pressure applied externally which lifts the membrane 1.1 mm from its seating in free.

The difference of corrected pressures (i.e., $p_1 - p_0$) may be converted into a modulus of elasticity of the soil (E_s) using elastic theory. The solution of the problem is achieved if the space surrounding the dilatometer is formed by two elastic half-space, be in contact along the plane of symmetry of the blade (Gravesen 1960). The solution is given to the following equation:

$$\mathbf{s_0 = 2D \times (p_1 - p_0).(1 - \nu^2)/(\pi \times E)} \quad (2.3)$$

For a membrane diameter D = 60 mm and S_0 = 1.1 mm, becomes:

$$\mathbf{E/(1 - \nu^2) = 34.7 \times (p_1 - p_0)} \quad (2.4)$$

Where,

ν = poison's ratio

The term $E/(1 - \nu^2)$ is defined by Marchetti as the Dilatometer Modulus (E_D) (Marchetti 1980). Two other indices values (i.e., material index and horizontal stress index) were also defined. The three index parameters are given as follow (Marchetti 1980; Marchetti et al. 2001):

Material Index (I_D) : $I_D = (p_1 - p_0)/(p_0 - u_0)$ (2.5)

Horizontal Stress Index (K_D) : $K_D = (p_0 - u_0)/\sigma'_v$ (2.6)

Dilatometer Modulus (E_D) : $E_D = 34.7 \times (p_1 - p_0)$ (2.7)

Where,

u_0 = the in-situ static pore water pressure prior to insertion of the DMT blade

σ'_v = in-situ effective vertical overburden pressure

2.1.4 INTERPRETED PARAMETERS FROM DMT TESTS

The original correlations were explained by Marchetti based on the available data obtained from eight numbers test sites, mostly in Italy (Marchetti 1980). The test sites comprised of variable sub-soil conditions ranging from cohesive to cohesionless soil with different stress history(Baldi et al. 1986; Marchetti et al. 1986, 1991; Konrad 1988; Marchetti and Totani 1989; Burghignoli et al. 1991). The basic three parameters of Dilatometer (Equation 2.5-2.7) obtained from those sites. These values were compared and empirically correlated to the laboratory results. An overview of these parameters is discussed below.

2.1.4.1 MATERIAL INDEX (I_D)

The material index parameter (I_D) merely indicates the type of soil and closely related to its grain size distribution(Iwasaki et al. 1991) (Kamei and Iwasaki 1995). Increasing or decreasing value of (I_D) mainly depends on presence of fine contents within the soil mass irrespective of the soil stress history(Iwasaki et al. 1991; Kamei and Iwasaki 1995).

The increasing amount of fine content sharply decreases the value of I_D and vice versa (Marchetti 1980; Powell and Uglow 1988; Iwasaki et al. 1991; Smith and Houlsby 1995). However, it cannot provide detail information on grain size distribution (Iwasaki et al. 1991). In this context, the value of I_D was considered as a function of the mechanical properties of the soil which depends on grain size as a whole (Powell and Uglow 1988; Lutenegger 1990a; Iwasaki et al. 1991; Smith and Houlsby 1995; Marchetti et al. 2001).

It was proposed that the Material Index is to be estimated as the ratio of soil stiffness (the difference of p_1 and p_0) and soil strength (as estimated by $p_0 - u_0$) (Marchetti 1980, 2015; Schmertmann 1986a; Marchetti et al. 2001; Penna 2006).

These two independent variables (i.e., soil stiffness and soil strength) depict wide range of I_D reflecting the soil behavioral qualities having different grain size. However, there was no correlation or range found between the plasticity index (PI) and Material Index (I_D). Soil classification system based on I_D is summarised in Table 2.1.

Table: 2.1 soil classification based on I_D values (Marchetti et al. 2001)

Peat or sensitive clays	Clay		Silt			Sand	
	Clay	Silty clay	Clayey silt	Silt	Sandy silt	Silty sand	Sand
I_D values	0.10	0.35	0.6	0.9	1.2	1.8	3.3

2.1.4.2 K_0 AND OCR

The 'lift-off' pressure, p_0 is induced by the horizontal pressure developed by soil during penetration of the blade. So, K_D is not a direct estimation of the horizontal stress (σ_h) induced by the soil (Mayne and Stewart 1988; Lawter Jr and Borden 1990; Mayne and Kulhawy 1990; Hamouche et al. 1995; Mayne and Martin 1998; Marchetti et al. 2001) . In this regard, the estimated field K_o (coefficient of earth pressure at rest condition) (Huang and Haefele 1990)value was plotted against measured value of K_D for individual test site (Marchetti 1980; Powell and Uglow 1988; Schmertmann 1988a; Lutenegger 1990a; Smith and Houlsby 1995), which revealed a unique relationship between these two parameters (Figure 2.6 (a) (Marchetti 1980; Marchetti et al. 2001). The equation (Equation 2.8) of this plot is given below (Marchetti 1980; Powell and Uglow 1988, 1989; Mayne and Martin 1998; Marchetti et al. 2001) (Marchetti 1985; Monaco and Marchetti 2004).

$$K_0 = (K_D/1.5)^{\wedge 0.47} - 0.6 \qquad (2.8)$$

It was also mentioned that this relationship was based on empirical relationship for uncemented clays (where materials are free from any attraction) (Marchetti 1980). Also, this relationship does not valid where the clays that have experienced aging, thixotropic hardening, naturally cemented, etc (Marchetti 1980, 2015; Schmertmann 1986a; Marchetti et al. 2001). In such soils, K_D probably depicts the higher values due to the additional strength contributed by these factors ((Marchetti 1980, 2015; Lutenegger and Timian 1986; Schmertmann 1986a; Jamiolkowski et al. 1988; Bogossian et al. 1989; Mayne and Martin 1998; Penna 2006; Marchetti et al. 2008b) (Marchetti et al. 2001) (Marchetti 1980).

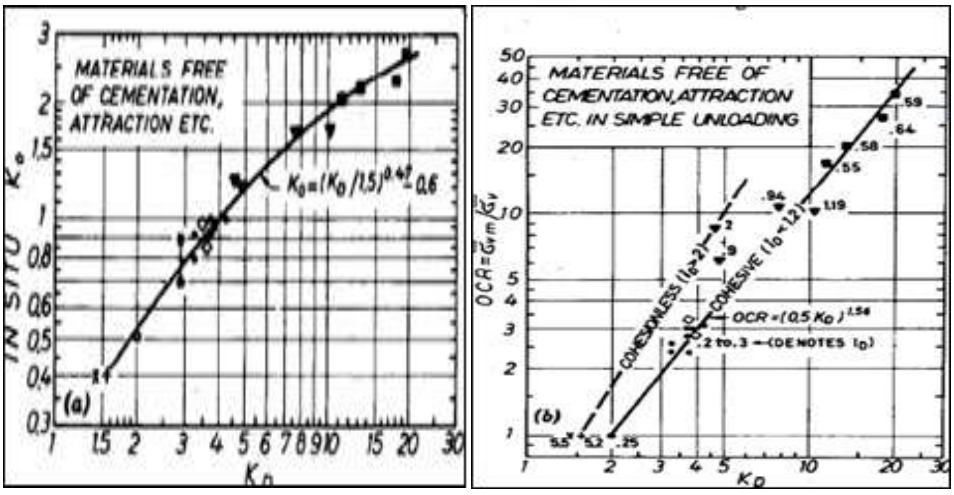

(a) (b)

Figure: 2. 6 Correlation between (a) K_0 and K_D; (b) OCR and K_D (Marchetti 1980; Marchetti et al. 2001)

On experimental study, it was observed that the value of K_D exhibited a consistent pattern in line with the overconsolidation ratio (OCR) (Figure 2.6 (b)). This relationship was mathematically stated by Marchetti in 1980 (Equation 2.9) (Marchetti 1980)(Marchetti 1979).

$$OCR = (0.5 \times K_D)^{\wedge 1.56} \quad (2.9)$$

However, it was mentioned that this relationship is only applicable for clayey soils (i.e., $I_D < 1.2$) (Marchetti 1980) . Whereas there was no definite correlation was found for cohesionless soils due to the limited experimental data(Marchetti 1980, 2015).

Moreover, it was mentioned that the range of K_D for normally consolidated clay, falls within the value of 1.8 to 2.3 (Averagely ≈2) (Marchetti 1980; Marchetti et al. 2001).

2.1.4.3 VERTICAL DRAINED CONSTRAINED MODULUS (M_{DMT})

There was no direct relationship between dilatometer vertical drained constrained modulus (M_{DMT}) with the reciprocal of volume compressibility ($1/m_v$) and dilatometer modulus (E_D) (Marchetti 1980; Marchetti et al. 2001; Marchetti and Monaco 2018). E_D is dependent variable which depends on many factors (Marchetti 1980). However, the Horizontal stress index (K_D) and Material Index (I_D) reflect the information on the stress history and soil type respectively(Marchetti 1980, 2010; Marchetti and Crapps 1981; Schmertmann 1982; Marchetti et al. 1993, 2001, 2006; Totani et al. 1999, 2001) . By considering these two parameters, it was found that a relationship exists between the dilatometer modulus (E_D) and vertical drained constrained modulus, M_{DMT} ($=1/m_v$), as given below (Equation 2.10) (Marchetti 1980; Marchetti et al. 2001).

$$M_{DMT} = R_M E_D \quad (2.10)$$

Where R_M is a non-dimension factor depends on I_D and K_D

From the experimental data (Figure 2.7), the following formulae (Equation 2.11(a) – 2.11(e)) for R_M were derived (Marchetti et al. 2001):

If $I_D \leq 0.6 \quad R_M = 0.14 + 2.36 \times \log K_D$ 2.11(a)

If $I_D \geq 3.0 \quad R_M = 0.5 + 2 \times \log K_D$ 2.11(b)

If $0.6 < I_D < 3.0 \quad R_M = R_{M,0} + (2.5 - R_{M,0}) \log K_D$, where $R_{M,0} = 0.14 + 0.15 (I_D - 0.6)$ 2.11(c)

If $I_D > 10 \quad R_M = 0.32 + 2.18 \times \log K_D$ 2.11(d)

If $R_M < 0.85, then\ set\ R_M = 0.85$ 2.11(e)

It was mentioned that the correlation between R_M with K_D was scattered in considerable amount because of some uncertainty of the M values used as reference (Marchetti 1980; Mayne 1987; Mayne and Martin 1998; Marchetti et al. 2001). However, it was assumed and stated that the margin of uncertainty for obtaining that correlation of data (Figure 2.7) was in the acceptable range as per the reliability based alternative methods (Marchetti 1980).

The local tangent values ($1/m_v$) were used as the reference values of M, which was used for establishing the correlation(Marchetti 1980). Therefore, the value of M is applicable in settlement analysis (De Beer 1965; Hayes 1986; Schmertmann 1986b; Leonards and Frost 1988; Skiles and Townsend 1994; Monaco et al. 2006a; Bandyopadhyay et al. 2020; Das et al. 2022). However, this small variation of M is only applicable for the aged clay or pre-consolidated clay. Beyond the pre-consolidation stress (P_c) or on the virgin consolidation side the value of M, estimated from dilatometer may be the small value (Schmertmann 1983; Mayne 1987).

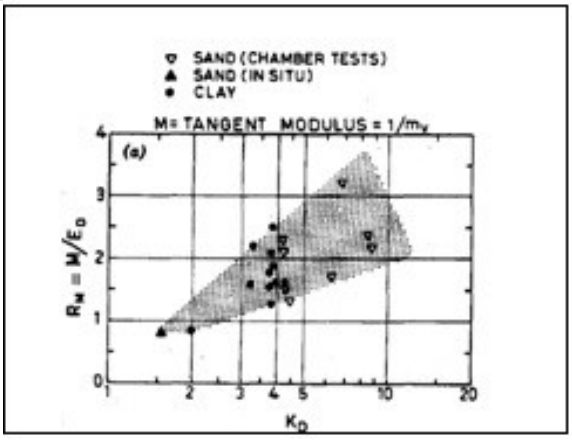

Figure: 2.7 R_M vs. K_D with M from experimental data (Marchetti 1980; Marchetti et al. 2001)

2.1.4.4 UNDRAINED SHEAR STRENGTH (C_u)

The prediction of undrained shear strength (C_u) from the dilatometer test is done based on the following relationship (Ladd et al. 1977; Marchetti 1980; Yu et al. 1992; Su et al. 1993; Bellotti et al. 1994; Kamei and Iwasaki 1995; Mello Vieira et al. 1999; Marchetti et al. 2001; Agaiby and Mayne 2015) (Equation 2.12):

$$(C_u/\sigma_v')_{OC} = (C_u/\sigma_v')_{NC}\, OCR^m \quad (2.12)$$

In this relationship, the ratio of undrained shear strength (Cu) to effective vertical stress (σv') for over-consolidated soil (OC) can be estimated. It includes multiplying the same ratio for normally consolidated (NC) soil by the over-consolidation ratio (OCR) raised to the power of 'm' (approximately 0.8). According to Ladd et al., when Equations (2.9) and (2.12) are equated, the relationship changes into the following form (Equation 2.13) (Ladd et al. 1977).

$$(C_u/\sigma_v')_{OC} = (C_u/\sigma_v')_{NC}.(0.5K_D)^{1.25} \quad (2.13)$$

Later on, 1980 the ratio of C_u and σ_v' against K_D was plotted for cohesive soils (based on experimental data, $I_D \leq 1.2$) (Figure 2.8) (Marchetti 1980). It was observed that the ratio of C_u and σ_v' for the NC soils, follows a value of 0.22

(Marchetti 1980). Also, it was found reasonable fit as suggested by Mesri (Mesri 1975) (Marchetti, 1980)(Terzaghi et al. 1996). Hence, Equation 2.13 can be rewritten as follow (Equation 2.14).

$$C_u = 0.22\,\sigma_v' \times (0.5K_D)^{1.25} \qquad (2.14)$$

In the Figure 2.8 (Marchetti 1980) (Marchetti et al. 2001), the dashed line indicates a lower strength than the average values of the experimental data. That means a conservative estimation of the in-situ C_u. It was also noted that (Marchetti 1980) the correlation (Figure 2.8 and Equation 2.14), applicable even if the clay is apparently overconsolidated due to aging, thixotropic hardening, cementation, etc.. However, it is not applicable for the removal of overburden. In that case, it would indicate a higher K_D value which results higher C_u, σ_v' ratio, irrespective of the origin of K_D (Marchetti 1980; Marchetti et al. 2001).

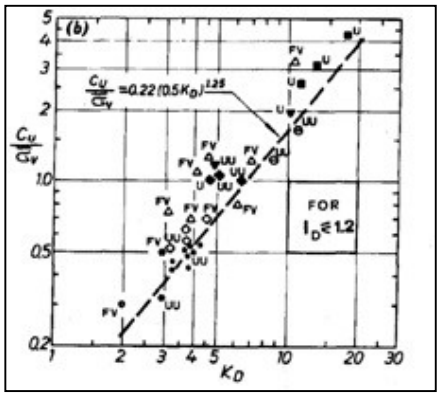

Figure: 2.8 Correlation between C_u/σ_v' and K_D (Marchetti 1980; Marchetti et al. 2001)

2.1.4.5 SUMMARY OF MARCHETTI CORRELATIONS

The empirical correlations were suggested by Marchetti (1980) (Marchetti 1980) on the basis for the existing data sets. Which was commonly used for interpreting the results obtained from Dilatometer test. Later on, (Marchetti S. 1997), the

correlation for friction angle (ϕ) for sand (I_D> 1.8) based on the value of K_D was suggested and included(ASTM International 2007). The summarised correlations are given in the following table (Table 2.2) proposed by Totani (Totani et al. 2001).

Table: 2.2 Marchetti DMT Interpretation Formulae (Marchetti et al. 2001; Totani et al. 2001)

SYMBOL	DESCRIPTION	BASIC DMT REDUCTION FORMULAE	
p_0	Corrected First Reading	$p_0 = 1.05\ (A - Z_M + \Delta A) - 0.05\ (B - Z_M - \Delta B)$	Z_M = Gage reading when vented to atm. If ΔA & ΔB are measured with the same gage used for current readings A & B, set $Z_M = 0$ (Z_M is compensated)
p_1	Corrected Second Reading	$p_1 = B - Z_M - \Delta B$	
I_D	Material Index	$I_D = (p_1 - p_0) / (p_0 - u_0)$	u_0 = pre-insertion pore pressure
K_D	Horizontal Stress Index	$K_D = (p_0 - u_0) / \sigma'_{v0}$	σ'_{v0} = pre-insertion overburden stress
E_D	Dilatometer Modulus	$E_D = 34.7\ (p_1 - p_0)$	E_D is NOT a Young's modulus E. E_D should be used only AFTER combining it with K_D (Stress History). First obtain $M_{DMT} = R_M E_D$, then e.g. $E \approx 0.8\ M_{DMT}$
K_0	Coeff. Earth Pressure in Situ	$K_{0,DMT} = (K_D / 1.5)^{0.47} - 0.6$	for $I_D < 1.2$
OCR	Overconsolidation Ratio	$OCR_{DMT} = (0.5\ K_D)^{1.56}$	for $I_D < 1.2$
c_u	Undrained Shear Strength	$c_{u,DMT} = 0.22\ \sigma'_{v0}\ (0.5\ K_D)^{1.25}$	for $I_D < 1.2$
Φ	Friction Angle	$\Phi_{safe,DMT} = 28° + 14.6°\ \log K_D - 2.1°\ \log^2 K_D$	for $I_D > 1.8$
c_h	Coefficient of Consolidation	$c_{h,DMTA} \approx 7\ cm^2 / t_{flex}$	t_{flex} from A-log t DMT-A decay curve
k_h	Coefficient of Permeability	$k_h = c_h\ \gamma_w / M_h$ ($M_h \approx K_0\ M_{DMT}$)	
γ	Unit Weight and Description	(see chart in Fig. 16)	
M	Vertical Drained Constrained Modulus	$M_{DMT} = R_M E_D$ if $I_D \le 0.6$ $R_M = 0.14 + 2.36 \log K_D$ if $I_D \ge 3$ $R_M = 0.5 + 2 \log K_D$ if $0.6 < I_D < 3$ $R_M = R_{M,0} + (2.5 - R_{M,0}) \log K_D$ with $R_{M,0} = 0.14 + 0.15\ (I_D - 0.6)$ if $K_D > 10$ $R_M = 0.32 + 2.18 \log K_D$ if $R_M < 0.85$ set $R_M = 0.85$	
u_0	Equilibrium Pore Pressure	$u_0 = p_2 = C - Z_M + \Delta A$	In free-draining soils

Further a chart was developed by Marchetti and Crapps (Marchetti and Crapps 1981) for predicting bulk unit weight corresponding to the soil type identified from the value of I_D and E_D. That chart is given in the following Figure 2.9. The aim behind to prepare this chart, was to predict the average value of unit weight for "normal soil". This was used to calculate the effective stress (σ'_v) and not to estimate accurate unit weight. The value of effective stress was used in the correlation suggested by Marchetti (Marchetti and Crapps 1981; Schmertmann and Marchetti 1981).

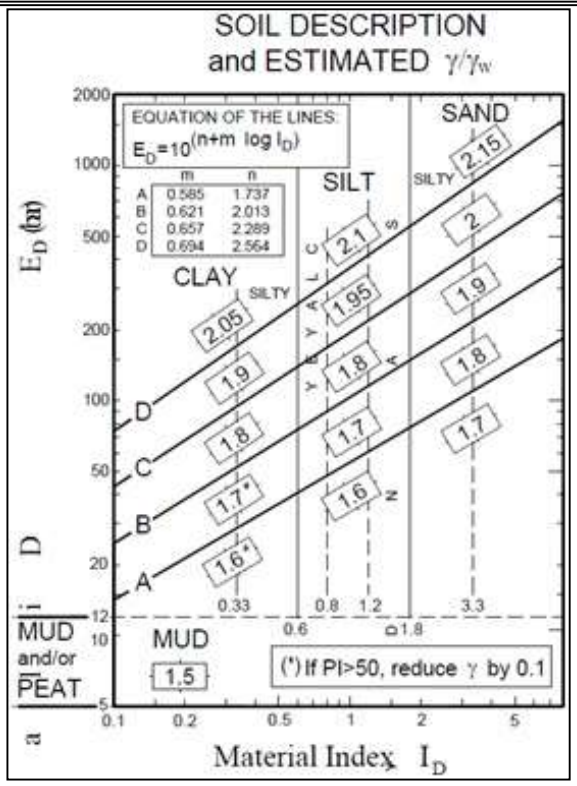

Figure: 2.9 Chart for predicting soil Unit Weight (Marchetti et al. 1981)

2.1.5 VERIFICATION TO THE MARCHETTI'S CORRELATIONS

Following the original work by Marchetti (1980), many research works had been carried out in the various part of world. The main focus of those studies were given to compare the DMT based test results with the conventional test results(Gabr and Borden 1988; Schmertmann 1988b, 1989, 1991; Baldi et al. 1989; Mayne and Bachus 1989; Borden 1991; Tanaka and Tanaka 1998; Cruz et al. 1999; Mayne and Liao 2004; Mayne 2006b, c, d, 2015; Nuno Cruz et al. 2006; Aykin et al. 2010; McNulty and Harney 2010)(Nandi et al. 2022)(ASTM International 1986; Schmertmann 1986b; Robertson 1988; Roque et al. 1988; Sanglerat 2012). The parameter wise research works are outlined below.

2.1.5.1 MATERIAL INDEX (I_D)

There have been few studies carried to compare the material index (I_D) to other conventional soil classification tests. Also, there are limited resources available on the comparison of soil unit weight as predicted from Dilatometer test. However, the Building Research Establishment (BRE) in the UK, attempted to establish a comparison of the DMT results with the known soil properties obtained from various test sites throughout the UK (Powell and Uglow 1988).

As a part of that research work, material index, (I_D) and the dilatometer modulus (E_D) for the various types of soils were plotted on the Marchetti density chart (Powell and Uglow 1988) (Figure 2.10). It was found that some of the soil types were accurately identified by the chart (mainly silty clays/clayey silts). Whereas, the soil more than 60% clay contents, were found to be scattered. It was concluded that the very high degree of over consolidation and relative age of those soils might affect the value of material index (I_D)(Mayne and Martin 1998).

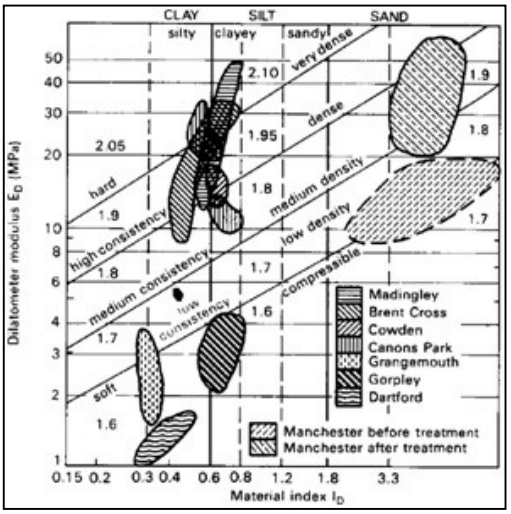

Figure: 2.10 Comparison chart for soil classification (Powell and Uglow 1988)

Besides, mixed responses were found in the comparison of unit weight. The predicted value from the chart indicated lower values for most of the soil (Figure

2.11). However, for certain soil types, there was a good agreement, indicating a trend of variation.

In the year 1991, another research work was carried out by Iwasaki on soft alluvial clays in Japan (Iwasaki et al. 1991). It was revealed an average relationship between the fines content and the material index, I_D (Figure 2.12). It was found that the fifty percent (50%) fine content lies within the I_D of 1.8, which belongs to the border line between silt and sand.

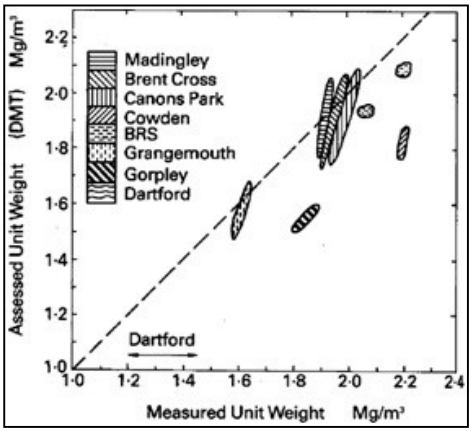

Figure: 2. 11 Comparison of unit weight (Powell and Uglow 1988)

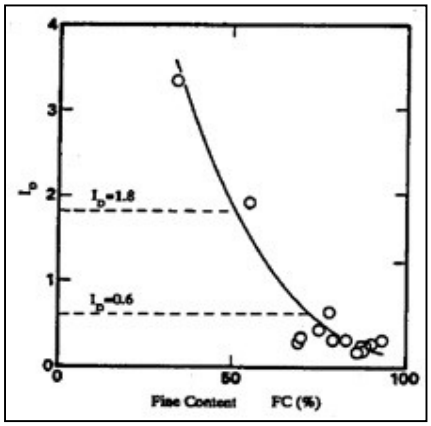

Figure: 2. 12 variation of I_D with fines content (Iwasaki et al. 1991)

2.1.5.2 OVER CONSOLIDATION RATIO (OCR) AND K_0

In the year of 1988 research was undertaken by Powell and Uglow (Powell and Uglow 1988, 1989) regarding the over-consolidation ratio (OCR) and K_0 values for various United Kingdom (UK) soils. Theses parameters were compared graphically with the dilatometer horizontal stress index (K_D). The results were then compared with the Marchetti proposed correlations(Marchetti et al. 2001; Totani et al. 2001) (Table 2.2). The corresponding graphs of those results are shown in Figure 2.13 and Figure 2.14.

The results show that, in heavily over-consolidated clays the OCR and K_0 values corresponding to value of K_D tended above the Marchetti correlation curve.

Whereas, these value lies below the correlation line for softer and younger clays. However, both the plots show the same general trend as mentioned in the correlation and it was suggested that site specific correlations could be made. The following correlations (Equation 2.15- 2.16) were proposed for the 'young' clays.

$$K_0 = 0.34 \times K_D^{0.55} \quad (2.15)$$

$$OCR = 0.24 \times K_D^{1.32} \quad (2.16)$$

On the other hand, it was also concluded that the determination of OCR for the heavily overconsolidated clays by oedometer test and thus establishing a generalised relationship is difficult.

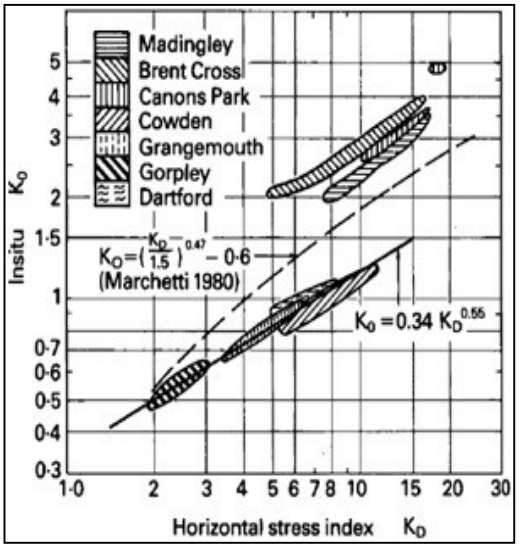

Figure: 2.13 Graph corresponding K_0 vs. K_D (Powell and Uglow 1986, 1988, 1989)

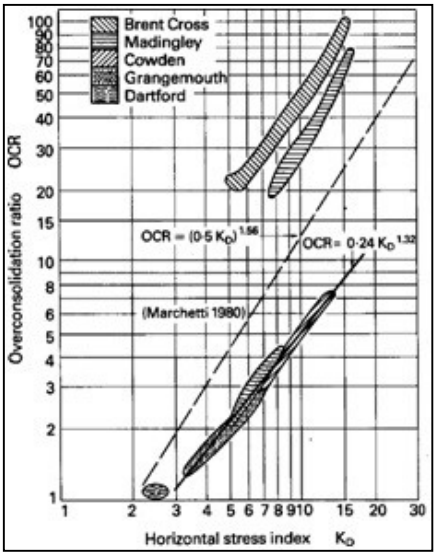

Figure: 2. 14 Graph corresponding OCR vs. K_D (Powell and Uglow 1986, 1988, 1989)

In report of ISSMGE Technical Committee 16 (Marchetti et al. 2001; Totani et al. 2001), it was mentioned that the original correlation was deviated as per the research by Powell & Uglow 1988(Powell and Uglow 1988, 1989). However, the report of the ISSMGE (Marchetti et al. 2001) indicated that:

- The original correlation line was intermediate between the UK test data points
- The data points of each UK site, were in a remarkably narrow band parallel to the original correlation line.
- The narrowness of the data point's band for each site, is a confirmation of the remarkable resemblance of the OCR and K_D profiles. Based on the parallelism of the data points, it was confirmed the same slope.

In 1991 (Iwasaki et al. 1991), for estimation of K_0, another research was conducted on soft alluvial clays in Japan. That study depicted a good comparison of dilatometer test with other tests (Figure 2.15). It was also observed that the results, predicted from dilatometer test were well tallied with other test results. Also, it was found to be close to the results estimated from self-boring pressuremeter and triaxial tests.

As per the research work done by Wong et al. conducted on 1993(Wong et al. 1993), it was revealed a good comparison between DMT and self-boring pressuremeter for estimating the K_0 values on soft alluvial soil (Figure 2.16)

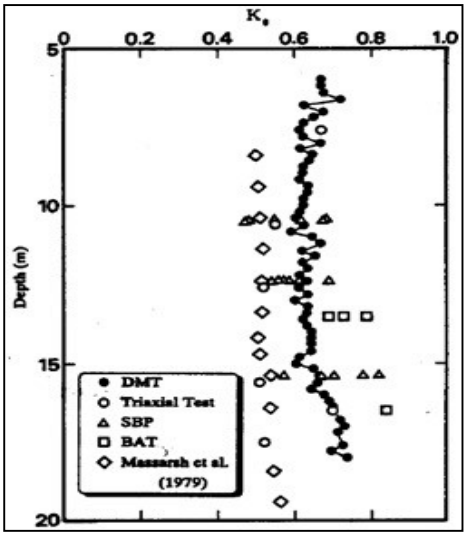

Figure: 2.15 Variation of K_0 values along depth (Iwasaki et al. 1991)

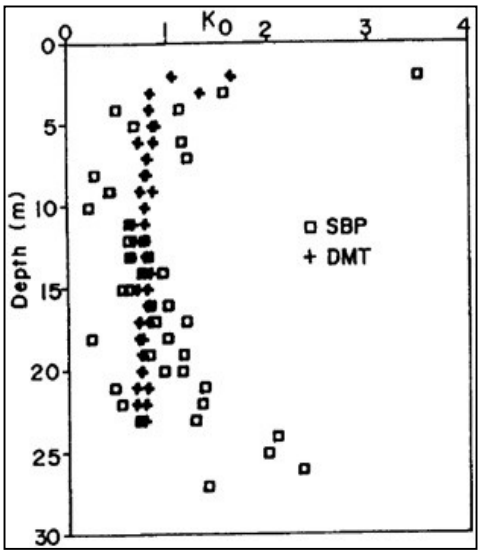

Figure: 2.16 K_0 values estimated from DMT and SBP (Wong et al. 1993)

Another good comparison was found on K_0 values estimated from DMT test and self-boring pressuremeter (SBP) (Nash et al. 1992) conducted at Bothkennar, UK and at Fucino, Italy (Burghignoli et al. 1991) (Figure 2.17).

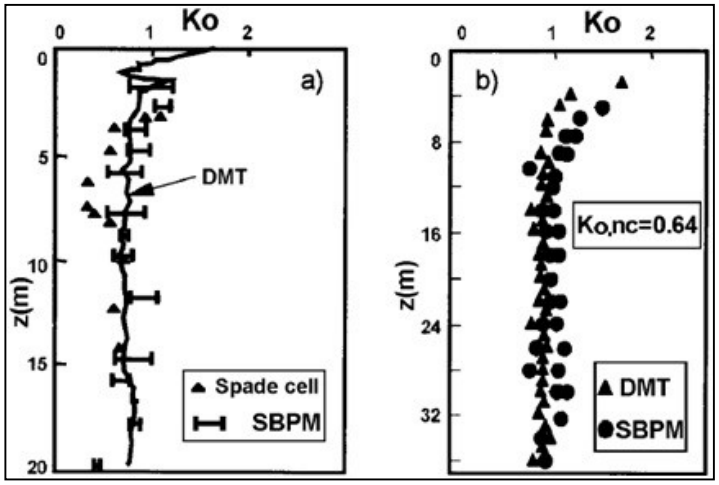

Figure: 2.17 Comparison of K_0 estimated from DMT tests with K_0 from other tests (Aversa and Evangelista 1993) (a) at Bothkennar (Nash et al. 1992) (b) at Fucino (Burghignoli et al. 1991)

The original correlation between over-consolidation ratio and K_D suggested by Marchetti (Marchetti 1980) (Equation 2.9). It was compared with a set of data by Kamei and Iwasaki (Kamei and Iwasaki 1995). Based on that study, an alternative relationship was suggested (Equation 2.17). It was also found that the correlation was remarkably similar to the Marchetti proposed equation. The illustrated plot is given in Figure 2.18.

$$\mathrm{OCR} = (0.47.\mathrm{K_D})^{1.43} \qquad (2.17)$$

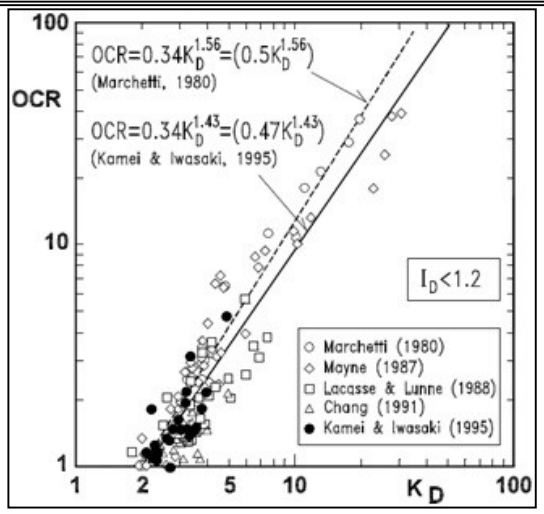

Figure: 2.18 Correlation of K_D and OCR for Cohesive Soils (Kamei and Iwasaki 1995)

Also, the relationship between K_D and OCR was confirmed by Finno on 1993 (Finno 1993) based on the comparison between field test results with a theoretical modeling. Which was based on three-dimensional strain path methods and anisotropic bounding space model suggested by Baligh et al. (Baligh and Scott 1975) on 1975. The illustrated graph is given in Figure 2.19.

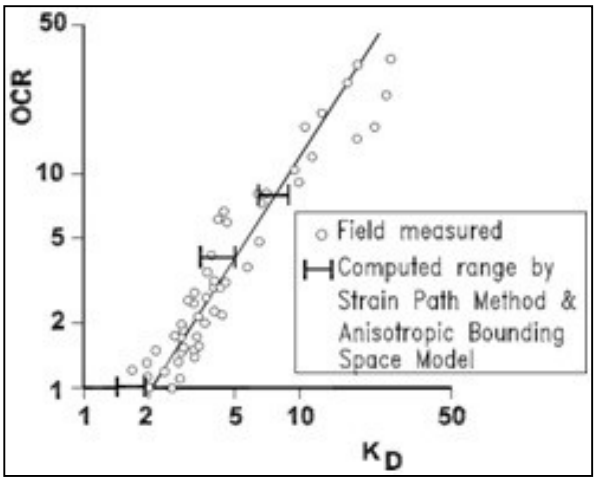

Figure: 2.19 K_D vs. OCR (Finno 1993)

2.1.5.3 VERITICAL DRAINED CONSTRAINED MODULUS (M)

The dilatometer modulus (E_D) was compared with the oedometer test results conducted for the UK test sites (Powell and Uglow 1986, 1988, 1989). It was found that there was an indication of linear relationship between the E_D and M. However, it had different gradients for different soil types as shown in Figure 2.20. Therefore, it revealed that the relationship between E_D and M depends on a factor $M = R_M.E_D$, depending upon the soil type. Which was suggested by Marchetti (Marchetti 1980).The factor, R_M, is not a constant. It depends on both the material index (I_D) and horizontal stress index (K_D). However, in this (Powell and Uglow 1988) study, the values of I_D and K_D (which was used for that study) were not mentioned. So, the Marchetti correlation was not compared fully.

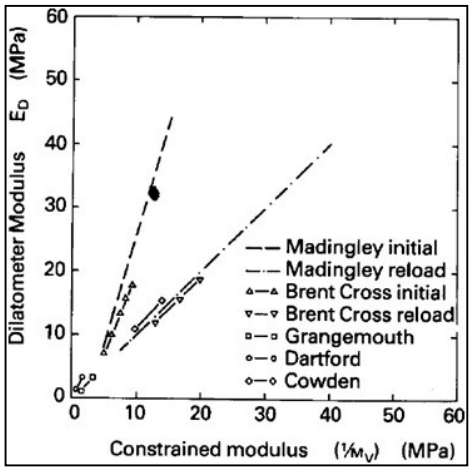

Figure: 2.20 Constrained Modulus ($1/m_v$) vs. Dilatometer Modulus (E_D)
(Powell and Uglow 1988, 1989)

On 1986 and 1991 two different studies were conducted on the constrained modulus obtained from oedometer test (i.e., $M_{oed} = 1/mv$) and Dilatometer for the soft clay at Norway (Lacasse 1986) and at Komatsugawa Japan (Iwasaki et al. 1991) respectively. The results from both the studies depicted a good

correlation. The results corresponding of those comparisons are given in Figure 2.21 and Figure 2.22.

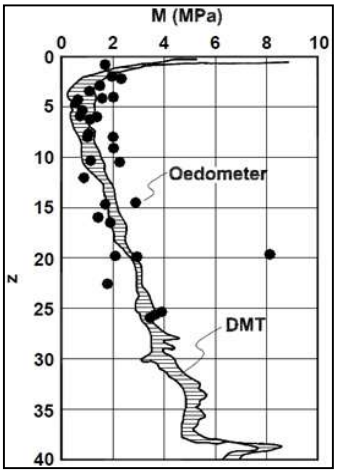

Figure: 2.21 Comparison between M determined from DMT and from Oedometer Test for Onsoy Clay, Norway (Lacasse 1986)

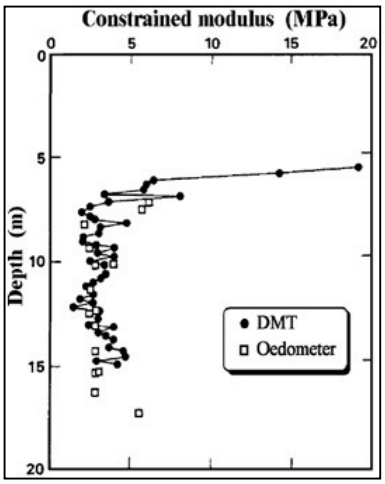

Figure: 2.22 Comparison between M determined from DMT and from oedometer test for Komatsugawa, Japan (Iwasaki et al. 1991)

In the year of1999, a study was conducted to compare the value of constrained modulus obtained from DMT with the oedometer test results for the alluvial soils and residual soils in Virginia, USA (Failmezger et al. 1999). The results depicted a good relationship as shown in Figure 2.23.

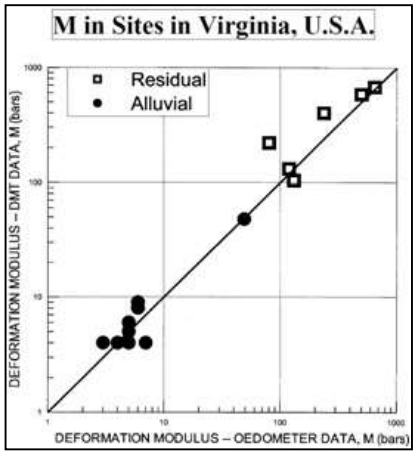

Figure: 2.23 Comparison of Oedometer results with DMT constrained modulus (Failmezger et al. 1999)

2.1.5.4 UNDRAINED SHEAR STRENGTH (C_u)

In 1998, research was undertaken by Powell & Uglow ((Powell and Uglow 1989) on UK soils. It was observed that a good correlation between horizontal stress index (K_D) and the ratio of shear strength (C_u) over effective overburden stress (σ_v') was exist (Figure 2.24). The original correlation proposed by Marchetti (1980) for C_u was plotted on the graph (Figure 2.24) and it had been observed that the data points were not so much scattered.

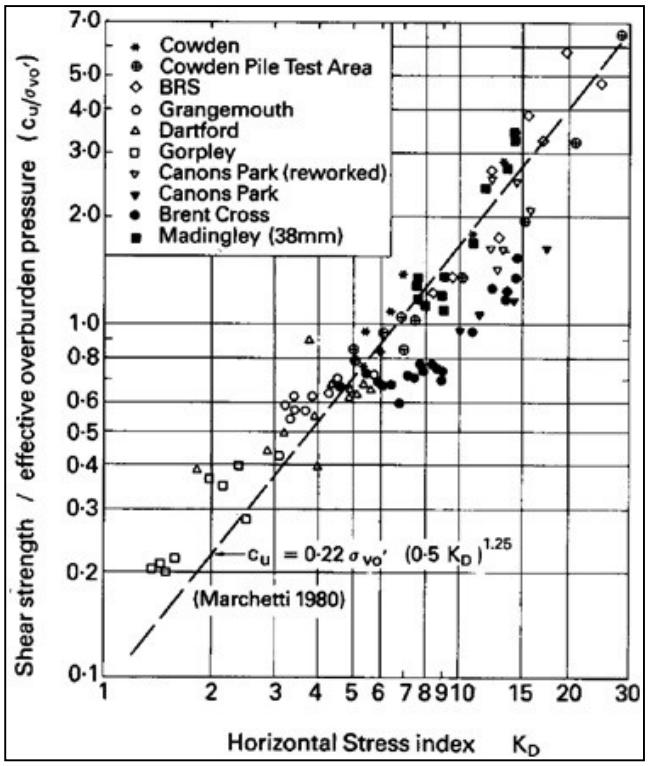

Figure: 2. 24 Shear Strength/effective Overburden Stress vs. K_D (Powell and Uglow 1988)

Apart from this study, several research programmes were undertaken to compare the DMT estimated C_u values with the values obtained from other laboratory and in-situ tests for various types of clay soils in different parts of the world. Some of these results are presented by graphically (Figure 2.25 - Figure 2.28). It was

observed that the DMT estimated C_u values were well tallied with the values obtained from the other tests.

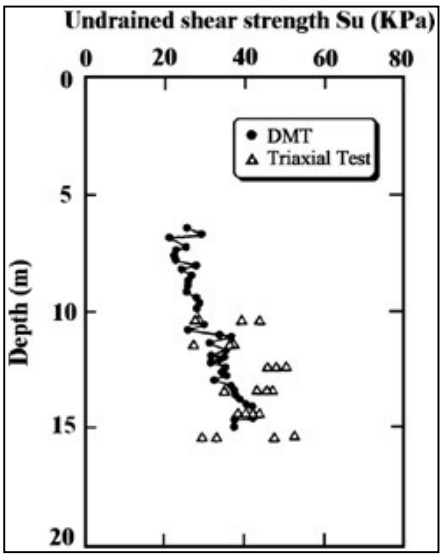

Figure: 2. 25 Comparison of undrained shear strength S_u for DMT and Triaxial (Iwasaki et al. 1991)

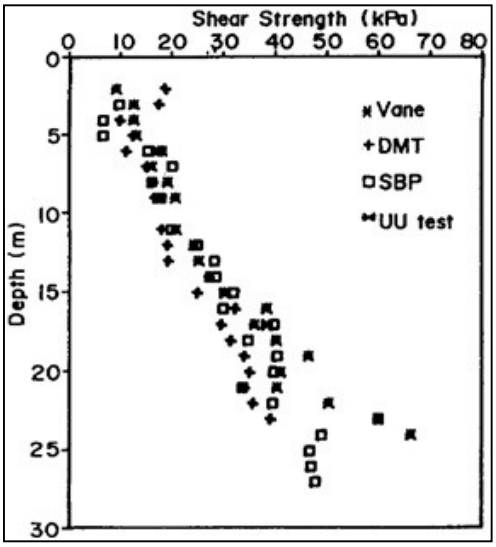

Figure: 2. 26 Comparison of shear strength assessed by Vane, DMT, SBP, UU test (Wong et al. 1993)

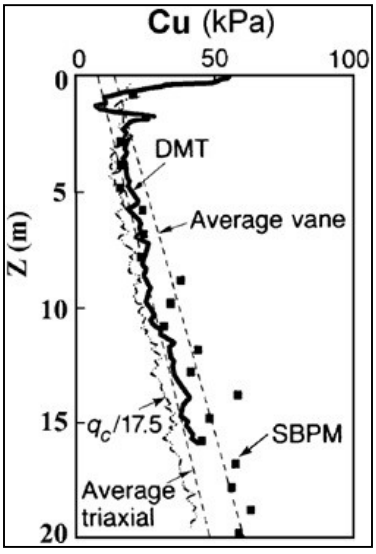

Figure: 2. 27 Comparison of undrained cohesion assessed by Vane, DMT, SBPM, Triaxial test (Nash et al. 1992)

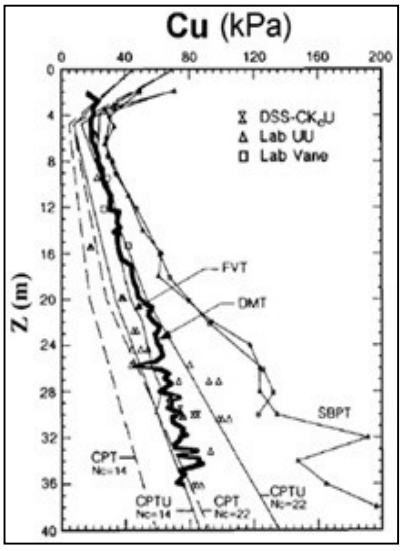

Figure: 2. 28 Comparison of undrained cohesion assessed by DSS-CK_0U, Lab UU, Lab Vane, DMT, SBPT, CPT_U, CPT test (Burghignoli et al. 1991)

A case study was made by Nandi et al. 2022 (Nandi et al. 2022), regarding the comparison of horizontal stress index (K_D) obtained from DMT test with the normalized cone resistance (Q_t) estimated from CPT test. In this regard, a correlation with good R^2 value, was found. In that study, the shear strength parameters (estimated from DMT, CPT, laboratory test and SPT test) were also compared with the shear strength parameters estimated from the predicted correlations. On that comparison, it was found that the assessment of the shear parameters depicted from the correlation was reasonably comparable with the other tests. The equations of the correlations are given below:

$$K_D = 1.475 * Q_t^{0.459} \quad (2.18)$$

$$C_u = [0.22 * \sigma'_{v0} * [0.5 * 1.475 * Q_t^{0.459}]^{1.25}] \quad (2.19)$$

2.1.5.5 DILATOMETER MODULUS (E_D) WITH SPT N VALUES

A standard correlation between SPT 'N' values with DMT estimated parameters has not been properly presented yet. On 1988, Schmertmann & Crapps (1988) (Schmertmann 1988a, c) stated that the prediction of SPT N value from dilatometer test might be misleading. However, some site-specific correlations were presented in the literature.

Mayne & Frost (Mayne and Frost 1988) proposed a correlation for sandy silts soils as shown in Figure 2.29. Another study was carried out by Tanaka et al. (Tanaka and Tanaka 1998) on three sandy soil sites in Japan. Based on this study, a relatively good correlation was found (Figure 2.30).

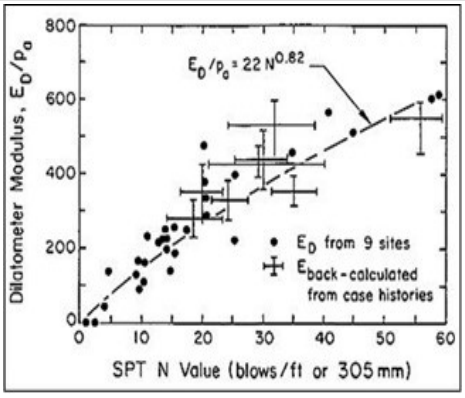

Figure: 2. 29 Correlation between E_D and SPT N value for Piedmont sandy silts (Mayne and Frost 1988) cited in (Kulhawy and Mayne 1990)

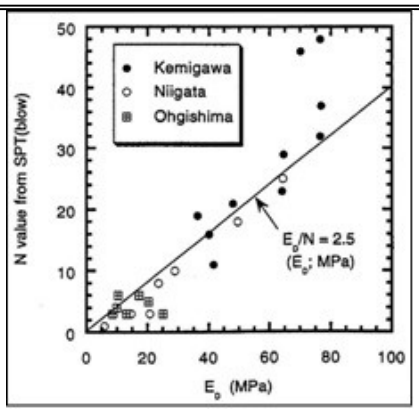

Figure: 2.30 Correlation between E_D and SPT N value for alluvial sands (Tanaka and Tanaka 1998)

2.1.5.6 DISCUSSION ON MARCHETTI (1980) CORRELATIONS

The original correlation was proposed by Marchetti (1980) based on the interpreted field test results for eight numbers of sites, which were mostly situated in Italy. However, in many cases, it was found that the original correlation (empirically predicted based on limited numbers of data) shows a good agreement for an extensive range of soil types in many parts of the world. In some cases, on cross-comparison research information's, it has been observed that the local variation of the original correlation may exist. Therefore, subsequent evaluation of new or improved relationships is required (e.g. (Powell and Uglow 1988, 1989), (Lacasse 1986, 1988; Lacasse and Lunne 1988) (Lunne et al. 1990b; Gabr et al. 1992)(Campanella and Robertson 1983, 1991; Greig et al. 1988).

On 1998, Mayne and Martin (Mayne and Martin 1998) tried to give a comprehensive review on the available correlations based on the comparative studies on DMT correlations. The exact method of interpretation of any soil parameters are dependent on various factors such as complexities of the blade penetration, stiffness of membrane, boundary and drainage conditions,

membrane inflation and deflation disturbance effects, rate of penetration effects etc. Therefore, the correlation for predicting the soil parameters, relies on empirical relationships and, thus it may differ for different soil types with different geology (Phoon and Kulhawy 1999).

Additionally, the computer software (i.e., SDMT Elab) used for analysing DMT test results, follows only standard Marchetti correlations, neglecting the local conditions. As such, for the design purpose, the use of these information should therefore, be taken considering the local soil type and its conditions. However, the Marchetti original correlations depict a useful initial approximation of sub-soil parameters, which can be assessed rapidly in economical manner. The results depicted from this test in absence of other tests, may be adopted for the design purpose depending on project concerned.

Lastly, for a specific project where the accurate measurements of the sub-soil properties are indispensable, the results from the DMT test should ideally be compared with other in-situ or laboratory test result. This helps confirm whether the original correlations will be applicable or if new one needs to be established.

2.2 CONE PENETRATION TEST (CPT)

2.2.1 BACKGROUND AND DEVELOPMENT OF THE CPT

On geotechnical engineering field a mechanical in-situ test namely Cone penetration test (CPT), was first introduced in 1930 at Netherlands (Vermeiden 1948; Schmertmann 1988a; Jamiolkowski et al. 1988; Baldi et al. 1989; Mayne and Bachus 1989; Danziger and Velloso 1995; Kaplan et al. 2004; Been et al. 2010; Presti and Meisina 2019; Bandyopadhyay et al. 2022). It was developed by using a 35mm diameter cone attached to smaller inner rod to a 35mm diameter hollow pipe as shown in Figure 2.31. Initially the test was carried out under quasi-static load for pushing the cone attached to the inner rod through outer hollow pipe (casing) at depth interval of 150mm (Campanella et al. 1983, 1985; Robertson and Campanella 1983a, b; Robertson 1986a; Robertson and Cabal 2015). The outer casing was then pushed down respect to the cone. Next, both the casing and the inner rod alongwith the cone, was pushed downward upto next test depth. This instrument was further improved by Vermeiden (Vermeiden 1948)(Holtrigter 2010), adding a conical part just above the cone to prevent entering of soil particles through the gap between the casing and the rods (Figure 2.32). On 1953, a significant modification (adding an 'adhesion jacket' behind the cone) of this instrument was made by Begemann (Begemann 1953). The test was named as 'Dutch cone test' (Figure 2.33) (Mayne and Bachus 1989; Holtrigter 2010; Robertson and Cabal 2015) . These two types of cone i.e., Begemann cone and Vermeiden cone are still regularly used in some parts of the world.

On further research, in 1965 an electric cone was designed by Fugro (de Ruiter 1971; Campanella et al. 1985). The main improvements compared to the mechanical cone penetrometers are listed below:

- Reducing frictional resistance between inner and outer rods and weight of inner rods to eliminate errors.
- To perform testing with a continuous rate of penetration by avoiding the adjustment of different parts of the penetrometer for unnecessary soil disturbance that may influence the cone resistance.
- Simplicity and reliability on the electrical measurement of cone resistance and sleeve friction.

Another add-on device was further introduced to predict pore water pressure by attaching with the Cone during the test (Campanella et al. 1983; Bihs et al. 2010), namely as piezocone (Senneset et al. 1989). By this device, the pore water pressure was predicted through a porous filter placed in the probe. The various piezocone was developed by placing the porous filter in different positions on the probe viz., u_1 position, u_2 position, u_3 position. In u_1 position porous filter is placed half-way up the cone. Besides, in u_2 position and u_3 position the porous filter is placed just behind the cone and in above to the friction sleeve respectively (Schmertmann 1988a; Kim et al. 1997). However, the most common and recommended position for placing porous filter is 'u_2' i.e., just behind the cone (Fonseca 2010) as shown in Figure 2.34.

Varying size of piezocones is available in the market as shown in Figure 2.34. However, the size of 10cm^2 is considered as the 'standard' for all type ground conditions. Although, sometime the piezocone of larger size (i.e., 15 cm^2) is used in hard ground condition (Robertson and Cabal 2015).

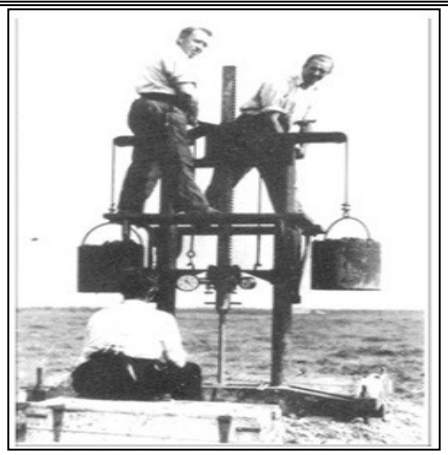

Figure: 2. 31 Early CPT rig in between 1930 to 1940 (Robertson and Cabal 2015)

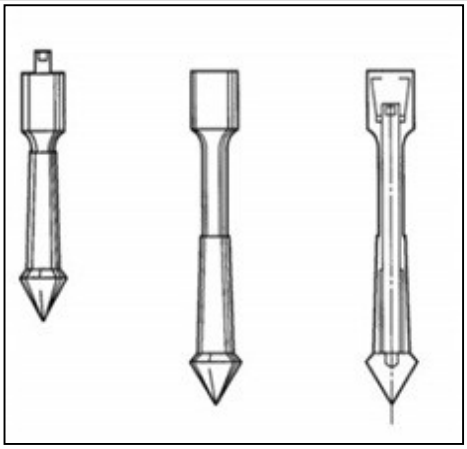

Figure: 2. 32 Schematic diagram of 'Vermeiden' cone (Robertson and Cabal 2015)

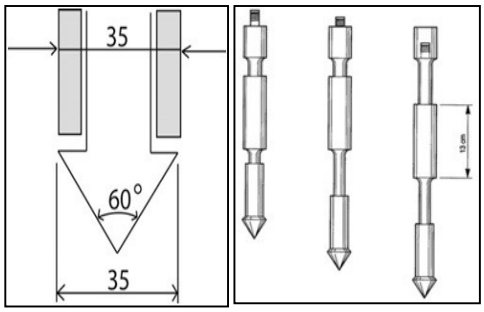

Figure: 2. 33 Schematic diagram of original 'Begeman' cone (Robertson and Cabal 2015)

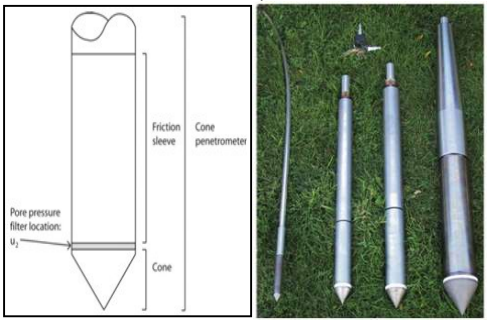

Figure: 2.34 Representative photographs of various Piezocone u_2 type (Robertson and Cabal 2015)

2.2.2 CPT TEST PROCEDURE AND BASIC RESULTS

The CPT probe is first attached to the extension rod then total assembly is pushed into the ground at a constant rate of (≈ 2cm/sec) (IS 4968 (Part-III) 1976; Schmertmann 1988a; ASTM Standard 2007; Fonseca 2010; Pagani Geotechnical Equipment (manual) 2014; Robertson and Cabal 2015). The digital load cell attached to the push rods produce continuous resistance (produce by the cone and sleeve) data which is reported as first reading (i.e., R_p during penetration of only the Cone), Second reading (R_p+R_L during the penetration of cone along-with the sleeve) and Third reading (R_T during penetration of total assembly of cone) (IS 4968 (Part-III) 1976; Schmertmann 1988a; ASTM Standard 2007; Pagani Geotechnical Equipment (manual) 2014; Robertson and Cabal 2015; Dagger et

al. 2018). Based on these three readings the cone resistance (q_t), sleeve friction (f_s) and total thrust (Q_T) are calculated (IS 4968 (Part-III) 1976; Pagani Geotechnical Equipment (manual) 2014; Robertson and Cabal 2015; Rocscience Inc. 2016). Also, dynamic pore pressure can be measured if the piezocone is used at site (Lunne et al. 1986; Robertson 1986b; Keaveny and Mitchell 1988; Mayne et al. 2000; ASTM Standard 2007; Robertson and Cabal 2015). The readings are to be recorded continuously on every 200 mm depth interval; in no case the depth interval should not be greater than 200mm (IS 4968 (Part-III) 1976; ASTM International 2000a; Pagani Geotechnical Equipment (manual) 2014; Robertson and Cabal 2015).

During the penetration of probe, the pore water pressure acts on the shoulder portion behind the cone and to the end portion of friction jacket. As a result, the equal distribution of pore pressure is affected, this phenomenon is often termed as the "unequal end area effect" (Campanella et al. 1983). This effect is presented as schematic diagram (Figure 2.35). This figure represents the key features for water pressure acting 'behind the cone' and to the 'end areas of the friction sleeve' (Lunne et al. 1986, 2002b) (Robertson and Cabal 2015) (Ahmadi and Robertson 2005). Thus, estimated q_c (mainly in soft clays and silts) is to be further corrected for pore water pressures i.e., corrected cone resistance q_t (Equation 2.20) (Mayne and Bachus 1989; Kulhawy and Mayne 1990; Mayne 2006a, 2007; Robertson and Cabal 2015; Rocscience Inc. 2016; Sakleshpur et al. 2022). However, in absence of pore water pressure measurement, the q_t will be equal to q_c (Rocscience Inc. 2016).

$$q_t = q_c + u_2 (1-a) \qquad 2.20$$

Here, 'a' (the net area ratio) is determined from laboratory calibration. The typical value ranges within 0.70 to 0.85. A similar correction is also to be applied to the sleeve friction as given in equation 2.21 (Robertson and Cabal 2015).

$$f_t = f_s - (u_2 \times A_{sb} - u_3 A_{st})/A_s \qquad 2.21$$

Where, f_s = measured sleeve friction (in absence of pore water pressure f_t=f_s), u_2 = water pressure at base of sleeve, u_3 = water pressure at top of sleeve, A_s = surface area of sleeve, A_{sb} = cross-section area of sleeve at base, A_{st} = cross-sectional area of sleeve at top

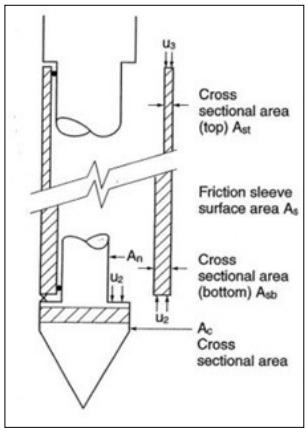

Figure: 2.35 Schematic diagram of cone geometry (Robertson and Cabal 2015)

For this test, the soil parameters are predicted from the three basic results (i.e., q_c or q_t, f_s and R_f) and thus the variation of these tests results with the depth are reported (R_f is the friction ratio that is equal to f_s/q_t) (IS 4968 (Part-III) 1976; Lacasse 1986; Schmertmann 1988a; Kulhawy and Mayne 1990; Mayne and Rix 1995; ASTM Standard 2007; Coutinho and Mayne 2012; Pagani Geotechnical Equipment (manual) 2014; Robertson and Cabal 2015; Rocscience Inc. 2016).

2.2.3 CPT DATA INTERPRETATION

2.2.3.1 SOIL BEHAVIOUR TYPE INDEX (I_C)

The cone penetration test may be used to identify the sub-soil profile in terms of soil type (Aas et al., 1986;(Robertson and Campanella 1983b, a; Aas 1986; Robertson 1990, 2009; Bowles 2001; Lunne et al. 2002b; Akca 2003; Salgado 2006; Fonseca 2010; Robertson and Cabal 2010, 2015; Rocscience Inc. 2016; Das 2019; Bandyopadhyay et al. 2020, 2022; Sakleshpur et al. 2022; Nandi et al. 2022). In this regard, it had been observed that the cone resistance, (q_c) is in higher side for sandy type soil and comparatively low for clayey soils (Robertson 1990; Ahmadi and Robertson 2005). Besides, the friction ratio (R_f) falls in lower side for sands and higher side in clays (Campanella et al. 1983; Robertson and Campanella 1983b, a; Robertson 1986b, a, 1990, 2009; Lunne et al. 2002b; Ahmadi and Robertson 2005; Robertson and Cabal 2010, 2015). However, it is not expected to get the accurate predictions of soil type based on CPT test in terms of physical characteristics (Robertson and Campanella 1983b, a; Robertson 1990; Lunne et al. 2002b; Robertson and Cabal 2010, 2015). However, it can provide a guideline about the mechanical characteristics (such as strength, stiffness etc.) of the sub-soil in terms of 'soil behavior type' (SBT) index (Robertson and Campanella 1983a; Robertson 1990; Lunne et al. 2002b; Robertson and Cabal 2010, 2015). Within the portion of the probe, the sub-soil behavior can be predicted based on the estimated value of SBT (Robertson and Campanella 1983a; Lunne et al. 2002b; Robertson and Cabal 2010, 2015). The prediction of sub-soil type based on CPT test results is termed as 'Soil Behavior Type' index (I_C) (Robertson and Campanella 1983a; Robertson 1986a, 1990; Lunne et al. 2002b; Robertson and Cabal 2010, 2015; Rocscience Inc. 2016).

A chart for the soil classification based on the I_C, was prepared by Robertson in the year of 1986 (Robertson and Campanella 1983b, a; Robertson 1986a, 1990; Schmertmann 1988a; Lunne et al. 2002b; Schnaid 2008).This chart was further modified by Robertson on 1990 (Figure 2.38) based on normalized CPT test results (Robertson 1990; Lunne 1997; Rocscience Inc. 2016) (Equation 2.21 - 2.22).

$$Q_t = (q_t - \sigma_{v0})/\sigma'_{v0} \quad (2.21)$$

$$F_r = [f_s/(q_t - \sigma_{v0})] \quad (2.22)$$

Where, Q_t = Normalized cone resistance, F_r= Normalized friction ratio, σ_{vo}= in-situ total vertical stress, σ'_{vo} = in-situ effective vertical stress

To determine the in-situ vertical overburden stress, bulk density of the sub-soil is required. Therefore, a chart was suggested Lunne, T in the year 1997 (Lunne 1997; Lunne et al. 2002b). This was suggested according to the value of I_C initially proposed by Robertson et al. 1986 (Robertson 1986a, 1990) (Figure 2.36 and 2.37). Besides in 2010, based on the experimental data Robertson and Cabal proposed another chart (Robertson and Cabal 2010, 2015) alongwith the general equation (Equation 2.23) to estimate approximate soil unit weight (unit weight).

Soil Behaviour Type (SBT)*	Approximate unit weight, γ (kN/m³)
1	17.5
2	12.5
3	17.5
4	18.0
5	18.0
6	18.0
7	18.5
8	19.0
9	19.5
10	20.0
11	20.5
12	19.0

*SBT based on charts by Robertson et al., (1986)

Figure: 2.36 Approximate soil unit weight (Robertson 1990)

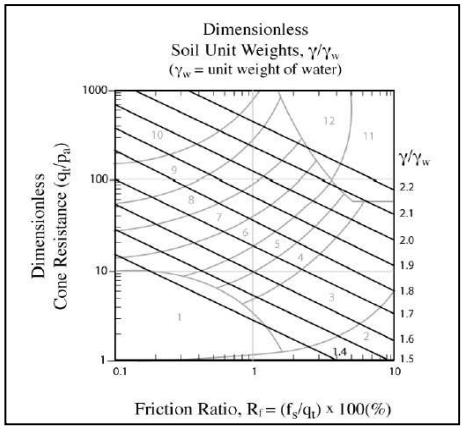

Figure: 2.37 Approximate soil unit weight (Lunne et al. 2002b)

$$\gamma/\gamma_w = [0.27 \times [\log R_f] + 0.36 \times [\log(q_t/p_a)] + 1.236] \times G_s/2.65 \quad (2.23)$$

Where, γ = in-situ unit weight of soil, γ_w= unit weight of water, R_f= friction ratio = (f_s/q_t) 100 %, p_a = atmospheric pressure in same units as q_t, G_s= The average specific gravity of soil (ranges between 2.6-2.7).

Another chart was proposed by Robertson (1990) (Robertson 1990; Lunne et al. 2002b; Robertson and Cabal 2010, 2015) after incorporating the pore pressure ratio (B_q) for eliminating the major errors on the measurements of sleeve friction. However, it was recommended to use of Q_t – F_r chart to predict the sub soil behavior (Robertson 1990; da Fonseca and Mayne 2004; Mayne 2006d; Robertson and Cabal 2010, 2015; Dagger et al. 2018) (Figure 2.38).

On the other hand, in the year 1993 Jefferies and Davies (Jefferies and Davies 1993) proposed an index related to the "Soil Behaviour Type" index (I_C). The definition of this index (I_C) was further modified by Robertson and Wride on 1998 ((Fear) Wride et al. 2000; Robertson et al. 2000; Holtrigter 2010; Rocscience Inc. 2016). The relationship of I_C with Q_t and F_r is given in below (Equation 2.24).

$$I_c = [(3.47 - \log Q_t)^2 + (\log F_r + 1.22)^2]^{0.5} \quad (2.24)$$

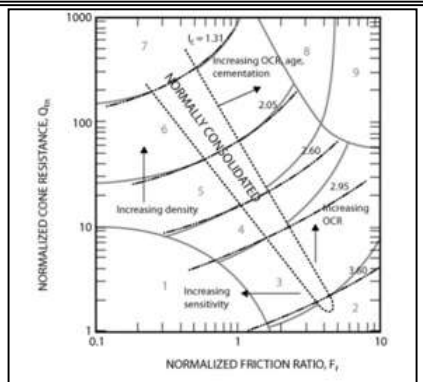

Zone	Soil Behavior Type	I_c
1	*Sensitive, fine grained*	N/A
2	*Organic soils – clay*	> 3.6
3	*Clays – silty clay to clay*	2.95 – 3.6
4	*Silt mixtures – clayey silt to silty clay*	2.60 – 2.95
5	*Sand mixtures – silty sand to sandy silt*	2.05 – 2.6
6	*Sands – clean sand to silty sand*	1.31 – 2.05
7	*Gravelly sand to dense sand*	< 1.31
8	*Very stiff sand to clayey sand**	N/A
9	*Very stiff, fine grained**	N/A

** Heavily overconsolidated or cemented*

Figure: 2. 38 Normalized soil behavior type chart (Robertson and Cabal 2015)

2.2.3.2 UNDRAINED SHEAR STRENGTH (C_u)

On the basis of classical bearing capacity theory (Equation 2.25) (Terzaghi 1943; Terzaghi et al. 1996; Bowles 2001), several theoretical and empirical correlations were reported in the literature (De Beer 1965; Nayak 1979, 2001; Leonards and Frost 1988; Kulhawy and Mayne 1990; Peck et al. 1991; Chang et al. 1999; Bowles 2001; Lunne et al. 2002b; Sargand et al. 2003; Karlsrud et al. 2005; Salgado 2006; Robertson and Cabal 2010, 2015; Das and Sivakugan 2018; Presti and Meisina 2019; Briaud 2019b; Sakleshpur et al. 2022), such that:

$$q_c = N_c . C_u + \sigma_{v0} \quad (2.25)$$

Where, C_u = undrained shear strength; N_c = bearing capacity factor (considered as cone factor, N_{kt}). Besides, the undrained shear strength was calculated by rearranging the Equation 2.25 (Senneset et al. 1982; Robertson and Cabal 2010;

Meigh 2013; Feda Aral and Gunes 2017; Dagger et al. 2018; Rindertsma et al. 2018) as given below (Equation 2.26):

$$C_u = (q_t - \sigma_{v0})/N_{kt} \quad (2.26)$$

Where N_{kt} = cone factor.

On 1987 (Teh and Houlsby 1991), a theoretical solution was developed for estimating the value of N_{kt} based on the strain path theory proposed by Baligh (Baligh 1985) (Figure 2.39). In this figure, it is observed that the cone penetration resistance is very much influenced by undrained shear strength (i.e., S_u), in-situ stress condition (i.e., σ'_{vo}, K_0), rigidity factor (I_r) and the roughness coefficient of cone (denoted as α).

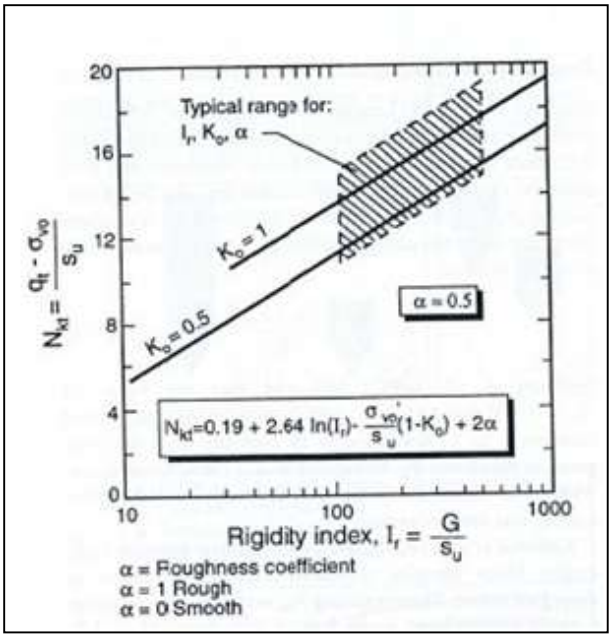

Figure: 2. 39 Theoretical Solution for N_{kt} (Teh and Houlsby 1991)

The mechanism of cone penetration is a complex and depends on several factors. As various factors are need to be considered, only theoretical approach (based on the assumptions), does not provide a complete solution, Therefore, empirical

correlations are always prioritized over the basic theoretical framework for establishing the empirical relationships (Lunne et al. 1990a, 2002b).

An experimental correlation for the cone factor (N_{kt}) was proposed based on the wide lab and field tests results, typically ranging between 10 to 18. However, an average value (i.e., 14) was suggested by Robertson and Cabal (Robertson and Cabal 2010, 2015).

In the year of 1986, it was evidential that the value of cone factor (N_{kt}) leans to increase with the increasing value of plasticity index (I_P) (Aas 1986; Holtrigter 2010). Besides, it was found that the value decreases with the increasing value of soil sensitivity (Aas 1986; Holtrigter 2010) (Figure 2.40).

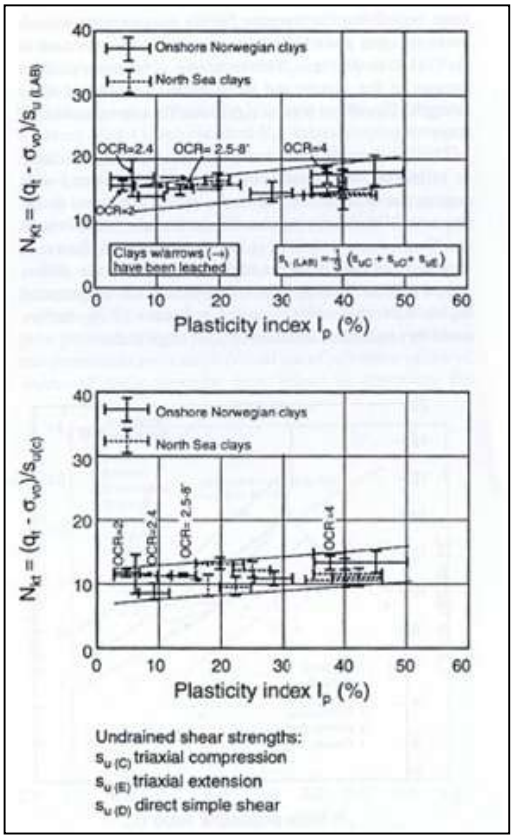

Figure: 2. 40 Variation of Cone Factor with Plasticity index and soil sensitivity (Aas 1986; Holtrigter 2010)

It was also observed that the value of N_{kt} varies with the pore pressure ratio (i.e., B_q) in which the value of N_{kt} decreases with the increasing of pore pressure ratio (Lunne et al. 1986, 2002b; Greig et al. 1988; Mayne and Bachus 1989; Lunne 1997; Karlsrud et al. 2005). The lowest value of N_{kt} (i.e., $N_{kt} = 6$) was observed at the pore pressure ratio 1.0 (i.e., $B_q \approx 1.0$). Further, it was noticed that the estimation of undrained shear strength (C_u) for very soft soil may be inaccurate due to the uncertainty of cone resistance value (q_t) (Schmertmann 1988a; Robertson and Cabal 2015; Dagger et al. 2018). In this regard, alternate method was proposed to predict C_u. This method was based on the measurement of excess porewater pressure (Kulhawy and Mayne 1990; Lunne 1997; Robertson and Cabal 2015) (Equation 2.27).

$$C_u = \Delta_u / N_{\Delta u} \tag{2.27}$$

Δ_u is excess pore pressure (i.e., u_2-u_0) and $N_{\Delta u}$ is the cone factor for excess pore pressure

Based on cavity expansion theory, it was found that the variation of $N_{\Delta u}$ ranged between 2 to 20, whereas, the variation was found to be 4 to10 considering the factor B_q (Lunne 1997; Holtrigter 2010; Robertson and Cabal 2015; Dagger et al. 2018) , the correlation is given below (Equation 2.28).

$$N_{\Delta u} = B_q N_{kt} \tag{2.28}$$

Where The factor 'Bq' is pore pressure ratio, as determined by the ratio of $(u_2 - u_0)/(q_t - \sigma_{v0})$; u_o is in-situ equilibrium pore water pressure

2.2.3.3 K_0 AND OCR

In general, the relationship between the undrained shear strength ratio (C_u/σ_v') for normally consolidated clay and over consolidated clay depends on the 'over

consolidation ratio (OCR)' as mentioned below (Equation 2.29) (Marchetti 1980; Schmertmann 1983; Boghrat 1987; Chang 1991a; Robertson et al. 2000; Lunne et al. 2002b):

$$(C_u/\sigma_v^{'})_{OC} = (C_u/\sigma_v^{'})_{NC} OCR^m \quad (2.29)$$

In this relationship it was assumed that the undrained shear strength ratio i.e $(C_u/\sigma_v^{'})$ for over consolidated (OC) condition may be obtained by factored up (i.e., OCR^m) ratio for normally consolidated (NC) state. In this equation the value of "m" was considered as 0.8 (Ladd et al. 1977; Powell and Uglow 1986; Boghrat 1987; Chang et al. 1999).

However, another relationship (based on the critical state theory), of the undrained shear strength ratio was proposed by (Robertson 2009; Robertson and Cabal 2010) (Equation 2.30). In this relationship, the undrained shear strength ratio for normally consolidated soil i.e. $(C_u/\sigma_v')_{NC}$ was evaluated under different loading condition.

$$(C_u/\sigma_v')_{NC} = 0.22 \quad (2.30)$$

Besides, Equation 2.25 may be rearranged and the ratio 'C_u/σ_v' may be written as given below (Equation 2.31).

$$(C_u/\sigma_{vo}^{'}) = [(q_t - \sigma_{vo}')/N_{kt}]/\sigma_{vo}' = Q_t/N_{kt} \quad (2.31)$$

Combining these three equations i.e. (Equation 2.29) (Equation 2.30) and (Equation 2.31), over consolidation ratio (OCR) was proposed by Robertson (Equation 2.32) (Robertson 2009).

$$OCR = 0.25 \times (Q_t^{1.25}) \quad (2.32)$$

In the year 1990, Kulhawy and Mayne (Mayne and Kulhawy 1990) also proposed alternate equation to predict the OCR as given in Equation 2.33

$$OCR = k \times Q_t \quad (2.33)$$

However, the above equation was valid for $Q_t < 20$. Furthermore, the value of 'k' ranged between 0.2 to 0.5 with an average of 0.3.

Anderson et al. 1979 (cited by (Holtrigter 2010)) suggested a chart (Figure 2.41) for direct measurement of K_0 and OCR values corresponding to the plasticity index (I_P) and undrained shear strength ratio (C_u/σ'_v). After that on 1990, Mayne and Kulhawy (Mayne and Kulhawy 1990) suggested a simple approach to determine the value of K_0 (Equation 2.34).

$$K_0 = 0.1 \times Q_t \quad (2.34)$$

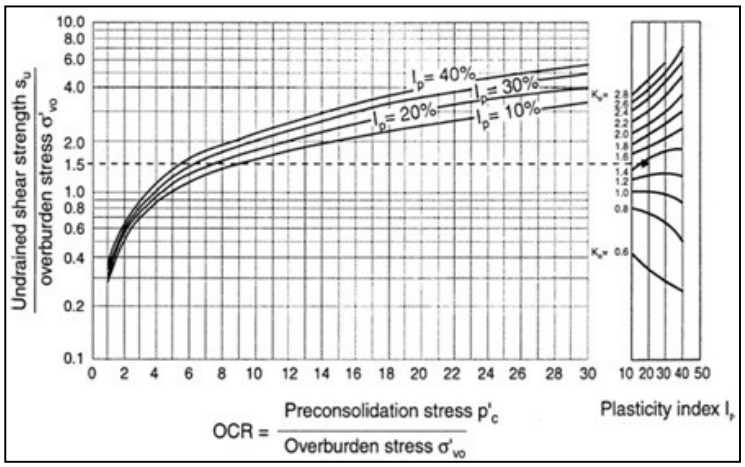

Figure: 2. 41 OCR and K_0 from s_u/σ'_{vo} and Ip proposed by Anderson et al. 1979 cited by (Holtrigter 2010)

2.2.3.4 CONSTRAINED MODULUS (M_{CPT})

Vertical drained constrained modulus, (M_{CPT}) can be predicted by using the cone resistance value (i.e., q_t) obtained from the CPT test. The relationship of

constrained modulus was first established by Senneset et al. in 1982 (Senneset et al. 1982, 1989). The original relationship is given in Equation 2.35

$$M = \alpha_M(q_t - \sigma_{v0}) \quad (2.35)$$

Where, α_M= empirically derived dimensionless factor

The value of the empirical factor (α_M) varies between 4 and 8 (Senneset et al. 1982, 1989). In previous research was conducted on 1972 (Holtrigter 2010; Sanglerat 2012). In that study, it was suggested that the value of the factor α_M depends on the type of soil, natural moisture content and cone resistance for fine grained soils. The detailed range is summarised below (Table 2.3).

Table: 2. 3 Range of α_M or values proposed by Sanglerat, 1972 (Sanglerat 2012)

Soil Type	Cone tip resistance (q_c) (MPa)	α_M value
Clay of low plasticity (CL)	$q_c < 0.7$	3 - 8
	$0.7 < q_c < 2.0$	2 – 5
	$q_c > 2.0$	1 –2.5
Silts of low plasticity (ML)	$q_c > 2.0$	3 – 6
	$q_c < 2.0$	1 – 3
Highly plastic silts and clay (MH,CH)	$q_c < 2.0$	2 – 6
Organic silts (OL)	$q_c < 1.2$	2 – 8
Peat and organic clay(Pt, OH)	$q_c < 0.7$	0.4 – 4 (depending onwater content)

In 1987, another study was conducted and it was suggested the range of α_M in between 2 to 8 (Meigh 2013).

In 1990, Mayne (Mayne and Kulhawy 1990) suggested a general correlation (Figure 2.42) between constrained modulus and cone resistance based on the twelve number of different sites.

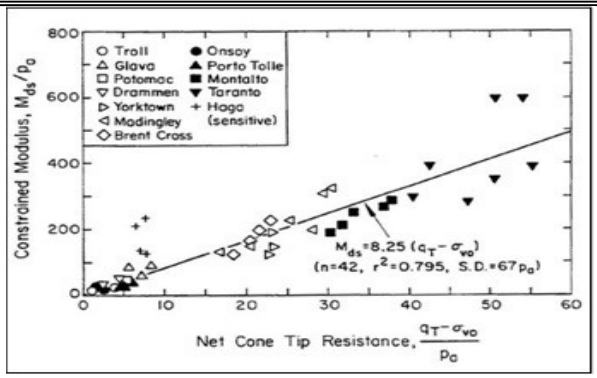

Figure: 2. 42 Correlation between constrained modulus and cone resistance (Mayne and Kulhawy 1990)

Further, in 2001 Mayne (2001) (Mayne 2001); (Rocscience Inc. 2016) proposed a general value of 8, whereas, Kulhawy and Mayne (Kulhawy and Mayne 1990) proposed a generalised value of 8.25. In 2009; Robertson suggested that the value of α_M varies with Q_t and I_C (Robertson 1990). So, When Ic> 2.2 α_M will be Q_t, (for Q_t<14) and α_M =14 (for Qt>14). Besides, for Ic< 2.2, α_M will be $0.0188*[10^{(0.55Ic + 1.68)}]$.

In 2004, Kaplan (Kaplan et al. 2004; Holtrigter 2010; Üzeler 2013) suggested a relationship (Figure 2.43) between the cone resistance with the factor α based on the results with laboratory test data obtained from two different clay sites.

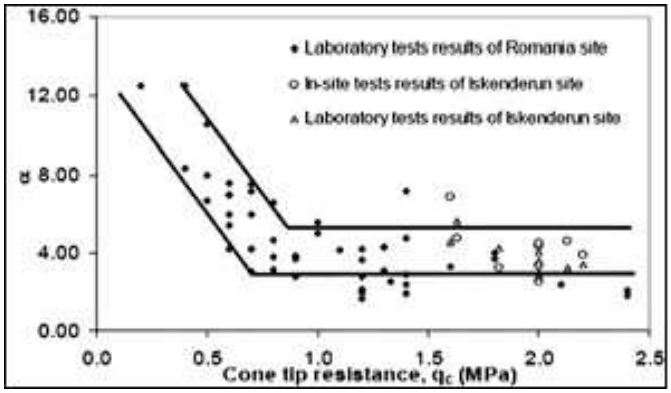

Figure: 2. 43 Tip resistance and factor α (Holtrigter 2010)

In 1997, Lunne (Lunne 1997) suggested that the total stress predicted from CPT test is based on the undrained measurements. Hence, it is difficult to establish a correlation with the drained parameters of soil without measuring the pore pressure variation during the CPT test. Therefore, these methods are used only for the rough estimate of soil compressibility characteristic (Lunne et al. 2002b). Furthermore, the estimation of drained behavior of sub-soil (i.e., $1/m_v$ or M) from cone resistance (without measuring of pore pressure) may portray erratic results (Ahmadi and Robertson 2005; Robertson and Cabal 2015).

2.2.3.5 ANGLE OF INTERNAL FRICTION (Φ)

The angle of internal friction may be determined from the cone resistance. Several research works were carried out to find out the effective shear strength parameters for coarse- and fine-grained soil. On 1972, Muromachi (Motaghedi and Eslami 2013; Mohammadi and Eslami 2016) assumed the slip surface produced during the insertion of cone resembled a logarithmic spiral. As such, the following correlation (Equation 2.36) was suggested for cohesionless soils (Motaghedi and Eslami 2013; Mohammadi and Eslami 2016):

$$q_c = 3/2 p_0 \cos\phi . e^{(2\pi\tan\phi - 1)} \quad (2.36)$$

Where, P_0 is effective overburden stress,

In the year 1974, Meyerhof (Meyerhof 1974; Motaghedi and Eslami 2013; Mohammadi and Eslami 2016) proposed another equation to determine friction angle (ϕ) for cohesionless soil based on the cone resistance and bearing capacity factor (Equation 2.37).

$$\phi = \tan^{-1}\left(\frac{q_c}{0.5 \times N_q}\right) \quad (2.37)$$

Where, Nq is the bearing capacity factor.

In the year 1983, Mitchell and Durgunoglu (Yu 2004; Holtrigter 2010; Motaghedi and Eslami 2013) proposed a chart of varying angle of internal friction (ϕ), with different value of q_c and effective overburden pressure (Figure 2.44).

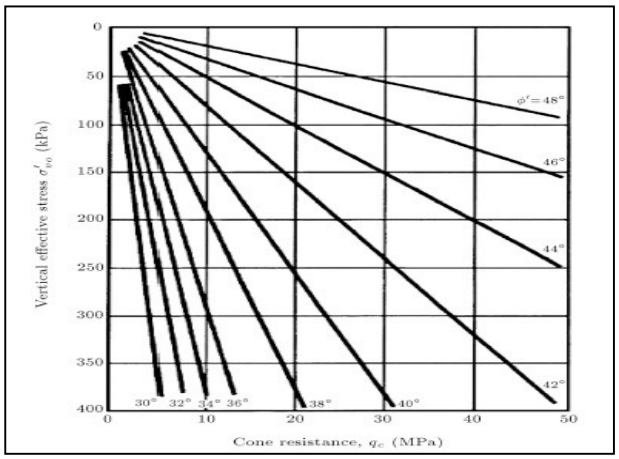

Figure: 2. 44 Friction angle varies with cone resistance (Holtrigter 2010; Motaghedi and Eslami 2013)

In the same year, a correlation was established by Robertson (Robertson and Campanella 1983b). They suggested that the angle of internal friction for sandy soil on drained condition depends on the cone resistance and effective overburden pressure (Equation 2.38).

$$\phi = \tan^{-1} \times [0.1 + 0.38 \log \left(\frac{q_c}{\sigma'_{v0}}\right)] \quad (2.38)$$

2.2.3.6 CPT CORRELATIONS

Among various in-situ tests, the Standard Penetration Test (SPT) is one of the common test which are used in many parts of the world. Standard Blow counts (SPT N) are commonly used to estimate various parameters such as shear strength, compressibility characteristics, shear wave velocity, along with

settlement analysis, liquefaction assessment etc. (Hasancebi and Ulusay 2007; Shiuly et al. 2018; Shiuly and Roy 2018). Also, it is well established and commonly used test in geotechnical field to characterize the sub-soil in terms of consistency (Terzaghi 1943; Terzaghi et al. 1996; Bowles 2001). Also, many design methods based on local SPT correlations are established by many geotechnical engineers. As such, when CPT test came into the geotechnical engineering field, initially it was intended to observe the CPT test results in the form of equivalent SPT N values (Terzaghi 1943; Terzaghi et al. 1996; Bowles 2001). In CPT test, cone penetration resistance (q_c) indirectly resembles the resistance imparted by the sub-soil (Akca 2003; Robertson and Cabal 2010, 2015). Intrinsically, the consistency of sub soil can also be predicted from CPT test (Terzaghi 1943; D. B. Campbell 1972; Bowles 2001; Lunne et al. 2002b). Initially Robertson et al. (1983) (Robertson and Campanella 1983a, b; Robertson 1986a) presented in a unique relation between the ratio of $(qc/pa)/N_{60}$ with mean grain size, D50 (varying between 0.001mm to 1mm) (Figure 2.45). Where, the 'pa' is atmospheric pressure with the same units as 'qc', and 'N_{60}' is the SPT N value corresponding to the 60% energy ratio. Based on CPT-SPT correlation, Robertson (Robertson 1986a) proposed the ratio of $(qc/pa)/N_{60}$ for different the soil type (by virtue of soil behavior type, I_C), Table 2.4.

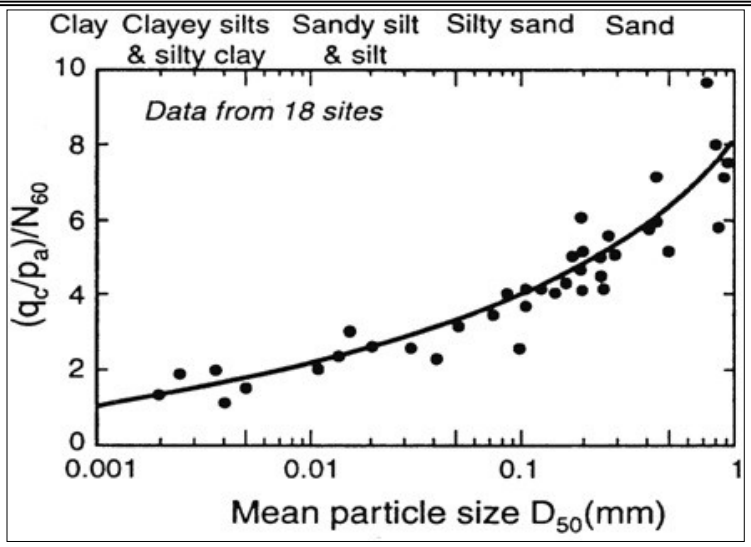

Figure: 2. 45 CPT-SPT correlation with D_{50} (Roberson et al. 1983)

Table: 2. 4 Range of $(q_c/p_a)/N_{60}$ ratio with SBT values (Robertson 1986a, 1990)

Zone	Soil Behavior Type (SBT)	$(q_c/p_a)/N_{60}$
1	Sensitive fine grained	2.0
2	Organic soils – clay	1.0
3	Clays: clay to silty clay	1.5
4	Silt mixtures: clayey silt & silty clay	2.0
5	Sand mixtures: silty sand to sandy silt	3.0
6	Sands: clean sands to silty sands	5.0
7	Dense sand to gravelly sand	6.0
8	Very stiff sand to clayey sand*	5.0
9	Very stiff fine-grained*	1.0

Later, in 1993, Jefferies and Davies (Jefferies and Davies 1993) suggested a correlation of CPT-SPT with respect to the soil behavior type index (I_C). The proposed correlation is given in Equation 2.39.

$$\frac{(q_t/p_a)}{N_{60}} = 8.5 \times \left(1 - \frac{I_c}{4.6}\right) \quad (2.39)$$

Further, the above correlation was updated by Robertson in the year 2012 to estimate the equivalent N_{60} values for insensitive clay (Robertson and Cabal 2015; Robertson 2016) (Equation 2.40).

$$\frac{(q_t/p_a)}{N_{60}} = 10^{(1.1268 - 0.2817 I_C)} \quad (2.40)$$

There also some correlations between SPT N and q_c, were suggested by many authors (Bowles 2001) (Danziger and Velloso 1995; Kara and Gündüz 2010; Onal and Özmen 2015; Costa et al. 2016; Feda Aral and Gunes 2017; Firuzi et al. 2019; Arifuzzaman and Anisuzzaman 2022; Moghadari Poor et al. 2023) for different soil types which is summarised in Table 2.5.

Table: 2. 5 Earlier established correlations for silty clay/ clayey silt soil

Author(s)	Soil Types	Relationship
De Alencar Velloso D.,1959	Clay and silty clay	$(q_c/ P_a)/N = 0.035$
FrankiPiles,1960	Silty clay	$(q_c/ P_a)/N = 0.030$
FrankiPiles,1960	Clays	$(q_c/ P_a)/N = 0.020$
Chang.,1988	Clayey silt, sandy clayey silt	$(q_c/ P_a)/N = 1.80$
Danzigeret al.,1998	Clayey silt	$(q_c/ P_a)/N = 3.1$
Danzigeret al.,1998	Clay	$(q_c/ P_a)/N = 4.5$
Atmospheric pressure (P_a) = 0.1 MPa, N is denoted for observed SPT N		

It is to be noted that, the earlier correlations are very much site specific or region based. As cone penetration test is rarely used in Indian condition (Bandyopadhyay et al. 2020, 2022; Nandi et al. 2022; Das et al. 2022), there is no specific correlation between qc with SPT N for the cohesive (silty clay/clayey silt) soil for this region for existing SPT-based design approach.

2.3 PRESSURE METER TEST (PMT)

2.3.1 BACKGROUND AND DESCRIPTION OF THE PMT TEST APPARATUS

Pressuremeter apparatus was developed by Louis Menard in 1954 in France based on the concept of Kogler in 1953 (Winter 1986). Later on, this test has become one of the popular and fundamental in-situ test in geotechnical investigation field (Cestari Ferrucio 2012). The basic idea of the pressuremeter test is the expansion of a cylindrical cavity in order to measure a relationship

between pressure and deformation of the sub-soil soil (Baguelin et al. 1978). In practice, the cavity formation is done by drilling a bore hole upto the desired test depth. Then probe is inserted into the borehole and inflated by using of gas pressure. During this expansion corresponding volume change is recorded (Clarke 1996). The probe is designed such a manner that during the radial expansion of the hole, length will not be changed (Baguelin et al. 1978; Hughes and Robertson 1985).Therefore, the increase of volume is only due to the radial expansion of the borehole (Baguelin et al. 1978).

At the initial period when the pressuremeter was introduced in the geotechnical investigation, the evaluation method (described by Menard) was mostly unknown (Hughes et al. 1977; Briaud and Jordan 1983; Winter 1986). The question arose whether the Menard's theory would suffice for the design or further research would be required for local subsoil condition and make necessary adjustments based on conventional test results (Baguelin et al. 1978). After more than 20 years of research work, based on large number of test results for particular geologic formations, it was established that the disturbance during installation and also the formation of borehole had significant effect on the test results (Baguelin et al. 1978; Amar et al. 1991; Clarke 1996; Briaud J.L 2013).

The apparatus consist of three components viz., 'probe', 'the control unit' and the 'coaxial tube' (Figure 2.46).

a. Probe: The original 'Menard' type pressuremeter probe consist of three different cells viz., Measuring Cell", top "Guard Cell" and bottom "Guard Cell" (Baguelin et al. 1978; Singh 1981; Nandi et al. 2024)., Measuring cell is placed in the middle portion of the probe. Measuring cell is covered with a flexible rubber membrane and is filled with water

during the test. Prior to the starting of the test, guard cells are filled with gas, in order to protect the membrane of measuring cell.

b. Control unit: control unit (or measuring unit) is placed on the ground near to the borehole. It contains a pressure gauge and a gate valve. It is used for both measuring the volume change of measuring cell and controlling the gas pressure applied to the probe.

c. Coaxial tube: A coaxial tube is used to connect the probe with measuring/ control unit. Main function of this tube to supply gas and water from the control unit to the probe.

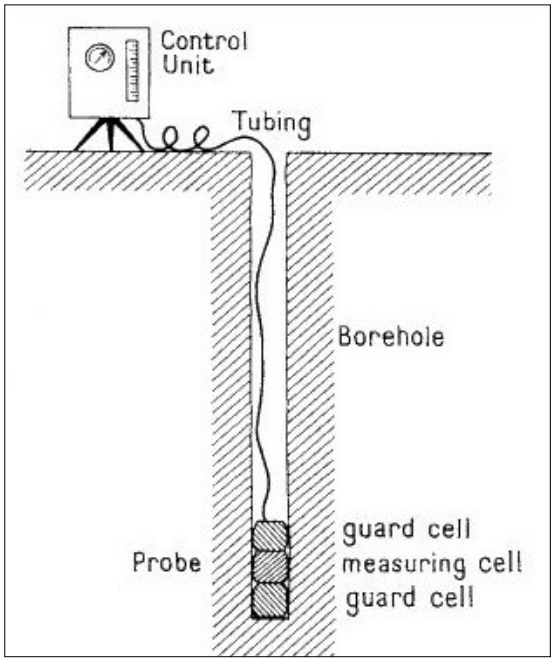

Figure: 2. 46 Components of pressuremeter apparatus (Baguelin et al. 1978)

The pressuremeter test is carried out either by measuring the volume change on every equal increment of pressure or measuring the pressure change on every equal increment of volume (Clarke 1996; British Standard 1997; ASTM International 2000b). In one word, the first method is termed as 'stress

controlled' whereas the second one is called 'strain controlled'. In stress-controlled method, it is preferable to increase pressure in 10 equal increments, so that the test is not run quickly or too slow (Baguelin et al. 1978). However, in common practice minimum 7 to 10 increments are to be kept during the test (Singh 1981; British Standard 1997; ASTM International 2000b; Cestari Ferrucio 2012). Generally, 25, 50, 100 or 200 kPa pressures increment are considered for the test conducted in soil (Clarke 1996; British Standard 1997; ASTM International 2000b). In order to select the approximate scale of the increment, one may divide the assumed limit pressure by the number of pressure increment (i.e., 10) (British Standard 1997; ASTM International 2000b; Cestari Ferrucio 2012) . In this context, the approximate limit pressure may be assumed from the past experiences obtained for the merely same sub-soil profile.

On every pressure increment, total pressure is held for 60 second and corresponding volume change is recorded for 15sec, 30second and 60 second (Hughes et al. 1977; Baguelin et al. 1978; Briaud 1992, 2019a; Clarke 1994; British Standard 1997; ASTM International 2000b). Ideally, the test is continued until the limit pressure is achieved (i.e., until the volume of the cavity is doubled) (Baguelin et al. 1978). As per ASTM standard, the test is carried out upto the yielding of the soil (measured from the volumeter) disproportionately large (ASTM International 2000b).

Baguelin et al. 1978 (Baguelin et al. 1978) also suggested that the test may be carried out upto the working range of the volumeter to avoid the risk of bursting of probe. However, this rule is applicable only when the bore-hole is calibrated properly.

In 'strain controlled' test, volume is increased usually in a rate of the 5 % of the nominal volume of the probe and it is held constant for 60 seconds and corresponding pressure reading is taken on same time interval as the stress-controlled method (Baguelin et al. 1978; British Standard 1997; ASTM International 2000b; Lukas 2013).

Prior to conduct the test, the instrument is to be calibrated to adjust for pressure loss and volume loss during the test (Baguelin et al. 1978; Clarke 1996; British Standard 1997; ASTM International 2000b). The calibration test is mainly of volume calibration and pressure calibration as explained below:

(i) *Volume calibration or Pipe calibration*: Volume losses are inherent in the pressuremeter test. These may occur due to the expansion of the tubing, compression of the rubber membrane, compression of the water etc. (Baguelin et al. 1978). Hence, these losses must be computed. In this regard, the probe is inserted into the heavy-duty steel casing which should withstand to the maximum capacity of the pressure range of the instrument, generally 80 Bar. The inner diameter should be same as the outer diameter of probe (e.g., for NX size probe the inner diameter of casing will be 76mm). Then the probe is allowed to be inflated so that the membrane seat against the inner side of the casing. Subsequently, the pressure is increased at a constant interval. In this stage, it is assumed that no 'volume change' is occurred. Furthermore, if there is any change in volume, it is ascribed to inherent losses in the pressuremeter. For this purpose, the pressure is increased at an increment of 100kPa or 500kPa depending upon the design pressure of the probe (i.e., 2.5 MPa or 5.0MPa) (Briaud 1992, 2019a; Clarke 1994; British Standard 1997; ASTM International 2000b). Each pressure is to be held for one minute and corresponding volume change is recorded. Then,

a curve corresponding to volume change with respect to the applied pressure is plotted. From the slope intercept of this curve, the correction volume (V_i) is computed and corresponding initial volume (V_0) of the probe is calculated (Equation 2.41)(Baguelin et al. 1978; Singh 1981; Winter 1986; Amar et al. 1991; British Standard 1997).

$$V_0 = (\pi/4) \times LD_i^2 - V_i \quad (2.41)$$

Where, D_i= inside diameter of the heavy-duty steel casing (for NX probe 76mm) L= Length of measuring cell of the probe, V_i= intercept of the slope with ordinate (Figure 2.47). The volume loss (V_c) of the system is computed from the following Equation 2.42.

$$V_c = V_r - aP_r \quad (2.42)$$

P_r = pressure increment, V_r = volume corresponding to each pressure increment i.e., P_r, a = slope intercept (Figure 2.47).

The volume loss correction is deducted from the measured volume corresponding to applied pressure. However, this volume loss is relatively small for the soil and may be neglected when slope of the volume loss curve is less than 0.1% of the nominal volume (V_0) of the probe per 100 kPa applied pressure (British Standard 1997; ASTM International 2000b). It is also mentioned that the maximum correction should not cross the 0.5% of the nominal volume per 100 kPa (British Standard 1997; ASTM International 2000b).

(ii) *Pressure calibration or Air calibration or Membrane correction*: As the probe inflates due to the increase of pressure, it is necessary to know the resistance of the rubber membrane and the sheath (Baguelin et al. 1978). Therefore, the pressure calibration is necessary to estimate the loss of pressure due to the membrane and sheath. Therefore, the probe is placed vertically

downward on ground surface at open air and pressure of about 10kPa (Baguelin et al. 1978; Clarke 1996; British Standard 1997; ASTM International 2000b) is applied. Subsequently, corresponding volume change is recorded for 1 minute. A graph is plotted and the pressure correction (P_c) is calculated. A schematic graph is shown in the Figure 2.47.

Once the calibration process is over, the probe is lowered into the bore hole (diameter according to the respective probe size) upto the desired test depth. Next, volume meter is filled up with water. After that, corresponding pressure increments, the change of volume is recorded (for stress-controlled method) (British Standard 1997; ASTM International 2000b). During the test, change in volume corresponding pressure change is recorded. Afterward, the corrected volume vs. pressure reading is plotted upon applying the calibrated value (as shown in Figure 2.48).

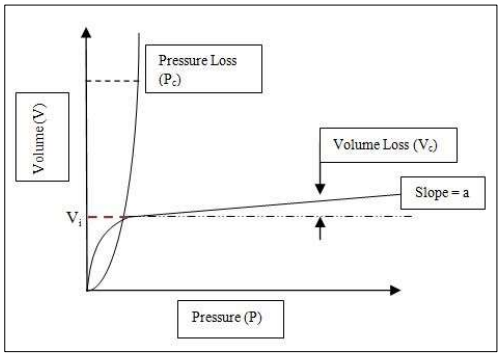

Figure: 2. 47 Schematic graph for calibration (ASTM International 2000b)

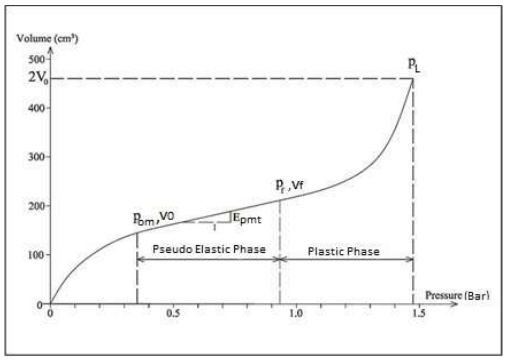

Figure: 2. 48 Schematic pressuremeter curve for soil (Singh 1981)

2.3.2 INTERPRETATION OF PMT TEST

From the Figure 2.48 it is revealed that, inside the borehole initially the probe inflates without any resistance upto touching the side wall of borehole. After touching the borehole wall, the volume increases slowly and the slope of the

curve turns into flatter (at pressure, P_{0m}). In this initial pressure, it is assumed that the membrane is in full contact with the side wall of bore hole. This initial pressure is often assumed as horizontal in-situ stress (Baguelin et al. 1978; Singh 1981). Subsequent increase of pressure, the slope of the curve (i.e., reading of the volumeter) increase slowly with a constant rate of change. This portion of the curve depicts the pseudo-elastic behavior of the soil (Baguelin et al. 1978; Singh 1981; Clarke and Wroth 1989). Further increase of pressure, soil becomes plastic at a pressure (P_f). Beyond this pressure, soil becomes permanently deformed and 'creeping phase' starts. In that stage, the volumetric expansion increases rapidly with a nominal change of pressure. Accordingly, the slope of the curve becomes much steeper (Hobbs and Dixon 1969; Baguelin et al. 1978; Singh 1981; Cassan 1988; Clarke and Wroth 1989; Clarke 1996; British Standard 1997; ASTM International 2000b; Sedran et al. 2013).

Referring to Figure 2.48, it is noteworthy that at the pressure P_{0m}, the volume is v_0, with the assumption that the probe inflates upon contact with the walls of the borehole. Thus, v_0 is marked as the start of the straight-line portion of the curve and it is termed as the initial volume of the cavity (Terzaghi 1943; Baguelin et al. 1978; Singh 1981; Bellotti 1986; Terzaghi et al. 1996; Bowles 2001). Theoretically, the limit pressure (P_L) is defined as the pressure corresponding to the doubled volume of the cavity (i.e $2v_0+V_0$) (Baguelin et al. 1978). However, to minimise the risk of probable damage to the probe, the limit pressure is often determined by indirect method rather than direct measurement (Baguelin et al. 1978; Singh 1981; Cestari Ferrucio 2012). In this method (Singh 1981; ASTM International 2000b; Cestari Ferrucio 2012), the corrected inverse volume reading (1/V) is plotted against the corrected pressure (p) and the intersection of

the straight line with $V = 2V_0$ termed as the limit pressure (P_L) as shown in Figure 2.49.

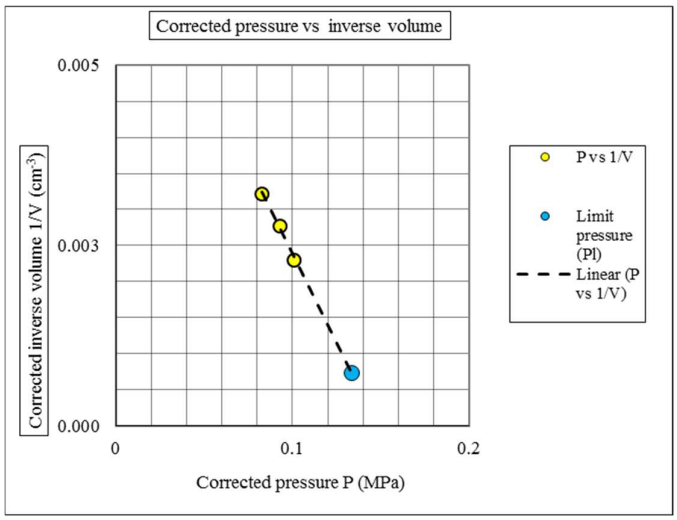

Figure: 2. 49 Schematic diagram for determination of limit pressure by inverse volume method (Cestari Ferrucio 2012)

It is also to be mentioned that the slope of the curve in pseudo-elastic phase (Figure 2.48) is termed as pressuremeter modulus (E_{PMT}). As per Baguelin 1978 (Baguelin et al. 1978; Lambe and Whitman 1991), the equation of the radial expansion of a cylindrical cavity in an infinite elastic medium was given as follows (Equation 2.41):

$$G = V.\Delta p/\Delta V \quad (2.41)$$

Where, G = Shear modulus, V=Volume of the cavity, p=pressure in the cavity

For the pressuremeter test, $\Delta V = \Delta v$, therefore the equation was converted as follows (Equation 2.42).

$$G = V.\Delta p/\Delta v \quad (2.42)$$

The ratio $\Delta p/\Delta v$ is constant in pseudo-elastic phase, but V is not. Approximately, the midpoint between v_0 and v_f was calculated in such a manner, so that $V = V_c+(v_0+v_f)/2 = V_m$. This volume ($V_m$) was then used to calculate "G" (which is termed as G_M) (Baguelin et al. 1978; Singh 1981). The volume 'V_c' was termed

as the initial volume of the probe (V_0). Hence, Equation 2.42 was rewritten as follows

$$G_M = V_m . \Delta p/\Delta v \quad (2.43)$$

Further, $G = E/2(1 + \upsilon)$

Henceforth, it was rewritten as following Equation2.44 (Baguelin et al. 1978)

$$G_M = \frac{E_{PMT}}{2\times(1+\upsilon)} \quad (2.44)$$

Or expressed as the following Equation 2.45 (Baguelin et al. 1978; Singh 1981; ASTM International 2000b)

$$E_{PMT} = 2(1 + \upsilon)(V_0 + v_m)\ \Delta p/\Delta v \quad (2.45)$$

Where, V_0=initial volume of the probe, υ=Poisson ratio=0.33 (ASTM International 2000b), and v_m= Corrected volume reading in the center portion of the Δv volume increase i.e., $(v_0+v_f)/2$.

The limit pressure (P_L) indicates the failure pressure of the soil, while the net limit pressure (P_{Ln} or P_L^*) is also used in geotechnical practice for the correlation purpose (Baguelin et al. 1978). The term 'net limit pressure' (Equation 2.46) is relatively insensitive to the disturbances in the borehole (Baguelin et al. 1978; Briaud 1992).

$$P_{Ln} = P_L - P_0 \quad (2.46)$$

Where, P_0 is horizontal in-situ stress. It can be obtained either directly from the graph drawn from the test (corrected volume vs corrected pressure) or calculated manually from the following Equation 2.47.

$$P_0 = K_0 . (\gamma . z - u_0) + u_0 \quad (2.47)$$

Where, γ is the unit weight of the soil at the test depth, z = test depth, u_0 = static pore water pressure at test depth and K_0 = coefficient of earth pressure at rest.

Theoretically, the pressure 'P_{om}' (Figure 2.41) is estimated from the pressuremeter curve which is equal to the horizontal stress P_0. However, it was observed that the estimation of P_{om} is very difficult due to the disturbances inside the borehole (Baguelin et al. 1978; Singh 1981).

The result obtained from the pressuremeter test is extensively used for foundation design (Clarke and Wroth 1989; Cestari Ferrucio 2012). This because the methodology of the test closely replicates the actual behavior footing. It is also observed that the test more accurately defines the in-situ boundary and stress-strain relationship than the other in-situ test like SPT, CPT (Lutenegger 1990b; Benoît and Lutenegger 1992; Mayne 1995). Further, this test can be carried out on any types of soil and rock (Nayak 1979, 2001; Amar et al. 1991; Clarke 1994; Terzaghi et al. 1996; Bowles 2001; Salgado 2006; Cestari Ferrucio 2012; Narimani et al. 2018).

2.3.3 PRESSUREMETER CORRELATIONS

From the nature of the pressuremeter curve, the characteristics of the sub-soil can be distinctively predicted. Also, this result may be used for the identification of the soils (Clarke and Wroth 1989; Clarke 1996).

The curve exhibits a sharp curvature (which is a clear indication of failure) on the transition phase between "pseudo-elastic" and "plastic" stage for clay soil. Whereas, sharp bend is typically absent in test curve for sand, as the shear strength of sand is primarily derived from their angle of internal friction (Hughes et al. 1977; Baguelin et al. 1978; Fahey and Carter 1993; Cheshomi and Ghodrati 2015; Naseem and Jamil 2016; Yildiz 2021). As such, the increase of normal forces creates better interlocking between the particles which result the increase of effective shear strength(Terzaghi 1943; Lambe and Whitman 1991; Terzaghi

et al. 1996). Besides, clay's shear strength primarily depends on undrained cohesion, which remains unaffected by applied normal stress (perpendicular to the borehole wall) during rapid test like 'pressuremeter'(Baguelin et al. 1978; Lambe and Whitman 1991; Briaud 1992, 2019a; Briaud J.L 2013; Ramdane et al. 2013; Robbins 2013; Ameratunga et al. 2016). Hence, during pressuremeter test, a 'clear failure point' is observed on the pressuremeter curve when the shear force exceeds the undrained shear strength of the clay soil.

In the year of 1978, Baguelin (Baguelin et al. 1978) suggested a typical range of net limit pressure (P_{Ln}) for different type of soils (Table 2.6). After that Briaud, (Briaud 1992) modified those range and suggested a new one (Table 2.7). On the other hand, the SPT test is popular and well accepted method by most of the engineers, owing to its low cost and easy to use in geotechnical exploration (Bowles 2001; Das and Sivakugan 2018; Das 2019). Nevertheless, the limited numbers of studies about the correlation between SPT and PMT test, were carried out till date. The SPT test results are used to predict many other characteristics of sub-soil such as shear strength parameters, Liquefaction potential, bearing capacity (Terzaghi 1943; Janbu and Senneset 1974; Mesri 1975; Mesri et al. 1975; Kulhawy and Mayne 1990; Terzaghi et al. 1996; Nayak 2001; Hasancebi and Ulusay 2007; Ku and Mayne 2013; Chatterjee and Choudhury 2013; Shiuly et al. 2018; Ramkrishnan et al. 2022). In this context, many research works were conducted to correlate P_L and E_{PMT} with SPT N values (Yagiz et al. 2008; Kayabasi 2012; Cheshomi and Ghodrati 2015; Balachandran et al. 2015, 2017; Anwar 2018; Özvan et al. 2018; Ramaswamy et al. 2021). In between the period of 1968 to 1969, correlation between P_L and SPT N were proposed for all type of soils (Hobbs and Dixon 1969; Cassan 1988). Further, in the year of 1978 a

general correlation between P_L and SPT N, for all type of soil was suggested (Baguelin et al. 1978). Another correlation between P_L and SPT N value was suggested for sandy soil of Singapore (Verruijt 2021). Further, in 1982, correlation between E_{PMT} and SPT N values were suggested for clay and sandy soil (Ohya et al. 2021).On 2008, a correlation between P_L and E_{PMT} with SPT N values was proposed for sandy silty clay soil (Yagiz et al. 2008). In the year of 2010, two numbers of separate correlations between E_{PMT} with SPT N were proposed for sandy and clayey soil respectively (Bozbey and Togrol 2010). In the next year 2011, correlation of P_L with SPT N value was proposed for all type of soil (Kayabasi 2012; Kayabaşı 2015). Another correlation of P_L and E_{PMT} with SPT N value for clayey soil was proposed in the year of 2012 (Kayabasi 2012; Aladag et al. 2013). In the year of 2014, separate correlations (P_L and E_{PMT} with SPT N) were proposed for the silty sand and silty clay soil (Cheshomi and Ghodrati 2015). Another attempt was made to correlate E_{PMT} with SPT blow count for both cohesive and cohesionless soil in the year of 2015 and 2017 (Balachandran et al. 2015, 2017). Between the year of 2016 and 2018 different correlations between P_L and E_{PMT} with SPT N for sandy soil, were suggested (Naseem and Jamil 2016; Özvan et al. 2018). During the period of 2019 to 2021 several correlations of P_L and E_{PMT} with SPT N, were proposed for different type of soil (Firuzi et al. 2019; Önal and Ceylan 2020; Yildiz 2021,). The earlier established correlations are tabulated below (Table 2.8).

Table: 2. 6 Approximate common values of the pressuremeter parameters (Baguelin et al. 1978)

PMT parameters	Soil type (Clay)					
	Very soft	soft	firm	stiff	Very stiff	Hard
P_{Ln} (kPa)	0-75	75-100	150-350	350-800	800-1600	>1600
	Soil type (Sand)					
	Very loose	Loose	Compact	Dense	Very Dense	
P_{Ln} (kPa)	0-200	200-500	500-1500	1500-2500	>2500	

Table: 2. 7 Approximate common values of the pressuremeter parameters (Briaud 1992)

PMT parameters	Soil Type (Clay)					
	Very soft	Soft	Firm	Stiff	Very stiff	Hard
P_{Ln} (kPa)	-	0 – 200	200 – 400	400 – 800	800 – 1600	> 1600
E_{PMT} (kPa)	-	0 – 2500	2500 – 5000	5000 – 12000	12000 – 25000	> 25000
	Soil Type (Sand)					
	Very loose	Loose	Compact	Dense	Very Dense	
P_{Ln} (kPa)	-	0 – 500	500 – 1500	1500 – 2500	> 2500	
E_{PMT} (kPa)	-	0 – 3500	3500 – 12000	12000 – 22500	> 22500	

Table: 2. 8 Earlier established correlations

Sl. No.	Author proposed	Correlation	Unit	R^2 value	Type of soil
1	Yagiz et al. (2008)	$E_{PMT} = 388.67 \times Ncor + 4554$	kPa	0.91	Sandy Silty Clay
		$P_L = 29.45 \times Ncor + 219.7$	kPa	0.97	Sandy Silty Clay
2	Bozbey et al (2010)	$E_{PMT} = 1.33 \times (N_{60})^{0.77}$	MPa	0.82	Sandy soil
		$E_{PMT} = 1.61 \times (N_{60})^{0.77}$	MPa	0.72	Clayey Soil
4	Chesho mi (2014)	$E_{PMT} = 0.98 \times N_{60} - 9.43$ $P_L = 0.1 \times N_{60} - 2.08$	MPa	0.7	Silty sand
		$E_{PMT} = N_{60} - 2.67$ $P_L = 0.05 \times N_{60} + 0.42$	MPa	0.85	Silty clay

Sl. No.	Author proposed	Correlation	Unit	R^2 value	Type of soil
5	Ohya et al. (1982)	$E_{PMT}/P_a = 19.3 \times N^{0.63}$		0.393	Clay
		$E_{PMT}/P_a = 9.08 \times N^{0.66}$		0.482	Sand
6	Baguilin e et al.(1978)	$N/P_L = 2$	kg/cm$_2$	-	All
7	Ramasw amy (1982)	Loose state $N/P_L = 10$ Dense state $N/P_L = 10$ (Average:$N/P_L = 10$)	MPa	-	Coarse to medium sand (Singapore)
		Loose state N/P_L = 35 to 45 Dense State N/P_L = 10 to 35 (Average: $N/P_L = 35$)	MPa	-	Calcareous Sand(Singapore)
		Loose State $N/P_L = 30$ Dense State N/P_L = 30 (Average:$N/P_L = 30$)	MPa	-	Silty Sand(Singapore)
8	Özgür YILDIZ et al. (2021)	$E_{PMT} = 0.52 \times N_{60} + 3.3673$	MPa	0.81	Sandy soil
		$E_{PMT} = 0.41 \times N_{60} + 6.1$	MPa	0.52	Clayey Soil
		$P_L = 0.026 \times N_{60} + 1.1745$	MPa	0.72	Sandy soil
		$P_L = 0.032 \times N_{60} + 0.8$	MPa	0.60	Clayey Soil
9	Ali Ozvan (2016)	$P_L = 0.142 \times N60 - 1.166$	MPa	0.895	Sandy silty clay (Clayey soil)
10	Kayabas ,i A. et. al. (2012)	$E_{PMT} = 0.29 \times (N60)^{0.71}$	MPa	0.74	Clayey soil
		$P_L = 0.043 \times (N60)^{1.2}$	MPa	0.74	Clayey soil
11	Cassan. M et. al. (1968)	$P_L = 0.028 \times (N) - 0.0021$	kPa	-	All soil
12	Hobbs et. al. (1969)	$P_L = 0.021 \times (N) + 0.33$	kPa	-	All
13	Waschko wski (2011)	$P_L = 0.0561 \times (N) - 0.092$	kPa	-	All
14	Naseem et. al. (2016)	$E_{PMT} = 165.88 \times (N) + 1364.1$	kpa	0.85	Sandy soils
		$P_L = 15.214 \times N60 + 89.276$	kPa	0.88	Sandy soils
15	Firuzi et al. (2019)	$E_{PMT} = 6.4 \times e^{0.04\,SPTN}$	MPa	0.83	Fine-grained soils
		$PL = 0.1 \times (N) + 0.26$	MPa	0.63	Fine-grained soils
		$E_{PMT} = 8.08 \times e^{0.04N}$	MPa	0.88	Coarse-grained soils
		$P_L = 30.93 \times e^{0.038N}$	MPa	0.75	Coarse-grained soils
16	Balachan dran et	$E_{PMT} = 1.12 \times N$	MPa	0.23	Cohesive soil

Sl. No.	Author proposed	Correlation	Unit	R^2 value	Type of soil
	al. (2015)	$E_{PMT} = 1.09 \times SPT\ N$	MPa	0.23	Cohesionless soil
17	Çigdem et. al. 2020	$E_{PMT} = 0.5304N_{60} + 4.5434$	MPa	0.53	Quaternary Alluvial
		$P_L = 0.0236 \times N_{60} + 0.4703$	MPa	0.60	gravel, sand, silt, and clay-intercalated mud

2.3.4 UNDRAINED SHEAR STRENGTH OF CLAYS (C_u)

In pressuremeter test, the load is rapidly applied to the bore hole wall, while the pore water drainage is restricted. Hence, a suitable method is required to directly estimate the value of undrained shear strength for cohesive sub-soil from the pressuremeter test results. In this regard, several different approaches are listed as "limit pressure method", "yield pressure method", "shear curve method" etc.(Terzaghi 1943; Terzaghi et al. 1996).

Amongst those methods, the "Yield pressure method" is one of the simple to estimate the undrained shear strength (Equation 2.47).

$$C_u = P_y - \sigma_{oh} \tag{2.47}$$

Where, p_y = yield pressure, σ_{0h} = total horizontal stress at rest.

However, Briaud did not recommend (Briaud 1992) this 'yield pressure' method. Sometimes, the yield pressure may lead to give overestimated prediction (Briaud 1992). So, another method was proposed i.e., "Shear curve method". However, this method was a graphical method and hence it was also not recommended for undrained shear strength estimations.

Clarke (Clarke 1994) suggested the "limit pressure" method based on the theoretical expression stated by Cassan (Cassan 1988) as given in Equation 2.48. This method is more reliable and commonly accepted in practice.

$$P_L = \sigma_{0h} + C_u \{1 + \ln(G/C_u)\} \quad (2.48)$$

P_L = limit pressure, σ_{0h} = total in-situ horizontal stress at rest, G = shear modulus of the soil, C_u= Undrained shear strength

Above equation may be written in simplified form as following Equation 2.49

$$C_u = P_{Ln}/\beta \quad (2.49)$$

The factor β in is referred as "pressuremeter constant". It mainly depends on the ratio of shear modulus (G) over the undrained shear strength (C_u). Generally, the value of β ranges between 5.5 to 7.5 (Briaud 1992; Briaud J.L 2013) with an average value of 6.5 (Baguelin et al. 1978) as given in Figure 2.50.

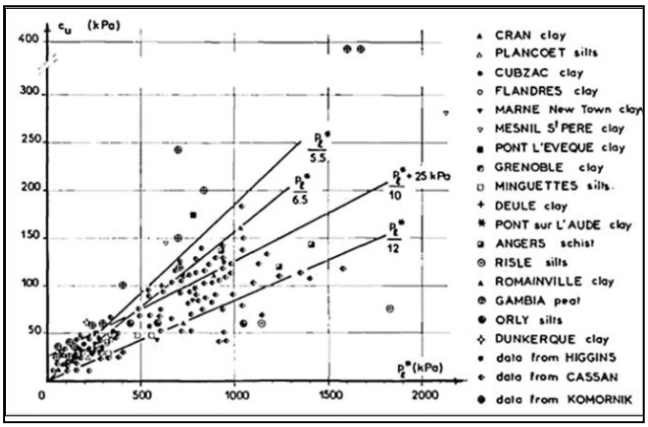

Figure: 2. 50 P_{Ln} vs. C_u correlation and proposed β factor (Baguelin et al. 1978)

B.G. Clark (1995) (Clarke 1994) also summarised the average value of β factor proposed by different researcher, as given in Table 2.9.

Table: 2. 9 Summarised values of the factor β (Clarke 1994)

Type of soil	β **factor**	Source
All clays	2 – 5	Menard, 1957
Soft to firm clays	5.5	Cassan, 1972, Amar & Jezequel, 1972
Firm to stiff clays	8	-
Stiff to very stiff clays	15	-

Type of soil	β **factor**	Source
Stiff clays	6.8	Marsland & Randolph, 1977
All clays	5.1	Lukas and LeClerc de Bussy, 1976
Stiff clays	10	Martin & Drahos, 1986

However, the variation of the "β" is related to uncertainties during the measurement of the σ_{h0}, due to influence of disturbance and anisotropy (Clarke 1994).

Baguelin et al. (1978) (Baguelin et al. 1978) also established a nonlinear correlation based on the different test results as shown in Figure 2.51.

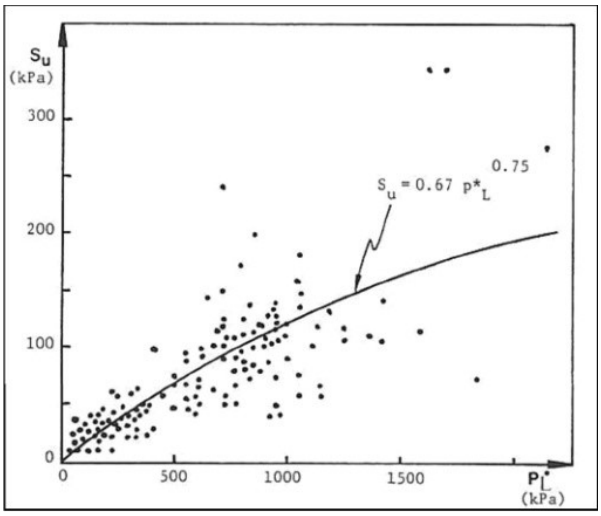

Figure: 2. 51 Correlation between net limit pressure and undrained shear strength (Baguelin et al. 1978)

2.4 SETTLEMENT PREDICTION OF SHALLOW FOUNDATIONS IN COHESIVE SOILS

2.4.1 DMT BASED SETTLEMENT

For predicting the settlement of shallow foundation from DMT test, M_{DMT} is an important tool (Fabius 1985). A model was proposed (by virtue of one-dimensional consolidation theory) to predict the settlement from M_{DMT} by Marchetti et al. 1997, (Fabius 1985; Borden et al. 1986; Schmertmann 1986b;

Chang 1987; Kalteziotis et al. 1991; Marchetti et al. 2001; Monaco et al. 2006a) as given in Equation 2.50.

$$S_t = (\Delta\sigma_v / M_{DMT}) \times z \quad (2.50)$$

S_t = Total settlement, $\Delta\sigma_v$ = Vertical stress increment, z = Thickness of compressible layers

Prior to this recommendation, many researchers had shown the comparison between the settlements predicted from DMT test with the other methods. A good agreement was reported by (Schmertmann 1986b) for 16 different case histories in different locations.

Also, a study was made by Hyes et al. in the year of 1986 (Hayes 1986) , about the comparison of flat dilatometer results and predicted settlement for different structures and earth work. It was found that the results were satisfactory. Also, in 1990, another comparison was made by Hyes et al. which was reported in TC16 (2001) (Marchetti et al. 2001). On those observations, it was found that DMT predicted settlement were in good agreement with the observed settlement (Figure 2.52)

In the year of 2006, a review on the DMT-predicted settlement vs observed settlements, was described by Monaco et al.(Monaco et al. 2006a). In this review, it was concluded that the M_{DMT} may be considered as an "operative modulus", for the prediction of settlement of foundation (which is in working conditions for a factor of safety of 2.5 to 3.5).

In India, a case study was made by Bandyopadhyay et al. for the comparison of settlement calculated by using M_{DMT} (Bandyopadhyay et al. 2020, 2022). It was found that the observed and the predicted settlement from DMT test was well comparable (Figure 2.53) with the observed settlement. Another study was made

by Das. K and Nandi. S in the year of 2022 (Das et al. 2022) for estimation of sub-soil parameters and settlement for the project in Kolkata city, the similar observations were found.

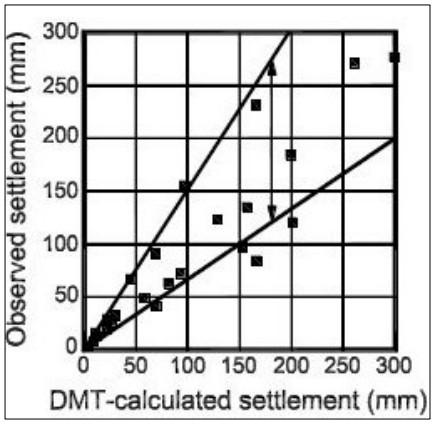

Figure: 2. 52 Observed vs DMT-calculated settlement by Hayes et al. 1990 (Marchetti et al. 2001)

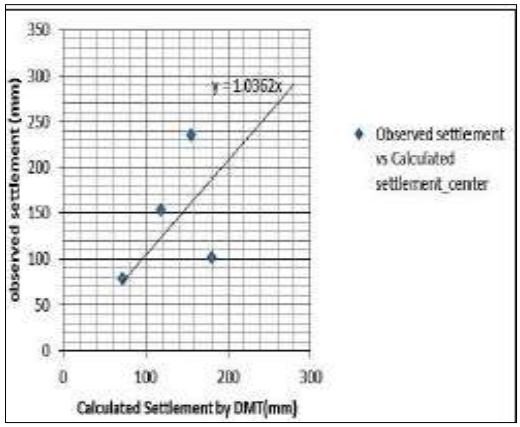

Figure: 2. 53 Predicted vs observed settlement (Bandyopadhyay et al. 2020)

2.4.2 CPT BASED SETTLEMENT

For the prediction of settlement, Meyerhof (1965) (Meyerhof 1974) used the CPT cone resistance (q_c) to evaluate the settlements of shallow foundation placed on cohesionless soils (i.e., sands). it was observed that the CPT based settlement was more conservative i.e., 1.2 to 1.5 times of field settlements (Sargand et al. 2003).

On the other hand, another refined method for the prediction of CPT-based settlement, was proposed by DeBeer (De Beer 1965). This method was based on the theory of the consolidation settlement of cohesive soil (Sargand et al. 2003). On the observations, it was found that the predicted settlement was twice more than the observed value.

In the year of 1970, another method was proposed by Schmertmann et al.(Schmertmann 1988a). This method was based on the linear elastic theory for the cohesionless soil. Also, a comparison was made with the laboratory model

and finite element method. In this regard, this method was found to be more realistic than other method (Sargand et al. 2003).

Besides, in Indian condition, there is no method to predict the settlement of the shallow foundation placed on the cohesive soil from CPT test results. However, an empirical equation was given in IS 8009 part-1 (IS 8009 Part-1 1985) based on average cone resistance (C_{KD}). This method was described to find the settlement for the cohesionless soils (based on CPT test results) by using Equation 2.51 and Equation 2.52. As no other methods were available for Indian condition, a case study was carried out by Bandyopadhyay et al.(Bandyopadhyay et al. 2022) to predict the settlement of shallow foundation placed on cohesive soil by using the same empirical equation. The estimated settlement was then compared with the values of observed settlement (estimated from settlement sensors) and with the values estimated from the numerical model (based on finite element-based software 'Plaxis 2D, Ver. 2016'). It was found that the value of predicted settlement was near to the other methods (Bandyopadhyay et al. 2022)

$$S_t = 2.303 \frac{H_t}{c} \log\left[\frac{\overline{p_0} + \Delta P}{\overline{p_0}}\right] \quad (2.51)$$

$$c = \frac{3}{2} \frac{C_{KD}}{\overline{p_0}} \quad (2.52)$$

Where, S_t = settlement, H_t = thickness of soil layer, $P_{0=}$ initial effective overburden pressure at mid height of the layer, ΔP = vertical stress increment, c = constant of compressibility, C_{KD}= average static cone resistance.

Chapter# 3
METHODOLOGY

3.1 GENERAL

In order to study the comparison of geotechnical parameters to establish relations, three distinct in-situ tests (i.e., CPT, DMT and PMT) were carried out adjacent to conventional boring accompanied by SPT test. All the tests were carried out at eleven numbers of different project sites in West Bengal (WB) and Odisha (OR) states, as detailed below.

i) Site-1 (HC): at Highcourt Site, Kolkata, WB

ii) Site-2 (PB): at Panchayet Bhaban site, Kolkata, WB

iii) Site-3(RJ): at Rajarhat CA94, Kolkata, WB

iv) Site-4 (HA): at Haldia Petrochem, Haldia, WB

v) Site-5 (DH): at Dhamra, OR

vi) Site-6 (SN): at Sonarpur, South 24 parganas, WB

vii) Site-7(LK): at Laketown project, Kolkata, WB

viii) Site-8 (BD): at Burdwan, Purba Bardhaman, WB

ix) Site-9 (VT): at Victoria, Kolkata, WB

x) Site-10 (PT): at Park Street, Kolkata, WB

xi) Site-11(ES): at Esplanade, Kolkata, WB

In this context, DMT, CPT or PMT tests were carried out at same starting 'Reduced Level' (R.L) corresponding to the adjacent bore holes. Besides, in absence of reduced level, it was assumed (+) 100.0 m. Irrespective of seasonal variation, the water level was assumed as same as the adjacent bore hole for the

respective DMT and CPT test's locations. On the other hand, for the PMT test, water level was measured 24 hours after completion of each test.

The DMT and CPT tests were carried out by using Pagani TG63-150 penetrometer (maximum thrust capacity of 150 kN) (Pagani Geotechnical Equipment (manual) 2014) as shown in Figure 3.1 and Pressuremeter test (PMT) were carried out by using 'pre-bored Menard Pressuremeter' (maximum capacity of 80 Bar), shown in Figure 3.2.

Figure: 3.1 Pagani Penetrometer TG63-150 (150 kN capacity)

Figure: 3.2 Prebored Menard Pressuremeter (80 Bar capacity)

The several parameters along with the shear strength parameters obtained from DMT and CPT tests, have been compared with the conventional field and laboratory test results. Besides, limit pressure (P_L) and pressuremeter modulus (E_{PMT}) have been compared with the observed SPT N values (N_{ob}). On the other hand, an attempt has been made to establish relations (based on the regression analysis) between some basic parameters obtained from DMT, CPT and PMT tests with the N_{ob} and laboratory test results. Also, the settlement of the shallow foundation has been evaluated by using empirical equation based on the average cone penetration resistance (i.e., C_{KD}) obtained from CPT test. These values have been compared with the settlement predicted from DMT tests (by using M_{DMT})

and numerical model (by using PLAXIS 2D ver.16 software) based on the geotechnical parameters predicted from CPT, DMT and laboratory tests on samples of soil obtained from adjacent boreholes.

The sub-soil of different project site comprises soils of varying nature due to the different geological condition. However, to meet the purpose of this study, focus is limited to the results obtained from DMT, CPT and PMT tests for the cohesive sub-soils.

3.2 SOIL EXPLORATION

3.2.1 CONVENTIONAL BORING AND SPT TEST

Conventional boring was done by wash boring method (IS 1892 1979) . The size of the bore hole was 150mm (SX). During the progress of the bore-hole the undisturbed samples were collected from the suitable depth intervals (IS 2132 2002) and Standard Penetration Test (SPT) were carried out as per IS 2131(IS 2131 2002).

Various laboratory tests viz. Grain size analyses (Sieve and Hydrometer Analysis), Atterberg's limits, Natural moisture content (w_n), Triaxial Unconsolidated Undrained test (UU) Unconfined Compressive strength test (UC) and Direct shear Test (DS), were carried out on undisturbed samples as per Indian Standards.

3.2.2 DMT TEST

The DMT test were carried out by pushing the "Dilatometer Blade" inside to the ground. Soon after penetration, by use of the control unit, the membrane was inflated by 'Nitrogen gas' pressure and corresponding two readings namely 'A-pressure' ('lift-off') reading and 'B-pressure' reading (i.e., required to move the center of the membrane 1.1 mm against the soil) were recorded from the 'pressure gauge' fitted to the control unit. On arriving of "A" reading (deactivating of signal from the 'Buzzer') the flow of gas pressure was continued upto the 'signal from the Buzzer' was reactivated. Immediate after reactivating of 'signal from Buzzer' the 'B' reading was recorded. After measuring 'B' reading, the DMT blade was further advanced to the next test depth. Before starting of each test, 'membrane calibration' was carried out to estimate the stiffness of the membrane. In this regard, 'ΔA' (on applying suction pressure to the membrane) and 'ΔB' (on applying positive pressure to the membrane) readings were recorded by attaching the 'DMT blade' to the control unit with short 'p-e' cable. This calibration process was done by a standardised 'Syringe' provided with control unit. The corresponding 'A' and 'B' pressure readings recorded during the test were then corrected to the pressure p_0 and p_1 respectively.

In accordance with standard method stated in TC16 2001(Marchetti et al. 2001), the minimum depth interval may be adopted as 10cm. However, for this study purpose, DMT test was carried out at 20cm depth intervals corresponding 2cm/s penetration rate (Marchetti et al. 2001).The standard computer program (i.e 'SDMT Elab') was (Prof. Marchetti S.r.l. Studio) used for analysing the field data.. The DMT tests were carried out to the adjacent boreholes at respective test

location. In this study, data from 29 numbers of DMT test are considered for analysis purpose

3.2.3 CPT TEST

In this study, total 25 numbers of CPT tests were carried out (Indian Standard 1976; Pagani Geotechnical Equipment (manual) 2014; Robertson and Cabal 2015) to the adjacent bore holes at respective test locations. It was conducted by using the CPT assembly attached with 'Pagani TG63-150' penetrometer as per 'Instruction Manual' provided by Pagani (Pagani Geotechnical Equipment (manual) 2014). The CPT test was carried out by pushing the cone assembly (Begemann cone) vertically into the ground surface at a constant strain rate (≈2cm/s). During the advancement of the cone three numbers of readings were recorded viz. first reading 'Rp' (i.e., during penetration of only the Cone), second reading 'R_p+R_L' (i.e., during the penetration of cone along-with the sleeve) and the third reading 'R_T' (i.e., during the penetration of total assembly of cone). Based on these three readings, two numbers of basic parameters i.e., cone resistance (q_c) and frictional resistance (f_s) were calculated. The readings were recorded at every 20cm depth intervals.

3.2.4 PMT TEST

For this study purpose, PMT test is carried out by using NX size (outer dia. ≈74mm) 'Prebored Menard Pressuremeter' having maximum capacity of 80 Bar (ASTM International 2000b). In this regard, NX size borehole (inside dia. 76 mm) is dug adjacent to conventional bore holes (SX size, i.e., Diameter ≈150mm) at respective test location. Total 48 numbers of PMT tests are carried out inside the 12 numbers of NX size boreholes at 5m depth intervals upto the average depth of 20m at three different locations viz., Site-9 (VT), Site-10 (PT) and Site-11 (ES). Before starting of each test, two numbers of calibration (i.e., pressure loss calibration and volume calibration) tests are performed. For pressure calibration, the probe is kept vertically downward at ground and all the connections are checked properly. Next, gas pressure is increased at average rate of 100kPa per minute and corresponding volume change is recorded at 15s, 30s and 60s time intervals. The pressure is increased upto the maximum pressure of 1Bar. After completion of pressure loss calibration, pressure is released and kept the instrument for reinstating its normal condition. For volume calibration, the probe is kept inside to a 'Heavy Duty' NX size (inside dia. 76mm) steel casing and gas pressure is increased at a rate of 1 Bar per minute upto the average pressure of 10 Bar. The volume reading corresponding to each pressure increment is recorded at the 15s, 30s and 60s interval. On completion of pressure loss calibration and volume loss calibration, the pressuremeter probe is then inserted into the Prebored 'NX' size hole at the test depth. Next, the test is performed by increasing the pressure in stages. On each pressure increment volume readings are recorded at time intervals of 15, 30 and 60 seconds from the time of application of pressure. The next incremental pressure is then applied.

3.3 DATA INTERPRETATION

3.3.1 DMT TEST

Two numbers of pressure readings are initially recorded from the DMT test. These two readings are further reduced to the corrected values (i.e., p_0 and p_1) after applying the membrane stiffness correction (i.e., 'ΔA' and 'ΔB'). Based on the corrected pressure readings three numbers of basic parameters are derived i.e., material index I_D, horizontal stress index K_D and Dilatometer modulus (E_D) (TC 16., 2001)(Marchetti et al. 2001). Also, shear strength parameters (C_u and ϕ) and compressibility characteristics in terms of vertical drained constrained modulus (M_{DMT}) are calculated. In arriving at these parameters, the vertical effective in-situ stress (σ'_v) is calculated based on the in-situ density chart proposed by Marchetti (Marchetti et al. 2001). In this purpose, 'SDMT Elab' software (Prof. Marchetti S.r.l. Studio) has been used. In each DMT test location, the classification of sub-soil has been predicted from the value of I_D (Marchetti et al. 2001) and density of sub-soil has been predicted from the chart proposed by Marchetti (Marchetti 1980; Marchetti et al. 2001).

3.3.2 CPT TEST

In CPT test, two numbers of basic parameters viz. cone resistance (q_c) and frictional resistance (f_s) are calculated as per 'Instruction Manual' provided by Pagani (as given in Equation 3.1 and 3.2) based on the recorded readings viz., R_P,R_P+R_L,R_T (Pagani Geotechnical Equipment (manual) 2014; Robertson and Cabal 2015; Rocscience Inc. 2016)

$$q_c = \frac{(R_P \times 10 + \text{number of sounding rod} \times \text{internal weight})}{10} \quad (3.1)$$

$$f_s = \frac{(R_P + R_L \times 10 - R_P \times 10)}{150} \quad (3.2)$$

On the other hand, cone resistance and sleeve friction are also calculated based on the method stated in Appendix A of IS 4968 (Part III) (Indian Standard 1976). Based on the cone resistance and sleeve friction, normalised parameters are estimated (Robertson and Cabal 2015).

The in-situ density (γ) and soil behavior type index (I_C), are estimated as per method stated by Robertson et. al. 2015 (Robertson and Cabal 2015; Rocscience Inc. 2016). Subsequently, shear strength parameters (C_u and ϕ), compressibility characteristics of soil (i.e., vertical drained constrained modulus, M_{CPT}) are estimated (Robertson and Cabal 2015; Rocscience Inc. 2016). On the calculation of M_{CPT}, the factor α_M is considered 8.25 (Kulhawy and Mayne 1990; Mayne and Kulhawy 1990; Rocscience Inc. 2016).

In each CPT test location, the classification and density of sub-soil is estimated from the value of I_C and density chart respectively (Robertson and Cabal 2015; Rocscience Inc. 2016).

3.3.3 PMT TEST

In PMT test, two numbers of parameters (i.e., limit pressure and pressuremeter modulus) are calculated. In estimating these parameters, pressuremeter curve is drawn corresponding to the corrected volume and corrected pressure (Baguelin et al. 1978; Clarke 1996). These corrections are calculated from the volume loss and pressure loss curve provided (Singh 1981; Clarke 1994, 1996)(ASTM International 2000b).

Limit pressure (P_L) and pressuremeter modulus (E_{PMT}) are calculated based on the inverse volume method and the standard equation respectively (Baguelin et al. 1978; Singh 1981; ASTM International 2000b). At all PMT test locations, the

sub-soil profile is predicted from the adjacent boreholes alongwith the visual inspection of soil during the progress of PMT test in the boreholes.

3.4 ANALYSIS

3.4.1 METHODOLOGY FOR COMPARISON OF ESTIMATED PARAMETERS AND PREDICTION OF SUB-SOIL PROFILE

In DMT and CPT tests, interpreted results are reduced over 200 mm depth intervals. In PMT test, the limit pressure and pressuremeter modulus are estimated on every 5m depth interval.

In this study, at each study location, the sub-soil profile predicted from DMT test (based on I_D), CPT test (based on I_C) and PMT test (based on PMT boreholes) is compared with the sub-soil obtained from adjacent bore holes (conventional boreholes).

In each project site, the variation of observed field SPT N value (N_{ob}) and shear strength parameters (i.e., C_u and ϕ) obtained from laboratory test, are plotted along depth.

In each CPT test location, the variation of q_c and f_s (calculated as per Robertson et. al. and IS 4968 part III) (IS 4968 (Part-III) 1976; Pagani Geotechnical Equipment (manual) 2014) are plotted along depth. Also, the variation of soil behaviour type index (I_C), vertical drained constrained modulus (M_{CPT}) and the shear strength parameters (i.e., C_u, ϕ; estimated from CPT test) are plotted along depth.

Besides, at each DMT test location, the basic parameters viz., E_D, M_{DMT}, I_D, alongwith the shear strength parameters (i.e., C_u and ϕ) are plotted along depth. Also, the variation of limit pressure and pressuremeter modulus is graphically presented along the depth for each of the PMT test locations.

The basic parameters obtained from DMT, CPT and PMT tests are side by side compared with the conventional field test (i.e. SPT test) and laboratory test results conducted in the adjacent boreholes.

3.4.2 METHODOLOGY TO PREPARE DESIGN CHART BASED ON PARAMETRIC COMPARISON

In arriving at the design chart or reference chart, some parameters are selected from DMT, CPT or PMT tests. These parameters are then related with some conventional test results. Based on that, the design or reference chart are prepared.

Based on the observations, on the variation of parameters (estimated from each DMT, CPT and PMT tests) along depth and the variation of conventional SPT N values (N_{ob}) and laboratory test results obtained from adjacent boreholes, the following parameters obtained from DMT, CPT and PMT tests, are selected for the relationship purpose.

- For DMT test, E_D and M_{DMT}
- For CPT test, q_c, f_s and M_{CPT}
- For PMT test, limit pressure (P_L) and pressuremeter modulus (E_{PMT}).

In this study, relationship between the selected parameters of DMT and CPT tests with the conventional SPT N values (N_{ob}), plastic limit (W_P) and plasticity index (PI) has been established for cohesive soils. In arriving at the relationship, average values of DMT or CPT based parameters and SPT N values (N_{ob}) alongwith plastic limit (W_P), plasticity index (PI) are considered corresponding to the collection depth of undisturbed samples from the adjacent boreholes.

Besides, the limit pressure and pressuremeter modulus have been related with the N_{ob} and liquidity index (I_L) for cohesive soils. In this regard, N_{ob} and I_L are estimated from the adjacent boreholes, corresponding to the PMT test depth.

The details of the methods to establish relations for the individual test are outlined below;

DMT test:

- In DMT test, the value of E_D and M_{DMT} are considered for relationship purpose.
- For each DMT test location the sub-soil profile predicted from I_D is compared with the sub-soil profile predicted from adjacent borehole.
- Average values of E_D and M_{DMT} corresponding to the collection depth of undisturbed cohesive soil are considered.

- Besides, average value of N_{ob} is considered corresponding to collection depth of undisturbed cohesive soil samples.
- Also, the value of plastic limit (W_P) and plasticity index (PI), estimated from the laboratory test are considered for the relationship purpose.

CPT test:

- In CPT test, the value of q_c, f_s and M_{CPT} are considered for establishing the relationship.
- For each CPT test location, the sub-soil profile predicted from I_C, is compared with the sub-soil profile predicted from adjacent borehole.
- Average values of q_c, f_s and M_{CPT} corresponding to the collection depth of undisturbed cohesive soil samples are considered.
- Besides, average value of N_{ob} is considered corresponding to the collection depth of undisturbed cohesive soil samples.

- Also, the value of plastic limit (W_P) and plasticity index (PI), estimated from the laboratory test are considered for the relationship purpose.

PMT test:

- Two numbers of basic parameters viz., P_L and E_{PMT} are considered for the relationship purpose.
- At each PMT test location, the sub-soil profile based on the PMT test boreholes is compared with the sub-soil profile predicted from the adjacent conventional boreholes.
- The average SPT N values (N_{ob}) (obtained from the conventional boreholes) are considered corresponding to PMT test (conducted in adjacent "NX" size borehole).
- Liquid limit, Plastic limit and natural moisture content are considered (corresponding to the adjacent PMT test depth) for establishing the relationship.

3.4.3 CPT-BASED PREDICTIVE MODEL FOR SHALLOW FOUNDATION SETTLEMENT ON COHESIVE SOIL

Another attempt is made to compare the settlement of shallow foundation (placed on cohesive soil) empirically predicted from average cone resistance (C_{KD}) from CPT test with the DMT based settlement and numerical model created based on conventional approach. The settlement of shallow foundation (placed on cohesive soils), having different shape and size are calculated against design load. This study, is carried out for selected locations where both the DMT and CPT tests have been conducted adjacent to common conventional borehole.

For calculating the settlement, numerical analyses were made by means of two numbers of computer-based softwares (i.e., Plaxis 2D ver.16 and DMT settlement).

In a particular test location, settlement of a particular foundation has been predicted by using an empirical equation based on the average cone resistance (C_{KD}) obtained from CPT test. Besides, effort was made to create individual soil model based on the borehole, DMT and CPT tests results using 'Mohr coulomb Model' in Plaxis 2D ver.16 software. Also, the settlement of the same foundation has been calculated (using DMT settlement software) based on the M_{DMT} values obtained from DMT test (Marchetti et al. 2001) by using DMT settlement software (Prof. Marchetti S.r.l. Studio).

In CPT test, the settlement has been estimated by using an empirical equation based on average cone resistance (C_{KD}), as no other code is available for Indian condition. Subsequently, these values have been compared with other results obtained from other methods. In this context, cone resistance (q_c) has been plotted along depth for a particular test. The average cone resistance (C_{KD}) has been calculated by virtue of the average line drawn through the similar type broken part of the curve. This value (C_{KD}) is then considered to calculate constant of compressibility (c) as given in Equation 3.4, the settlement ($S_{t\,CPT}$) of each layer being calculated as per Equation 3.5. The total settlement is then calculated by summation of each layer settlement. The vertical stress increment (Δp) has been calculated from Boussinesq's equation.

$$c = \frac{3}{2}\frac{C_{KD}}{\overline{p_0}} \tag{3.4}$$

$$S_{t\,CPT} = 2.303\ \frac{H_t}{c}\ \log\left[\frac{\overline{P_0} + \Delta P}{\overline{p_0}}\right] \tag{3.5}$$

Where,

$\overline{S}_{t\,CPT}$ = settlement, H_t = thickness of soil layer, $P_{0\,=}$ initial effective overburden pressure at mid height of the layer, ΔP = vertical stress increment (calculated using Boussinesq's equation) , c = constant of compressibility, C_{KD} = average static cone resistance.

Besides, using DMT settlement software, the total settlement is calculated below both the center and the corner of the footing. Observing that the estimated settlement below the center is higher than that below the corner, the settlement value at the center of the footing is considered for the analysis.

In this case, the settlement of the foundation is calculated based on one dimensional consolidation theory by taking thickness of each layer (Δz) as 20cm (Marchetti et al. 2001). In this regard, the vertical drained constrained modulus estimated from DMT test (i.e., M_{DMT}) and vertical stress increment (i.e., $\Delta\sigma_v$, estimated using Boussinesq's equation) is taken for the calculation purpose (Bandyopadhyay et al. 2022, TC-16; 2001). The relevant equation (Equation 3.3) is given below:

$$S_{t\,DMT} = \sum(\Delta\sigma_v/M_{DMT})\,\Delta z \qquad (3.3)$$

PLAXIS 2D (ver. 2016) software is used to estimate the settlement of shallow foundation by creating numerical model. For the purpose of creating soil profile in Plaxis 2D software based on the DMT and CPT tests results, the sub- soil layer is identified based on the I_D (for DMT test) or I_C (for CPT test) and the vertical drained constrained modulus (M_{DMT} or M_{CPT}) for respective DMT or CPT test. The shear strength parameters for the particular layer, is estimated by averaging total number of results obtained within that thickness of layer. The layer wise modulus of elasticity of soil (E_{sDMT}) in the soil model (i.e. created based on DMT test), is calculated by multiplying 0.8 to the averaged value of M_{DMT} (Marchetti

et al. 2001) for that layer. Similarly, the modulus of elasticity (E_{sCPT}) from M_{CPT} (to create numerical model based on CPT test), is estimated by adopting the same procedure as described for the DMT test (Marchetti et al. 2001)(Poenaru 2016). On the other hand, estimation of modulus of elasticity (E_{sBH}) to create the numerical model on Plaxis 2D software based on conventional borehole, is carried out by using conventional equation (Equation 3.6 and 3.7) (Terzaghi 1943; Peck et al. 1991; Terzaghi et al. 1996; Bowles 2001).

For Sand (normally consolidated) (Bowles 2001)

$$E_{sBH} = 500 \times (N + 15) \quad (3.6)$$

For Silts, Sandy Silts or Clayey Silt (Bowles 2001)

$$E_{sBH} = 300 \times (N + 6) \quad (3.7)$$

Here, E_{sBH} is in kPa

Moreover, the footing section is modelled by considering it as a plate element. the key parameters such as Young's modulus (E) of the plate elements (specific to M25 grade concrete), plate area (A), and moment of inertia (I) are calculated. The effective depth (d_{eff}) of the plate is defined as 150mm. Settlement value, derived from PLAXIS 2D software under plain strain condition, are integrated for comparative assessment (Bandyopadhyay et al. 2022).

Chapter# 4
LOCATION AND DESCRIPTION OF SITES

4.1 GENERAL

The DMT, CPT and PMT tests have been carried out at 11 numbers of different sites within the eastern part of India. The locations of 11 numbers of sites are presented in Figure 4.1.

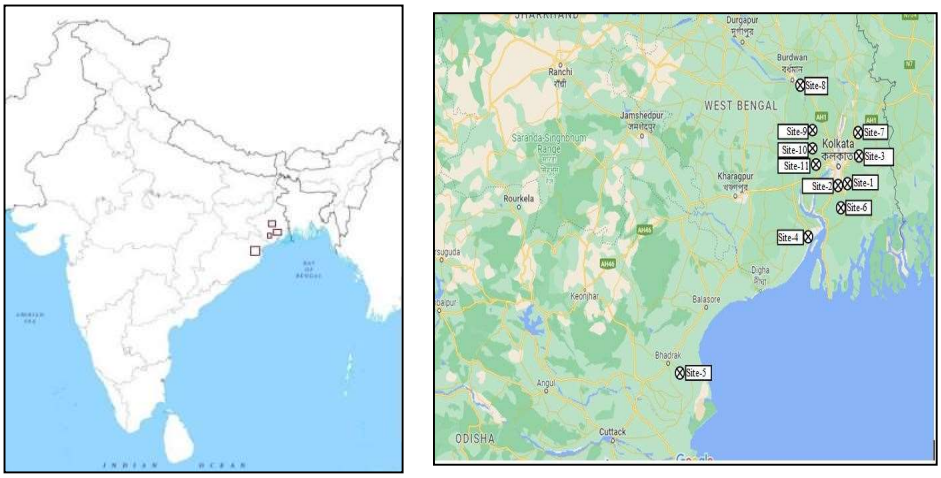

Figure: 4.1 Indicative location plan of the study area

In most of the project sites, the laboratory test results along with conventional SPT test results are gathered from the original conventional geotechnical investigation report for research purpose.

DMT, CPT and PMT tests have been carried at different project sites. At Site-1 to Site-8, DMT and CPT tests have been conducted adjacent to the conventional boreholes accompanied with SPT tests. On the other hand, at Site-9 to Site-11, PMT tests have been carried out adjacent to the conventional boreholes accompanied with SPT tests. Site-wise test details are given in the following Table 4.1.

Table: 4. 1 Project site details

Site	Project Location	DMT test	CPT Test	PMT test	Conventional Borehole	Water Level (b.g.l) (m)	Termination Depth of DMT, CPT and PMT test (b.g.l)	Soil Type	Soil Deposition
Site-1 (HC)	Highcourt site, Kolkata, WB	yes	yes	-	yes*	3.0	11.2 m for DMT; 10m for CPT	Silty clay/ Clayey silt	Alluvial
Site-2 (PB)	Panchayet Bhaban, Kolkata, WB	yes	yes	-	yes**	3.0	10.0m for DMT; 9.0m for CPT	Silty clay/ Clayey silt	Alluvial
Site-3 (RJ)	Rajarhat CA94, Kolkata, WB	yes	yes	-	yes*	3.5	19m for DMT and CPT	Silty clay / Clayey silt	Alluvial
Site-4 (HA)	Haldia, Purba Medinipur, WB	yes	yes	-	yes*	0.45	13.0m for DMT; 19.0m for CPT	Silty clay / Clayey silt	Alluvial
Site-5 (DH)	Dhamra, Bhadrak, OR	yes	yes	-	yes*	0.8	15m for DMT; 12m for CPT	Silty clay / Clayey silt	Alluvial
Site-6 (SN)	Sonarpur, South 24 parganas, WB	yes	yes	-	yes*	2.5	19.0m for both DMT and CPT	Silty clay / Clayey silt; Sandy silt / Silty Sand	Alluvial
Site-7 (LK)	Laketown, Kolkata, WB	yes	yes	-	yes*	2.3	19.0m for DMT; 17.0m for CPT	Silty clay / Clayey silt, Sandy silt / Silty Sand	Alluvial
Site-8 (BD)	Burdwan, Purba Bardhaman, WB	yes	yes	-	yes*	4.0	8.0m for DMT; 9.0m for CPT	Silty clay / Clayey silt; Sandy silt / Silty Sand	Alluvial
Site-9 (VT)	Victoria, Kolkata, WB	-	-	Yes	yes#	7.0	20m	Silty clay / Clayey silt; Sandy silt / Silty Sand	Alluvial
Site-10 (PT)	Park Street, Kolkata, WB	-	-	Yes	yes#	1.3	20m	Silty clay / Clayey silt	Alluvial
Site-11 (ES)	Esplanade Kolkata, WB	-	-	Yes	yes#	1.5	20m	Silty clay / Clayey silt	Alluvial

'b.g.l' below ground level

digging of conventional Borehole were done
* Borehole results were collected

** Nearest Borehole was considered as reference for analysis purpose

4.2 DESCRIPTION OF SITE:

4.2.1 SITE-1 (HC): (Lat: 22.5693^{o} N, Long: 88.3434^{o}E)

This site is located inside the North West block of Hon'ble High court building in Kolkata, WB. Based on the scope of work, four numbers of DMT tests (i.e., DMT-1_HC, DMT-2_HC, DMT-3_HC and DMT-4_HC) and four numbers of CPT tests viz. CPT-1_HC, CPT-2_HC, CPT-3_HC and CPT-4_HC, have been carried out on the specific location adjacent to three numbers of conventional boreholes (namely BH-1_HC, BH-2_HC and BH-3_HC) as shown in Figure 1. On each test location, both the DMT and CPT tests have been carried out (Figure4.1). Since, the locations is filled up with Brick bats, Rubbish etc. with an average thickness of 1.5m. As such, four numbers of pits have been excavated each of the test locations as shown in location plan (Figure 4.2). In order to carrying out the tests, four numbers of steel ramps (2.72 m in length, 0.4 m in width and 0.18 m in thickness) have been converted into two numbers of longer ramps by joining two shorter ramps through bolts such as longer ramps having length of 5.4m.Next, the two longer ramps have been placed horizontally in parallel way by keeping a clearance of 200mm (Figure 4.2) and Pagani TG63-150 penetrometer has been placed over this platform by which the CPT and DMT tests have been carried out (Figure 4.2). Both the DMT and CPT tests have been conducted upto the average depth of 11.2m.

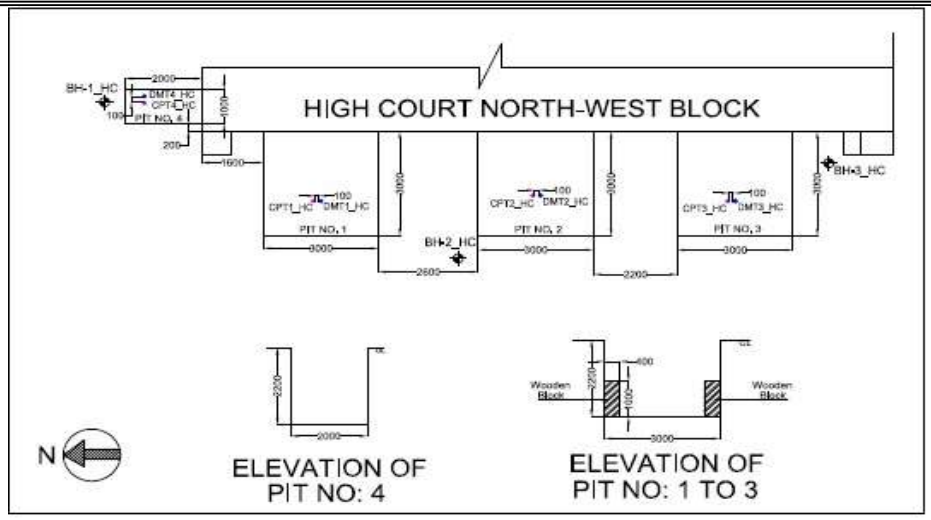

Figure: 4.2 Schematic location plan of Site-1 (HC)

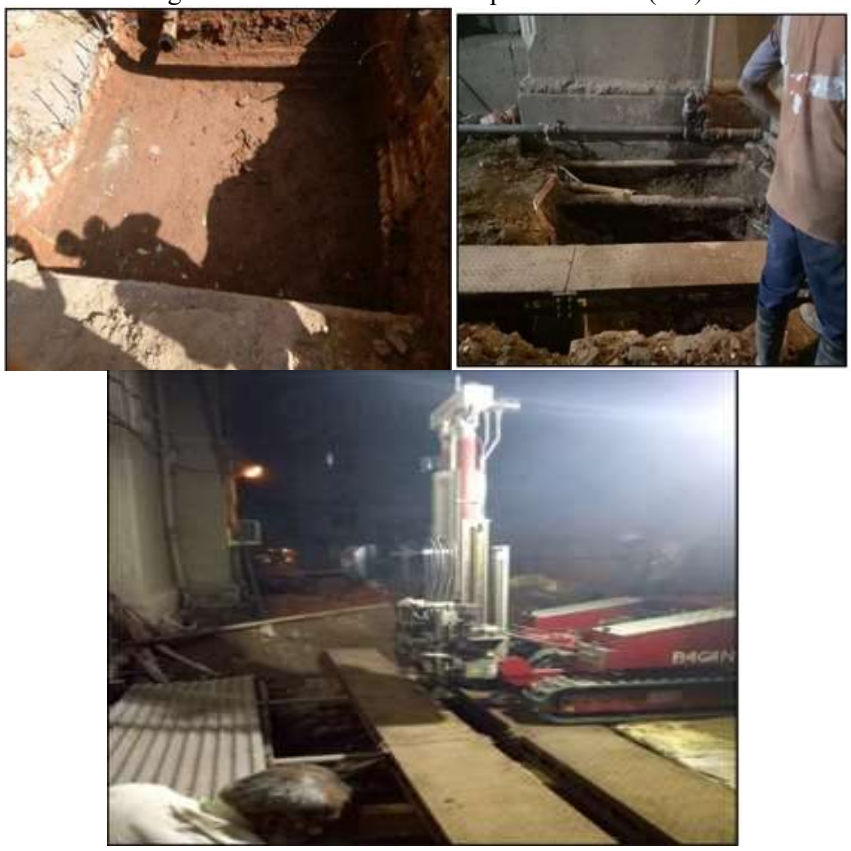

Figure: 4. 3 Photographs of test pit and test set up

4.2.2 SITE-2 (PB) : (Lat: 22.5701° N, Long: 88.3437°E)

This study area is located near to the Panchayet Bhaban, Kolkata, WB which is adjacent to the Site-1 (HC). Therefore, for the study purpose two numbers of boreholes (i.e., BH-2_HC and BH-3_HC) have taken as reference. In this location two numbers of CPT

tests and two numbers of DMT tests (namely DMT-1_PB, DMT-2_PB, CPT-1_PB and CPT-2_PB) have been carried out adjacent to the borehole BH-2_HC. Besides, one DMT test has been carried out adjacent to the borehole BH3_HC as shown in Figure 4.4.

The DMT and CPT tests have been conducted upto the average depth of 9.0m below the ground level for the test point of DMT-1_PB, DMT-2_PB, CPT-1_PB and CPT-2_PB. On the other hand, DMT-3_PB has been conducted upto the average depth of 10.2m below ground level. A representative photograph is given in Figure 4.5.

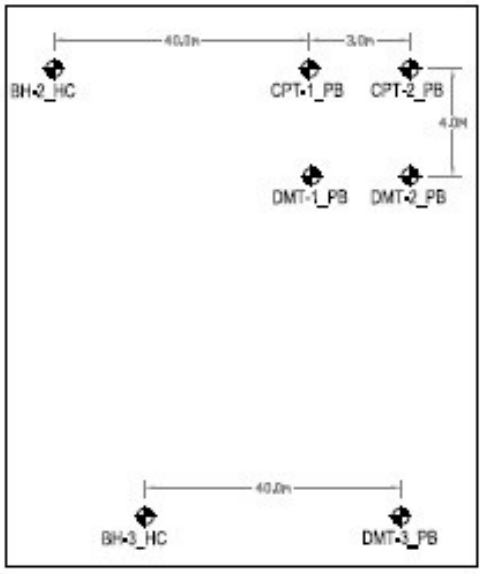

Figure: 4. 4 Schematic location plan of Site-2 (PB)

Figure: 4.5 Photograph showing test conducted at Site-2 (PB)

4.2.3 SITE-3 (RJ): (Lat: 22.5776°N, Long: 88.4640°E)

In this study area, two numbers of DMT tests (i.e., DMT-1_RJ and DMT-2_RJ) and two numbers of CPT tests namely, CPT-1_RJ and CPT-2_RJ has been carried out adjacent to two numbers of Boreholes viz., BH-1_RJ and BH-2_RJ respectively. The test location plan is given in Figure 4.6.

Both the DMT and CPT tests have been carried out upto the average depth of 18.0m. A representative photograph of the test is given in Figure 4.7

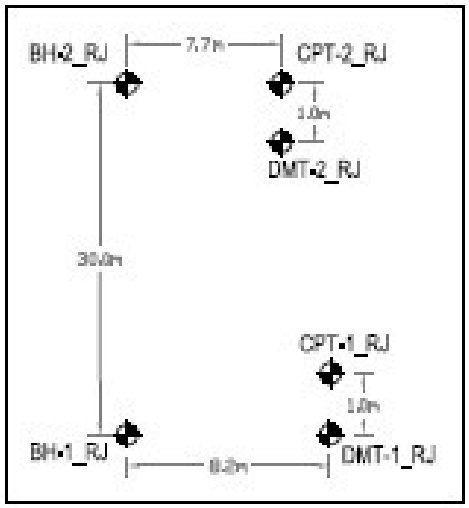

Figure: 4.6 Schematic test location plan at Site-3 (RJ)

Figure: 4.7 Representative Photograph of test at site-3 (RJ)

4.2.4 SITE-4 (HA): (Lat: 22.0666°N, Long: 88.1145°E)

This study area is located at Haldia, Purba Medinipur, WB. In this study area one DMT test and three numbers of CPT tests have been carried out in three different locations adjacent to three numbers of boreholes namely BH-1_HA, BH-2_HA, BH-3_HA as shown in schematic test location plan given in Figure 4.8.

For the study purpose, a DMT test (DMT-3_HA) and a CPT test (CPT-3_HA) have been conducted adjacent to BH-3_HA, upto a depth of 12.40m and 19.20m below ground level respectively.

On the other hand, other two CPT tests (i.e., CPT-1_HA and CPT-2_HA) have been carried out upto the average depth of 19.20m adjacent to BH-1_HA and BH-2_HA. A representative photograph is given in Figure 4.9.

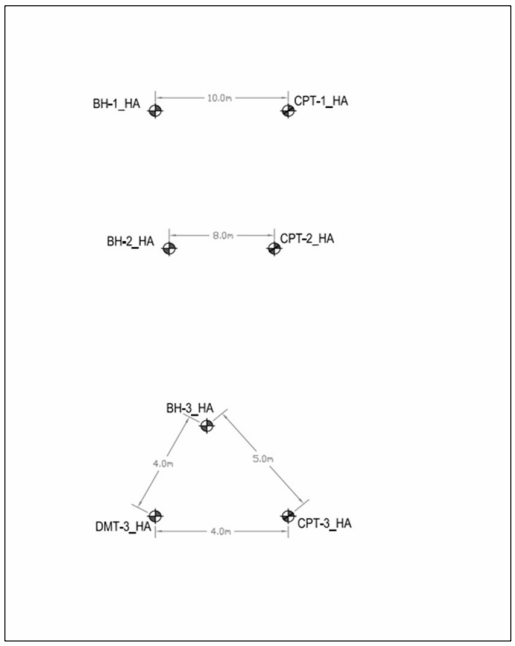

Figure: 4.8 Schematic test location plan at Site-4 (HA)

Figure: 4.9 Representative Photograph of test at site-4(HA)

4.2.5 SITE-5 (DH) : (Lat: 20.9930° N, 86.6390° E)

This study area is located at Dhamra, in the state of Odisha (OR). In this study area four numbers DMT tests and three numbers CPT tests were carried out in three different locations adjacent to three numbers of boreholes viz., BH-7_DH, BH-12_DH, BH-15_DH as shown in schematic test location plan given in Figure 4.10.

For the study purpose, four numbers DMT tests namely, DMT-1_DH, DMT-2_DH, DMT-3_DH, DMT-5_DH have been conducted upto the depth of 10.60m, 15.80m, 16.00m and 15.0m respectively. On the other hand, three numbers of CPT tests namely CPT-1_DH, CPT-2_DH, CPT-3_DH, have been carried out upto the depth of 10.60m, 11.20m and 13.40m depth respectively. A representative photograph is given in Figure 4.11.

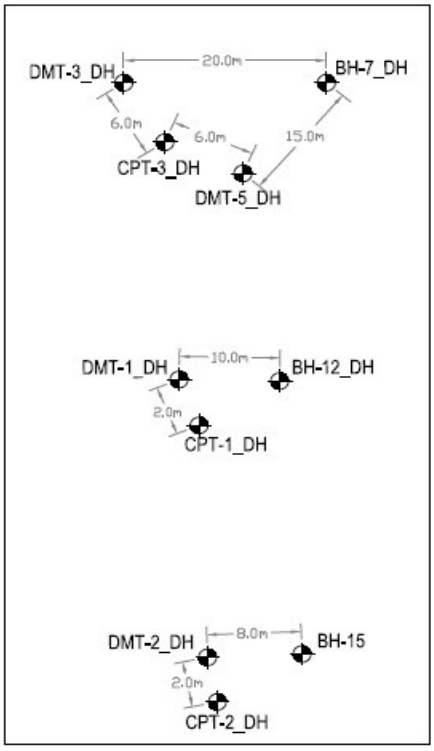

Figure: 4.10 Schematic test location plan at site-5 (DH)

Figure: 4.11 Representative Photograph of test at site-5 (DH)

4.2.6 SITE-6 (SN): (Lat: 22.4050˚N, 88.4077˚ E)

This study area is located at Chowhati, South 24 parganas, in the state of West Bengal. In this area five numbers of DMT tests and five numbers of CPT tests have been carried out adjacent to five numbers of Boreholes viz., BH-1_SN, BH-2_SN, BH-3_SN, BH-5_SN, BH-6_SN. A schematic location plan is given in Figure 4.12.

Here, five numbers DMT (i.e., DMT-1_SN, DMT-2_SN, DMT-3_SN, DMt-5_SN, DMT-6_SN) tests have been carried out upto the depth of 20.20m, 20.00m, 19.60m, 19.60m and 20.40m respectively. Contemporarily, five numbers of CPT tests have been carried out upto the depth of 10.40m, 19.20m,19.20m, 19.40m and 19.40m depth respectively. A representative photograph is given in Figure 4.13.

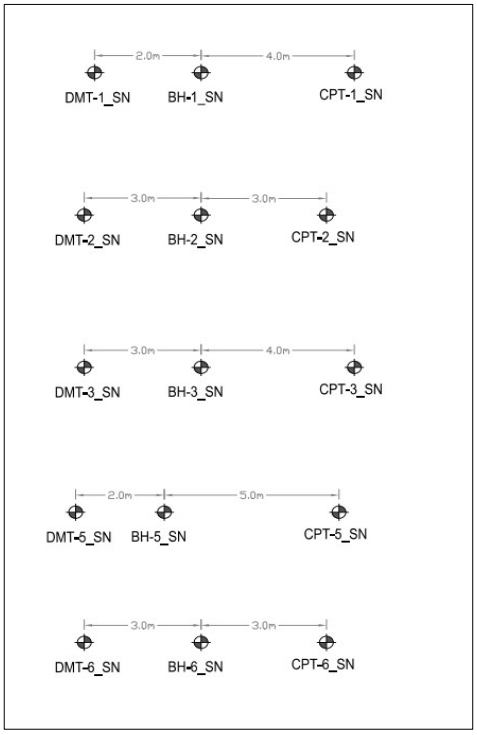

Figure: 4.12 Schematic test location plan at site-6 (SN)

Figure: 4.13 Representative Photograph of test at site-6 (SN)

4.2.7 SITE-7 (LK): (Lat: 22.6035° N, 88.4040° E)

This study area is located at Laketown area in Kolkata, WB. In this area four numbers of DMT tests four numbers of CPT tests have been carried out adjacent to four numbers of Boreholes viz., BH-1_LK, BH-3_LK, BH-4_LK, BH-5_LK. A schematic location plan is given Figure 4.14.

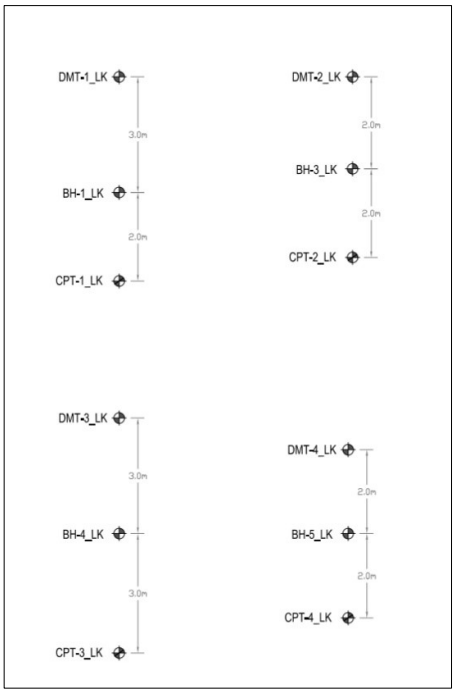

Figure: 4.14 Schematic test location plan at site-7 (LK)

Figure: 4.15 Representative Photograph of test at site-7 (LK)

Here, four numbers of DMT (i.e., DMT-1_LK, DMT-2_LK, DMT-3_LK, DMT-4_LK) tests have been carried out upto the depth of 19.80m, 18.60m, 18.60m and 19.90m respectively. Contemporarily, four numbers of CPT tests viz., CPT-1_LK, CPT-2_LK, CPT-3_LK, CPT-4_LK, have been carried out upto the depth of 19.20m,16.40m, 19.20m and 16.00m depth respectively. A representative photograph is given in Figure 4.15.

4.2.8 SITE-8 (BD): (Lat: 23.2588° N, 87.8279° E)

This study area is located at Burdwan in Purba Bardhaman district, WB. In this area six numbers of DMT tests and two numbers of CPT tests have been carried out adjacent to six numbers of Boreholes viz., BH-1_BD, BH-2_BD, BH-3_BD, BH-4_BD, BH-5_BD, BH-6_BD.

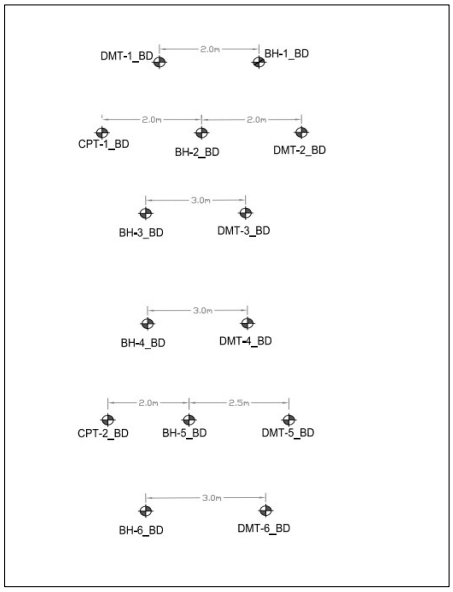

Figure: 4.16 Schematic test location plan at site-8 (BD)

Figure: 4.17 Representative Photograph of test at site-8 (BD)

In this area six numbers of DMT tests (i.e., DMT-1_BD, DMT-2_BD, DMT-3_BD, DMT-4_BD, DMT-5_BD, DMT-6_BD) have been conducted upto the maximum depth of 7.0m, 13.80m,7.80m, 7.20m, 11.0m, 9.20m respectively. Besides, two numbers of CPT tests viz., CPT-1_BD and CPT-2_BD, have been carried out upto the depth of 7.0m and 10.40m adjacent to BH-2_BD and BH-5_BD respectively. A schematic location plan is given in Figure 4.16. Also, an representative photograph of the test is given in Figure 4.17.

4.2.9 SITE-9 (VT): (Lat: 22.5483° N, Long: 88.3432° E)

This study area is located near to the Victoria Memorial of Kolkata, WB. In this area, 20 numbers of pressuremeter tests (PMT) have been conducted inside five numbers of "NX" size boreholes (diameter ≈75mm) at 5m depth interval upto the maximum depth of 20m at each borehole. The pressuremeter tests have been conducted adjacent to five numbers of SX (diameter ≈150mm) size boreholes.

In this study area, pressuremeter tests have been conducted inside the boreholes designated as BH-28A_VT, BH-29A_VT, BH-30A_VT, BH-31A_VT, BH-32A_VT adjacent to the conventional SX size boreholes namely BH-28, BH-29, BH-30, BH-31 and BH-32 respectively. A schematic layout of test location is presented in Figure 4.18. Also, the representative photograph of the test is given in Figure 4.19.

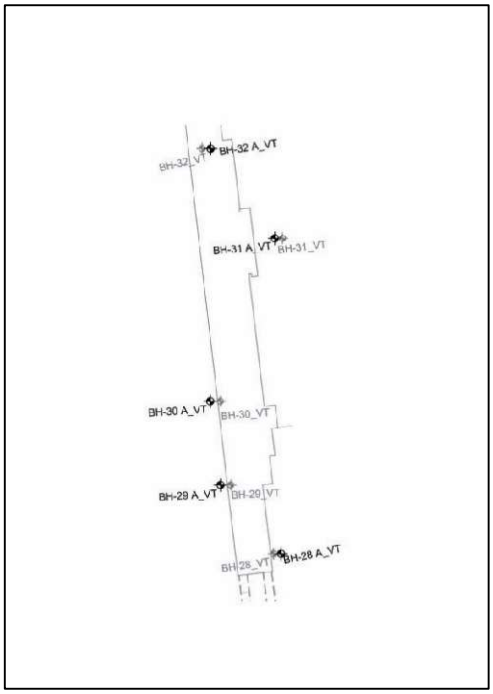

Figure: 4.18 Schematic test location plan at site-9 (VT)

Figure: 4.19 Representative photograph of test at site-9 (VT)

4.2.10 SITE-10 (PT): (Lat: 22.5170° N, Long: 88.3459° E)

This study area is located in the Park street area, Kolkata, WB. In this area, 16 numbers of pressuremeter tests (PMT), have been conducted inside four numbers of NX size boreholes at 5m depth interval upto the maximum depth of 20m at each borehole. The pressuremeter tests have been conducted adjacent to four numbers of SX size boreholes. In this study area, pressuremeter tests have been conducted inside the boreholes designated as BH-42A _PT, BH-43A_PT, BH-46A_PT and BH-47A_PT adjacent to the conventional SX size boreholes namely BH-42, BH-43, BH-46, and BH-47

respectively. A schematic layout of test location is presented in Figure 4.20. Also, the representative photograph of the test is given in Figure 4.21.

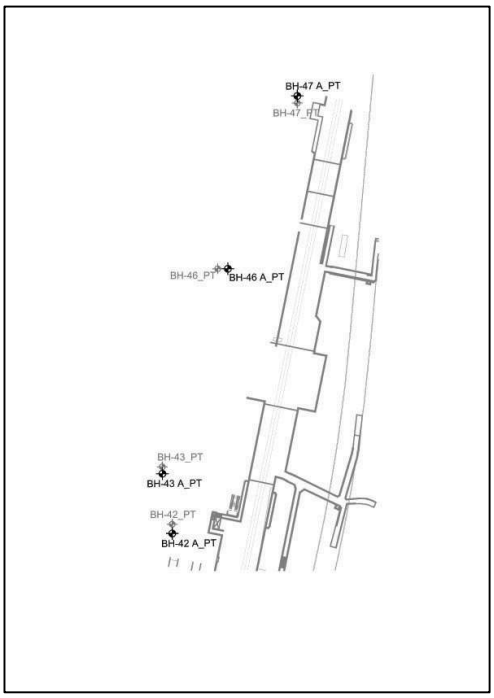

Figure: 4.20 Schematic test location plan at site-10 (PT)

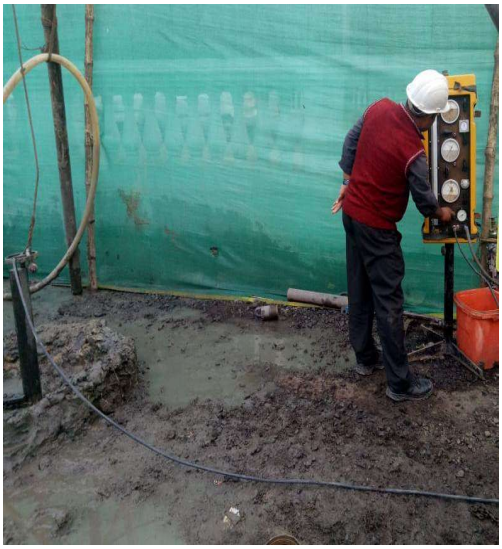

Figure: 4.21 Representative photograph of test at site-10 (PT)

4.2.11 SITE-11 (ES): (Lat: 22.5653° N, Long: 88.3519° E)

This study area is located in the Esplanade area, Kolkata, WB. In this area, 12 numbers of PMT tests have been conducted inside four numbers of NX size boreholes (diameter ≈75mm) at 5m depth interval upto the maximum depth of 20m at each borehole. The pressuremeter tests have been conducted adjacent to three numbers of SX (150mm) size boreholes.

In this study area, pressuremeter tests have been conducted inside the boreholes designated as BH-50A_ES, BH-51A_ES and BH-54A_ES and adjacent to the conventional SX size boreholes namely BH-50, BH-51 and BH-54 respectively. A schematic layout of test location is presented in Figure 4.22. Also, the representative photograph of the test is given in Figure 4.23.

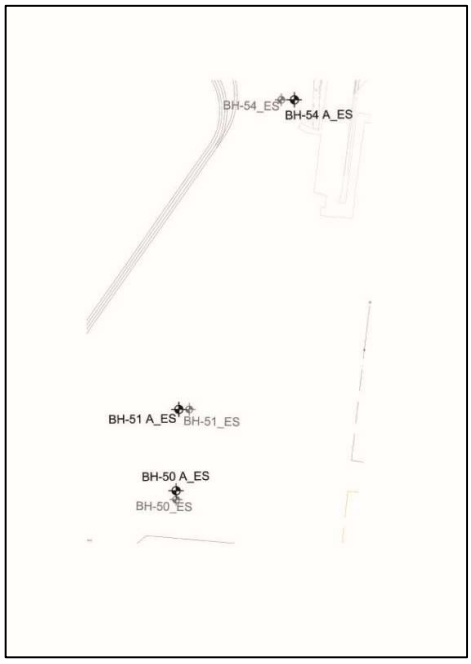

Figure: 4.22 Schematic test location plan at site-11(ES)

Figure: 4.23 Representative photograph of test at site-11 (ES)

Chapter# 5

DETERMINATION OF GEOTECHNICAL PARAMETERS AND COMPARISON OF THE SAME FROM DIFFERENT TESTS

5.1 GENERAL

In this section, focus is given on the site- wise test results obtained from the DMT, CPT and PMT tests. Also, the site- wise test results (field SPT N values along with relevant laboratory test results viz. shear parameters and index properties, conducted on collected undisturbed samples) obtained from the adjacent conventional bore-holes are presented. The DMT, CPT and PMT based sub-soil profile has been drawn and compared with the sub-soil profile predicted from the conventional boring.

The Shear strength parameters (Undrained cohesion C_u, Angle of internal friction Φ), the vertical drained constrained modulus (M_{DMT}/M_{CPT}) , sub-soil behaviour type index (I_D or I_C), Dilatometer modulus (E_D) , cone penetration resistance (q_c), sleeve friction (f_s) and field SPT N values, have been determined along depth for each site where those tests had been carried out.

Besides, at three numbers of test locations (i.e., Site-9 (VT), Site-10 (PT) and Site-11 (ES)) where PMT tests have been carried out, the Limit pressure (P_L) and Pressuremeter modulus (E_{PMT}) were determined along depth. Also in those areas, the SPT N values and undrained cohesion (C_u) were obtained from conventional soil exploration tests and results based on these were compared with those obtained from DMT, CPT and PMT tests.

Apart from this, an attempt has been made to draw a design or reference chart based on the field and laboratory test results for individual tests i.e., DMT, CPT and PMT tests. In this regard, firstly, a comparison has been made on the

selective parameters obtained from the individual DMT, CPT and PMT results with the conventional SPT N value and laboratory test results of conventional boreholes. Subsequently, relations have been formulated based on these comparisons. Finally, respective design or reference charts have been proposed. Besides, the settlement of the different type of shallow foundation (placed on cohesive soil) has been calculated by using average cone resistance (C_{KD}) from CPT tests, based on the empirical relation as detailed before. In this regard, the settlement of the same footing has been analysed based on M_{DMT} (by using DMT settlement software) estimated from the adjacent DMT tests and also from the numerical modeling on Plaxis 2D (ver.16) software. Last but not the least, the settlement value predicted by using C_{KD}, are compared with those obtained from other methods.

5.2 SUB-SOIL PROFILE

For all test locations, identification of sub-soil profile for the conventional borehole, has been drawn based on the laboratory tests results (conducted on undisturbed samples collected from the conventional bore-hole) along with the visual inspection during SPT tests. Contemporarily, for DMT and CPT tests, identification of sub-soil profile, are made from the value of I_D and I_C respectively. Apart from this, at PMT test locations, the sub-soil profile has been identified from the adjacent conventional boreholes alongwith the visual inspection during the PMT tests.

5.2.1 SITE-1 (HC): (Lat: 22.5693^o N, Long: 88.3434^{o}E)

In High Court test location, it is observed that the top layer consists of rubbish and brickbats with an average depth up to 3.0m below ground level. This top

layer is followed by soft/ firm brownish grey silty clay/clayey silt (Layer-I) with an average depth of 3.0m. Layer-II starts from 6m below the ground level with soft dark grey silty clay/ clayey silt along with organic matter and decomposed vegetation having average depth of 9.0m. A representative sub soil profile is given in Figure 5.1.

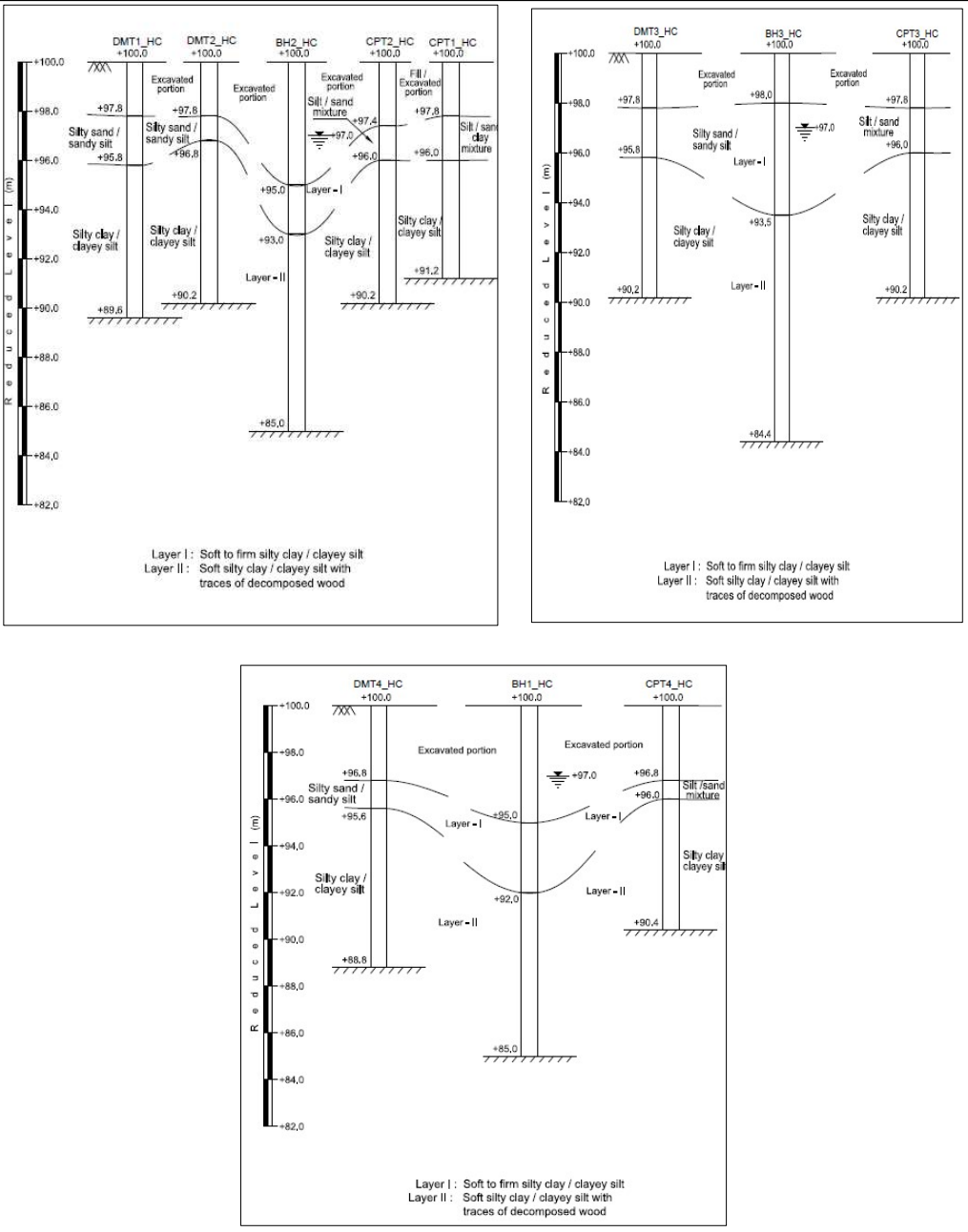

Figure: 5. 1 Sub-Soil profile of Site-1 (HC)

5.2.2 SITE-2 (PB): (Lat: 22.5701^{o} N, Long: 88.3437^{o}E)

In this site (i.e., Site-2 (PB)), it has been observed that the top layer consists of rubbish and brickbats with an average depth up to 3.0 m below ground level. This top layer is followed by soft/ firm brownish grey silty clay/clayey silt (Layer-I) with an average depth of 3.0 m. Layer-II starts from 6m below the ground level with soft dark grey silty

clay/ clayey silt along with organic matter and decomposed vegetation having average depth of 10.0 m. Figure 5.2, demonstrates the subsoil profile.

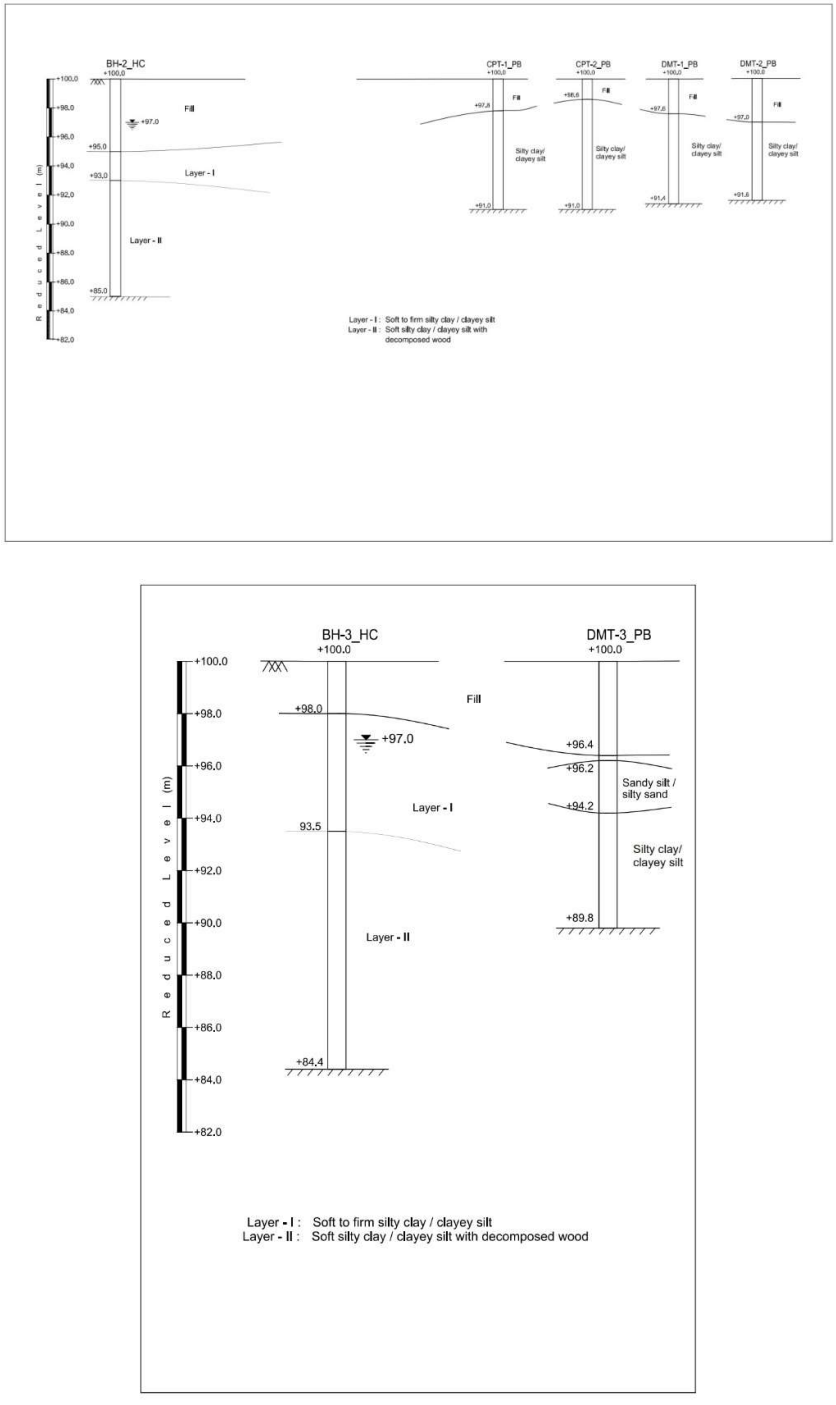

Figure: 5.2 Sub-Soil profile of site-2 (PB)

5.2.3 SITE-3 (RJ): (Lat: 22.5776°N, Long: 88.4640°E)

In this test location, it has been identified that the top layer consists of brickbats and kankars with an average depth up to 1.5 m below ground level. This top layer is followed by firm grey silty clay/clayey silt (Layer-I) upto the average depth of 3.0m. This Layer-I is underlain by soft grey silty clay / clayey silt with occasional presence of decomposed wood (Layer II) with an average depth of 9.0 m below Layer-1. This layer is under-lain by silty clay/clayey silt with occasional traces of calcareous nodules (i.e., Layer III) with an average depth of 4.0 m below Layer I & II. This layer is finally followed by stiff silty clay (Layer IV) (with an average thickness of 1.0m) and fine sand/sandy silt (Layer V) (with an average thickness of 3.5 m). Figure 5.3 demonstrates the subsoil profile.

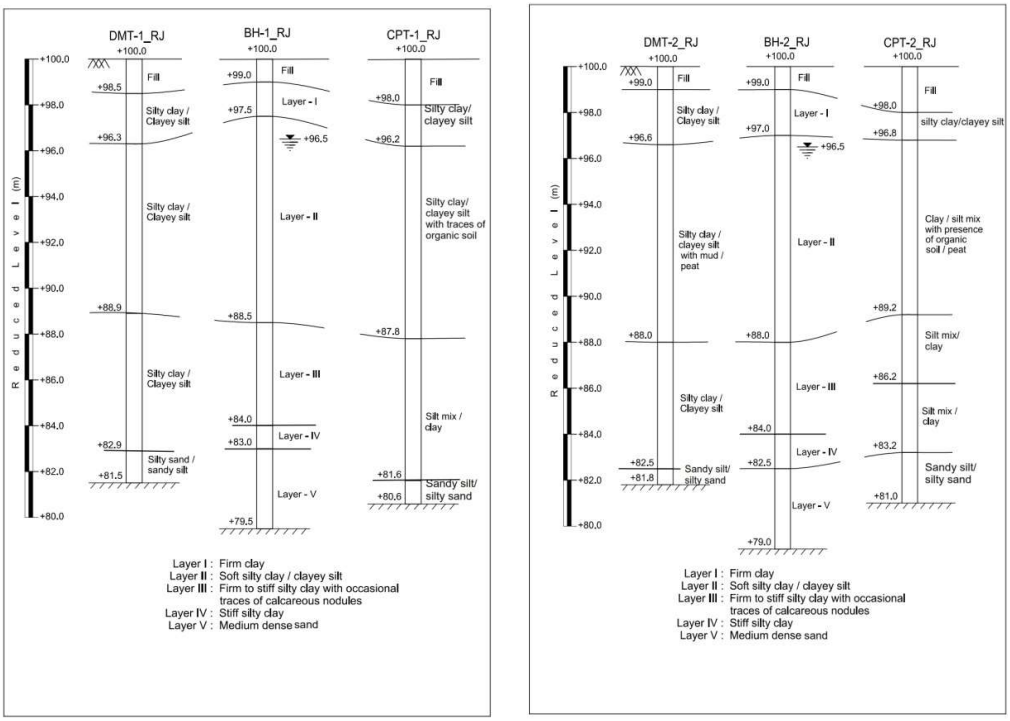

Figure: 5.3 Sub-Soil profile of site-3 (RJ)

5.2.4 SITE-4 (HA): (Lat: 22.0666^{o}N, Long: 88.1145^{o}E)

At Haldia test location, it has been observed that the top layer consists of sandy silty clay with brick bats etc. with an average depth up to 1.4 m below ground level. This top layer is followed by medium stiff / soft brownish grey to grey silty clay (Layer-I and Layer-II) with an average depth of 6.0 m. This layer is followed by loose grey clayey sandy silt (Layer-III) with an average depth of 3.0 m. Finally, this layer is followed by soft grey silty clay with varying percentages of decomposed wood/ organic matter and calcareous nodules (Layer-IV and Layer-V) upto the termination depth. The soil profile is shown in Figure 5.4.

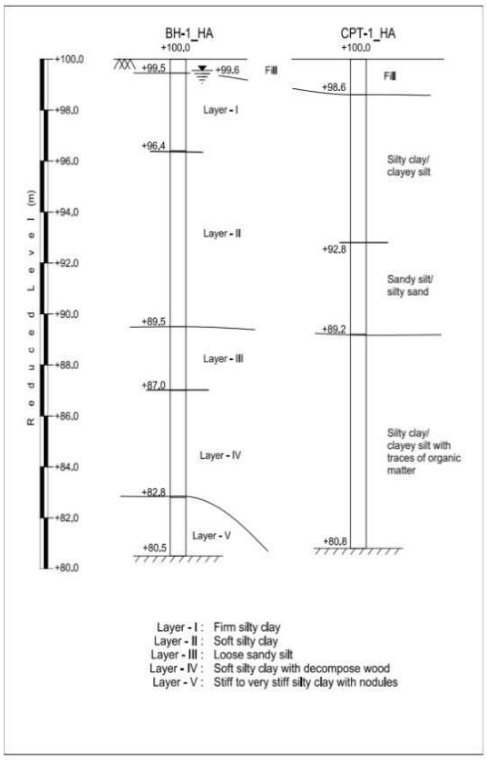

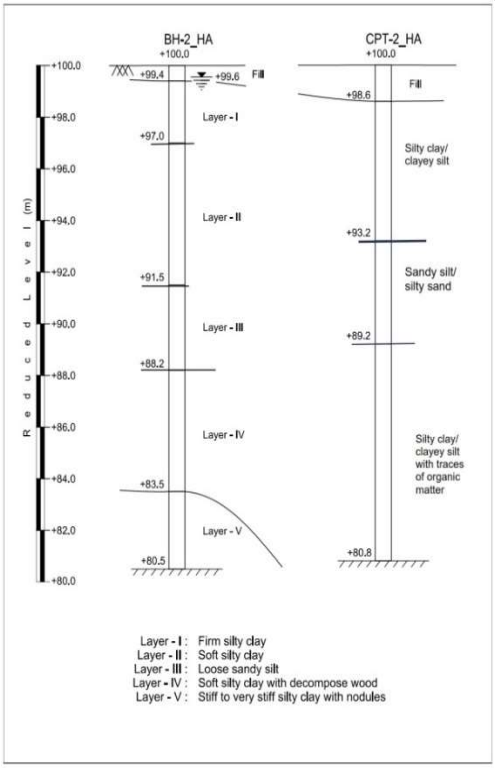

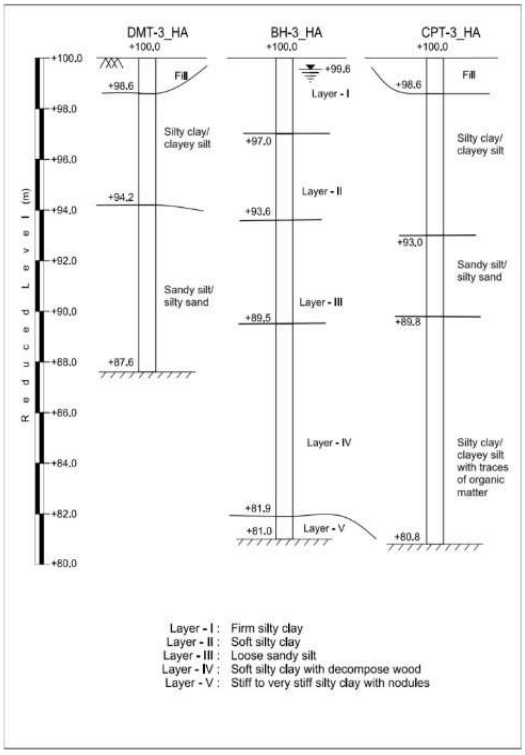

Figure: 5.4 Sub-Soil profile of Site-3 (HA)

5.2.5 SITE-5 (DH): (Lat: 20.9930° N, 86.6390° E)

In Dhamra test site (i.e., Site-5 (DH)), DMT and CPT tests have been carried out in three different locations adjacent to the BH-7_DH, BH-12_DH and BH-15_DH boreholes.

In BH-7_DH bore hole location, it has been identified that the top layer (fill) consists of brick bats, moorum with kankars with a depth of 1.0m below ground level. This layer is followed by very soft/soft silty clay (Layer-I) with a depth of 9.0m consisting of 0.5m pocket of sandy silty clay. This Layer-I is underlain by medium dense sand (Layer-IV). The sub soil profile is presented in Figure 5.5(a).

Based on the laboratory test results and visual identification of soil samples collected from boreholes, it has been found that there are four numbers of soil layers exist in BH-12_DH location. It has been observed that the top layer consists of reddish brown silty clayey sand with moorum, kankars etc. with an average depth up to 1.0 m below ground level. This top layer is followed by very soft / soft silty clay (Layer-I) with an average depth of 1.0 m. This layer (i.e., Layer- I) is underlain by very soft to soft silty clay with decomposed wood (Layer II) (consisting of 1.5m thick band of silty clayey sand) upto the termination depth. The sub soil profile is presented in Figure 5.5(b).

In BH-15_DH location, it has been observed that the top soil layer (Fill) consisting of moorum, brick bats etc. with a depth of 2.0m below ground level. This layer is followed by Layer-I, comprising very soft/ soft silty clay upto a depth of 8.5 m with two pockets consisting of sandy silt. This Layer-I is underlain by stiff silty clay (Layer-III) upto the termination depth. The sub soil profile is shown in Figure 5.5(c).

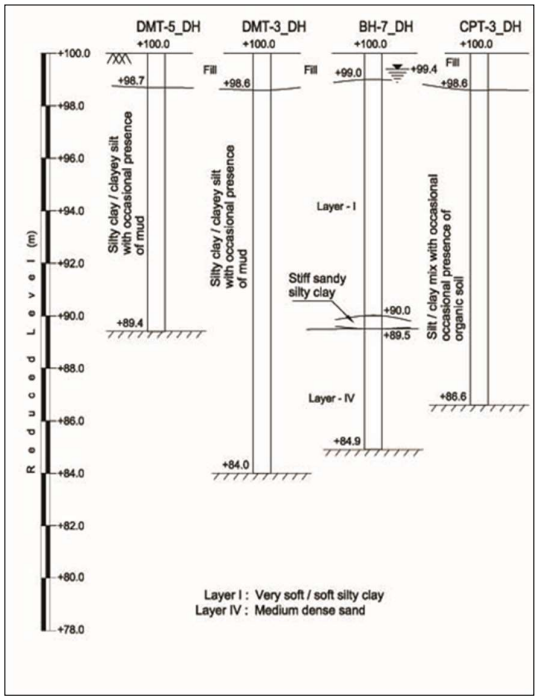

(a)

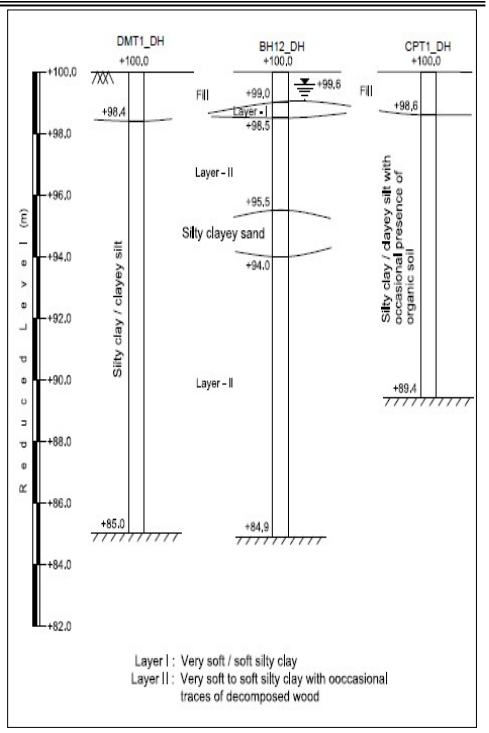

(b)

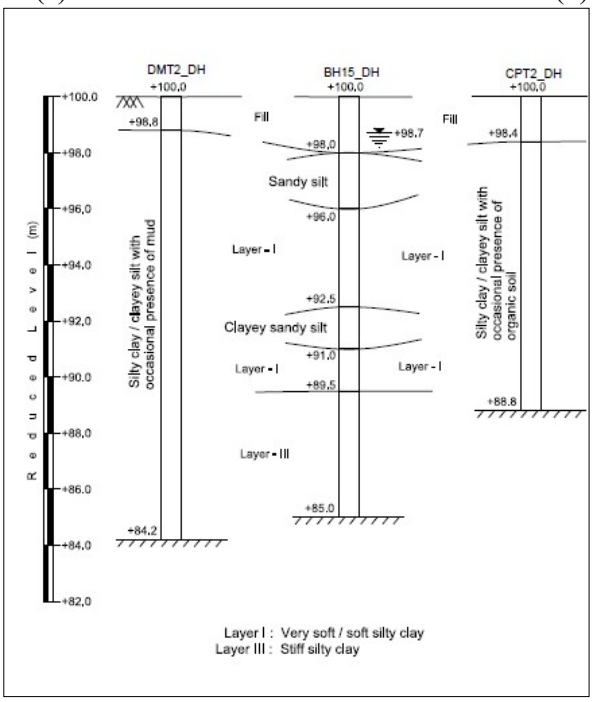

(c)

Figure: 5.5 Sub-Soil profile of Site-5 (DH), (a) BH-7_DH location, (b) BH-12_DH location and (c) BH-15_DH locations

5.2.6 SITE-6 (SN): (Lat: 22.4050°N, 88.4077° E)

In Sonarpur site, it has been observed that the top layer (fill) consists of clayey silt mixed with brick pieces, roots etc. upto an average depth of 0.5m below ground level. This fill layer is followed by soft to medium silty clay to clayey silt (Layer-I) with an average depth of 3m. This Layer-I is underlain by Layer-II comprising medium to very dense sandy silt to silty sand upto the termination depth. The sub-soil profile is shown in Figure 5.6.

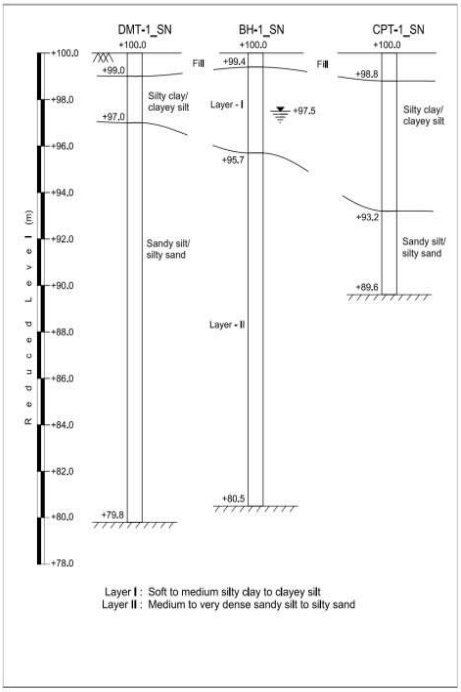

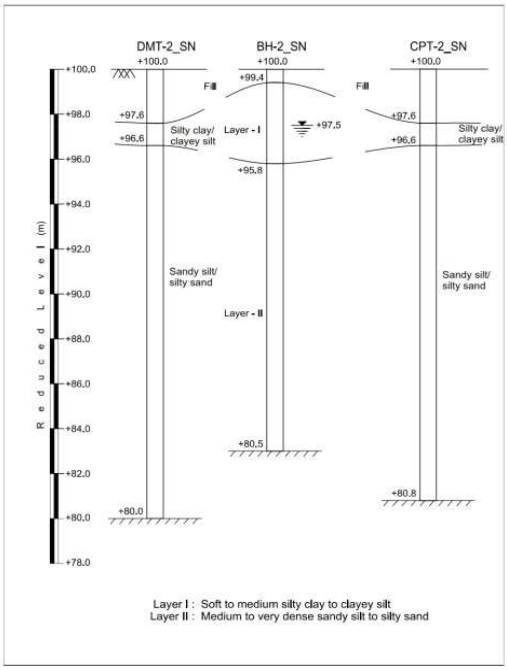

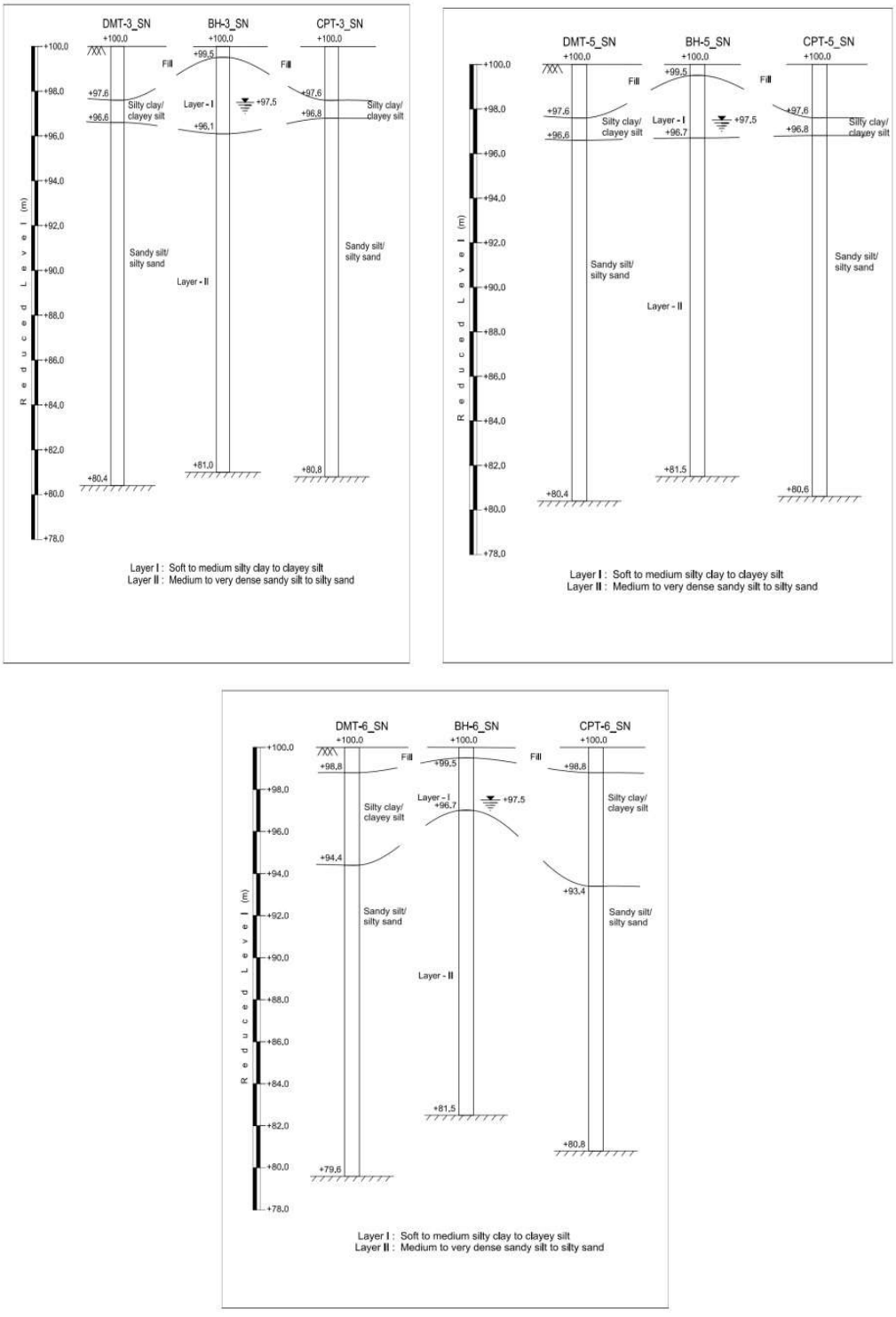

Figure: 5.6 Sub-Soil profile of Site-6 (SN)

5.2.7 SITE-7 (LK): (Lat: 22.6035° N, 88.4040° E)

In Laketown site (i.e., Site-7 (LK)), it has been observed that the top layer (fill) consists of clayey silt mixed with brick bats, roots etc. with an average depth of 0.80m below ground level. This fill layer is followed by Layer-I consisting of firm silty clay with an average depth of 2.5m. This Layer-I is underlain by Layer-II consisting of very soft/soft silty clay containing decomposed wood with an average depth of 4.0m. The Layer-II is underlain by Layer-III consisting of very stiff/stiff clayey silt/clayey sandy silt with an average depth of 3.0m. Layer-III is underlain by Layer-IV consisting of dense/very dense grey silty fine sand with traces of mica upto the termination depth. The sub-soil profile is shown in Figure 5.7.

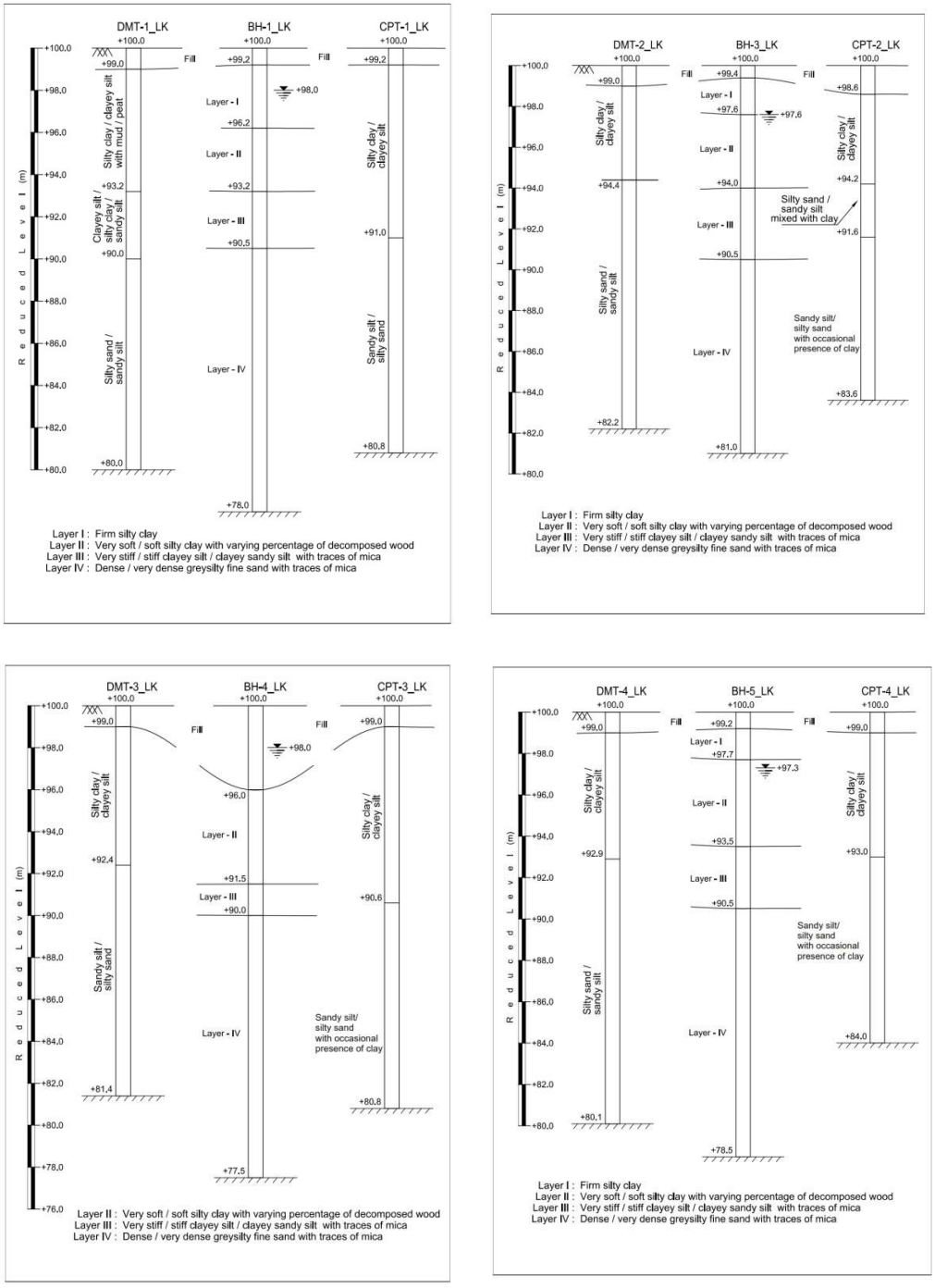

Figure: 5.7 Sub-Soil profile of Site-7 (LK)

5.2.8 SITE-8 (BD): (Lat: 23.2588°N, 87.8279°E)

In Burdwan test site (i.e., Site-8 (BD)), it has been observed that the top layer (Fill) consists of grey to black stone chips, ash fills, sand and coal having an average thickness

of 1.4 m below ground level. This filling layer is followed by medium stiff brown/brownish grey silty clay/clayey silt with kankars and ferruginous spots (Layer-I) with an average depth of 3.0 m. This layer is followed by stiff/very stiff mottled blue/yellowish-grey sandy silt clay with kankars & rusty sports (Layer-II) with an average depth of 3.4 m. This layer is followed by dense/very dense yellow/yellowish brown silty sand with traces of mica (Layer-III) with an average depth of 3.5m. This layer is followed by a very stiff silty clay (Layer-IV) upto termination depth. The sub-soil profile is shown in Figure 5.8.

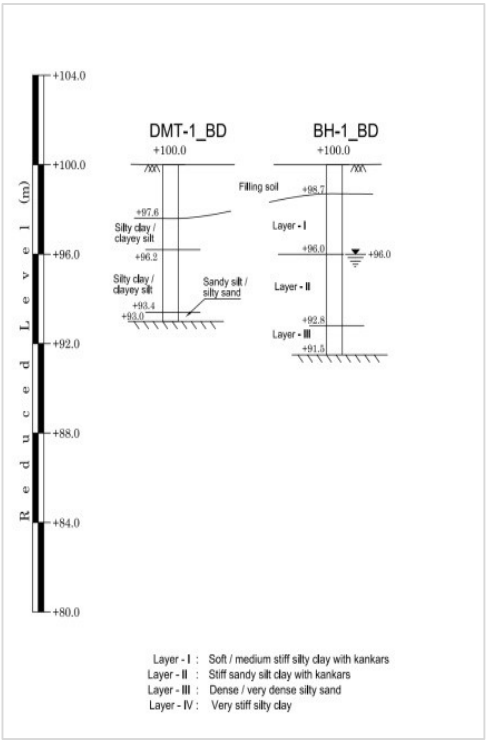

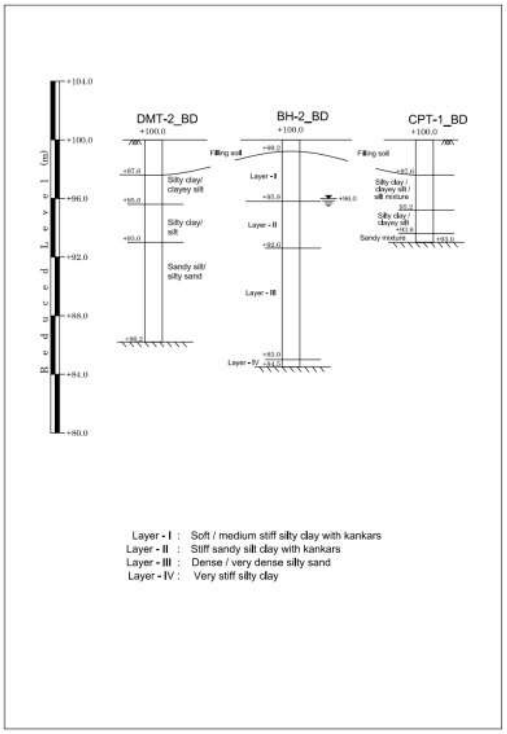

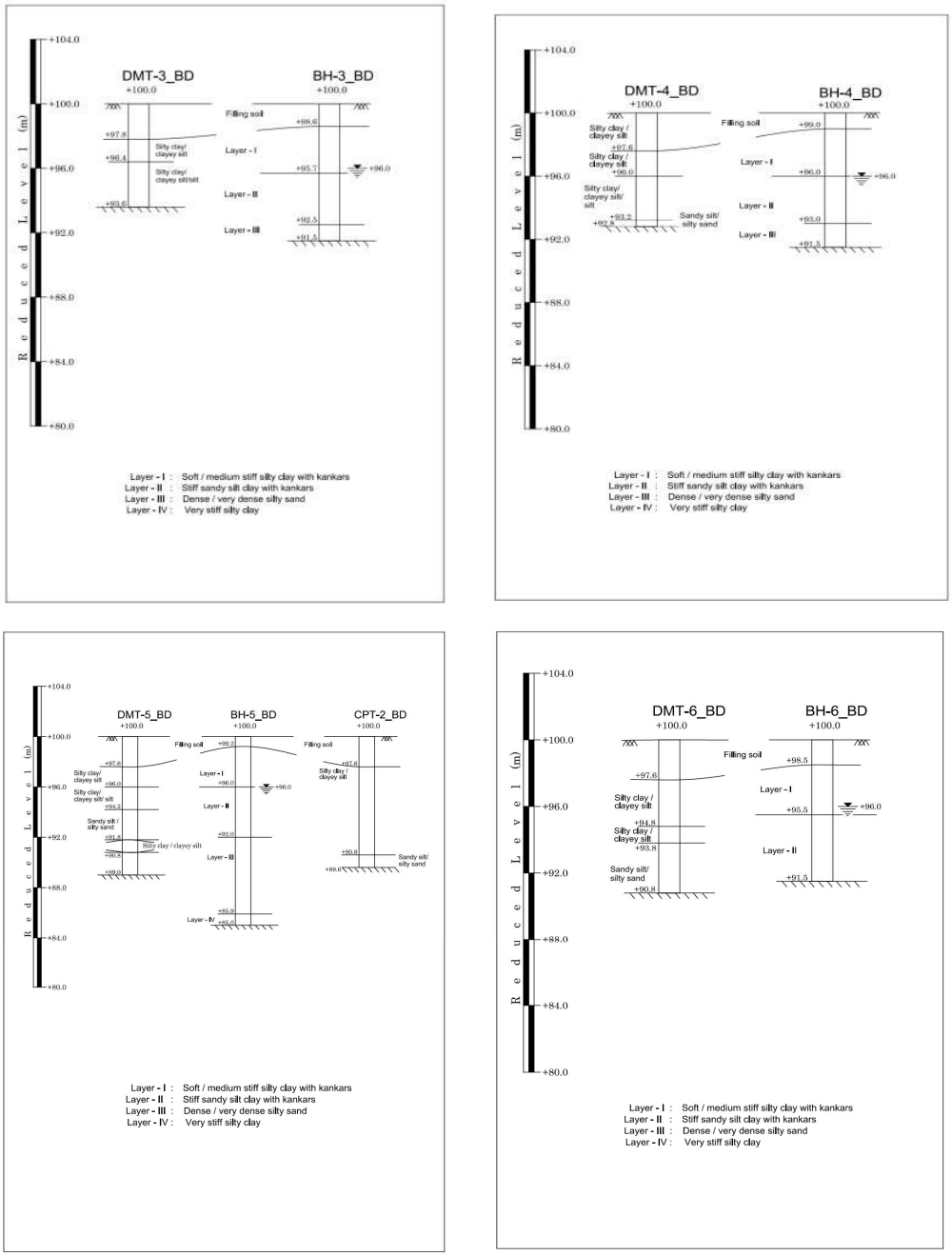

Figure: 5. 8 Sub-Soil profile of Site-8 (BD)

5.2.9 SITE-9 (VT): (Lat: 22.5483° N, Long: 88.3432° E)

At this test site (i.e., Site-9 (VT)), the top soil comprises sandy silty clay / silty clay /clayey sand/ clayey silt with kankars, roots, brick pieces etc. with an average depth of 1.0m. This top soil layer is followed by Layer-IA consisting of soft / firm silty clay with an average depth of 6m. This Layer-IA is underlain by Layer-IB which consists of firm

/ stiff silty clay with high silt content / clayey silt / loose sandy silt with traces of clay with an average depth of 5.0m. The Layer-IB is underlain by Layer-IVA consisting of medium dense / dense silty sand upto the termination depth. The sub-soil profile is shown in Figure 5.9.

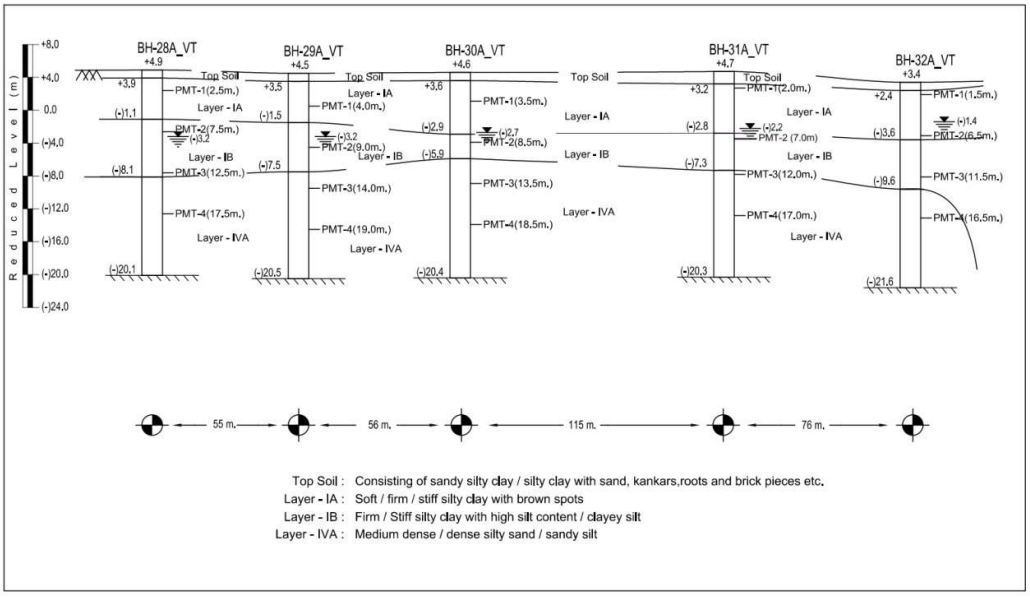

Figure: 5. 9 Sub-Soil profile of Site-9 (VT)

5.2.10 SITE-10 (PT): (Lat: 22.5170° N, Long: 88.3459° E)

In this study area (i.e., Site-10 (PT)), the top layer (Layer-IA) comprises soft / firm silty clay with an average depth of 4.0m. This layer is followed by Layer-IB consisting of firm / stiff silty clay with high silt content / clayey silt / loose sandy silt with traces of clay with an average depth of 4.0m. This Layer-IB is underlain by Layer-II comprises soft / firm silty clay / clayey silt with varying percentage of decomposed wood with an average depth of 5.50m. This Layer-II is underlain by Layer-III consisting of firm / stiff to very stiff silty clay with occasional traces of calcareous nodules with an average depth of 4.50m. This Layer-III is underlain by Layer-IV consisting of stiff / very stiff / hard silty clay with high silt content / clayey silt with an average depth of 3.0m. This

soil layer (Layer-IV) is underlain by stiff / very stiff / hard silty clay with brown spots (Layer-V) upto the termination depth. The sub-soil profile is shown in Figure 5.10.

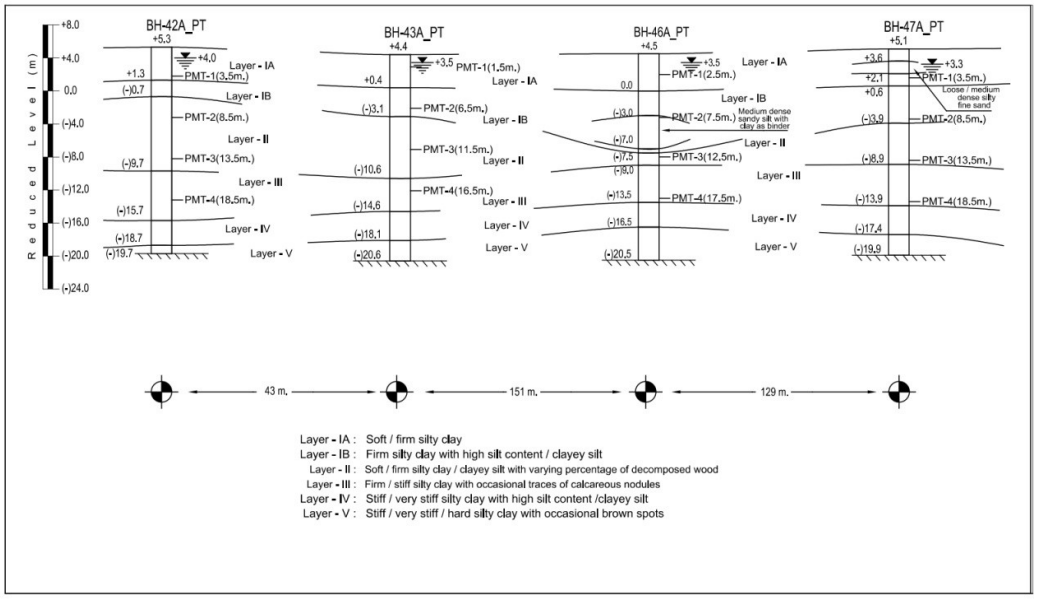

Figure: 5.10 Sub-Soil profile of Site-10 (PT)

5.2.11 SITE-11 (ES): (Lat: 22.5653° N, Long: 88.3519° E)

In this site area (i.e., Site-11 (ES)), only at BH-54A_ES, it has been observed that the top soil (fill) comprises sandy silty clay / silty clay / clayey sand /clayey silt with kankars, roots, brick pieces etc. with a depth of 1.50m below ground level whereas, in other two numbers of boreholes (i.e., BH-50A, BH-51A) there was no filling soil observed on that depth. The Layer-IA consists of soft / firm silty clay with an average depth of 2.50m. This Layer-IA is followed by Layer-IB consists of firm / stiff silty clay with high silt content / clayey silt / loose sandy silt with an average depth of 2.50. This layer (Layer-IB) is underlain by Layer-II, consisting of soft / firm silty clay / clayey silt containing of varying percentage of decomposed wood with an average depth of 11.0m. This layer (Layer-II) is underlain by Layer-III, and consists of firm / stiff to very stiff silty clay with occasional traces of calcareous nodules with an average depth of 4.50m. This Layer-III is underlain by stiff / very stiff / hard silty clay with high silt content /

clayey silt (Layer-IV) with an average depth of 4.0m. This Layer-IV is underlain by stiff / very stiff / hard silty clay (Layer-V) upto the termination depth. The sub-soil profile is shown in Figure 5.11.

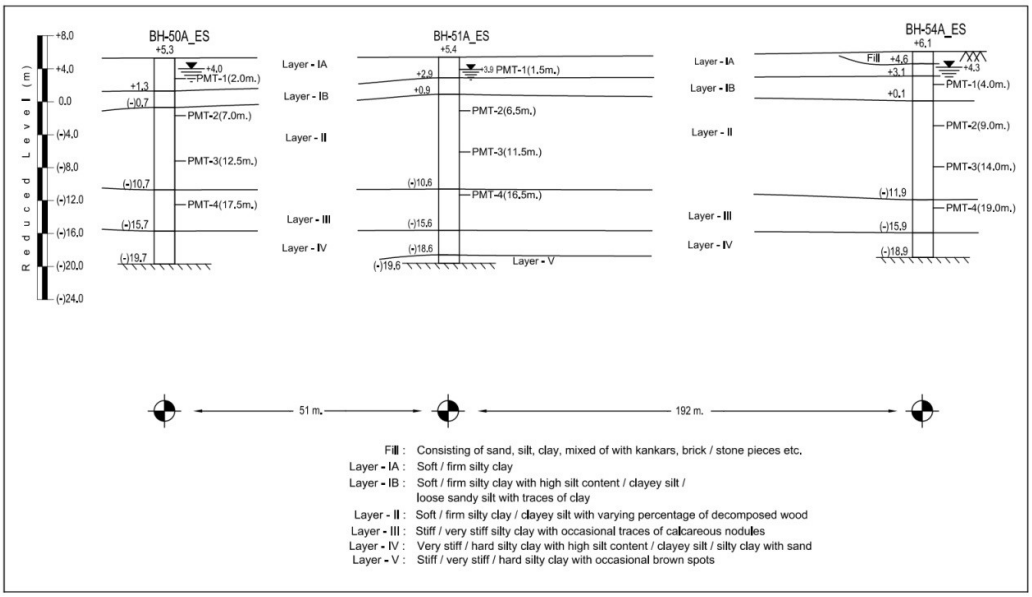

Figure: 5. 11 Sub-Soil profile of Site-11 (ES)

5.3 IN-SITU TEST RESULTS

In this section, summary of all the geotechnical parameters with depth are presented for each test location.

5.3.1 OBSERVED (FIELD) SPT N VALUE (N_{OB})

At each test location, the variation of SPT N (conducted in adjacent boreholes) values has been plotted along depth.

In Site-1 (HC), the variation of SPT N values along depth is presented in Figure 5.12.

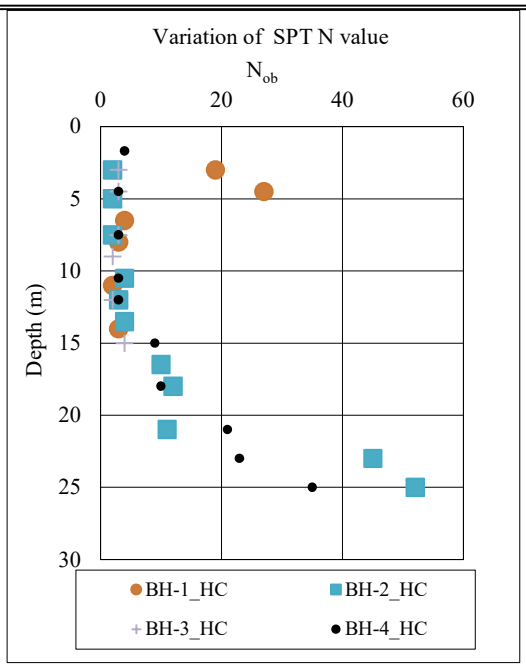

Figure: 5. 12 Variation of $_{Nob}$ along depth for Site-1 (HC)

At Site-2 (PB), two numbers of boreholes namely BH-2_HC and BH-3_HC, has been considered for the study purpose. The variation of SPT N values along depth is presented in Figure 5.13.

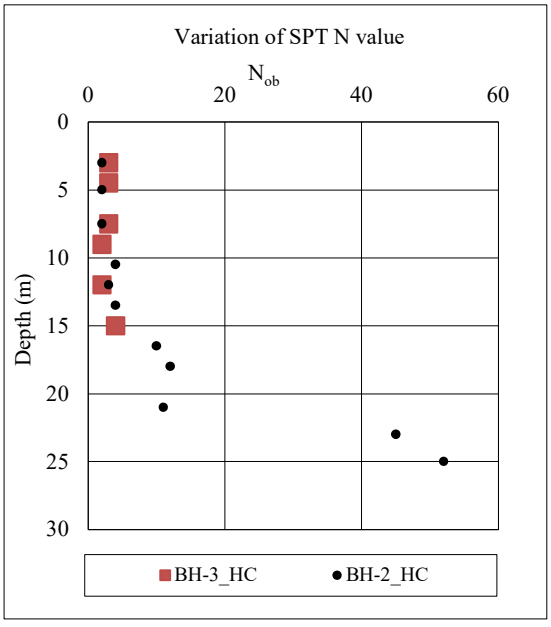

Figure: 5. 13 Variation of $_{Nob}$ along depth for Site-2 (PB)

At Site-3 (RJ), two numbers of boreholes (namely BH-1_RJ and BH-2_RJ) has been considered for the study purpose. The variation of SPT N value along depth is presented in Figure 5.14.

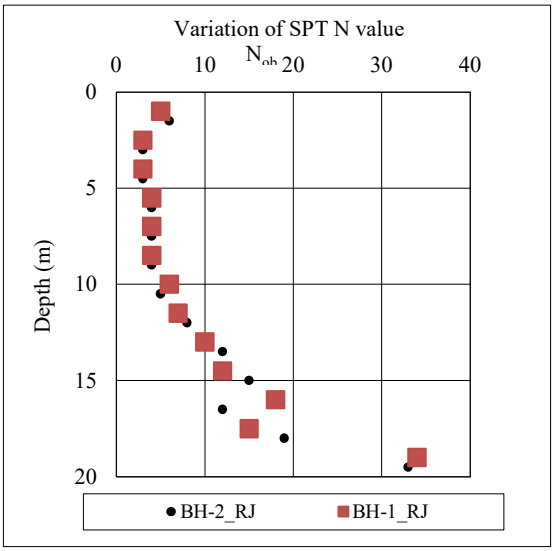

Figure: 5. 14 Variation of N_{ob} along depth for Site-3 (RJ)

At Site-4 (HA), three numbers of boreholes viz. BH-1_HA, BH-2_HA and BH-3_HA) have been considered for the study purpose. The variation of SPT N value along depth, is presented in Figure 5.15.

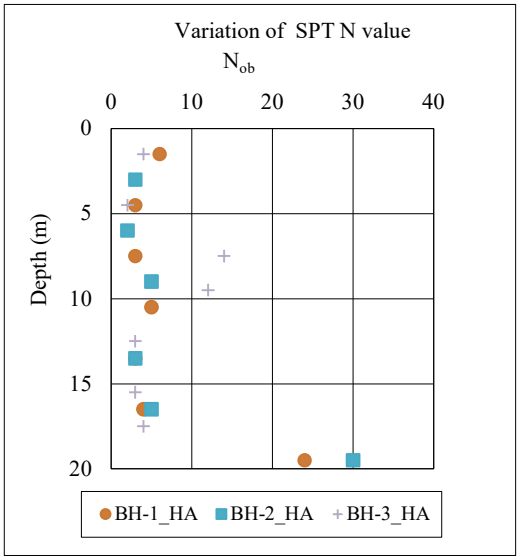

Figure: 5.15 Variation of N_{ob} along depth for Site-4 (HA)

At Site-5 (DH), three numbers of boreholes viz., BH-7_DH, BH-12_DH and BH-15_DH have been considered for the study purpose. The variation of SPT N value along depth, is presented in Figure 5.16.

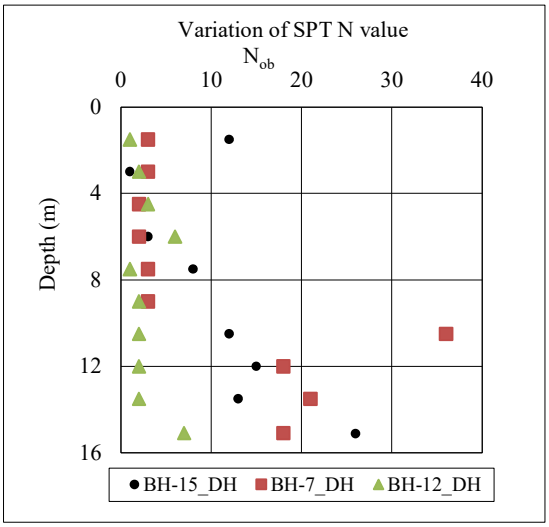

Figure: 5. 16 Variation of N_{ob} along depth at Site-5 (DH)

At Site-6 (SN), five number of boreholes (namely BH-1_SN, BH-2_SN, BH-3_SN, BH-5_SN and BH-6_SN) have been considered for the study purpose. The variation of SPT N value along depth, is presented in Figure 5.17.

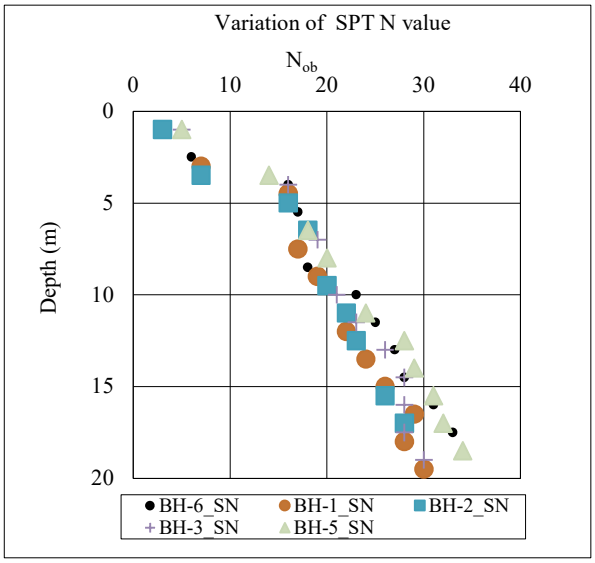

Figure: 5. 17 Variation of N_{ob} along depth at Site-6 (SN)

At Site-7 (LK), three number of boreholes viz., BH-1_LK, BH-2_LK, BH-3_LK, BH-4_LK and BH-5_LK, have been considered for the study purpose. The variation of SPT N value along depth, is presented in Figure 5.18.

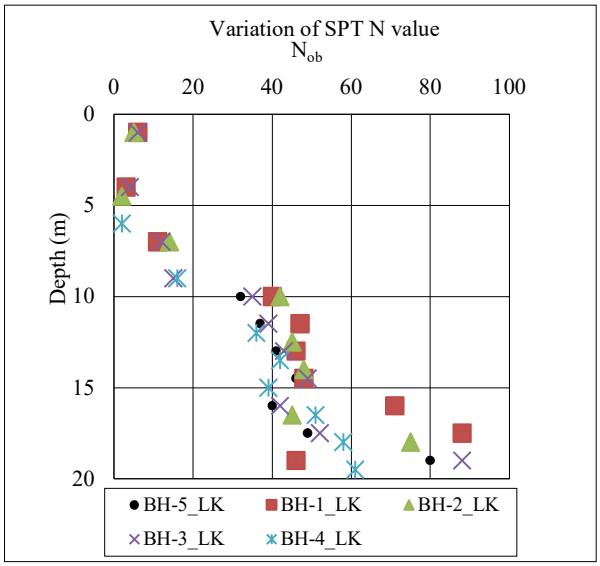

Figure: 5. 18 Variation of N_{ob} along depth at Site-7 (LK)

At Site-8 (BD), six number of boreholes viz., BH-1_BD, BH-2_BD, BH-3_BD, BH-4_BD, BH-5_BD and BH-6_BD) have been considered for the study purpose. The variation of SPT N value along depth is presented in Figure 5.19.

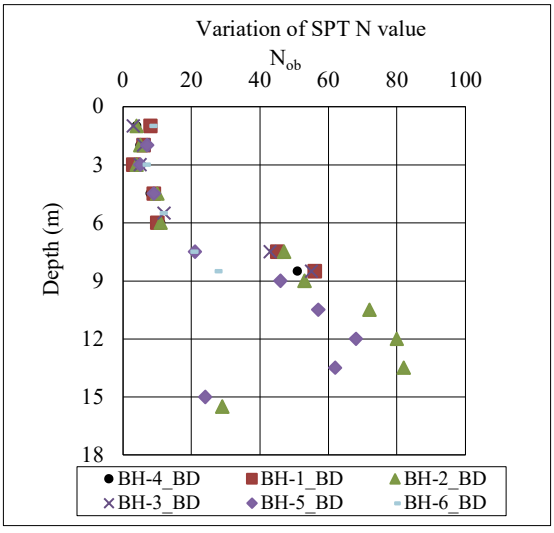

Figure: 5. 19 Variation of N_{ob} along depth at Site-8 (BD)

At Site-9 (VT), In five numbers of boreholes (namely BH-28A_VT, BH-29A_VT, BH-30A_VT, BH-31A_VT and BH-32A_VT) have been considered for the study purpose. The variation of SPT N value along depth, is presented in Figure 5.20.

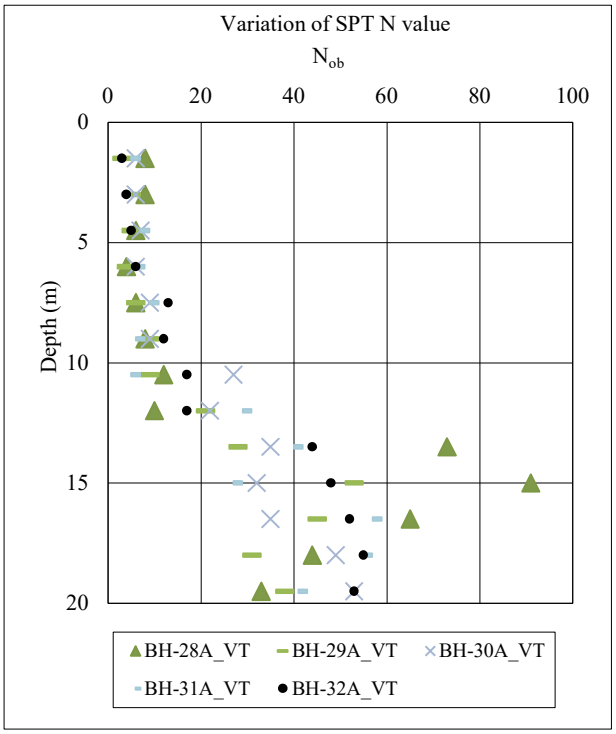

Figure: 5. 20 Variation of N_{ob} along depth at Site-9 (VT)

At Site-10 (PT), four number of boreholes viz., BH-42A_PT, BH-43A_PT, BH-46A_PT and BH-47A_PT have been considered for the study purpose. The variation of SPT N value along depth, is represented in Figure 5.21.

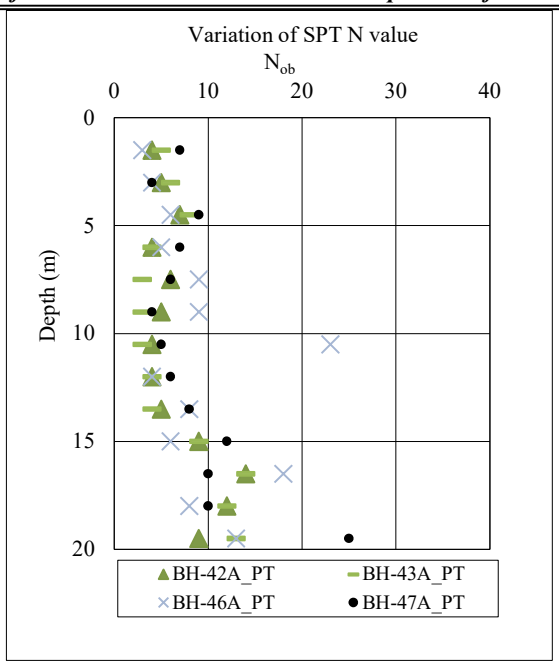

Figure: 5. 21 Variation of N_{ob} along depth at Site-10 (PT)

At Site-11 (ES), three numbers of boreholes viz., BH-50A_ES, BH-51A_ES and BH-54A_ES, have been considered for the study purpose. The variation of SPT N value along depth is presented in Figure 5.22.

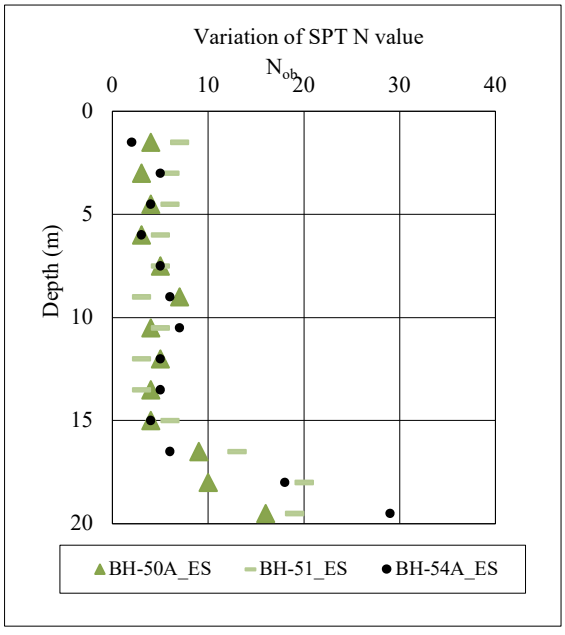

Figure: 5. 22 Variation of N_{ob} along depth at Site-11 (ES)

5.3.2 UNDRAINED COHESION (C_u)

At eight numbers of test locations, where DMT and CPT tests have been carried out, the undrained cohesion (C_u) is estimated from CPT and DMT tests. Also, standard laboratory triaxial (UU) tests have been carried out on undisturbed samples collected from adjacent boreholes for comparison purpose. At eight test locations, the value of undrained cohesion (C_u) estimated from DMT and CPT tests, are found to be consistent with UU test results.

It has been observed that the value of undrained cohesion (C_u) estimated from DMT test are closer to the value estimated from laboratory triaxial (UU) test results. The possible reason is due to less disturbance of the sub-soil during the penetration of Dilatometer blade into the soil as suggested by Marchetti (Marchetti 1980). Besides, estimated undrained cohesion (C_u) from CPT tests lie at higher side compared to other two set of tests (i.e., DMT and Laboratory triaxial UU test) owing to higher influence zone of CPT cone during the penetration (Robertson and Cabal 2015).

Site wise, variation of undrained cohesion (C_u) along depth are plotted in Figure 5.23 to 5.32.

Besides, at other three sites viz., Site-9 (VT), Site-10 (PT) and Site-11 (ES), the undrained cohesion (C_u) has been estimated from the laboratory triaxial (UU) tests conducted on collected undisturbed samples from adjacent boreholes. The variation of (C_u) are plotted along depth (Figure 5.33 to 5.35).

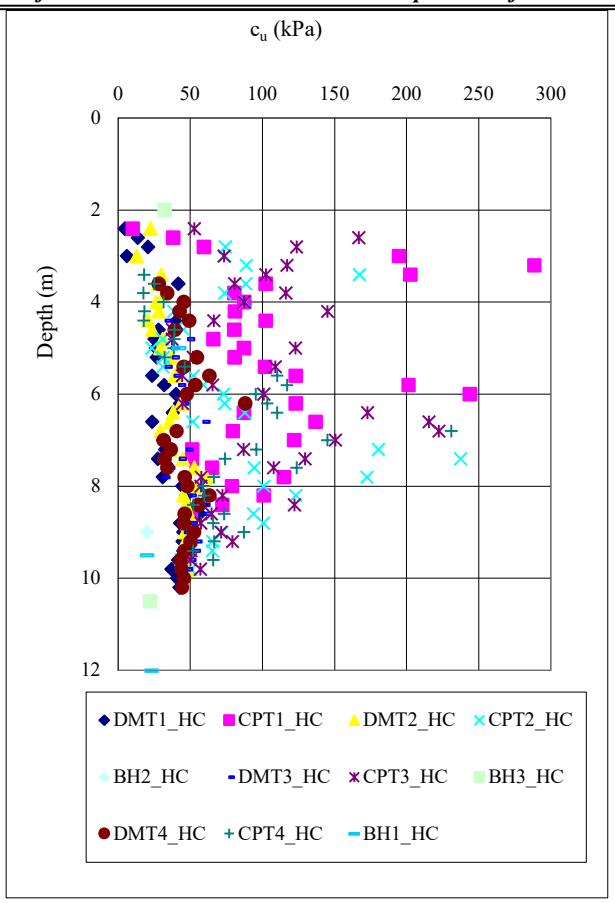

Figure: 5. 23 Variation of undrained cohesion (C_u) along depth for DMT-1_HC, DMT-2_HC, DMT3_HC, DMT-4_HC, CPT-1_HC, CPT-2_HC, CPT-3_HC, CPT-4_HC, BH-1_HC, BH-2_HC, and BH3_HC test points at Site-1(HC)

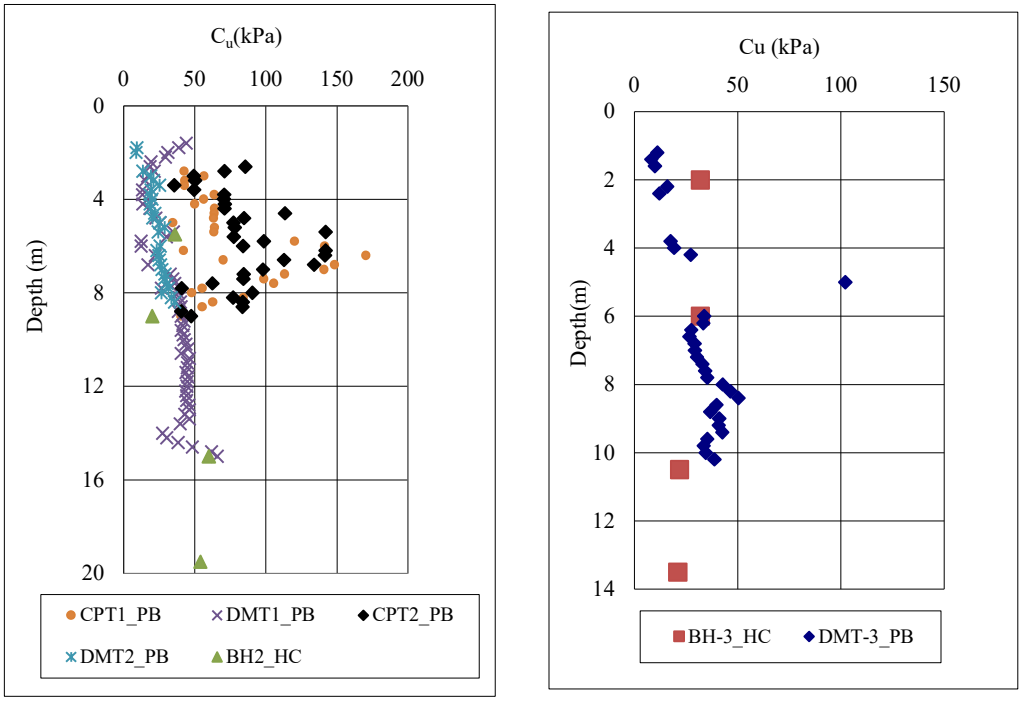

Figure: 5. 24 Variation of undrained cohesion (C_u) along depth for DMT1_PB, DMT2_PB, CPT-1_PB,CPT-2_PB, BH-2_PB,DMT3_PB and BH3_HC test points at Site-2 (PB)

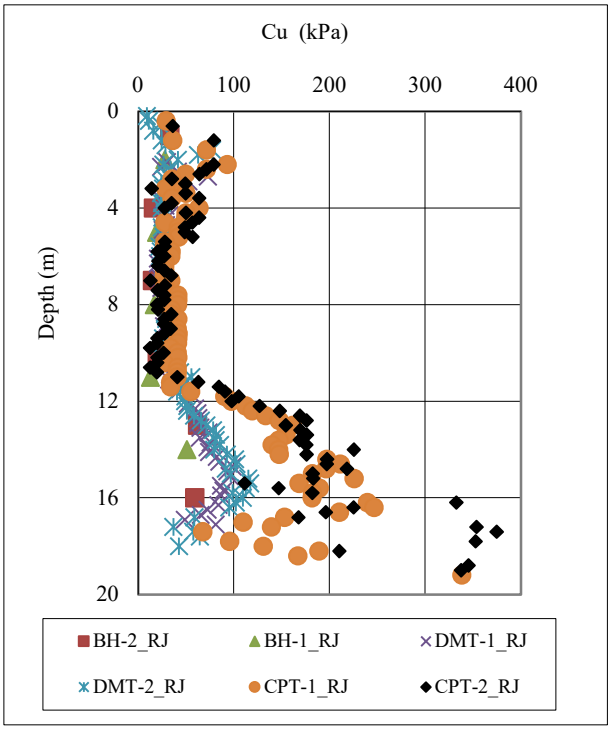

Figure: 5. 25 Variation of undrained cohesion (C_u) along depth for DMT-1_RJ, DMT-2_RJ, CPT-1_RJ, CPT-2_RJ_ and BH-1_RJ, BH-2_RJ test points at Site-3 (RJ)

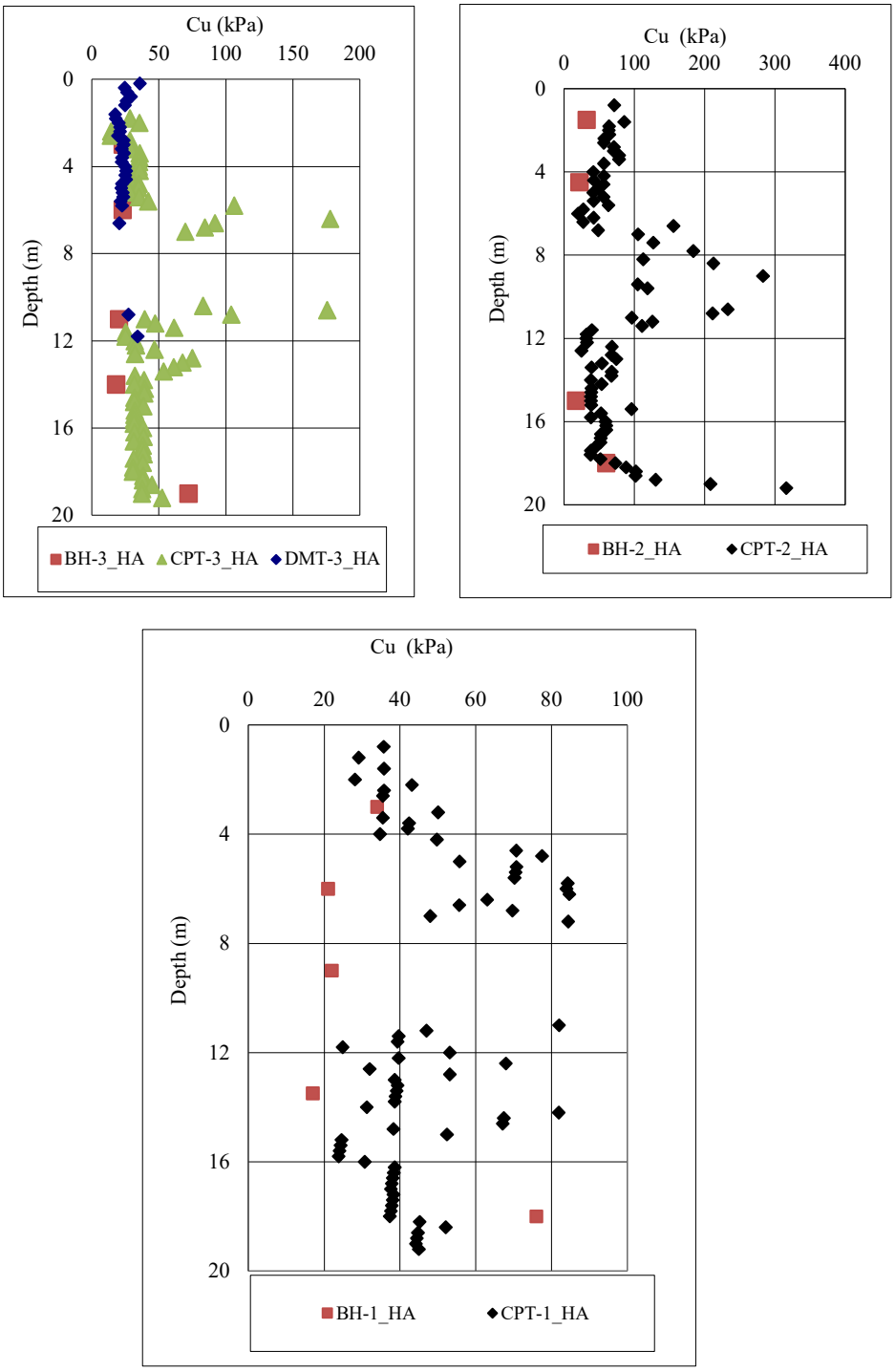

Figure: 5. 26 Variation of undrained cohesion (C_u) along depth for DMT-3_HA,CPT-3_HA, BH-3_HA,CPT-1_HA, BH-1_HA, CPT-2_HA, BH-2_HA test points at Site-4 (HA)

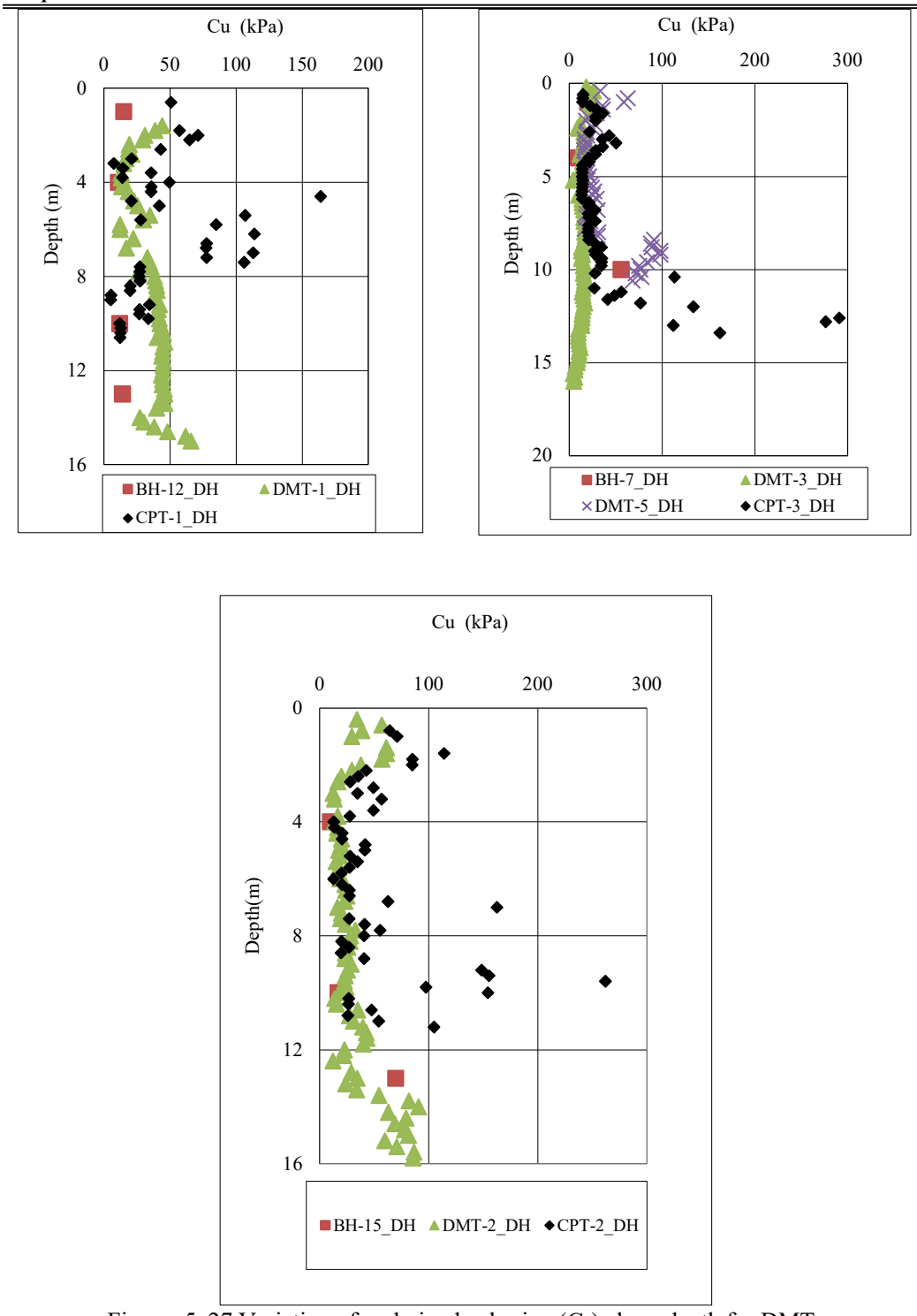

Figure: 5. 27 Variation of undrained cohesion (C_u) along depth for DMT-1_DH,CPT-1_DH, BH-12_DH, DMT-2_DH, CPT-2_DH, BH-15_DH, DMT-3_DH, CPT-3_DH, DMT-5_DH and BH-7_DH,test points at Site-5 (DH)

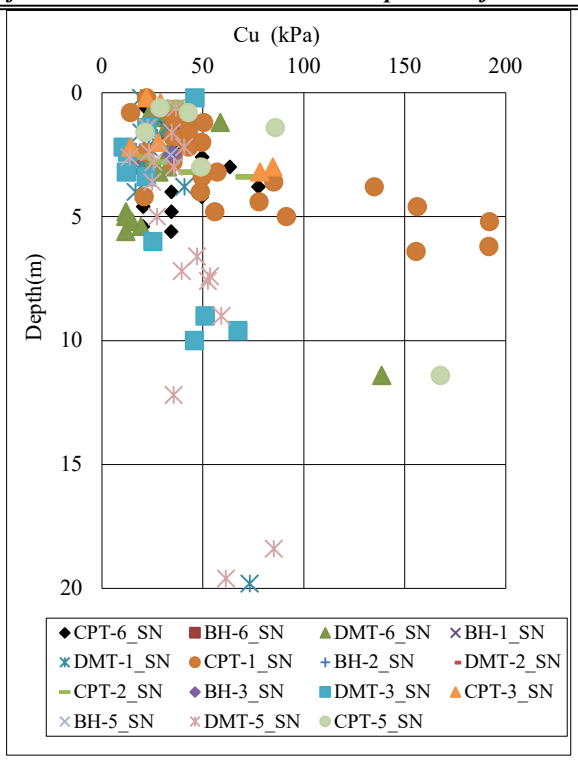

Figure: 5. 28 Variation of undrained cohesion (C_u) along depth for DMT-1_SN,CPT-1_SN, BH-1_SN, DMT-2_SN, CPT-2_SN, BH-2_SN,DMT-3_SN,CPT-3_SN, DMT-5_SN, CPT-5_SN,BH-5_SN, DMT-6_SN,CPT-6_SN and BH-6_SN test points at Site-6 (SN)

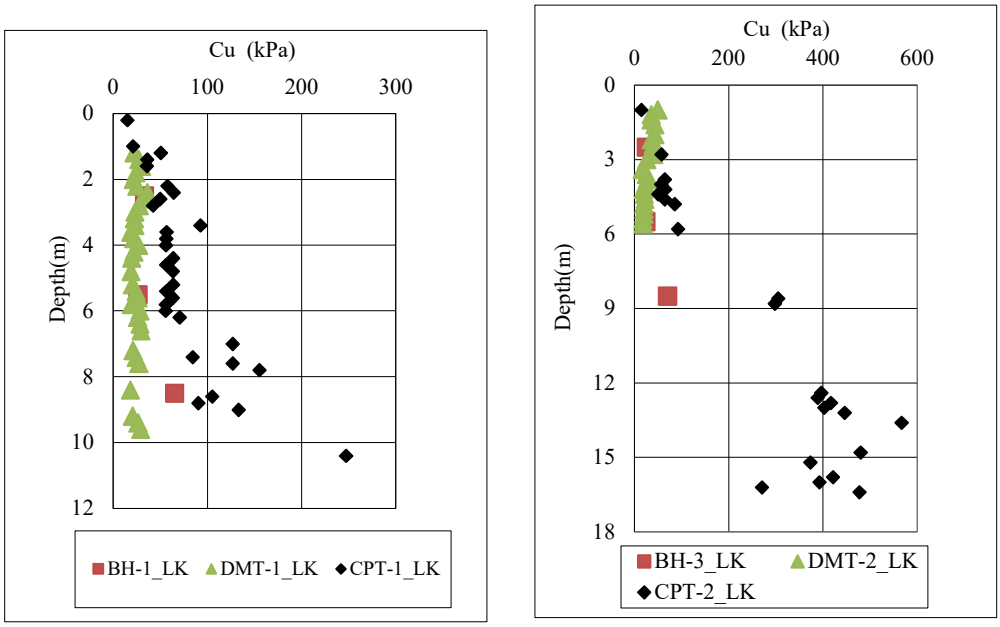

Figure: 5. 29 Variation of undrained cohesion (C_u) along depth for DMT-1_LK,CPT-1_LK, BH-1_LK, DMT-2_LK, CPT-2_LK, BH-3_LK test points at Site-7 (LK)

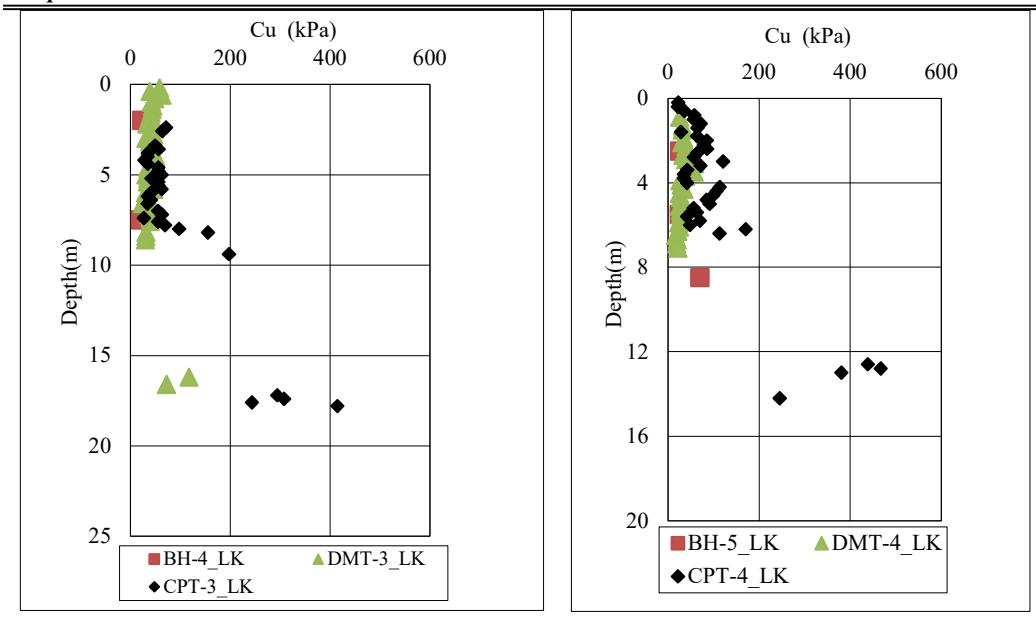

Figure: 5. 30 Variation of undrained cohesion (C_u) along depth for DMT-3_LK,CPT-3_LK,BH-4_LK, DMT-4_LK, CPT-4_LK, and BH-5_LK, test points at Site-7 (LK)

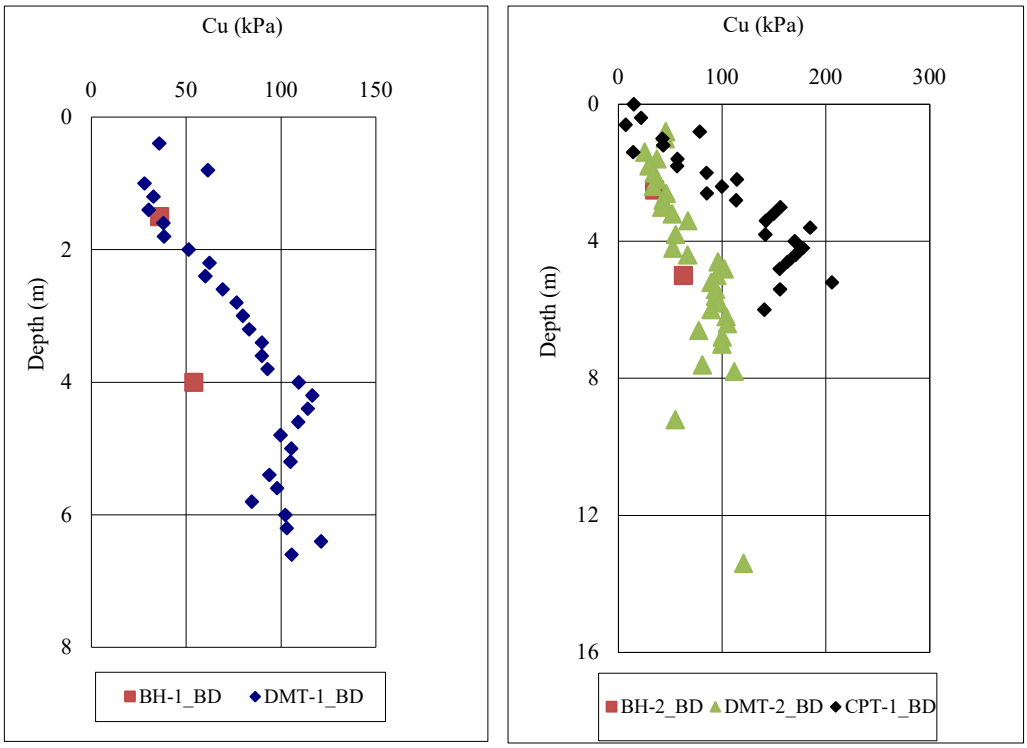

Figure: 5. 31 Variation of undrained cohesion (C_u) along depth for DMT-1_BD, BH-1_BD, DMT-2_BD,CPT-1_BD,BH-2_BD test points at Site-8 (BD)

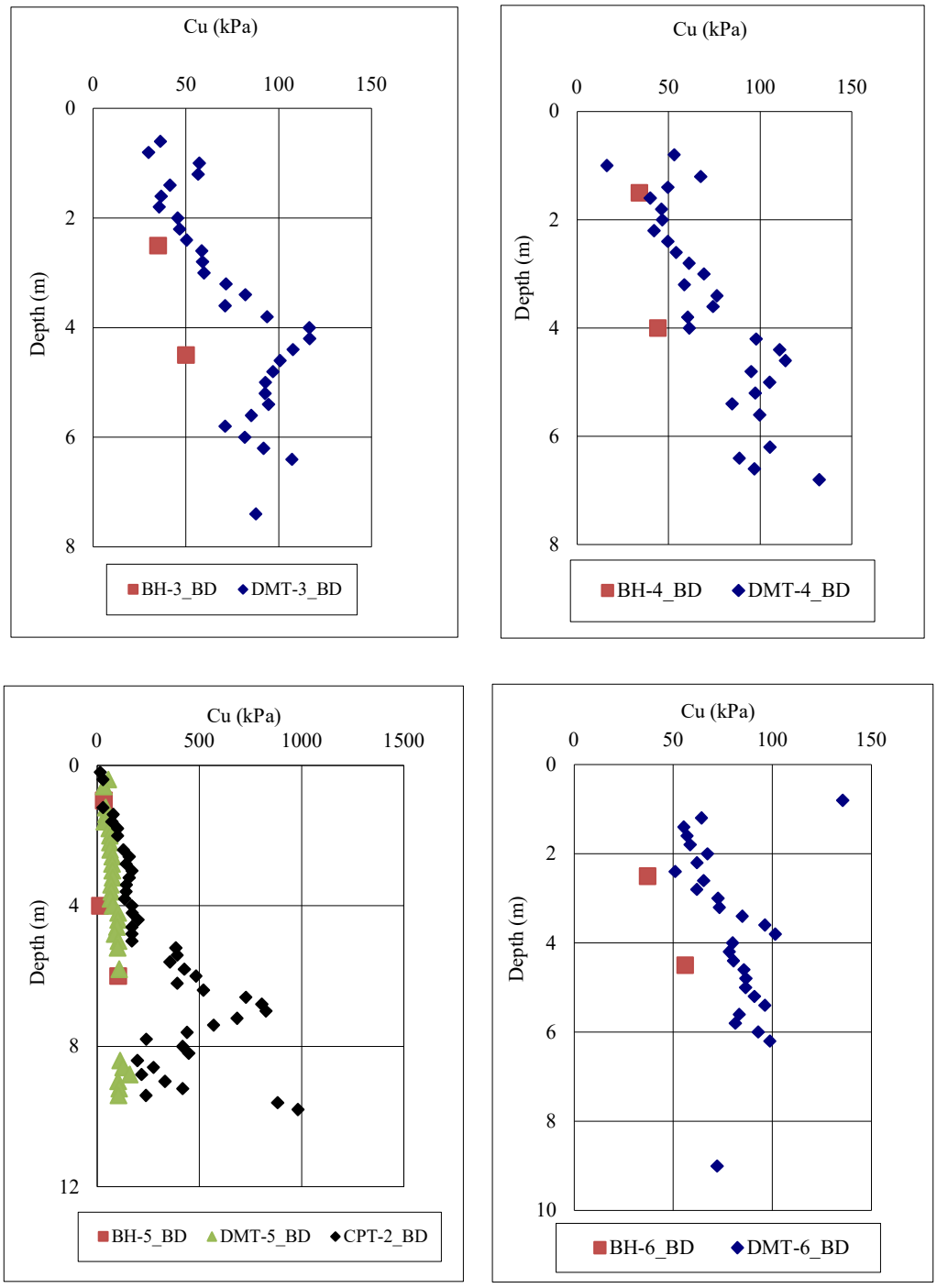

Figure: 5. 32 variation of undrained cohesion (C_u) along depth for DMT-3_BD, BH-3_BD, DMT-4_BD,BH-4_BD,DMT-5_BD,CPT-2_BD, BH-5_BD and DMT-6_BD,BH-6_BD test points at Site-8 (BD)

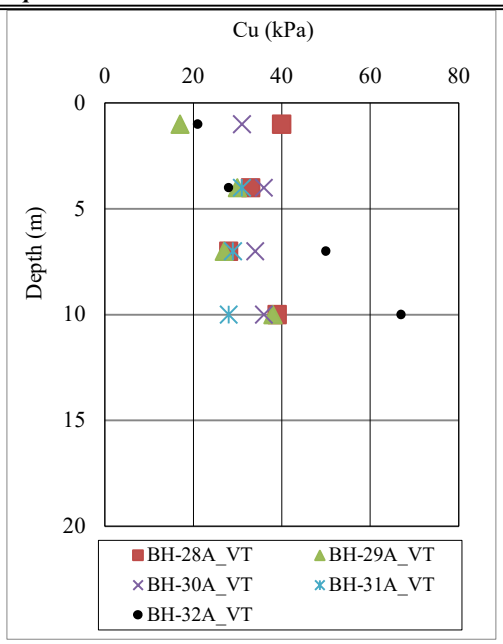

Figure: 5. 33 Variation of undrained cohesion (C_u) along depth for BH-28A_VT, BH-29A_VT, BH-30A_VT, BH-31A_VT and BH-32A_VT at Site-9 (VT)

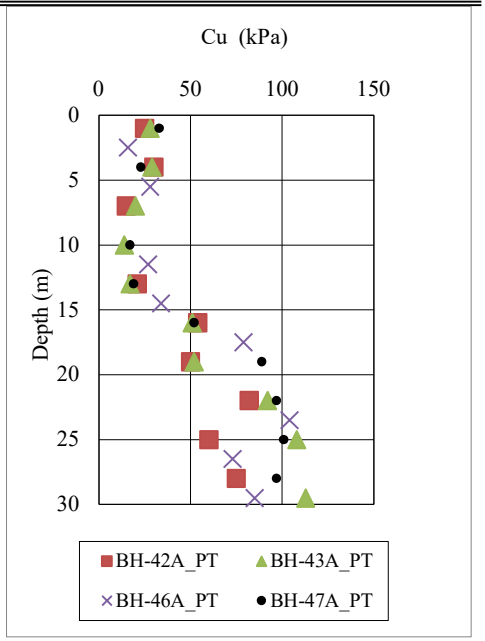

Figure: 5. 34 Variation of undrained cohesion (C_u) along depth for BH-42A_PT, BH-43A_PT, BH-46A_PT and BH-47A_PT at Site-10 (PT)

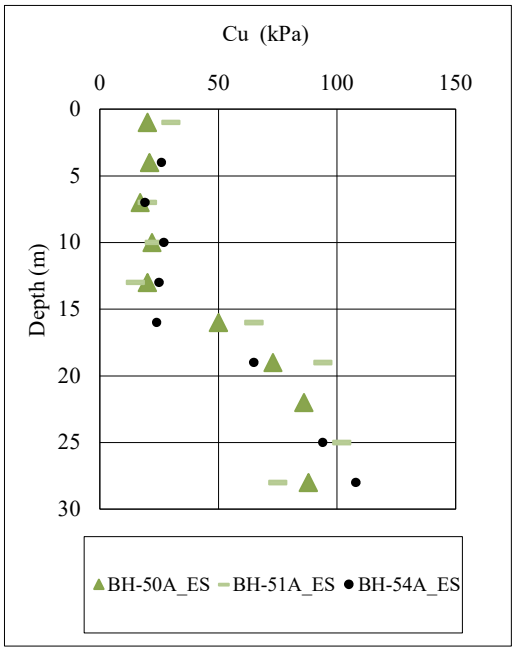

Figure: 5. 35 Variation of undrained cohesion (C_u) along depth for BH-50A_ES, BH-51A_ES and BH-54A_ES at Site-11 (ES)

5.3.3 ANGLE OF INTERNAL FRICTION (ϕ)

Variation of angle of internal friction (ϕ) along depth, has been plotted for each test location. It is also observed that the variation of ϕ (estimated from DMT and CPT tests) along depth, is similar in nature with the results estimated from laboratory tests. This variation is graphically presented in Figure 5.36 to 5.43.

For Site-9 (VT), site wise variation of ϕ along depth has been plotted and presented in Figure 5.44.

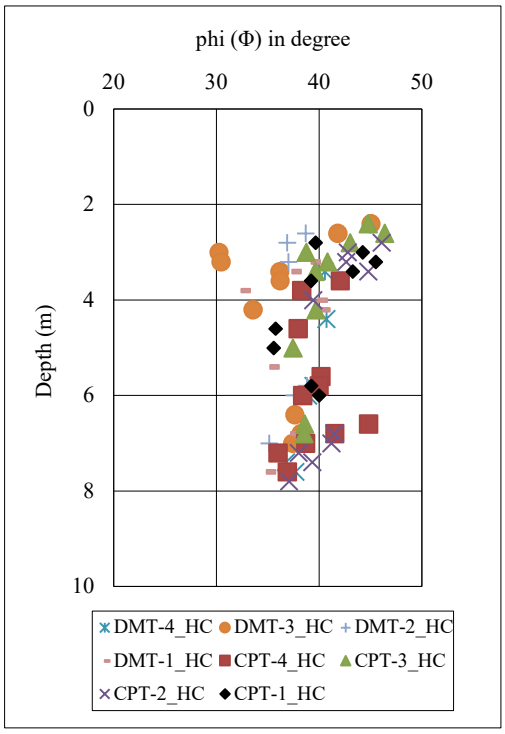

Figure: 5. 36 Variation of angle of internal friction (ϕ) along depth for DMT-1_HC, DMT-2_HC, DMT3_HC, DMT-4_HC, CPT-1_HC, CPT-2_HC, CPT-3_HC, and CPT-4_HC test points at Site-1 (HC)

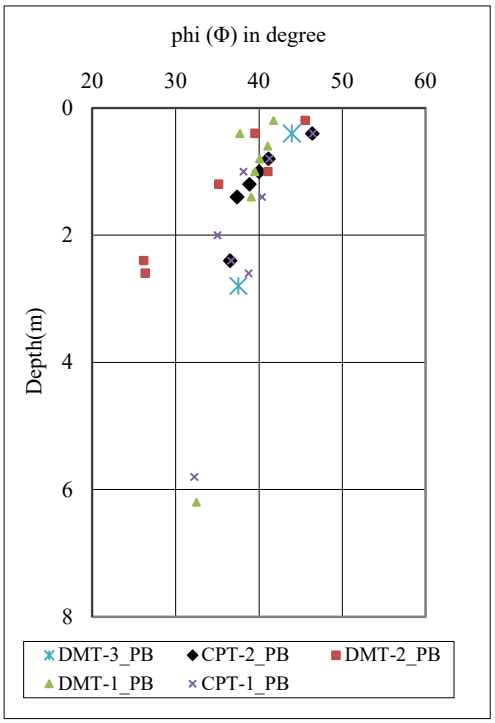

Figure: 5. 37 Variation of angle of internal friction (ϕ) along depth for DMT-1_PB, DMT-2_PB, DMT-3_PB , CPT-1_PB and CPT-2_PB test points at Site-2 (PB)

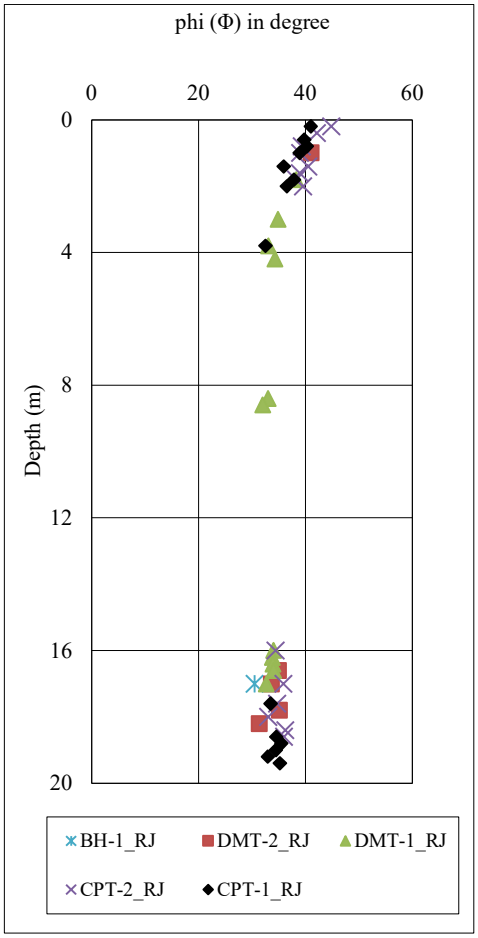

Figure: 5. 38 Variation of angle of internal friction (ϕ) along depth for DMT-1_RJ, DMT-2_RJ, CPT-1_RJ, CPT-2_RJ_ and BH-1_RJ, test points at Site-3 (RJ)

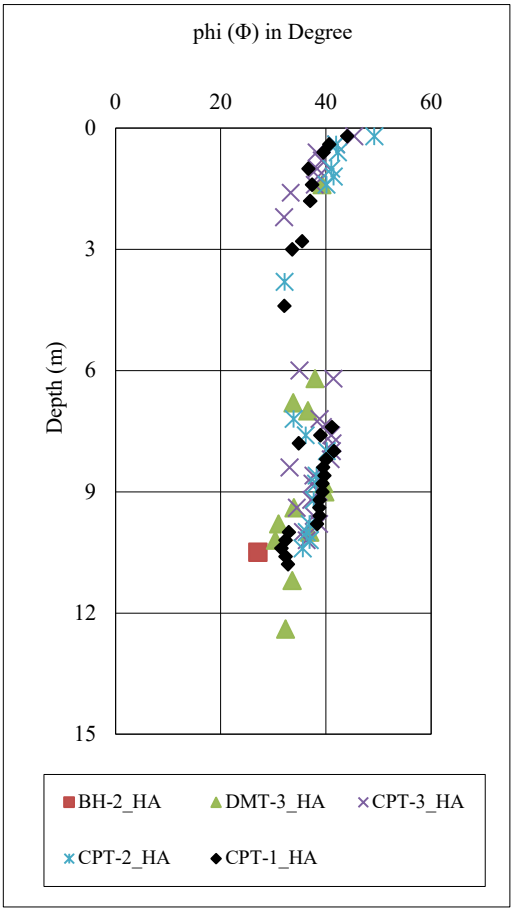

Figure: 5. 39 Variation of angle of internal friction (ϕ) along depth for DMT-3_HA,CPT-3_HA,CPT-1_HA,CPT-2_HA and BH-2_HA test points at Site-4 (HA)

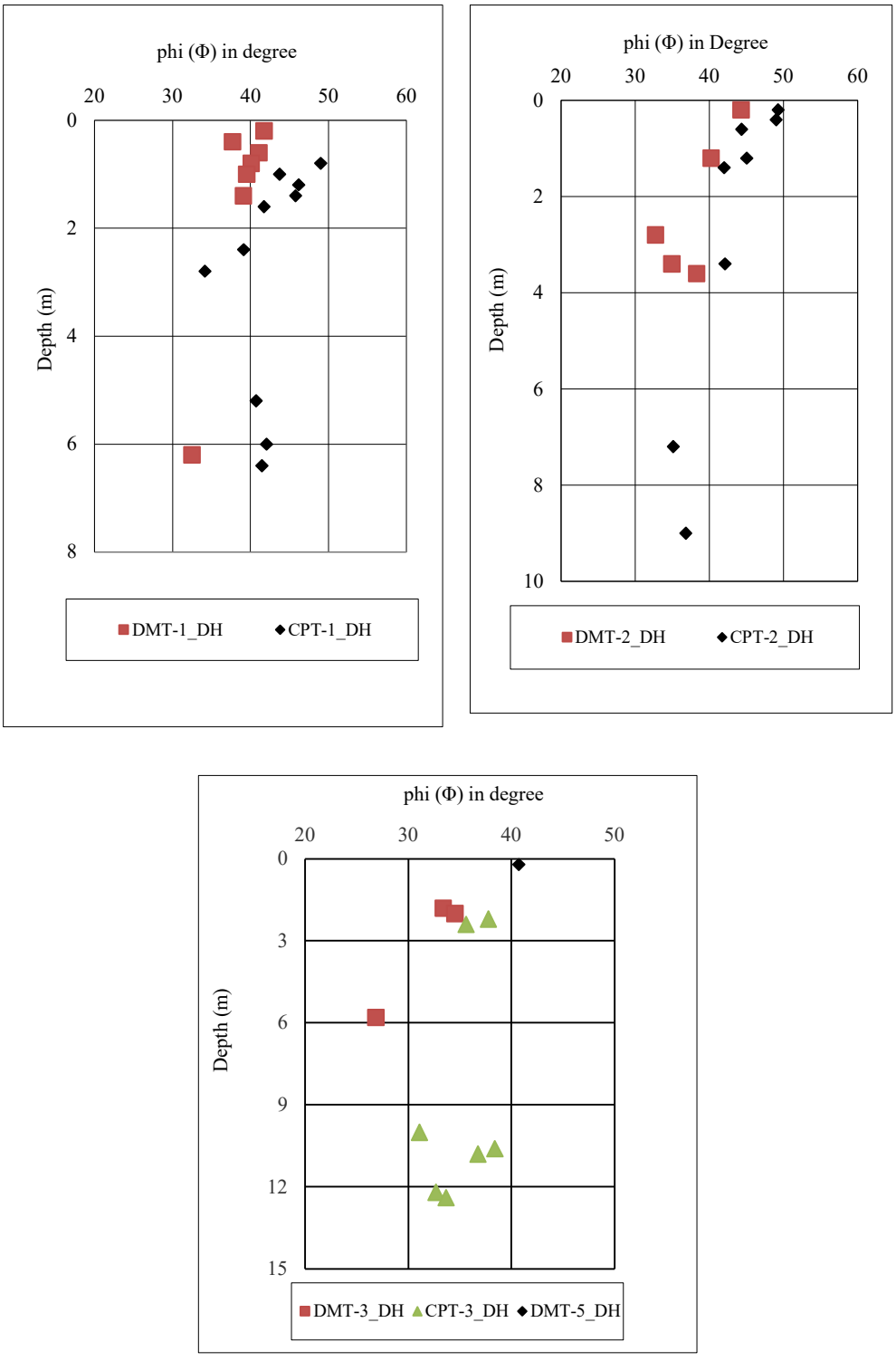

Figure: 5. 40 Variation of angle of internal friction (ϕ) along depth for DMT-1_DH,CPT-1_DH, DMT-2_DH, CPT-2_DH,DMT-3_DH,CPT-3_DH and DMT-5_DH test points at Site-5 (DH)

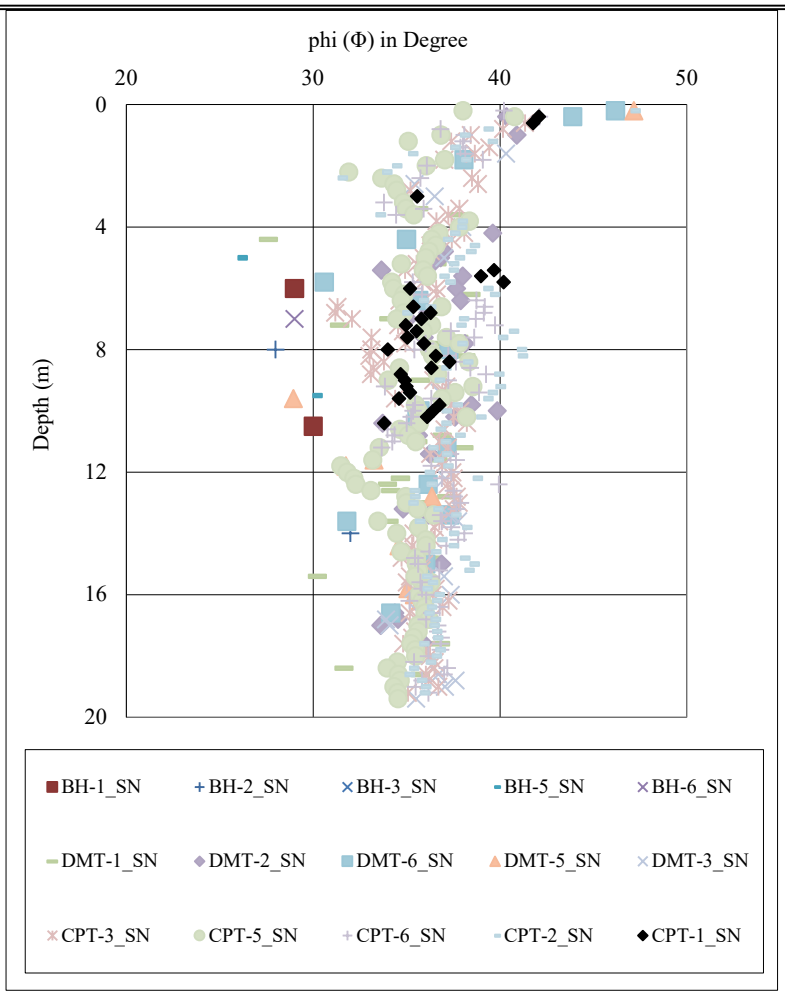

Figure: 5. 41 Variation of angle of internal friction (ϕ) along depth for DMT-1_SN,CPT-1_SN, BH-1_SN, DMT-2_SN, CPT-2_SN, BH-2_SN,DMT-3_SN,CPT-3_SN, DMT-5_SN, CPT-5_SN,BH-5_SN, DMT-6_SN,CPT-6_SN and BH-6_SN test points at Site-6 (SN)

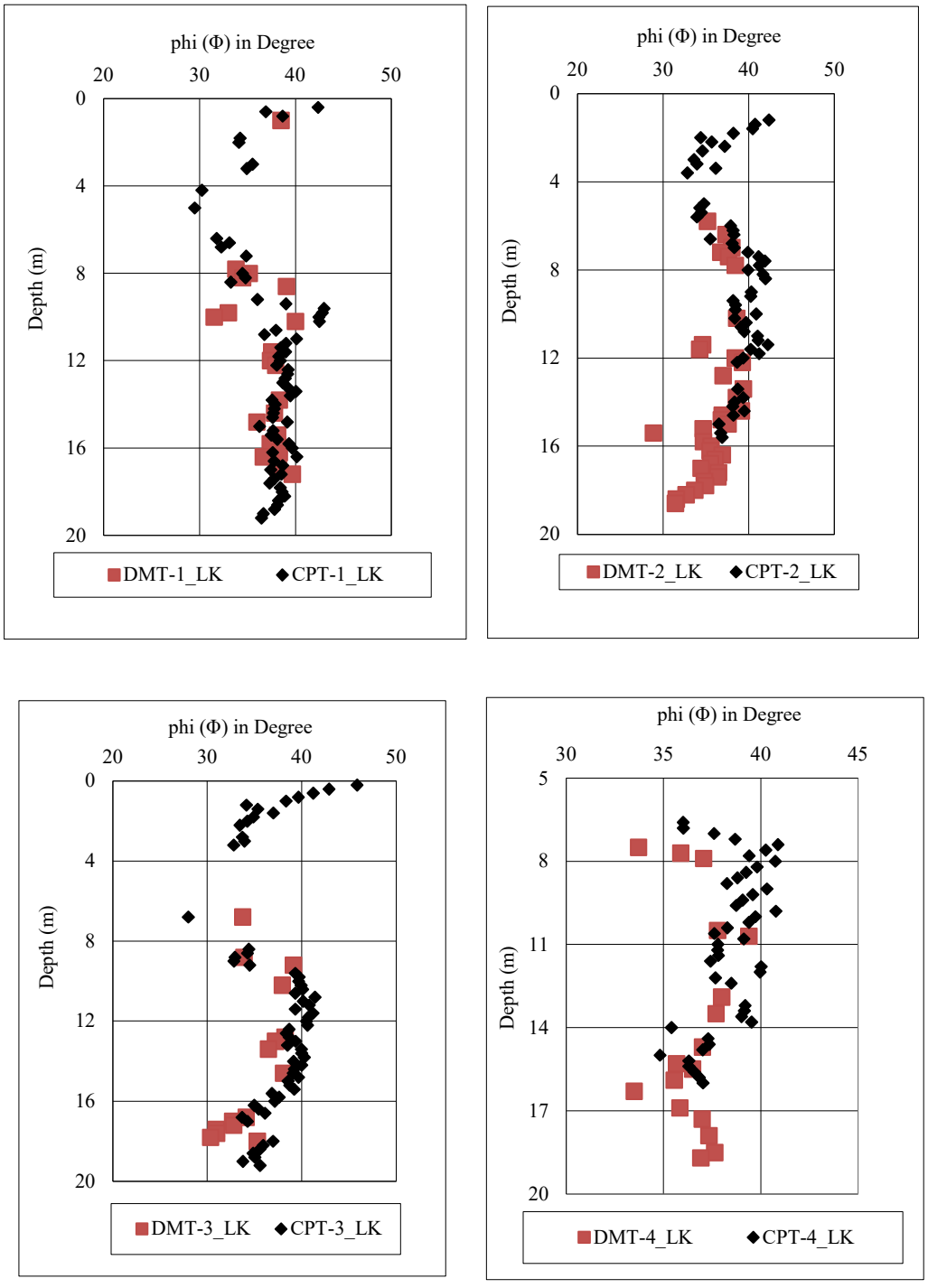

Figure: 5. 42 Variation of angle of internal friction (ϕ) along depth forDMT-1_LK,CPT-1_LK, DMT-2_LK, CPT-2_LK, DMT-3_LK,CPT-3_LK, DMT-4_LK, and CPT-4_LK test points at Site-7 (LK)

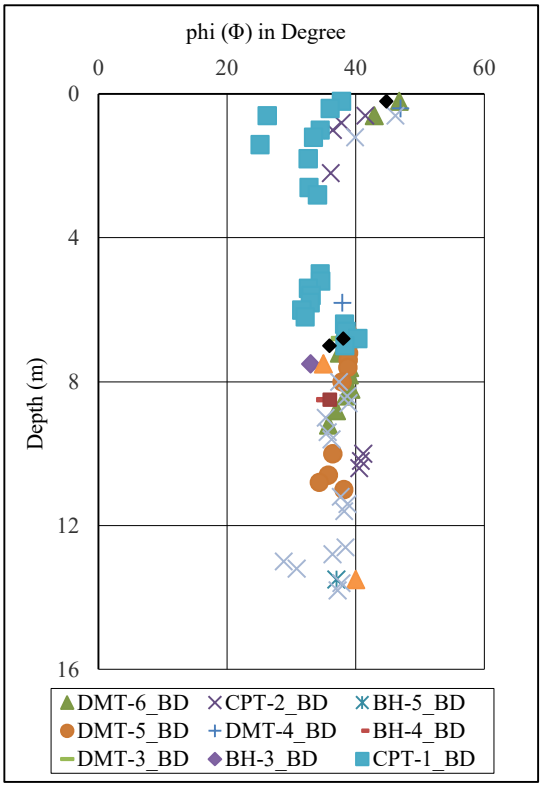

Figure: 5. 43 Variation of angle of internal friction (ϕ) along depth forDMT-1_BD, BH-1_BD, DMT-2_BD,CPT-1_BD, BH-2_BD, DMT-3_BD,BH-3_BD, DMT-4_BD,BH-4_BD,DMT-5_BD,CPT-2_BD, BH-5_BD and DMT-6_BD test points at Site-8 (BD)

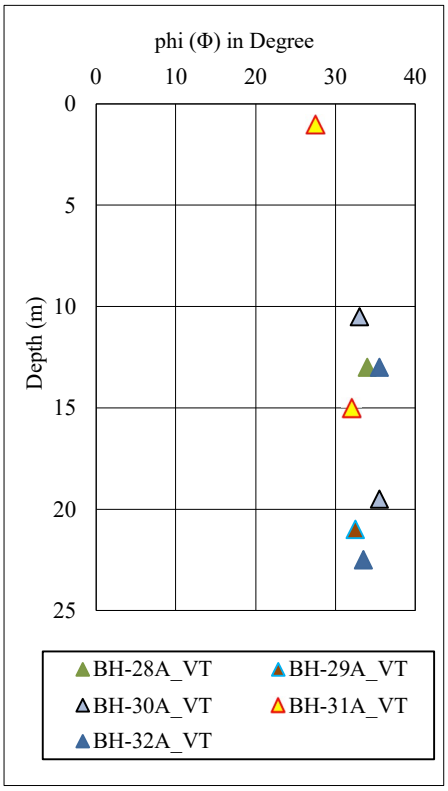

Figure: 5. 44 Variation of angle of internal friction (ϕ) along depth for -28A_VT, BH-29A_VT, BH-30A_VT, BH-31A_VT and BH-32A_VT at Site-9 (VT)

5.3.4 VERTICAL DRAINED CONSTRAINED MODULUS (M)

In eight number of sites, the compressibility characteristics (in terms of vertical drained constrained modulus i.e., M) of sub-soil has been estimated from DMT (M_{DMT}) and CPT (M_{CPT}) tests. Site wise, the variation of this parameter along depth are presented in Figure 5.45 to 5.52.

It has been observed that the value of vertical drained constrained modulus (M_{DMT} and M_{CPT}) estimated from DMT and CPT tests are in agreement for both the tests.

At Site-1 (HC), variation (as shown in Figure 5.45) of M_{DMT} (estimated from DMT tests) and M_{CPT} (estimated from CPT tests) along depth, shows scatter of values at different depth interval (between 4.0m to 6.0m depth below ground level). It is mainly due to the presence of silty sand/ sandy silt at that particular depth. Otherwise, the value is more or less similar in nature for both the tests.

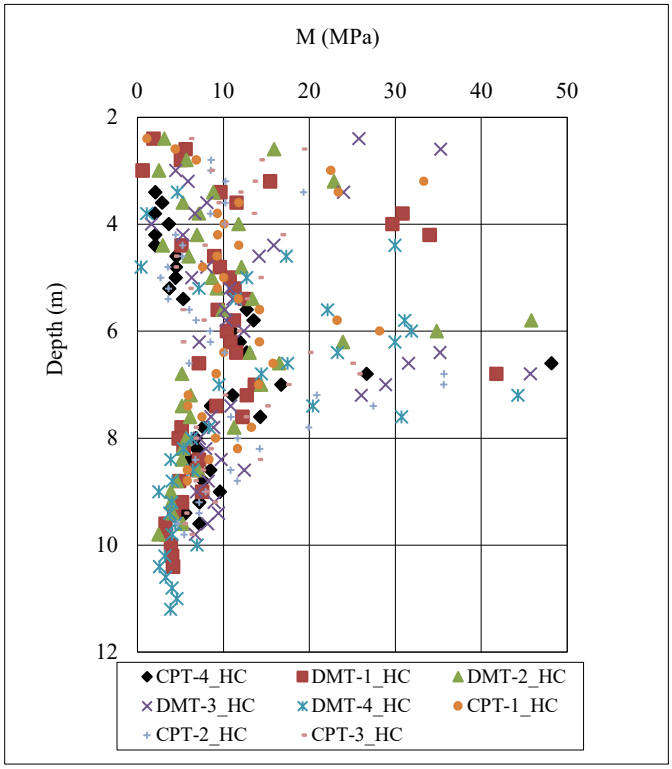

Figure: 5. 45 Variation of M (M_{DMT} and M_{CPT}) along depth for DMT-1_HC, DMT-2_HC, DMT3_HC, DMT-4_HC, CPT-1_HC, CPT-2_HC, CPT-3_HC, CPT-4_HC, test points at Site-1 (HC)

At Site-2 (PB), in DMT-2_PB and DMT-3_PB test locations, it is observed that the variation of M_{DMT} along depth (as shown in Figure 5.46) shows scatter of values at different depth interval (in between 0.0m to 6.0m below ground level). It is mainly due to the presence of silty sand/ sandy silt within this depth range. On the other hand, the value of M, for CPT-1_PB, CPT-2_PB and DMT-1_PB test locations, are found to be more or less similar for both the tests.

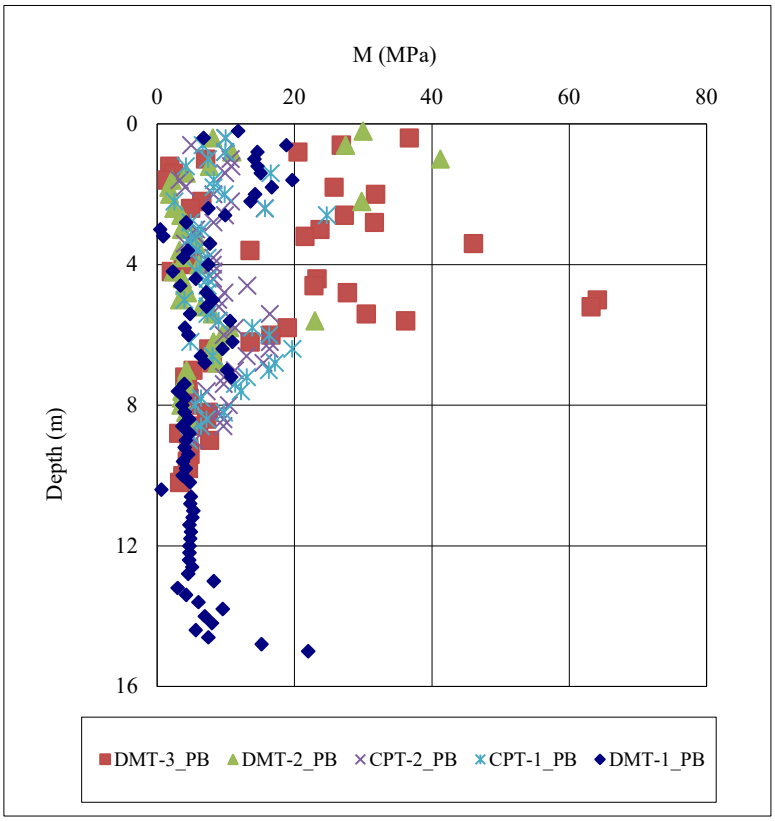

Figure: 5. 46 Variation of M (M_{DMT} and M_{CPT}) along depth for DMT-1_PB, DMT-2_PB, DMT3_PB, CPT-1_ PB and CPT-2_PB test points at Site-2 (PB)

At Site-3 (RJ), variation of M_{DMT} (estimated at DMT-1_RJ location) along depth, shows scatter of values in between 5.0m to 8.0m depth below ground level. It is mainly due to the presence of decomposed wood particles (Figure 5.47), identified from adjacent bore hole results. Otherwise, the variation of M along depth (estimated from both DMT and CPT tests), is found to be similar in nature for other test locations.

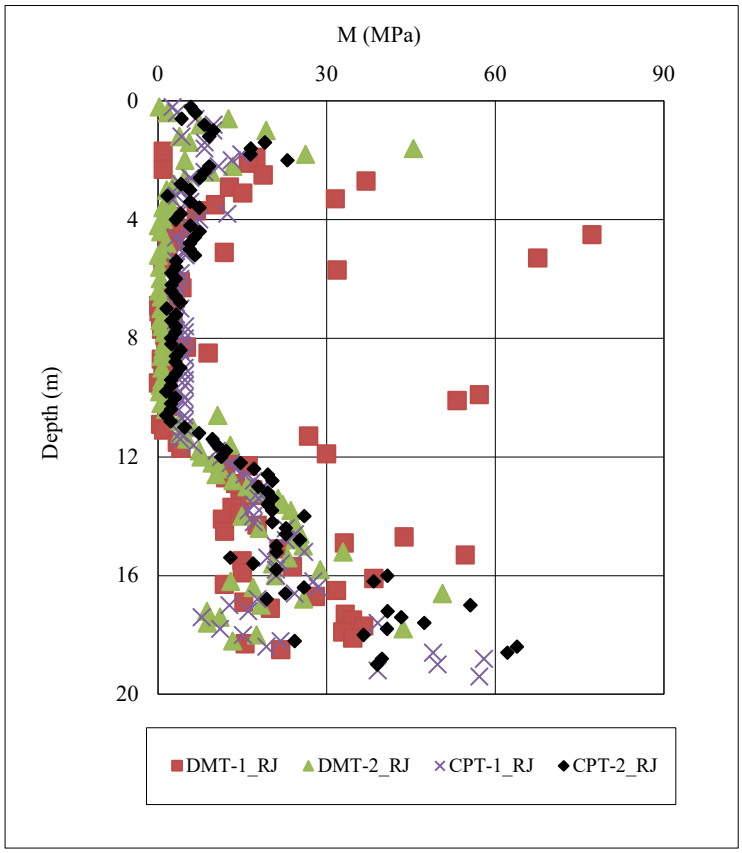

Figure: 5. 47 Variation of M (M_{DMT} and M_{CPT}) along depth for DMT-1_RJ, DMT-2_RJ, CPT-1_RJ, CPT-2_RJ_ and BH-1_RJ, test points at Site-3 (RJ)

At Site-4 (HA), the variation of M_{DMT} (estimated at DMT-3_HA location) along depth, shows some scatter of values within the depth of 8.0 to 10.0m below ground level (Figure 5.48). It is mainly due to the presence of silty sand/sandy silt (identified from adjacent bore hole i.e., BH-3_HA results). Otherwise, the overall variation of M along depth (estimated from both DMT and CPT tests), is found to be similar in nature.

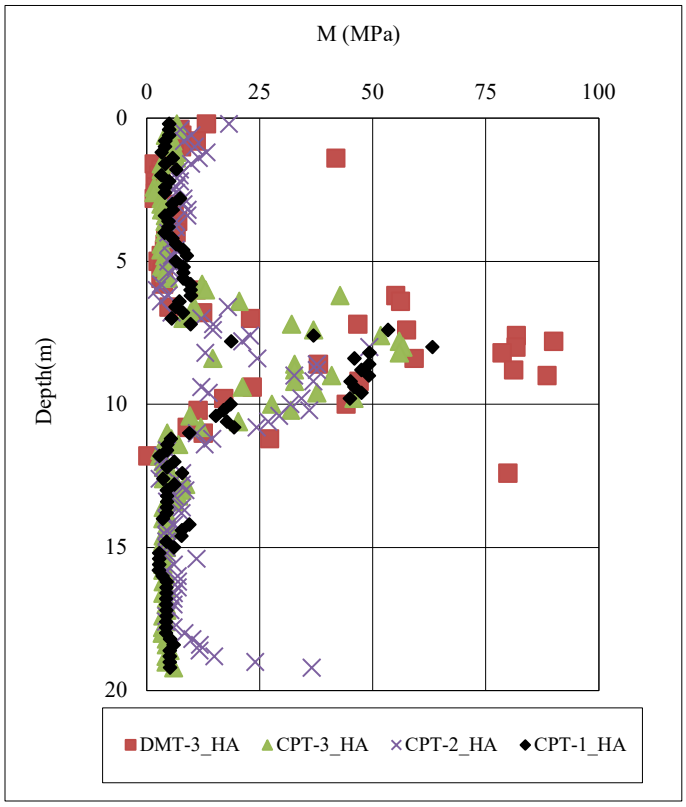

Figure: 5. 48 Variation of M (M_{DMT} and M_{CPT}) along depth for DMT-3_HA, CPT-3_HA, CPT-1_HA and CPT-2_HA test points at Site-4 (HA)

At Site-5 (DH), the value of M (estimated from both DMT and CPT tests) are found to be more or less similar in nature (Figure 5.48). However, the presence of sandy silty clay within the depth of 10.0m to 13.0m below ground level, was observed from laboratory tests of BH-7_DH. Consequently, estimated M is found to be somewhat scattered within this depth at DMT-5_DH and CPT-3_DH test

location. However, the overall variation of M is found to be more or less similar in nature for both the CPT and DMT tests at all the locations.

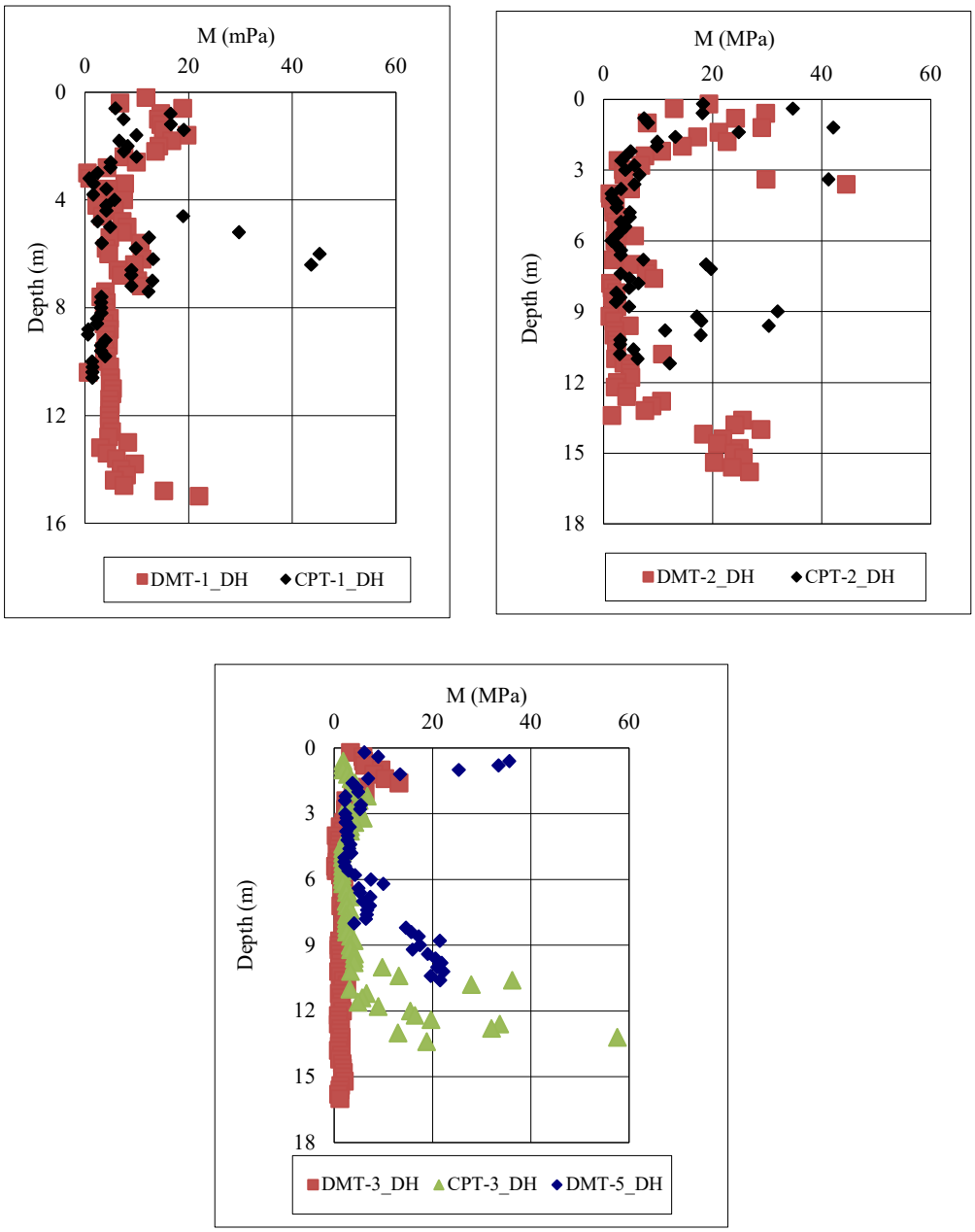

Figure: 5. 49 Variation of M (M_{DMT} and M_{CPT}) along depth for DMT-1_DH,CPT-1_DH, DMT-2_DH, CPT-2_DH,DMT-3_DH,CPT-3_DH and DMT-5_DH test points at Site-5 (DH)

At Site-6 (SN), the variation of vertical drained constrained modulus (M) (estimated from DMT and CPT tests) along depth, are found to be more or less similar in nature for all test locations (Figure 5.50).

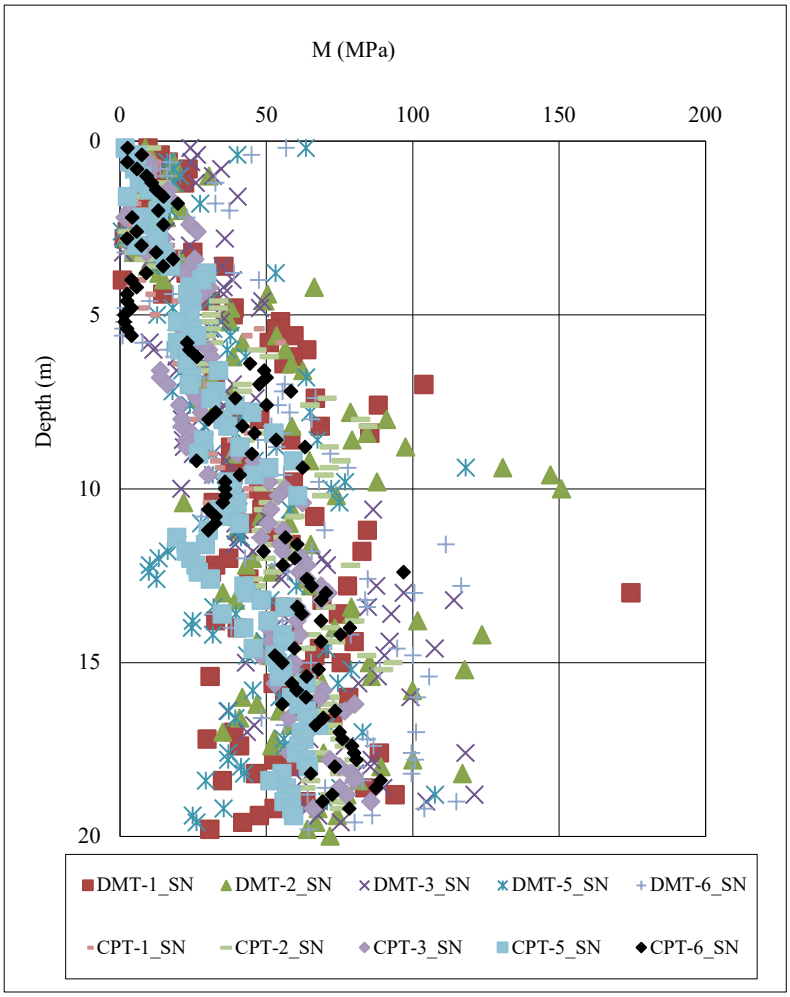

Figure: 5. 50 Variation of M (M_{DMT} and M_{CPT}) with depth for DMT-1_SN, CPT-1_SN, DMT-2_SN, CPT-2_SN, DMT-3_SN, CPT-3_SN, DMT-5_SN, CPT-5_SN, DMT-6_SN and CPT-6_SN test points at Site-6 (SN)

At Site-7 (LK), it has been observed that the depth wise variation of vertical drained constrained modulus (M) estimated from DMT and CPT tests are more or less similar in nature for all the tests. Variation of constrained modulus along depth is shown in Figure 5.51.

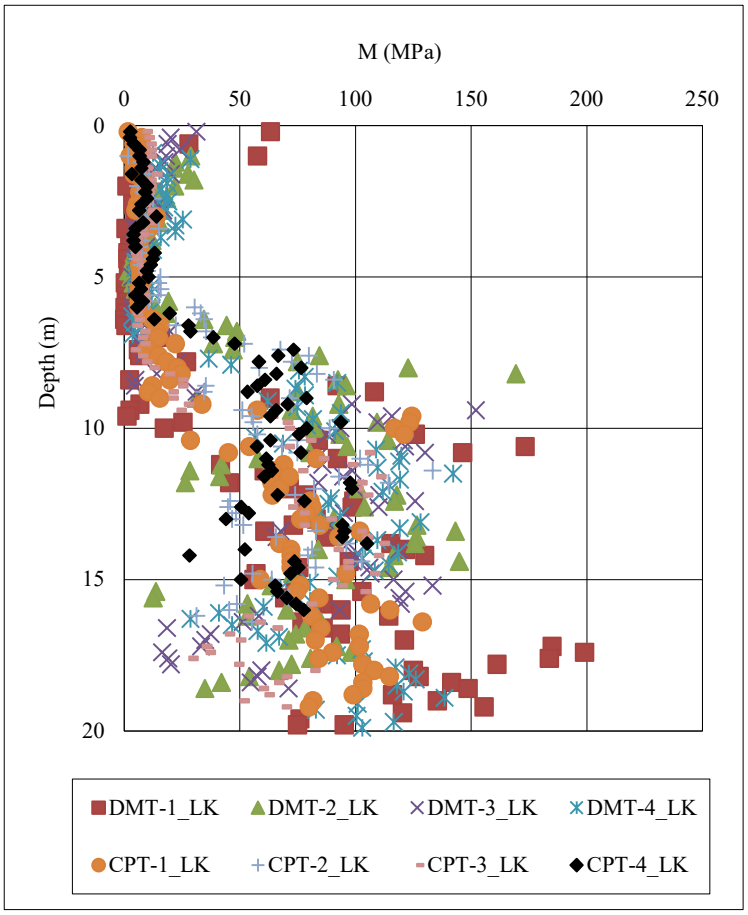

Figure: 5. 51 Variation of M (M_{DMT} and M_{CPT}) with depth for DMT-1_LK,CPT-1_LK, DMT-2_LK, CPT-2_LK, DMT-3_LK,CPT-3_LK, DMT-4_LK, and CPT-4_LK test points at Site-7 (LK)

At Site-8 (BD), it has been observed that the depth wise variation of vertical drained constrained modulus (M_{DMT} and M_{CPT}) estimated from DMT and CPT tests, are more or less similar in nature for all the test points. Variation of constrained modulus is shown in Figure 5.52.

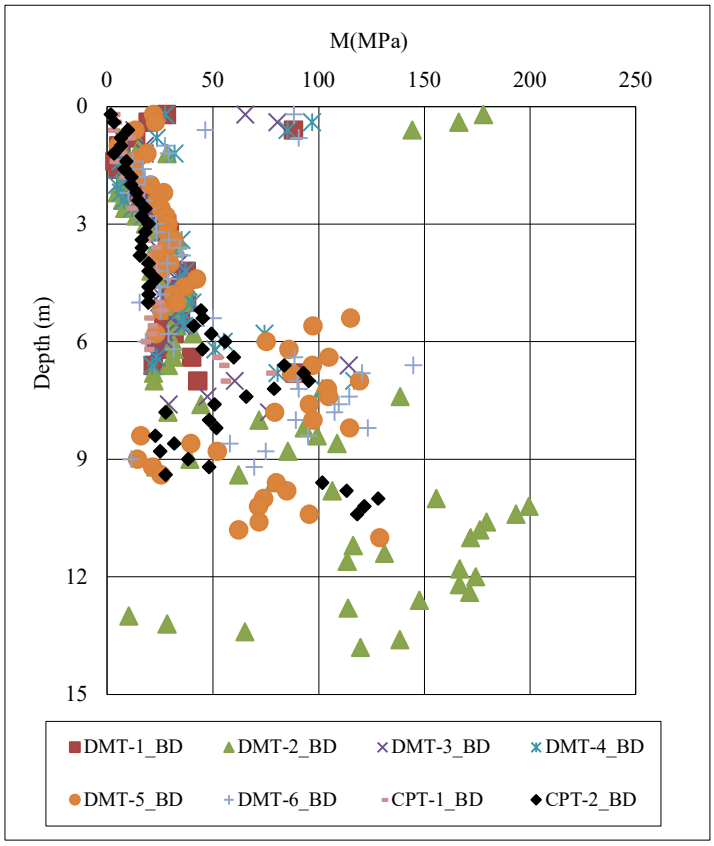

Figure: 5. 52 Variation of M (M_{DMT} and M_{CPT}) with depth for DMT-1_BD, DMT-2_BD, CPT-1_BD, DMT-3_BD, DMT-4_BD, DMT-5_BD, CPT-2_BD, and DMT-6_BD test points at Site-8 (BD)

5.3.5 DILATOMETER MODULUS (E_D)

At eight numbers of test locations (where DMT tests were carried out), site wise Dilatometer modulus (E_D) was estimated and plotted along depth. The variation of E_D along depth is presented in Figure 5.53 to 5.60.

At Site-1 (HC), it has been observed that the presence of silt/silty sand /sandy silt is identified from DMT tests in between the average depth of 4.0m to 8.0m below ground level. However, the presence of soft to firm silty clay/clayey silt with

traces of decomposed wood was observed from laboratory tests. Consequently, the variation of E_D is found to be somewhat scattered within this depth. The variation of E_D is plotted for this site and is shown in Figure 5.53.

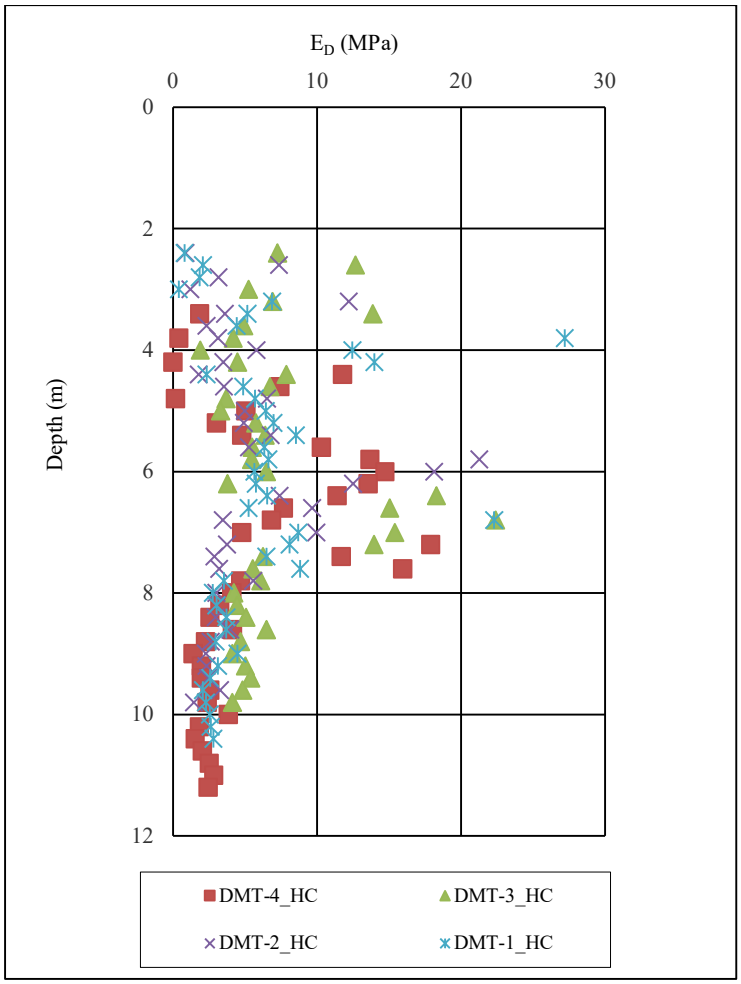

Figure: 5. 53 Variation of E_D with depth for DMT-1_HC, DMT-2_HC, DMT-3_HC and DMT-4_HC at Site-1 (HC)

At Site-2 (PB), Panchayet Bhaban site, three numbers of DMT tests were carried out. The variation of Dilatometer modulus (E_D) with depth is presented in Figure 5.54. In this graph it has been observed that the value of E_D is scattered upto the depth of 6.0m below ground for DMT-3_PB test location compared to other two DMT test points (i.e., DMT-1_PB and DMT-2_PB). In this regard, at DMT-3_PB test location, the filling soil was observed upto the depth of 3.6m below

ground level and from 3.60m to 5.80m depth the presence of pockets of sandy silt was identified from the tests results. Whereas, in other two DMT test points the presence of clayey sit/ silty clay was identified. Contemporarily, beyond the depth of 6.0m below ground level the variation of E_D is consistent for all DMT test points (i.e., DMT-1_PB, DMT-2_PB and DMT-3_PB).

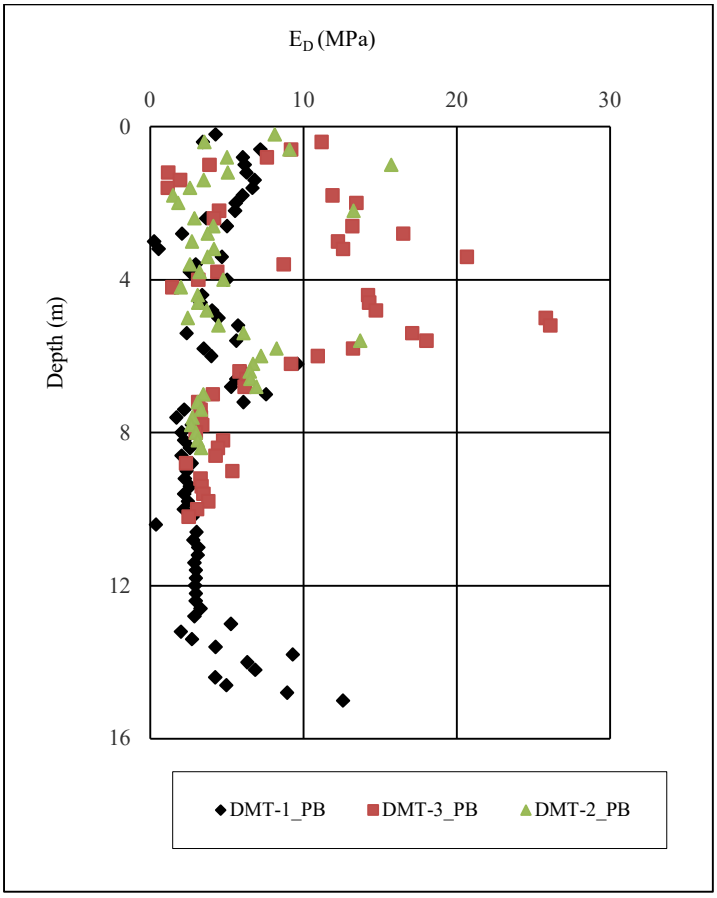

Figure: 5. 54 Variation of E_D with depth for DMT-1_PB, DMT-2_PB, DMT-3_PB at Site-2 (PB), Panchayet Bhaban, Kolkata, WB, India

At Site-3 (RJ), two numbers of DMT tests were conducted. The variation of Dilatometer Modulus (E_D) with depth is presented in Figure 5.55. At DMT-1_RJ test point, some scattered values of E_D are observed at few depths. This may be due to the presence of decomposed wood particles. However, the overall variation of E_D with depth is more or less similar for both DMT tests points.

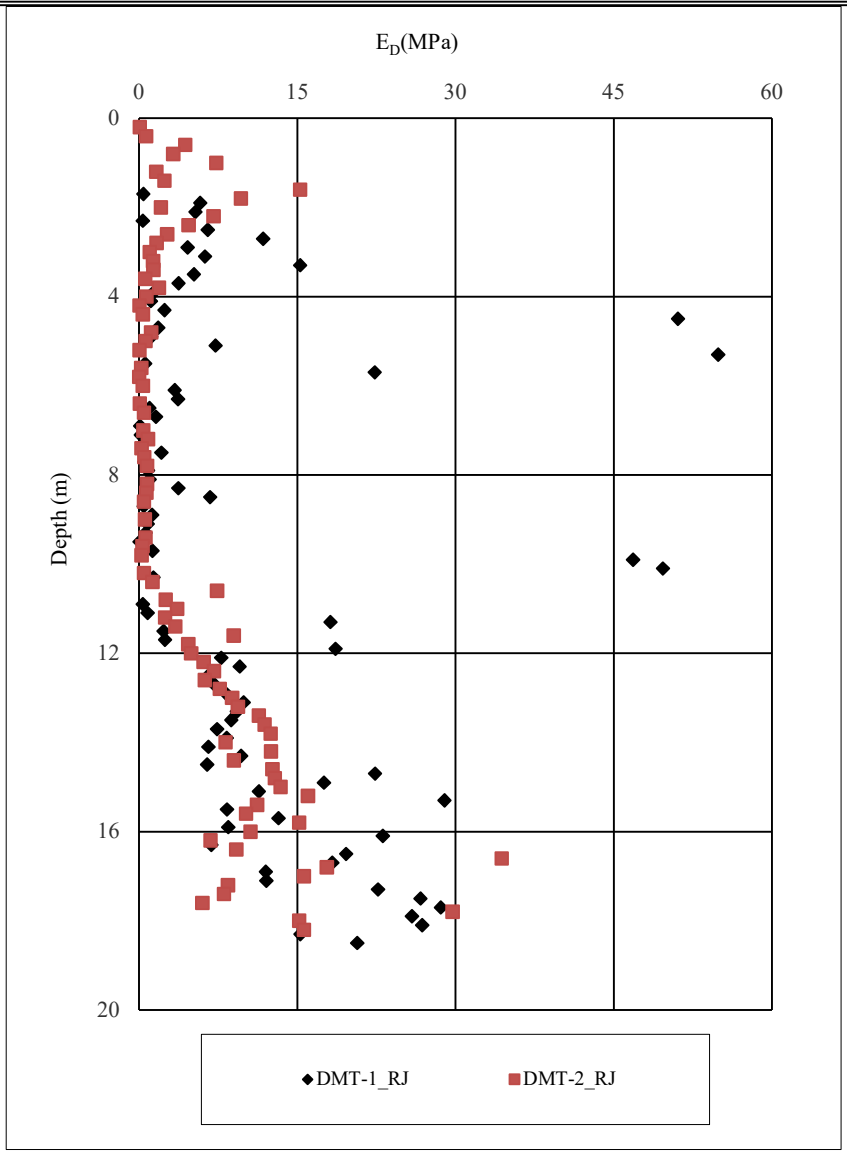

Figure: 5. 55 Variation of E_D with depth for DMT-1_RJ and DMT-2_RJ at Site-3 (RJ), Rajarhat Site, Kolkata, WB, India

At Site-4 (HA), one DMT test was carried out namely DMT-3_HA. The variation of Dilatometer modulus (E_D) with depth is presented in Figure 5.56. It is observed that the E_D is consistent upto the depth of 5.80m below ground level. However, some higher values of E_D are observed at few depths. This may be due to the presences of sandy silt / silty sand.

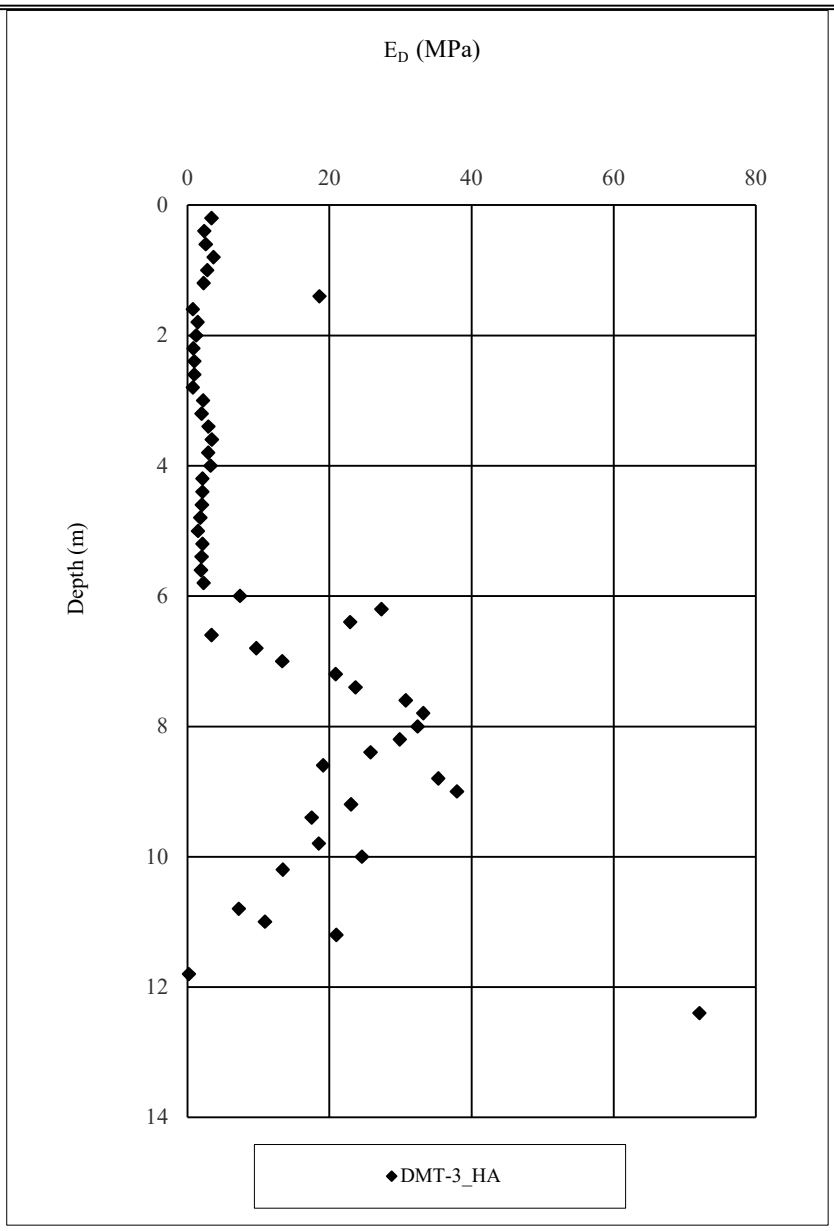

Figure: 5. 56 Variation of E_D with depth for DMT-3_HA at Site-4 (HA)

At Site-5 (DH), four DMT tests (i.e., DMT-1_DH, DMT-2_DH, DMT-3_DH and DMT-5_DH) were carried out. The variation of E_D with depth is presented in Figure 5.57. At each test point, some scattered values of E_D are observed at few depths. This may be due to the presences of filling material. However, the overall variation of E_D with depth is more or less similar for all DMT test points.

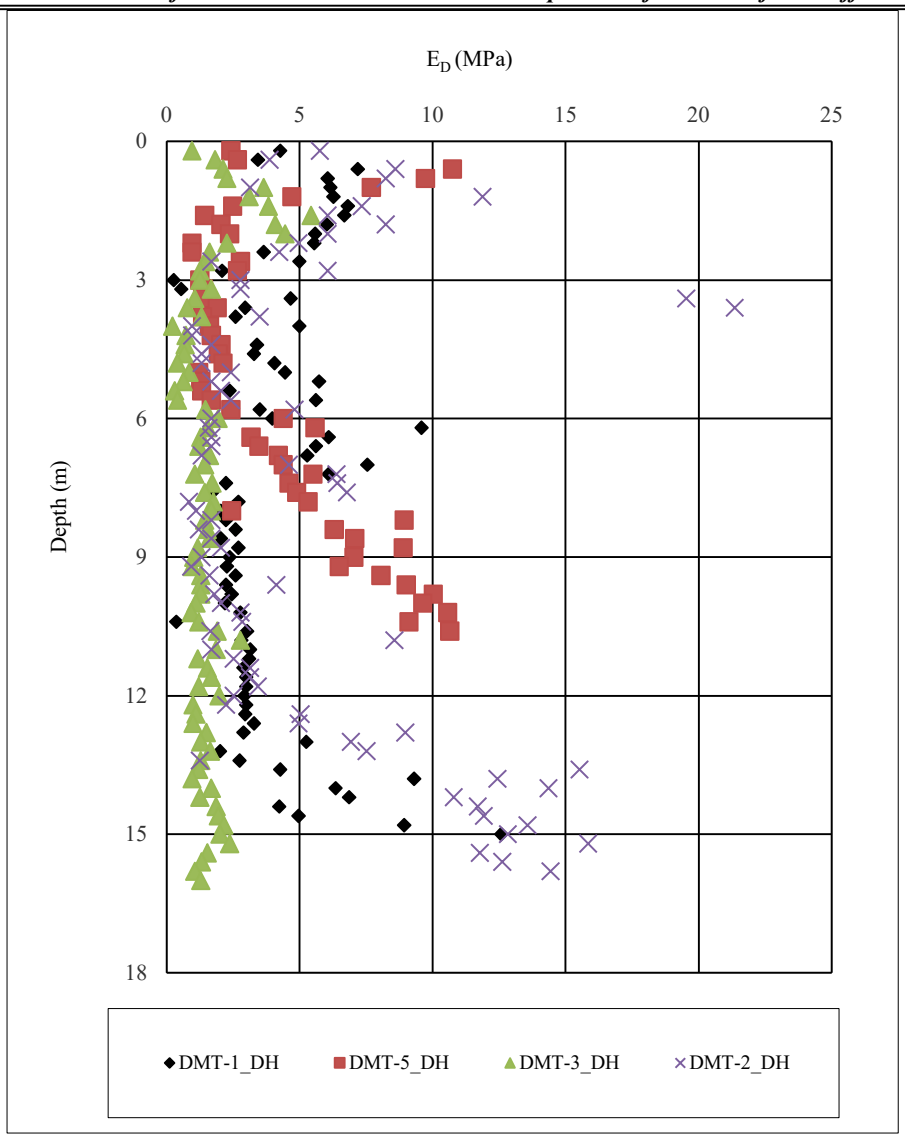

Figure: 5. 57 Variation of E_D with depth for DMT-1_DH, DMT-2_DH, DMT-3_DH and DMT-5_DH at Site-5 (DH)

At Site-6 (SN), five numbers of DMT tests were carried out. The variation of E_D along depth is presented in Figure 5.58. The overall variation of E_D with depth is more or less similar for all DMT test points.

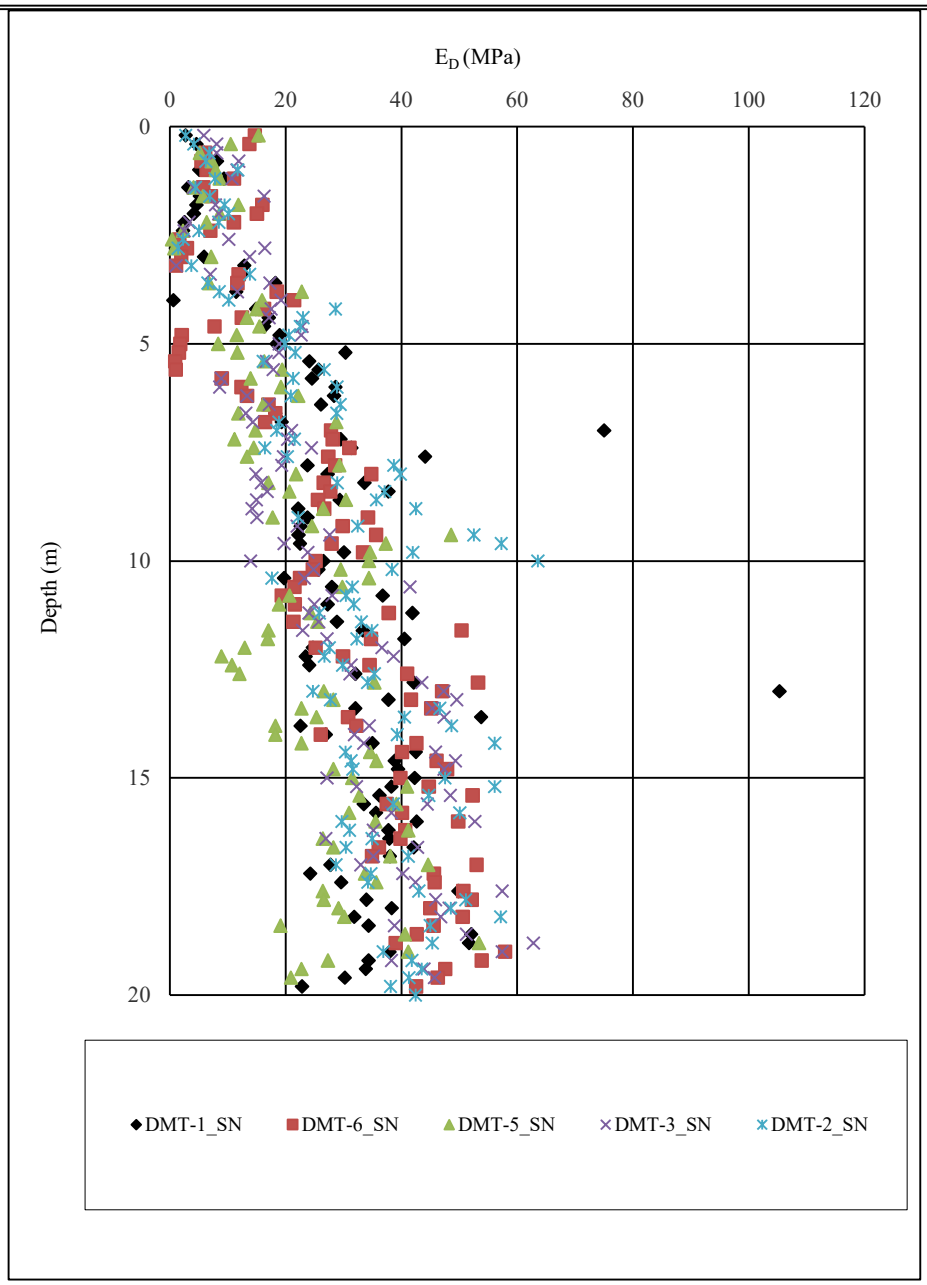

Figure: 5. 58 Variation of E_D with depth for DMT-1_SN, DMT-2_SN, DMT-3_SN, DMT-5_SN, DMT-6_SN at Site-6 (SN)

At site-7 (LK), four numbers DMT tests were carried out. The variation of E_D along depth is presented in Figure 5.59. The overall variation of E_D with depth is more or less similar for all DMT test points.

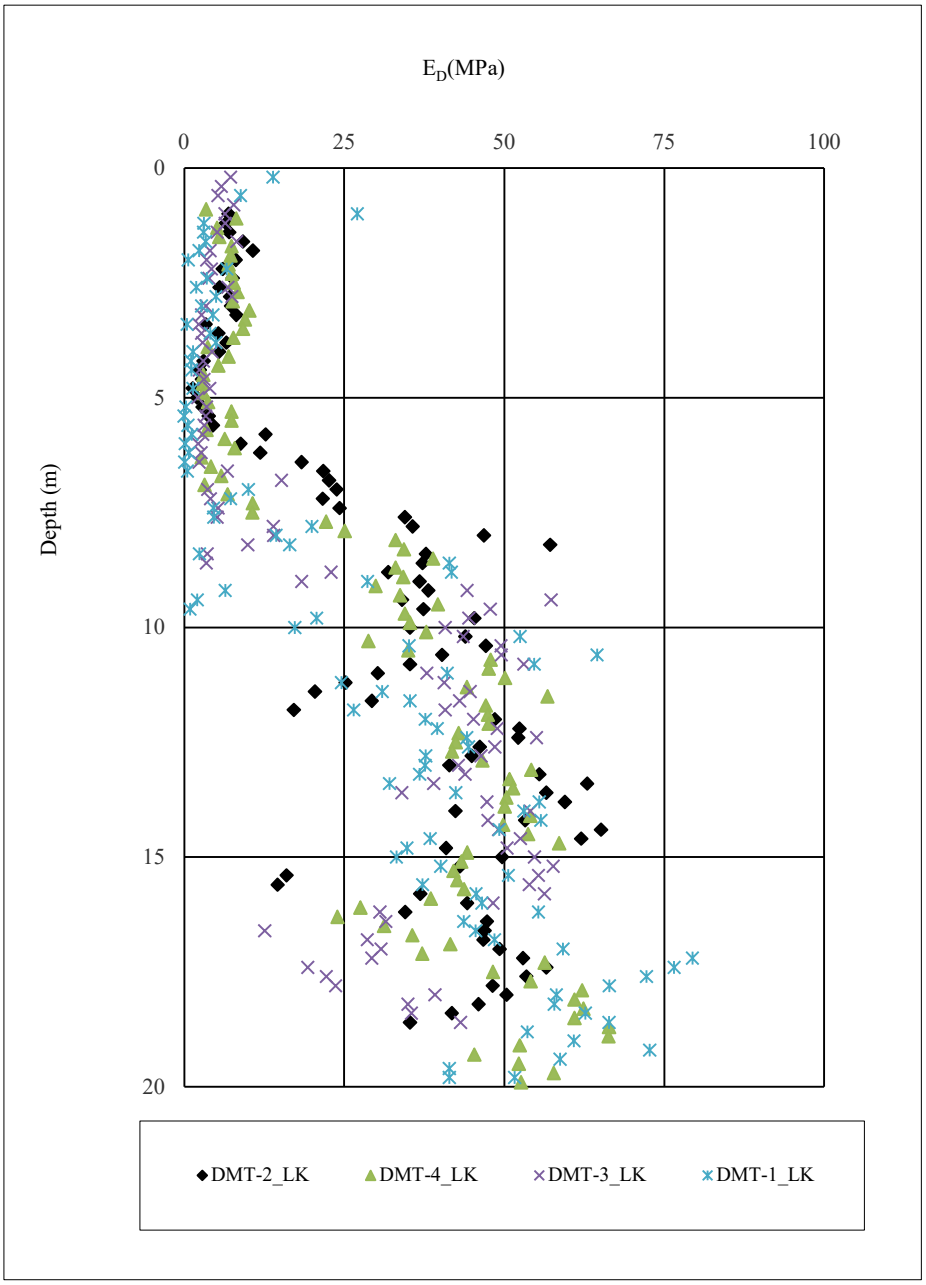

Figure: 5. 59 Variation of E_D with depth for DMT-1_LK, DMT-2_LK, DMT-3_LK, DMT-4_LK, at Site-7 (LK)

At Site-8 (BD), four numbers DMT tests were carried out. the variation of E_D along depth is presented in Figure 5.60. Some higher values of E_D are observed at few depths. This may be due to the presences of sandy silt/silty sand. However, the overall variation of E_D is found to be consistent.

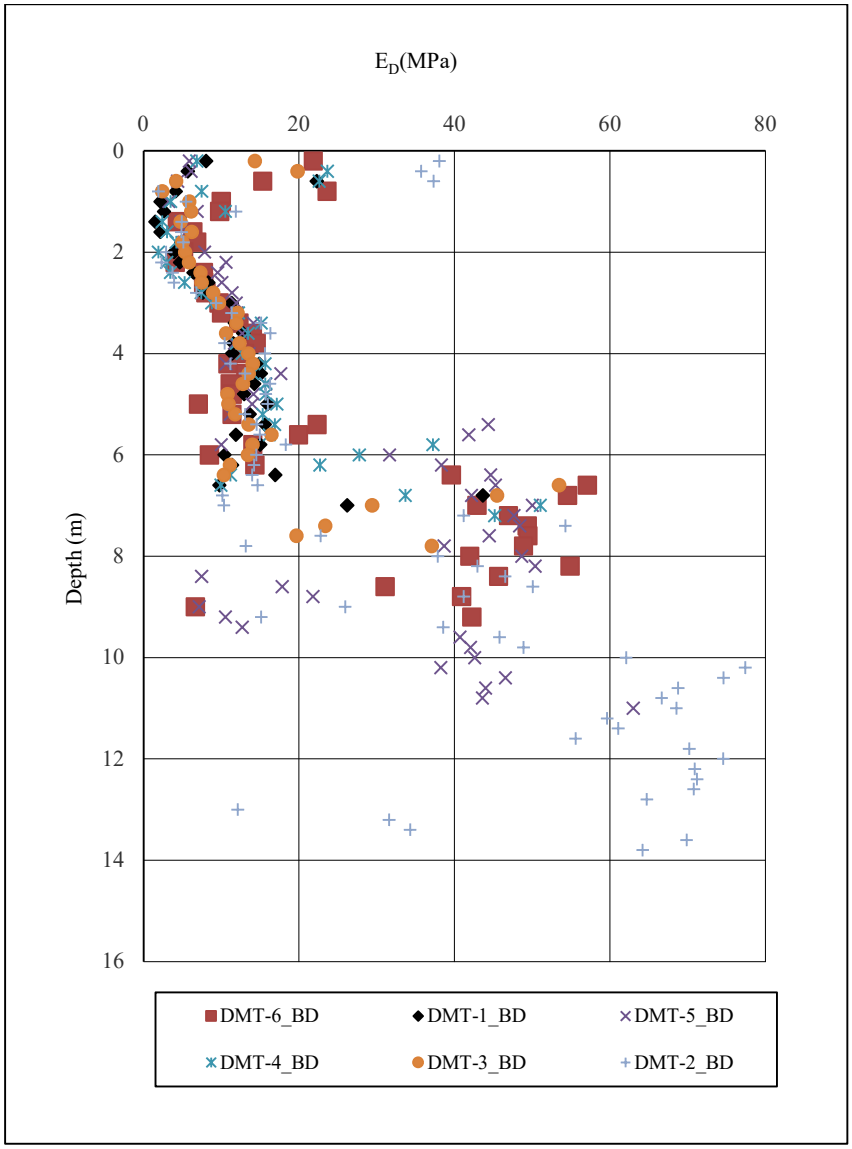

Figure: 5. 60 Variation of E_D with depth for DMT-1_BD, DMT-2_BD, DMT-3_BD, DMT-4_BD, DMT-5_BD, DMT-6_BD at Site-8 (BD)

5.3.6 CONE PENTRATION RESISTANCE (q_c)

Variation of cone penetration resistance (q_c) is plotted along depth for all CPT tests carried out at respective site.

At site-1(HC), four numbers of CPT tests were carried out. The variation of estimated q_c is plotted along depth and presented in Figure 5.61. In this graph, it has been observed that the variation of q_c is consistent and more or less similar in nature for all CPT tests.

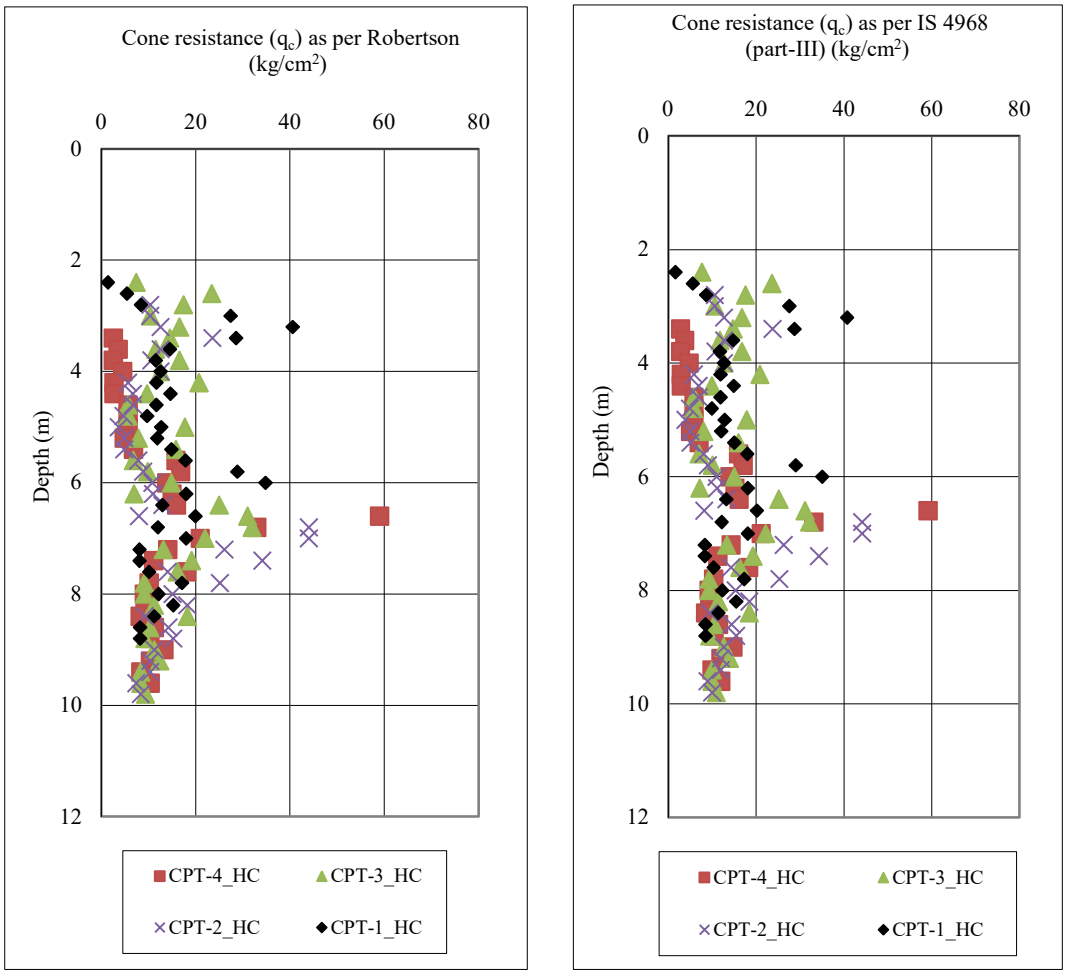

Figure: 5. 61 Variation of q_c with depth for CPT-1_HC, CPT-2_HC, CPT-3_HC, CPT-4_HC, at Site-1(HC)

At Site-2 (PB), two numbers of CPT tests were carried out. The variation of estimated q_c is plotted along depth and presented in Figure 5.62. In this graph, it has been observed that the variation of q_c is scattered probably due to the occasional presence of sand mixture (i.e., silty sand to sandy silt) identified at different depth for both CPT tests.

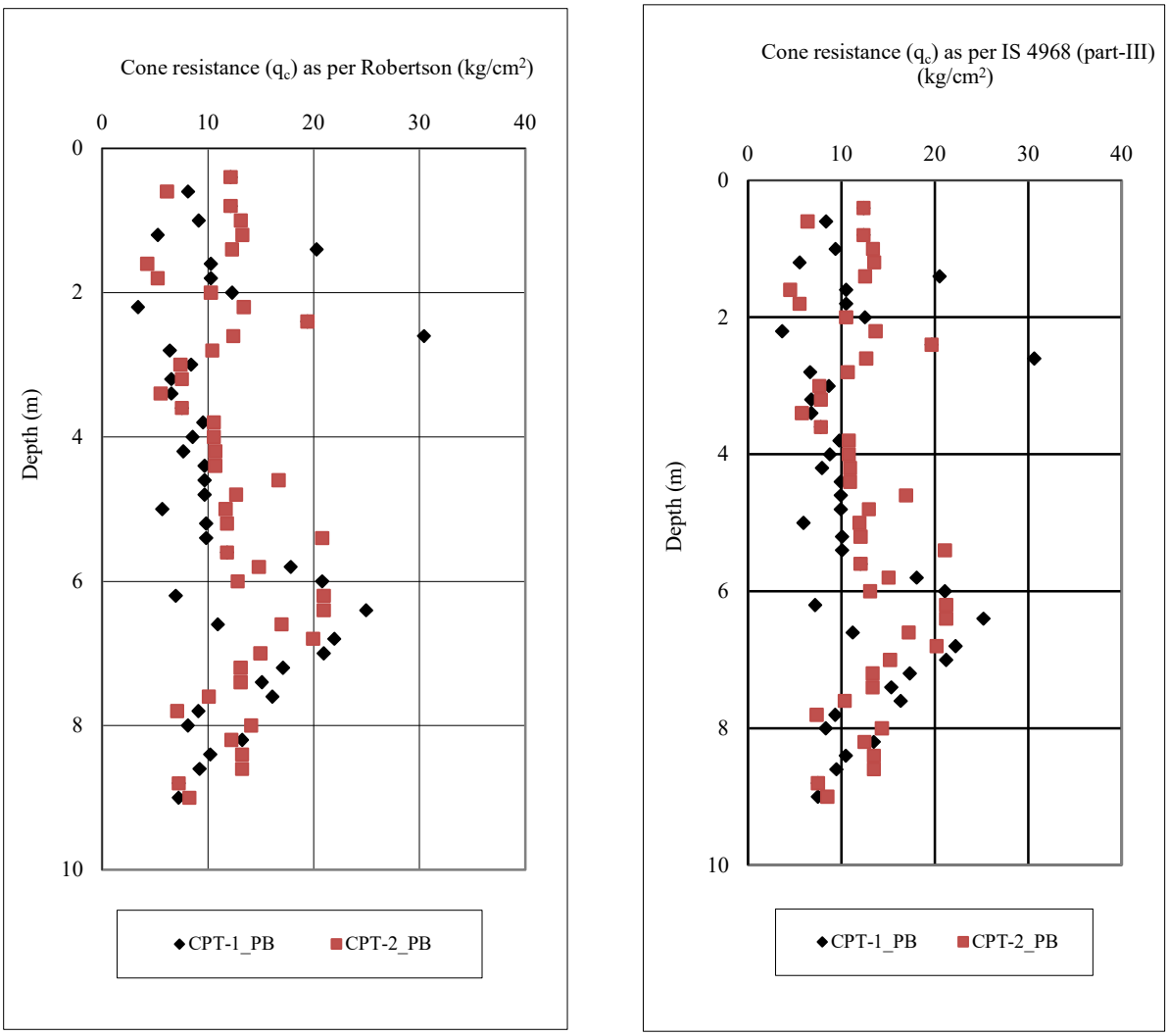

Figure: 5. 62 variation of q_c with depth for CPT-1_PB, CPT-2_PB, at Site-2 (PB

At site-3 (RJ), two numbers of CPT tests were carried out. The variation of q_c is plotted along depth and presented in Figure 5.63. In this graph it is observed that the variation of q_c along depth, is similar in nature and consistent upto the average

depth of 16.0m below ground level. Beyond this depth, values are found to be on the higher side due to the presence of sand mixture (i.e., silty sand to sandy silt).

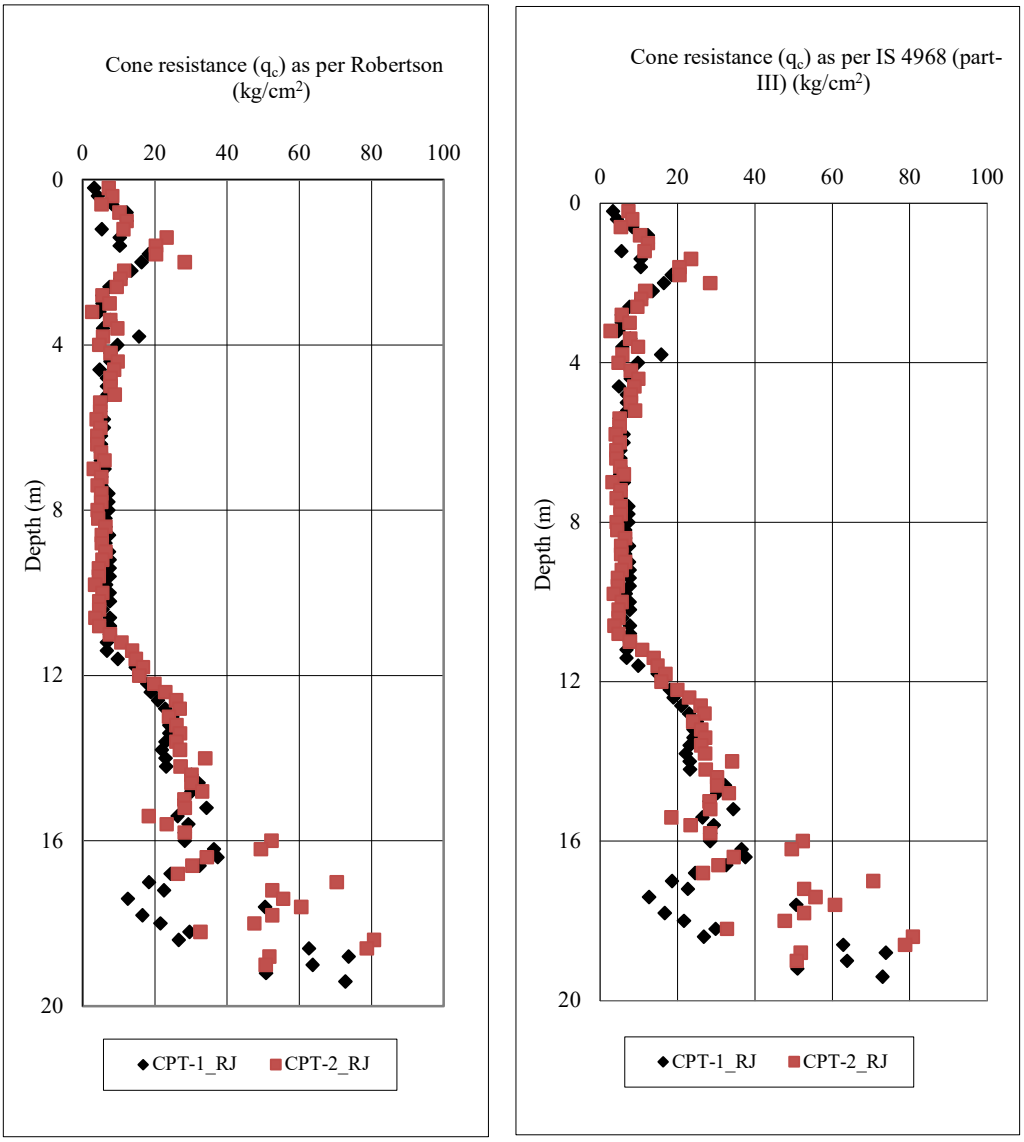

Figure: 5. 63 variation of q_c with depth for CPT-1_RJ, CPT-2_RJ at Site-3(RJ)

At site-4 (HA), three numbers of CPT tests were carried out. The variation of q_c is plotted along depth and presented in Figure 5.64. In this graph, it is found that the variation of q_c along depth is similar for all CPT tests. It is also found that for all the tests, the value of q_c is on the higher side from the average depth of 7.0m

to 10.0m below ground level due to presence of sand mixture (silty sand/sandy silt).

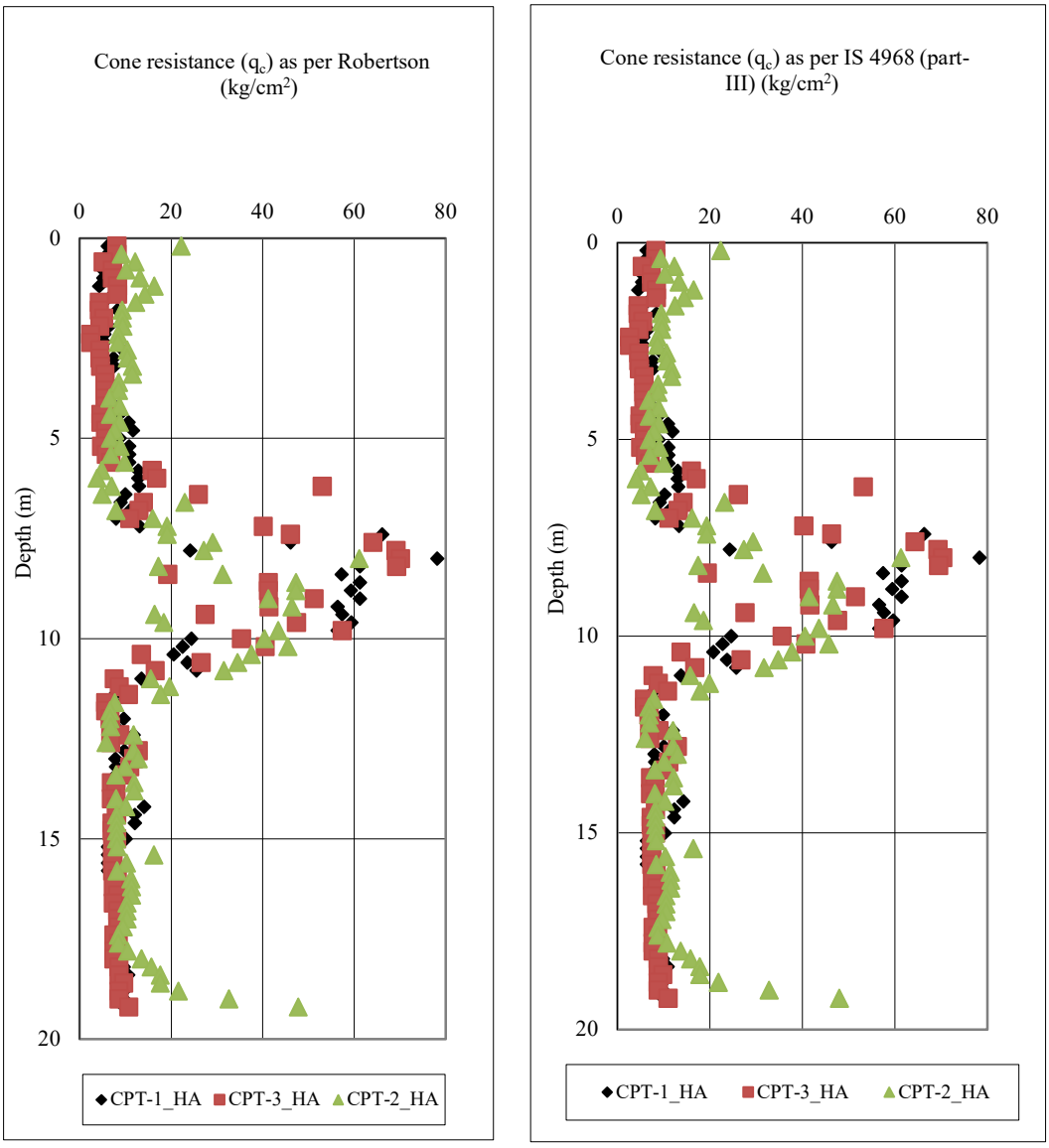

Figure: 5. 64 Variation of q_c with depth for CPT-1_HA, CPT-2_HA and CPT-3_HA, at Site-4 (HA)

At Site-5 (DH), three numbers of CPT tests were carried out. The variation of q_c is plotted along depth and presented in Figure 5.65. In this graph, it is found that the overall variation of q_c along depth are similar in nature at all CPT tests. However, some scattered values are found within the 5.0m to 8.0m depth below

ground level at CPT-1_DH and CPT-3_DH tests points, probably due to the occasional presence of organic soil.

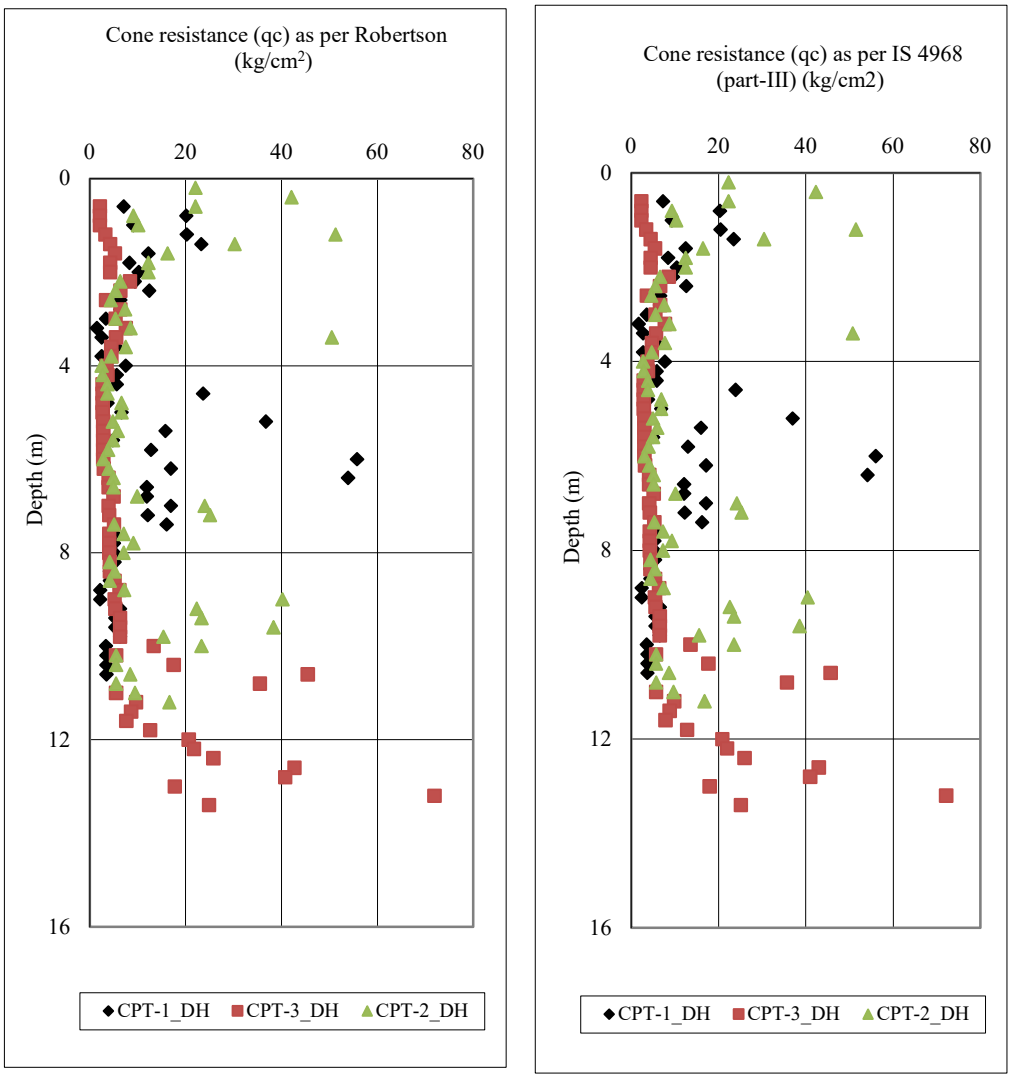

Figure: 5. 65 Variation of q_c with depth for CPT-1_DH, CPT-2_DH and CPT-3_DH, at Site-5 (DH)

At site-6 (SN), five numbers CPT tests were carried out. The variation of q_c is plotted along depth and presented in Figure 5.66. In this graph, it is observed that the variation of q_c is similar in nature and also consistent for all CPT tests.

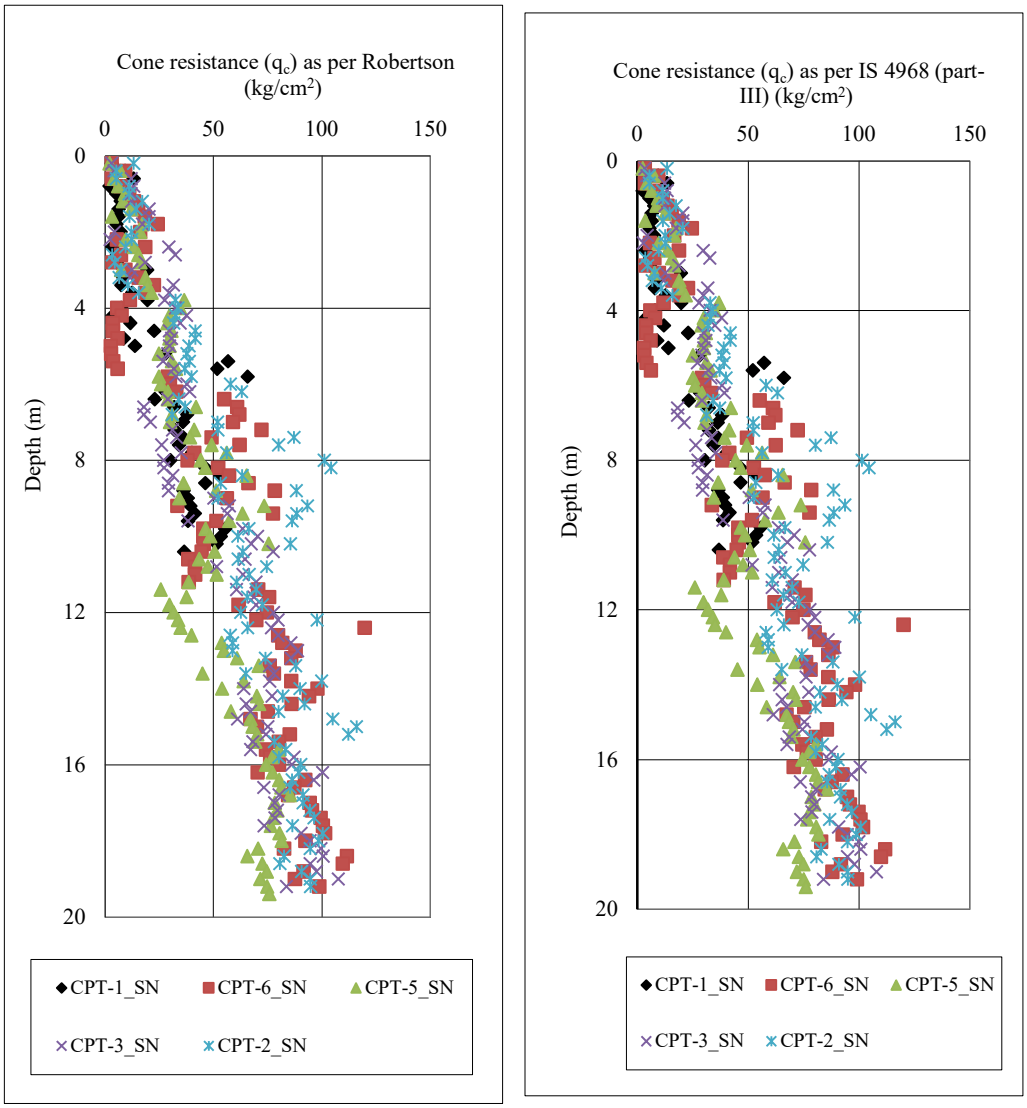

Figure: 5. 66 Variation of q_c with depth for CPT-1_SN, CPT-2_SN and CPT-3_SN, CPT-5_SN and CPT-6_SN at Site-6 (SN)

At Site-7 (LK), four numbers of CPT tests were carried out. The variation of q_c is plotted along depth and presented in Figure 5.67. In this graph, it is observed that the variation of q_c is similar in nature and also consistent for all CPT tests upto the average depth of 8.0m below ground level. Below this depth, it is

observed that the values are consistently on the higher side upto the termination depth due to presence of sand mixture (i.e., sandy silt/ silty sand) soil.

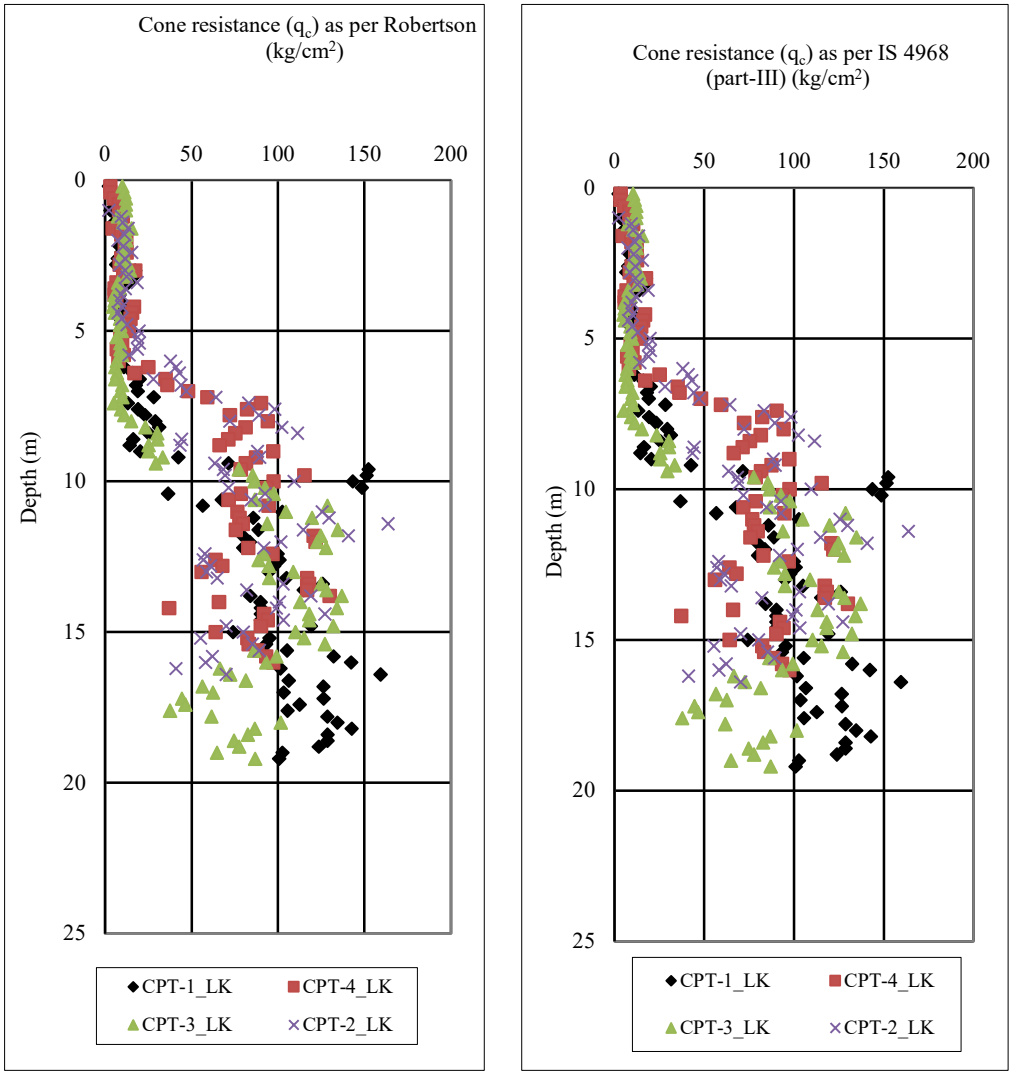

Figure: 5. 67 Variation of q_c with depth for CPT-1_LK, CPT-2_LK and CPT-3_LK and CPT-4_LK at Site-7 (LK)

At Site-8 (BD) site, two numbers of CPT tests were carried out. The variation of q_c is plotted along depth and presented in Figure 5.68. In this graph, it has been observed that the variation of q_c along depth, are consistent and similar in nature for both the tests upto the average depth of 6.0m below ground level. Below this depth the value of q_c is found to be on the higher side upto the termination depth, probably due to the presence of sand mixture i.e., sandy silt / silty sand.

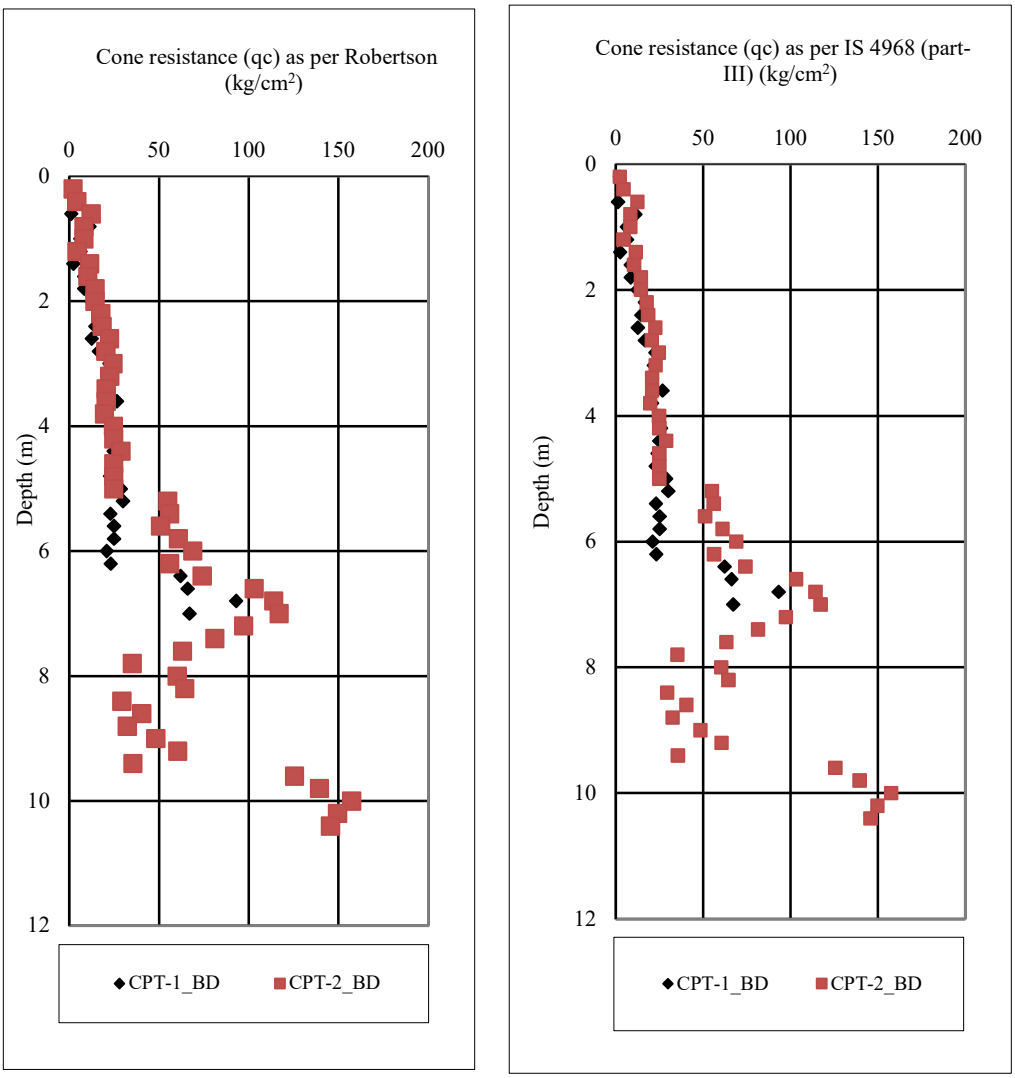

Figure: 5. 68 Variation of q_c with depth for CPT-1_BD, CPT-2_BD at Site-8 (BD)

5.3.7 SLEEVE FRICTION (f_s)

The variation of sleeve fiction (f_s) along depth has been plotted for all CPT test points conducted at different test site. The variation of f_s for each site, is shown in Figure 5.69 to 5.76.

At Site-1(HC), variation of f_s along depth for four numbers of CPT test, is shown in Figure 5.69. In this graph it has been observed that the nature of the variation of f_s along depth is more or less similar for all CPT test.

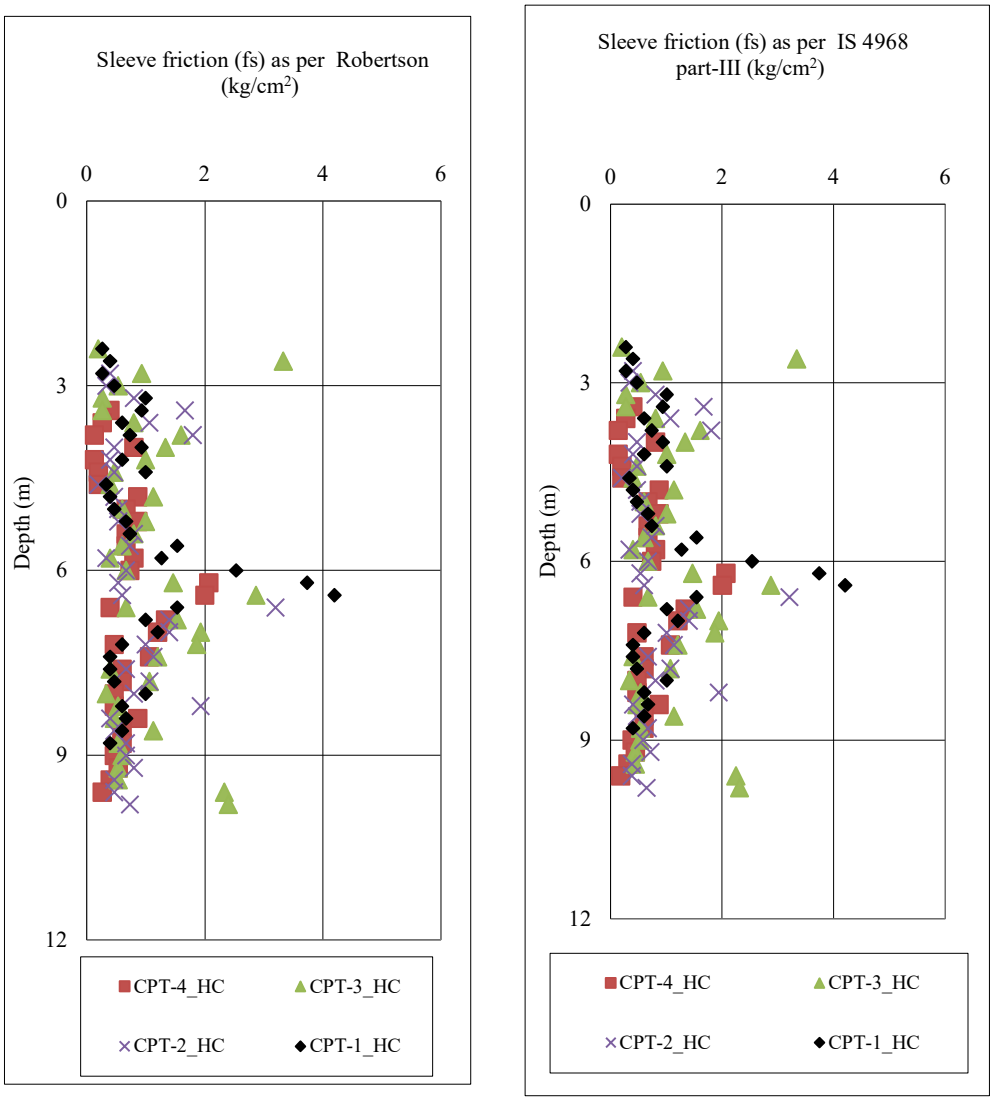

Figure: 5. 69 Variation of f_s with depth for CPT-1_HC, CPT-2_HC, CPT-3_HC, CPT-4_HC, at Site-1(HC)

At site-2 (PB), variation of f_s along depth is plotted for two numbers of CPT tests. In this graph, it has been observed that the variation of f_s is scattered due to the presence of sand mixture identified at different depth. The variation of sleeve friction is shown in Figure 5.70.

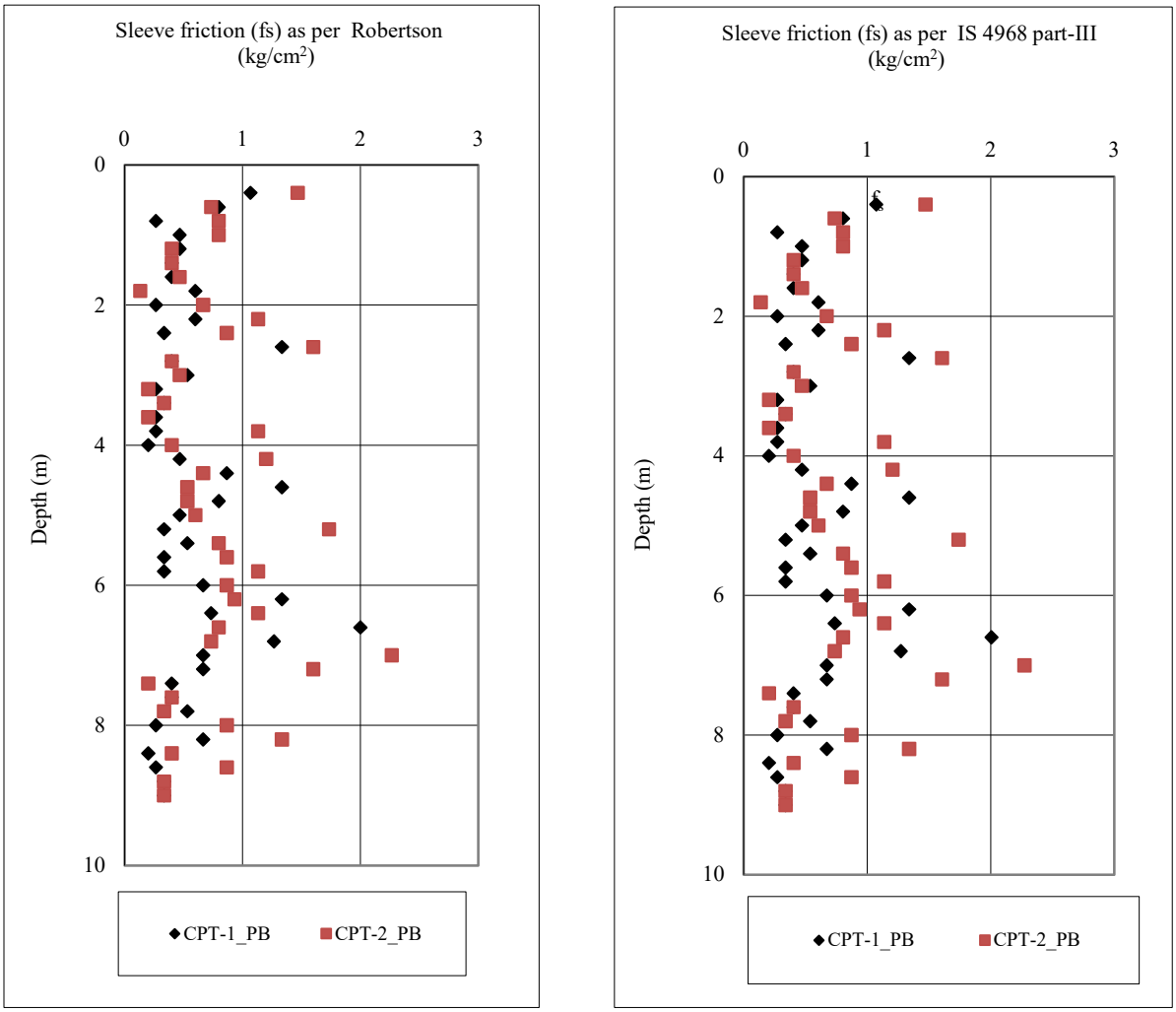

Figure: 5. 70 Variation of f_s with depth for CPT-1_PB, CPT-2_PB at Site-2 (PB)

At site-3 (RJ), variation of f_s along depth is plotted for two numbers CPT tests as shown in Figure 5.71. In this graph it is observed that the variation of f_s along depth is similar in nature and consistent upto the average depth of 16.0m below ground level. Beyond this depth, values are found to be on the higher side due to the presence of sand mixture (i.e., silty sand to sandy silt).

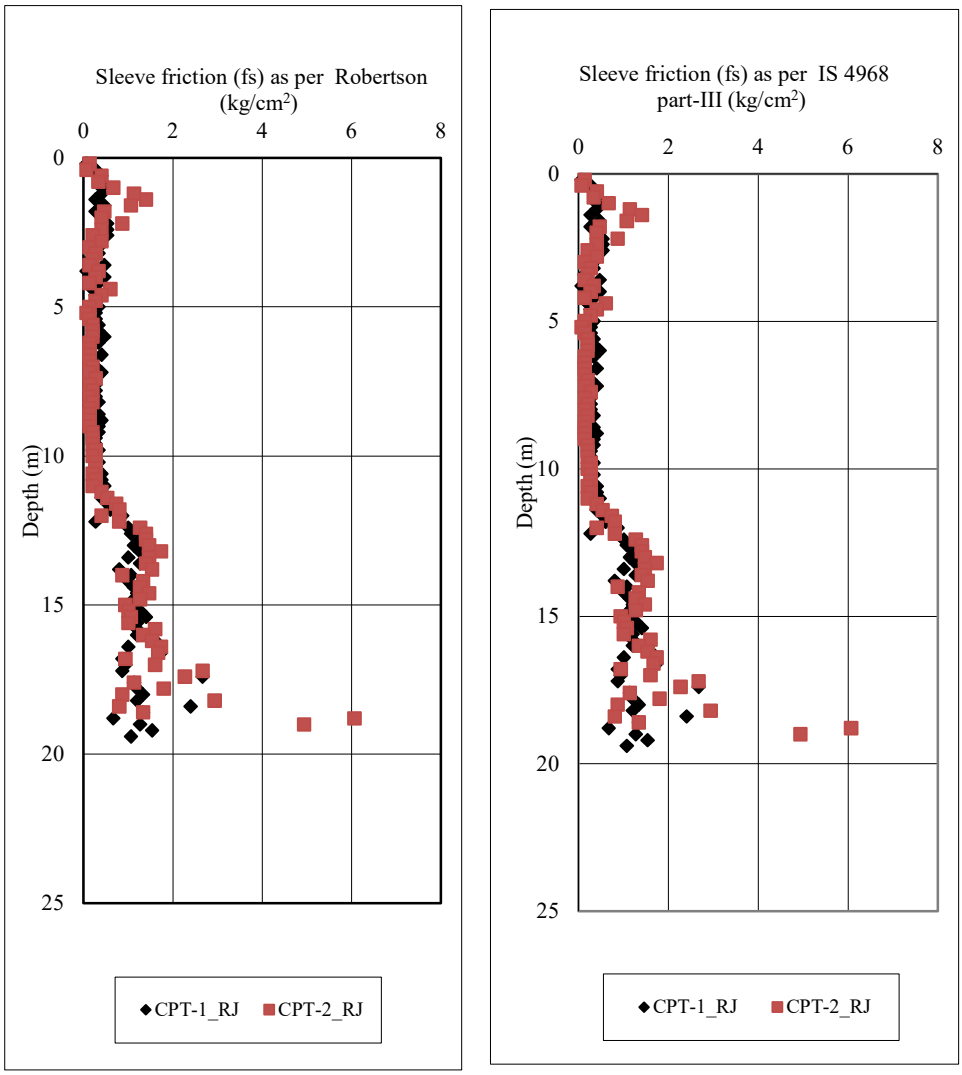

Figure: 5. 71 Variation of f_s with depth for CPT-1_RJ, CPT-2_RJ at Site-3 (RJ)

At site-4 (HA), three numbers CPT tests were carried out. The variation of f_s is plotted along depth and presented in Figure 5.72. In this graph, it is found that the pattern of the variation of f_s along depth is similar for all CPT tests. It is also found that for all the tests, the value of f_s is on higher side from the average depth of 5.0m to 10.0m due to presence of sand mixture (silty sand/sandy silt).

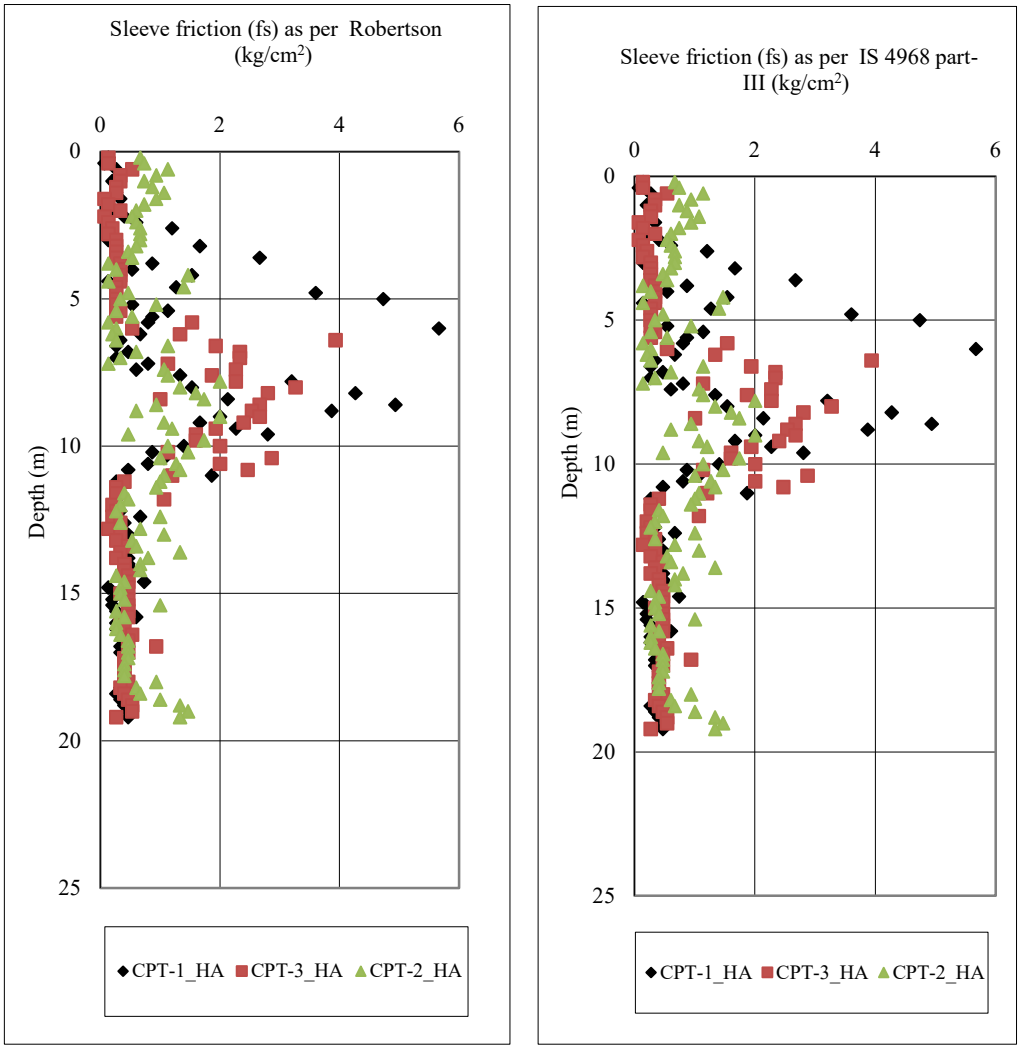

Figure: 5. 72 Variation of f_s with depth for CPT-1_HA, CPT-2_HA and CPT-3_HA, at Site-4 (HA)

At Site-5 (DH), three numbers CPT tests were carried out. The variation of f_s is plotted along depth and presented in Figure 5.73. In this graph, it is found that the overall variation of f_s along depth is similar in nature at all CPT tests. However, some scattered values are found within the 5.0m to 8.0m depth below ground level at CPT-1_DH and CPT-3_DH tests points, due to the occasional presence of sand mixture/organic soil.

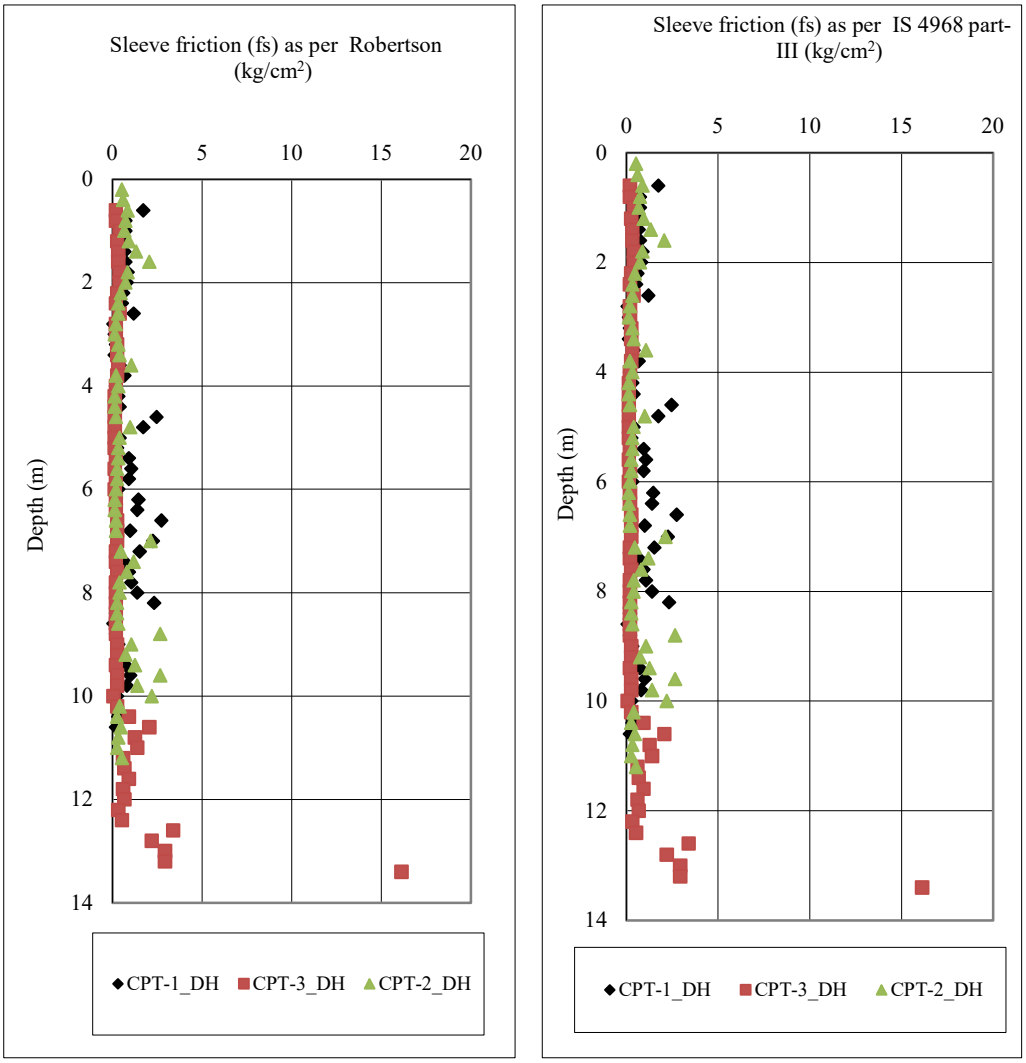

Figure: 5. 73 Variation of f_s with depth for CPT-1_DH, CPT-2_DH and CPT-3_DH, at Site-5 (DH)

At site-6 (SN), the variation of f_s is plotted along depth and shown in Figure 5.74. In this graph, it is observed that the variation of f_s is similar in nature and also consistent for all CPT tests.

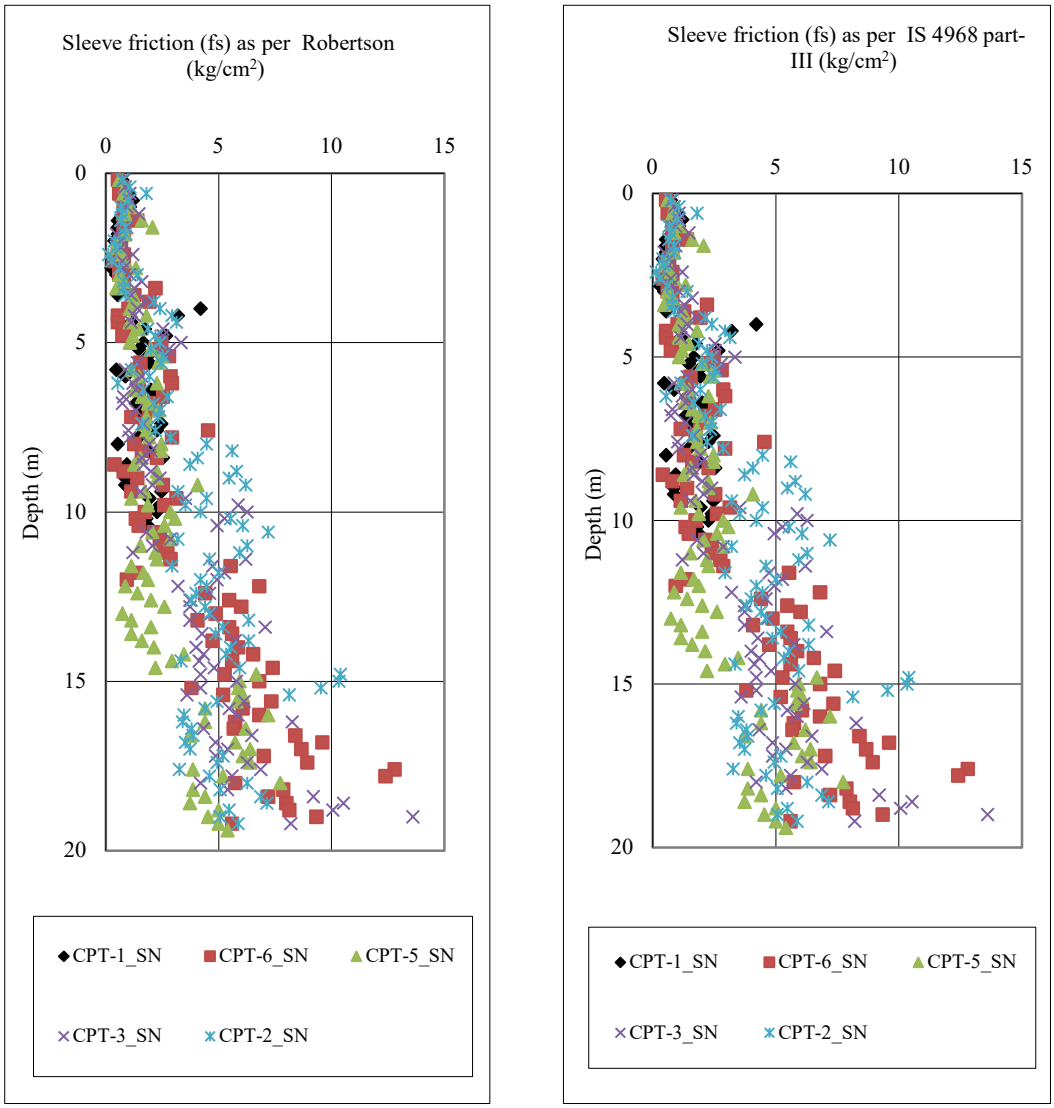

Figure: 5. 74 Variation of f_s with depth for CPT-1_SN, CPT-2_SN and CPT-3_SN, CPT-5_SN and CPT-6_SN at Site-6 (SN)

At Site-7 (LK), the variation of f_s is plotted along depth and presented in Figure 5.75. In this graph, it is observed that the variation of f_s is similar in nature and also consistent for all CPT tests upto the average depth of 8.0m below ground level. Below this depth, it is observed that the values are consistently on the higher side upto the termination depth.

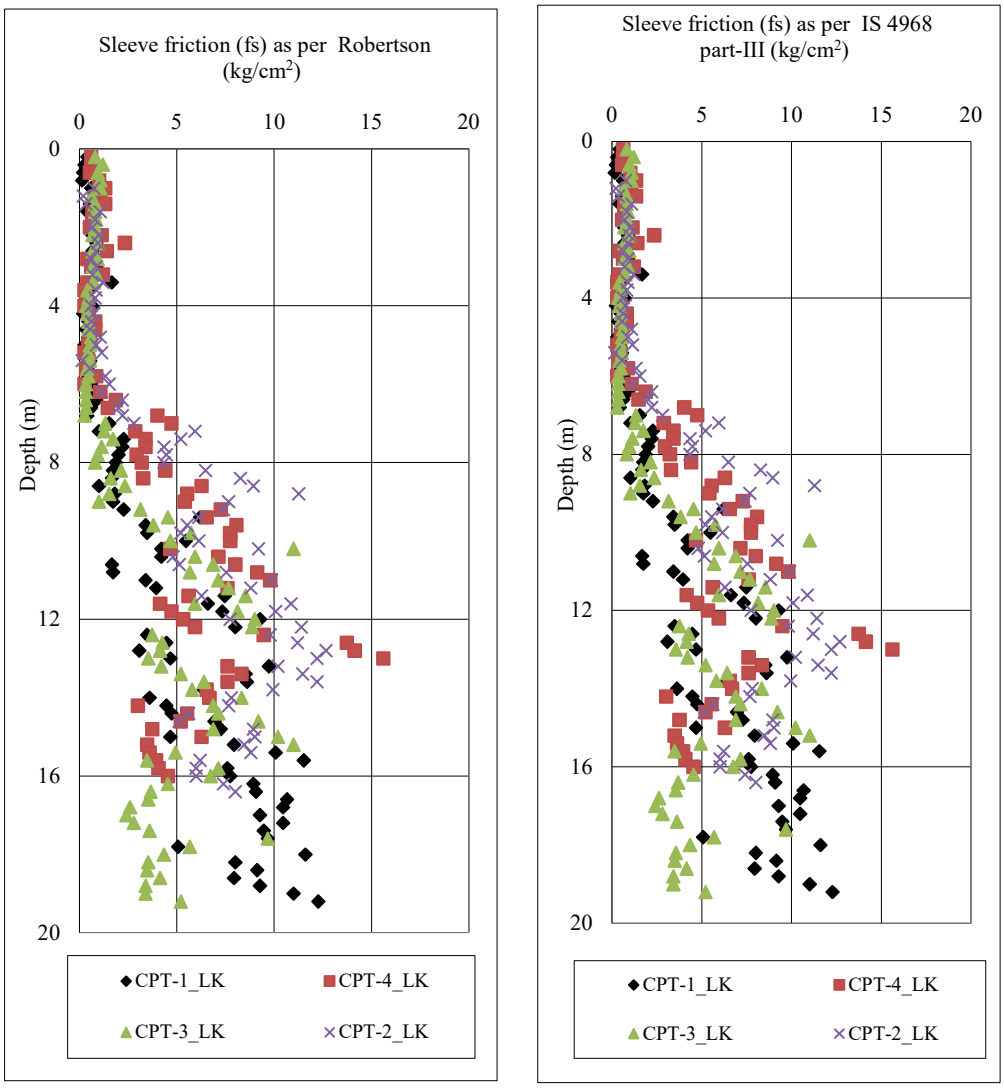

Figure: 5. 75 Variation of f_s with depth for CPT-1_LK, CPT-2_LK and CPT-3_LK and CPT-4_LK at Site-7 (LK)

At Site-8 (BD), the variation of f_s is plotted along depth and presented in Figure 5.76. In this graph, it has been observed that the variation of f_s along depth, are consistent and similar in nature for both the tests upto the depth of 6.0m below ground level. Below this depth the value of f_s is found to be on the higher side upto the termination depth, probably due to the presence of sand mixture i.e., sandy silt / silty sand.

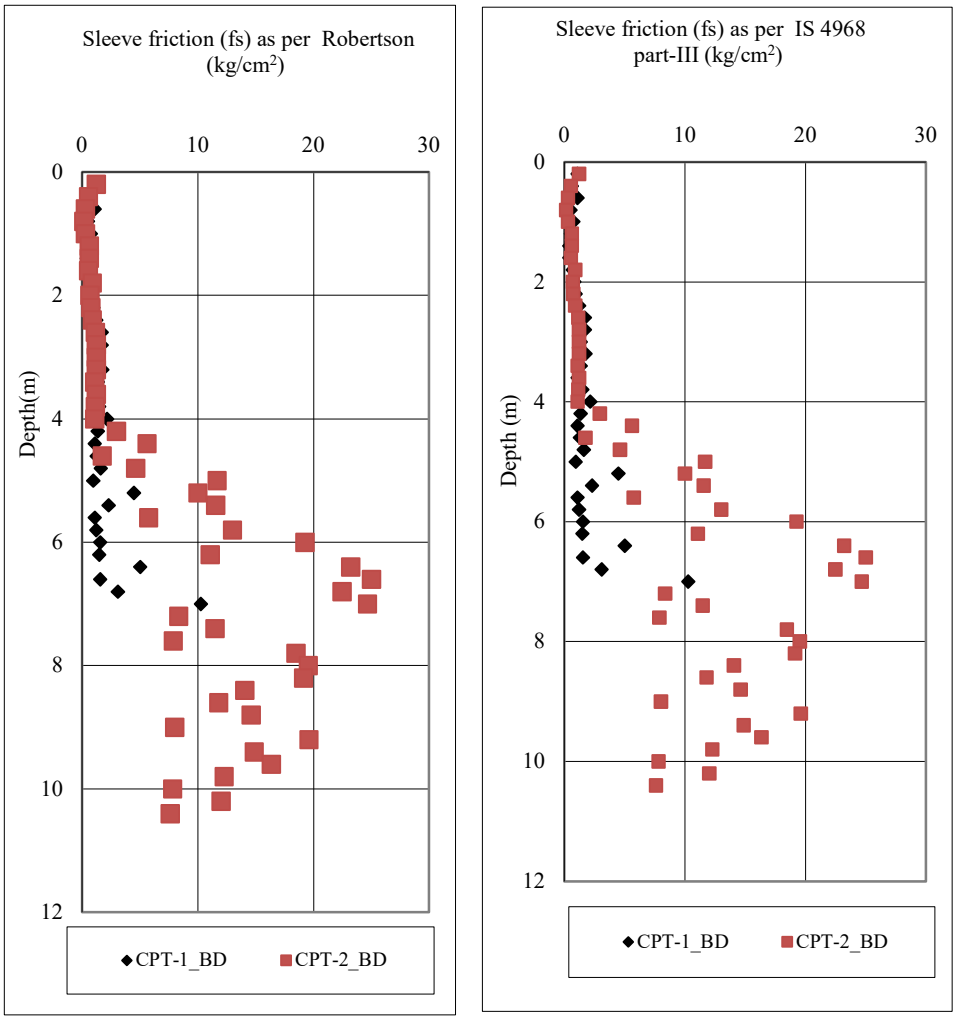

Figure: 5. 76 Variation of f_s with depth for CPT-1_BD, CPT-2_BD at Site-8 (BD)

5.3.8 MATERIAL INDEX (I_D) AND SOIL BEHAVIOUR TYPE INDEX (I_C)

The material index (I_D) and soil behaviour type index (I_C), have been plotted with depth for eight number of sites where both DMT and CPT tests were carried out. Based on the I_D and I_C values, it is observed that at most of the sites, cohesive subsoil is predominant up to the test depth. In few cases, presence of silt mix/sandy mixture/silty sand/sandy silt have been noticed. Site wise, variation of material index (I_D) and soil behaviour type index (I_C) with depth, are shown in Figure 5.77 to 5.84.

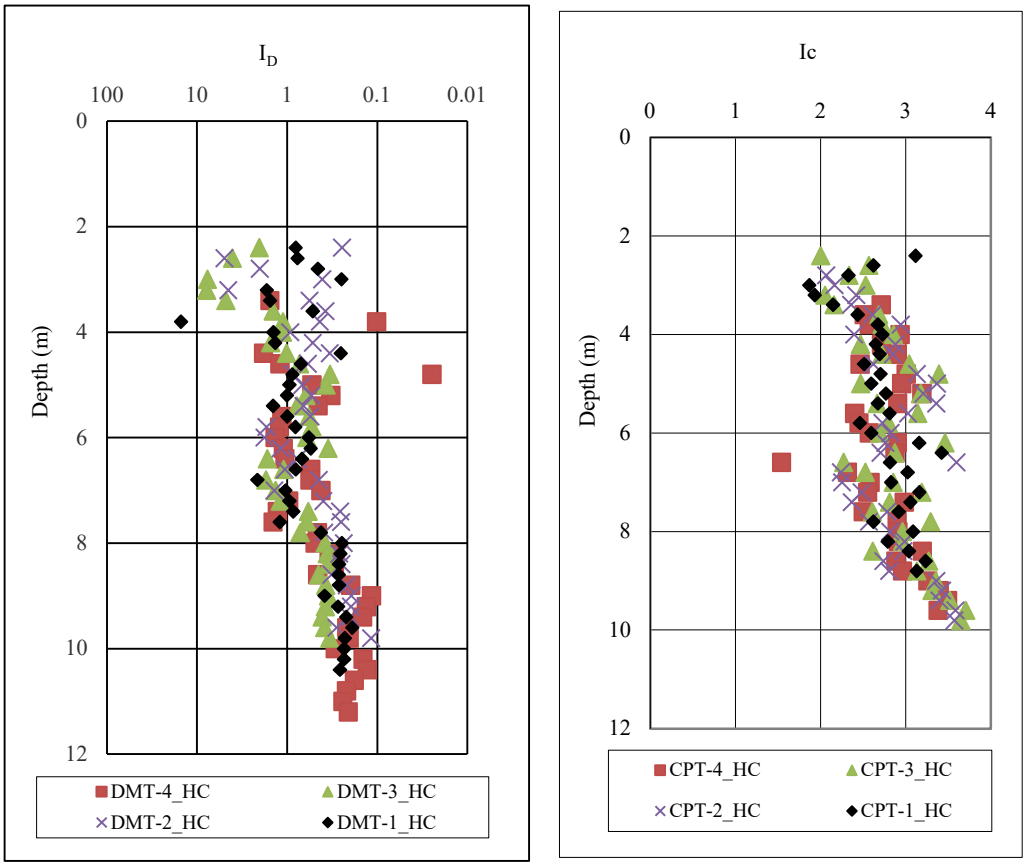

Figure: 5. 77 Variation of I_D and I_C with depth at Site-1 (HC)

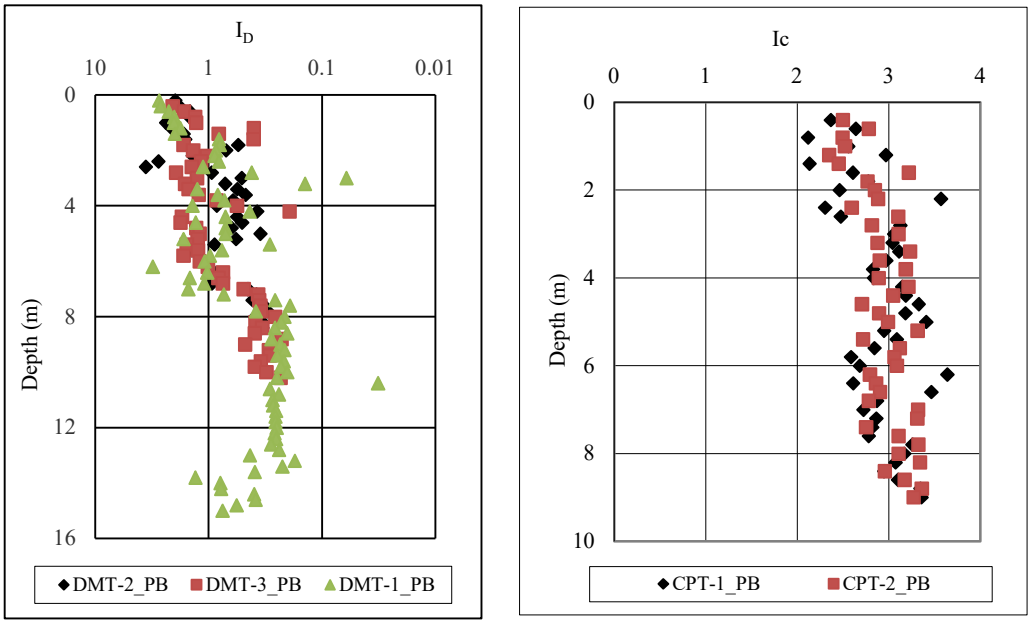

Figure: 5. 78 variation of I_D and I_C with depth at Site-2 (PB)

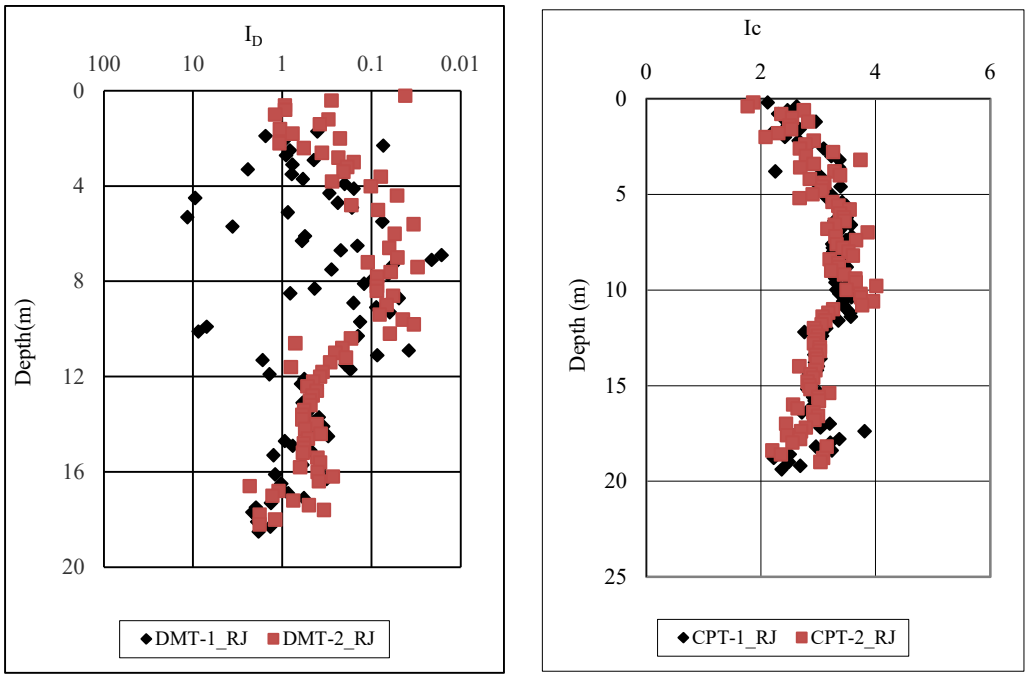

Figure: 5. 79 variation of I_D and I_C with depth at Site-3 (RJ)

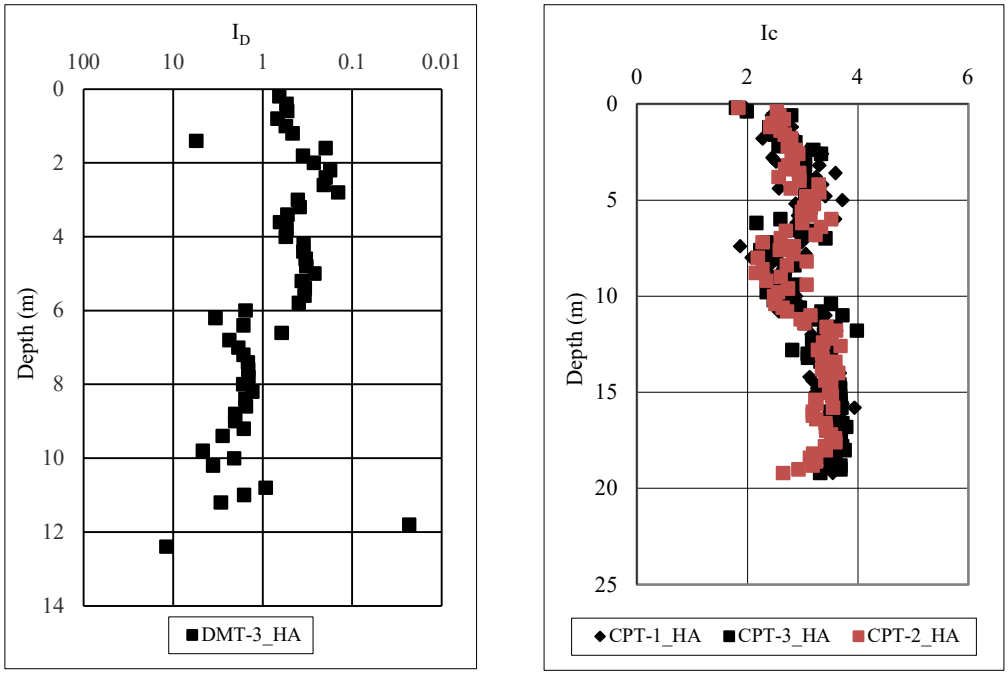

Figure: 5. 80 Variation of I_D and I_C with depth at Site-4 (HA)

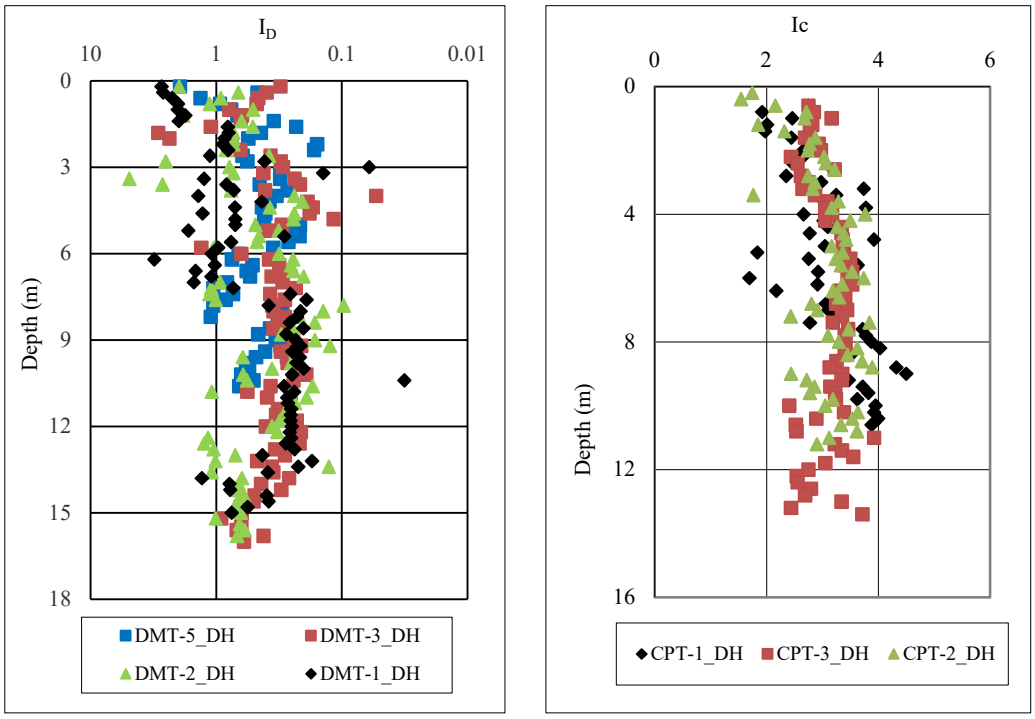

Figure: 5. 81 Variation of I_D and I_C with depth at Site-5 (DH)

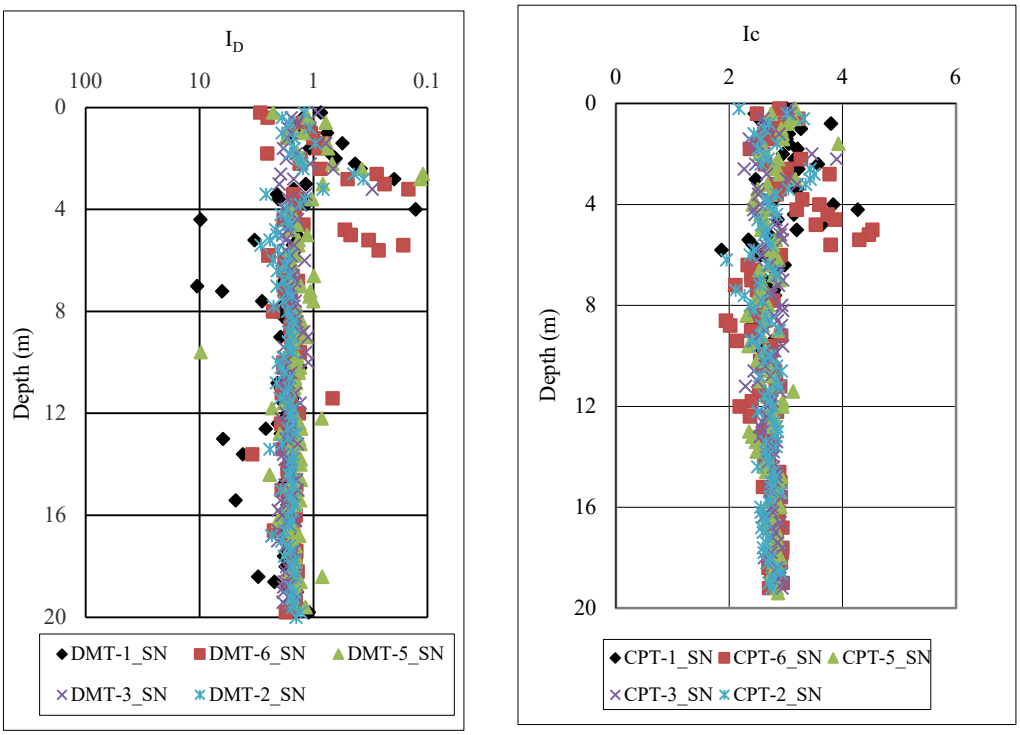

Figure: 5. 82 Variation of I_D and I_C with depth at Site-6 (SN)

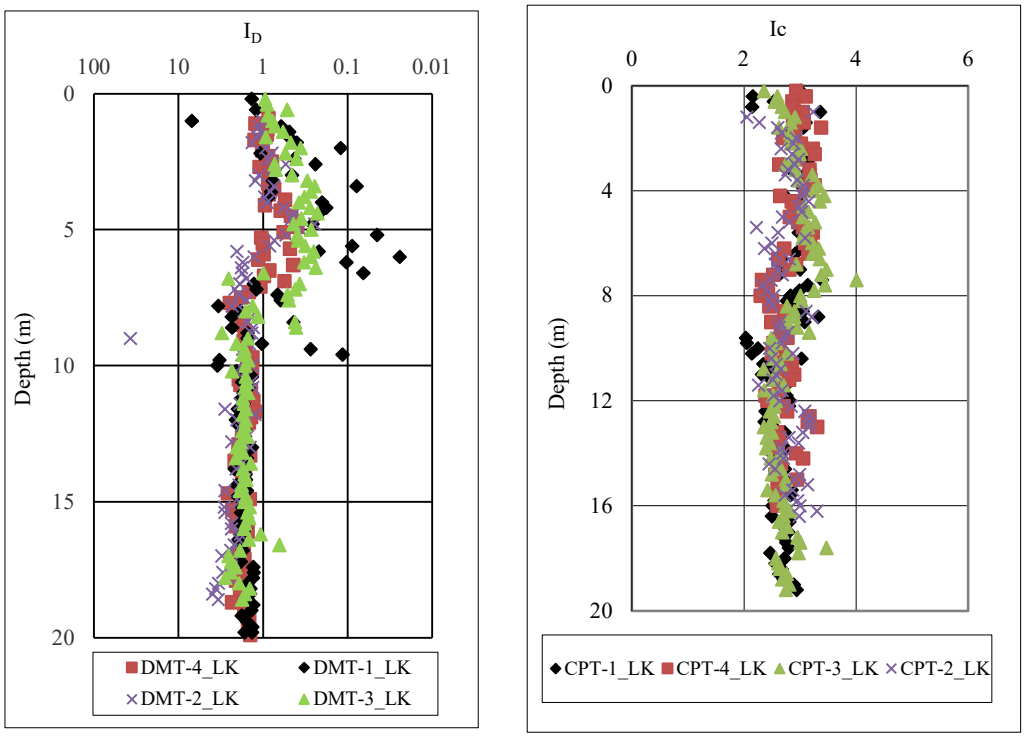

Figure: 5. 83 Variation of I_D and I_C with depth at Site-7 (LK)

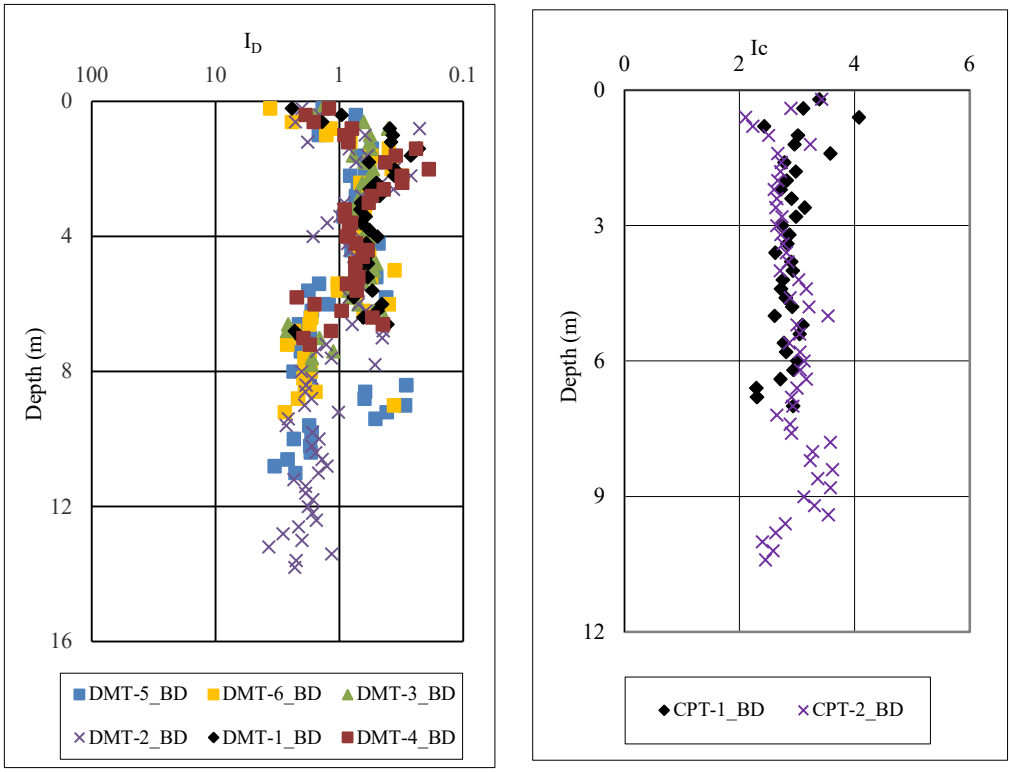

Figure: 5. 84 Variation of I_D and I_C with depth at Site-8 (BD)

5.3.9 LIMIT PRESSURE (P_L) AND PRESSUREMETER MODULUS (E_{PMT})

At three sites viz., Site-9 (VT), Site-10 (PT) and Site-11 (ES), Pressuremeter tests were carried out to determine Limit pressure (P_L) and Pressuremeter modulus (E_{PMT}). Variation of Limit pressure (P_L) and Pressuremeter modulus (E_{PMT}) along depth have been plotted.

At Site-9 (VT), twenty numbers of PMT tests were carried out at five test locations. The variation of limit pressure (P_L) along depth, is plotted (Figure 5.85). At these test locations, presence of silty sand/sandy silt was observed below the average depth of 9.0m. Consequently, the value of P_L is found to be on higher side below that depth. However, it has been observed that the variation of limit pressure along depth is consistent and similar in nature for the entire site.

Besides, the variation of Pressuremeter modulus (E_{PMT}) along depth has also been plotted for these five numbers of test points (Figure 5.86). The higher value of E_{PMT}, has been found below the average depth of 9.0m. However, the overall nature of the variation of E_{PMT}, is found similar and consistent for all PMT test points.

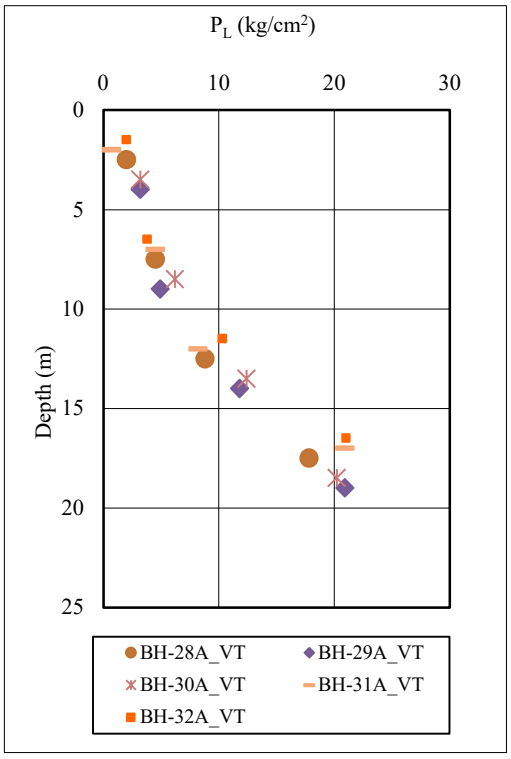

Figure: 5. 85 Variation of limit pressure (P_L) along depth at Site-9 (VT)

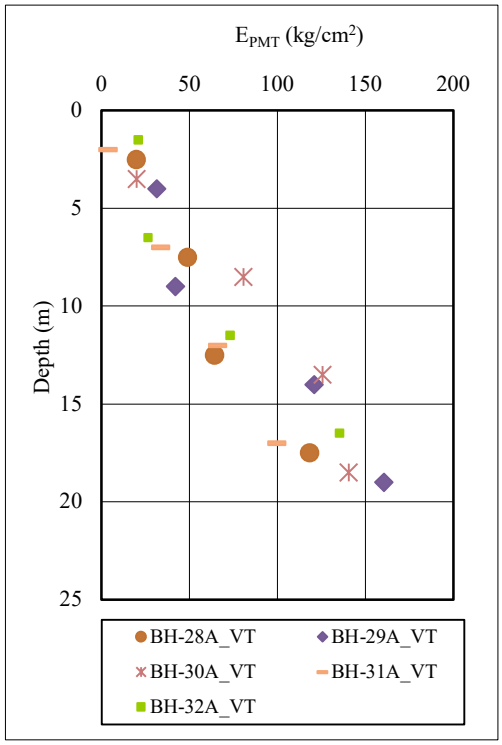

Figure: 5. 86 Variation of Pressuremeter Modulus (E_{PMT}) along depth at Site-9 (VT)

At Site-10 (PT), sixteen PMT tests were carried out at four locations. Limit pressure (P_L) is plotted along depth (Figure 5.87). In this plot, it is observed that the variation of P_L along depth is consistent and similar in nature. Besides, the variation of E_{PMT} along depth has been plotted (Figure 5.88). It is found to be consistent and similar in nature for all test locations. At these test locations, it was observed that the sub-soil consists of soft/ firm to very stiff silty clay/clayey

silt upto the average depth of 18.5m below ground level. Subsequently, the value of P_L and E_{PMT} are found to be on lower side.

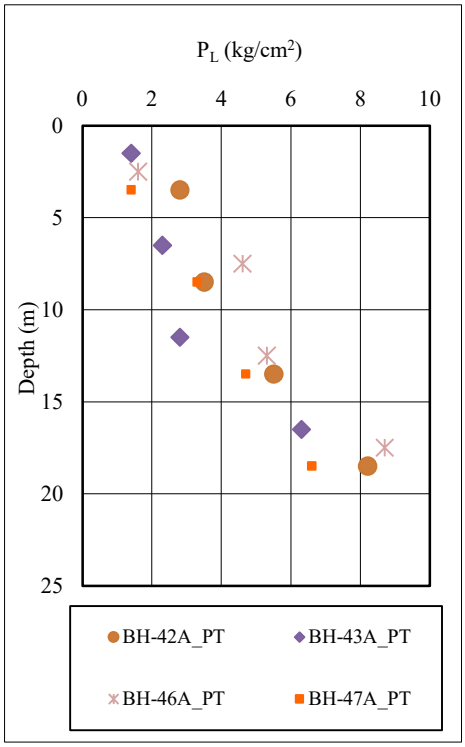

Figure: 5. 87 Variation of limit pressure (P_L) along depth at Site-10 (PT)

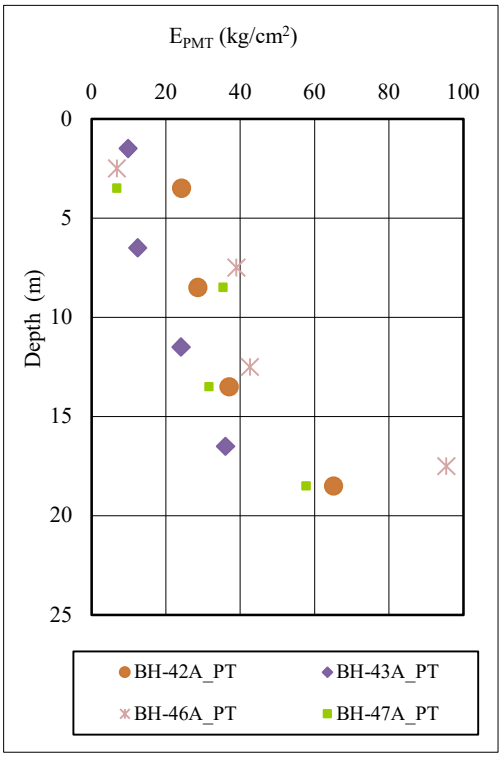

Figure: 5. 88 Variation of Pressuremeter Modulus (E_{PMT}) along depth Site-10 (PT)

At Site-11, twelve number of PMT tests were carried out at three locations. Limit pressure (P_L) is plotted along depth (Figure 5.89). Besides, the variation of E_{PMT} along depth has been plotted (Figure 5.90). In these plots, it has been observed that the overall variation of P_L and E_{PMT} along depth is consistent and similar in nature for the entire test locations. At these locations, it was observed that the sub-soil consists of soft/ firm to very stiff silty clay/clayey silt upto the average depth of 19.0m below ground level. Subsequently, the value of P_L and E_{PMT} are found to be on the lower side.

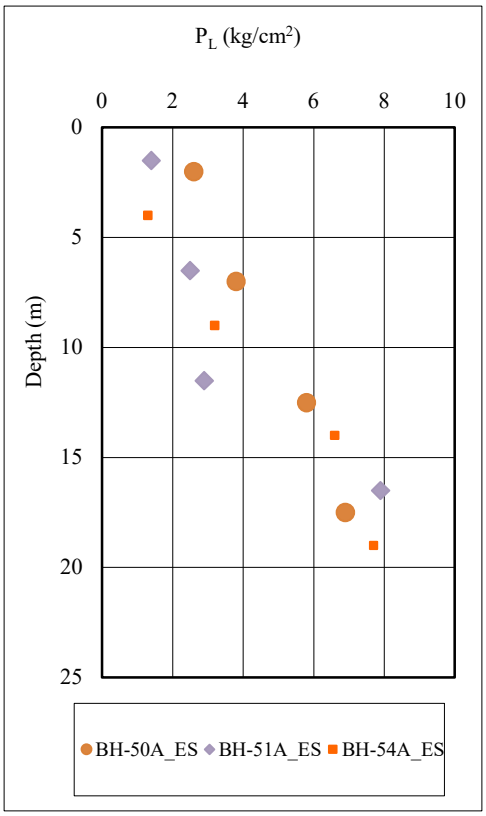

Figure: 5. 89 Variation of limit pressure (P_L) along depth at Site-11 (ES)

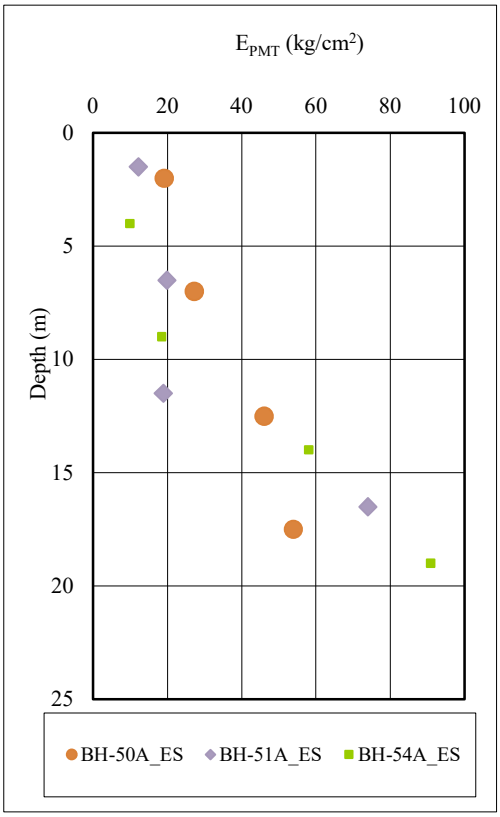

Figure: 5. 90 Variation of Pressuremeter Modulus (E_{PMT}) along depth at Site-11 (ES)

5.4 SUMMARY

DMT test, CPT test and PMT test were carried out at different locations. In this study the selected parameters obtained from DMT, CPT and PMT tests, have been considered to compare with the conventional SPT N values and shear strength parameters. Apart from this, the sub-soil profiling estimated from DMT and CPT (based on I_D and I_C) have been compared with that obtained from the conventional boring technique. Also, the value of pressuremeter modulus (E_{PMT}) and Limit pressure (P_L) have been observed for the typical normal Calcutta soil deposits. The principal observations are summarised below:

- It has been observed that the undrained cohesion (C_u) estimated from DMT test, are more comparable than that the C_u estimated from CPT test.
- The angle of internal friction estimated from DMT and CPT tests are comparable with the values estimated from laboratory direct shear test (DS).
- Compressibility characteristics of sub-soil in terms of vertical drained constrained modulus (M) are found to be more or less similar for both DMT and CPT tests.
- It is observed that the variation of both M_{DMT} and M_{CPT} is well tallying with the SPT N values for entire study location.
- It is also observed that the variation of Dilatometer Modulus (E_D) is well tallying with the SPT N values for all the study locations.
- In CPT tests, the variation of both cone penetration resistance (q_c) and sleeve friction (f_s) closely matches with the SPT N values throughout the entire study area.
- It has also been observed that the value of cone resistance (q_c) and sleeve friction (f_s) estimated as per IS 4968 (Part-III) are very close with the values estimated as per (Robertson and Cabal 2015).
- Moreover, the sub soil profile (identified from conventional boring work at adjacent bore holes) is alike with predicted sub-soil profile by DMT and CPT tests (based on the I_D and I_C values).
- In PMT tests, it has been observed that the variation of P_L and E_{PMT} are more or less similar for the individual site. However, the value of these parameters depends on the consistency of the sub-soil. Consequently, the variation of both the parameters P_L and E_{PMT} is found to be well comparable with the observed SPT N values.

- It has also been noticed that the presence of decomposed wood particles in sub-soil badly affects the test results obtained from DMT, CPT and PMT tests.
- In some cases, it is noticed that the sub-soil is identified as silty sand/sandy silt from DMT or CPT tests while the presence of silty clay/clayey silt soil mixed with decomposed wood was observed from conventional boring technique. Consequently, the value of M_{DMT} or M_{CPT} is found to be on higher side compared to the silty clay/clayey silt soil.

Chapter# 6
DESIGN CHARTS BASED ON PARAMETRIC COMPARISON

6.1 GENERAL

This chapter focuses on comparing the basic parameters viz., E_D, M, q_c, f_s, P_L, and E_{PMT} with SPT N values (N_{ob}) (conducted at adjacent conventional boreholes, (BH)) at each test location. Following that, an attempt has been made to create a design chart for predicting the values of those parameters for cohesive soil (with varying consistency) based on N_{ob} value.

Furthermore, another attempt has been made to predict the index properties of cohesive soil using the parameters obtained from the DMT, CPT, and PMT tests.

6.2 DMT TEST

In this study, two basic parameters viz., E_D and M_{DMT} are considered for comparison purpose. In DMT test, dilatometer modulus (E_D) is obtained from the pressure difference applied to the membrane during the test (Marchetti et al. 2001). It should be noted that the value of E_D does not represent the stress history of soil (Marchetti 1980; Marchetti et al. 2001). Additionally, the observed (field) SPT blow count (N_{ob}) does not represent the soil stress history(Terzaghi 1943). Therefore, at each test location, E_D is compared with the N_{ob}. Both results are plotted with depth to notice the nature of the variation.

Further, in DMT test, the compressibility characteristics of soil can be estimated by virtue of vertical drained constrained modulus i.e., M_{DMT}. This is one key parameter to estimate settlement from the DMT tests data in geotechnical design field (Marchetti et al. 2001). Also, the compressibility characteristics and

modulus of elasticity of soil can be predicted from this parameter(Chang 1986, 1991b). Hence, at each test location, the estimated value of M_{DMT} is compared with the N_{ob} by plotting along depth.

6.2.1 DMT ESTIMATED BULK UNIT WEIGHT

At each test location, bulk unit weight (γ) of sub soil (estimated from both the laboratory test and DMT test), is compared. In arriving at the comparison, laboratory measured bulk unit weight is kept as abscissa and DMT estimated bulk unit weight(Marchetti 1980; Powell and Uglow 1988; Smith and Houlsby 1995; Marchetti et al. 2001) is kept as ordinate (Figure 6.1). In view of the comparison, it is evident that the bulk unit weight estimated from DMT is more or less at par with the laboratory tested value.

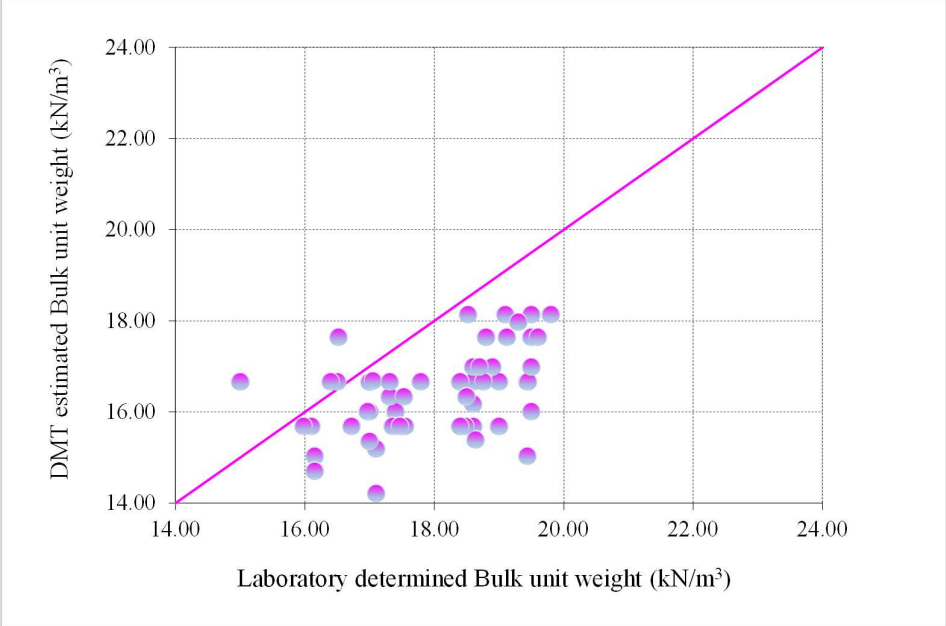

Figure: 6. 1 comparison of laboratory determined bulk unit weight with DMT estimated bulk unit weight

6.2.2 COMPARATIVE INTERPRETATION OF SPATIAL VARIATION OF E_D AND N_{OB} WITH DEPTH

The variation of E_D and N_{ob} values are plotted along depth for each site. In this variation it is observed that depth wise variation of E_D is similar in nature with N_{ob} in cohesive sub-soil. The depth- wise variation of E_D is found to be scattered for the cohesive sub soil (in some cases) which comprises decomposed wood as well as for the cohesionless sub-soil (mainly sandy silt/silty sand). The depth wise variation is presented in Figure 6.2 to Figure 6.9.

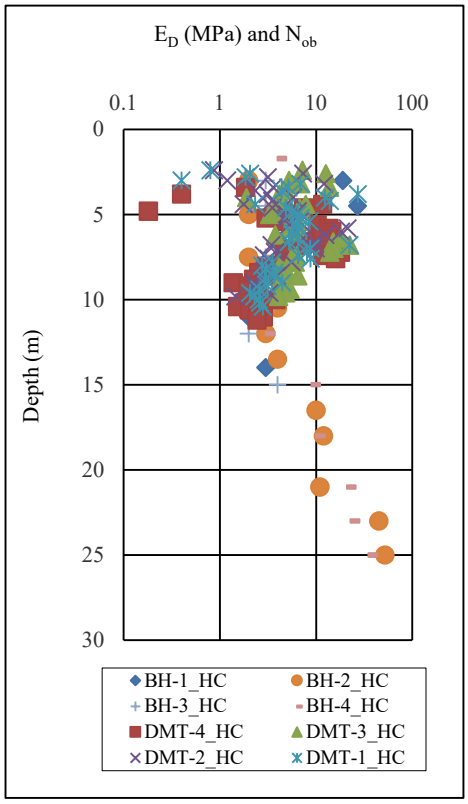

Figure: 6. 2 Variation of E_D (from DMT) and N_{ob} (from BH) along depth for Site-1 (HC)

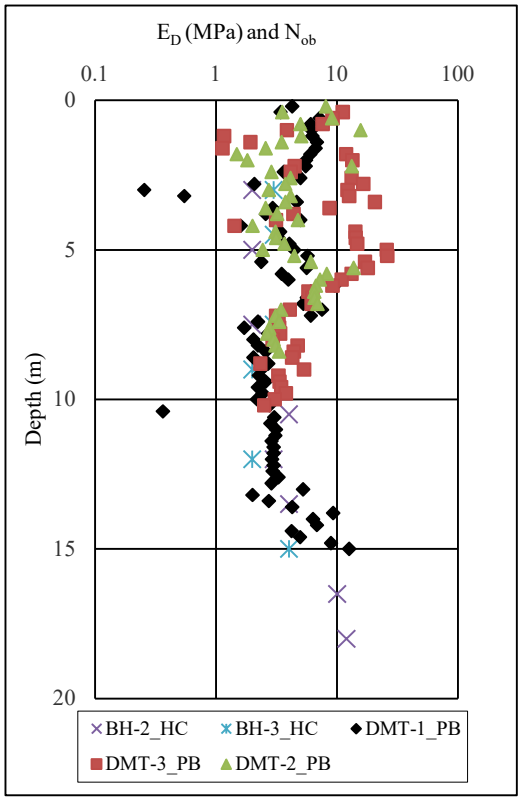

Figure: 6. 3 Variation of E_D (from DMT) and N_{ob} (from BH) along depth for Site-2 (PB)

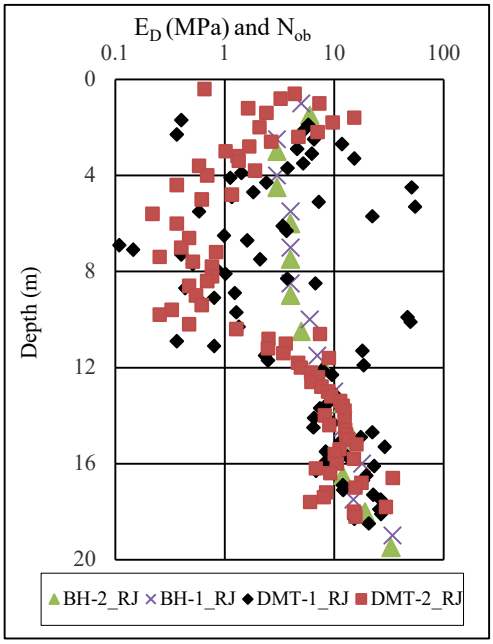

Figure: 6. 4 Variation of E_D (from DMT) and N_{ob} (from BH) along depth for Site-3 (RJ)

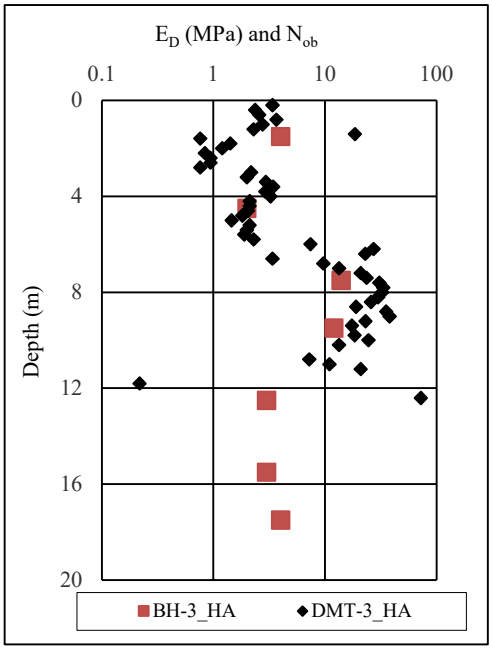

Figure: 6. 5 Variation of E_D (from DMT) and N_{ob} (from BH) along depth for Site-4 (HA)

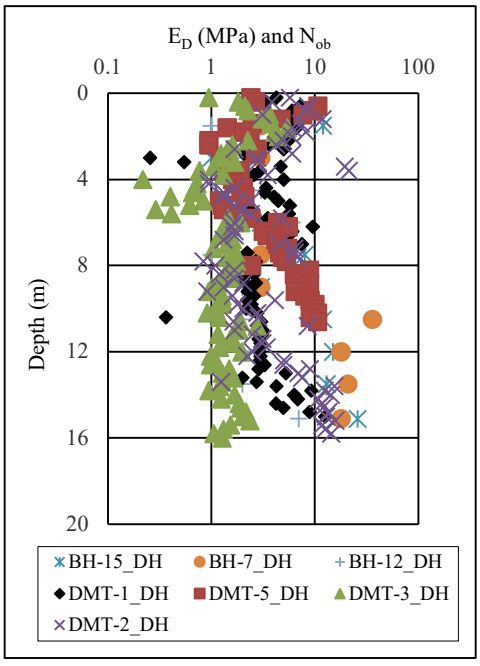

Figure: 6. 6 Variation of E_D (from DMT) and N_{ob} (from BH) along depth for Site-5 (DH)

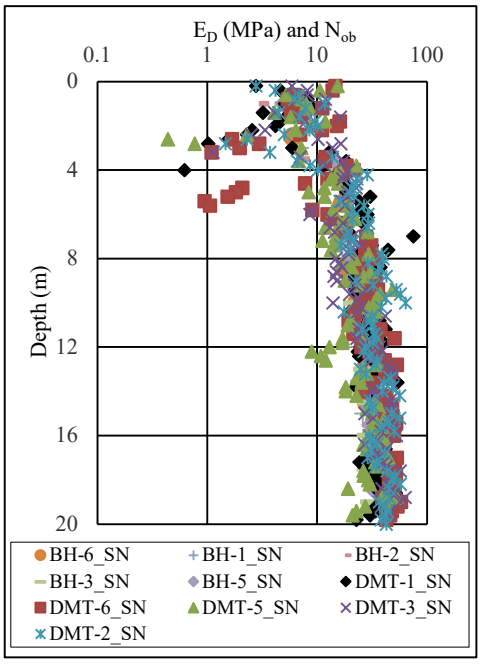

Figure: 6. 7 Variation of E_D (from DMT) and N_{ob} (from BH) along depth for Site-6 (SN)

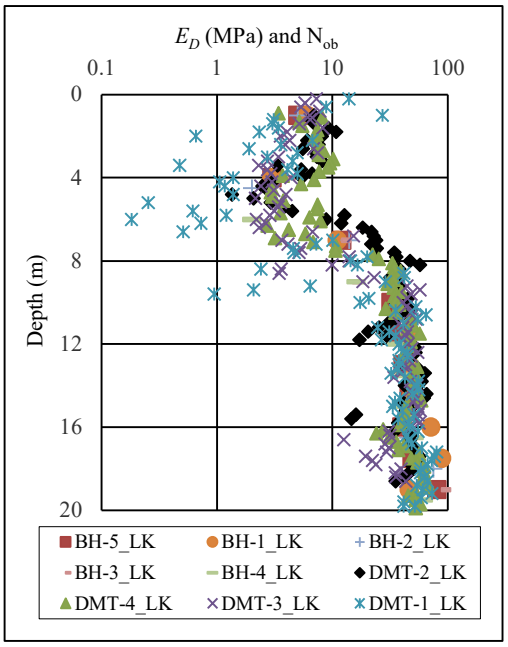

Figure: 6. 8 Variation of E_D (from DMT) and N_{ob} (from BH) along depth for Site-7 (LK)

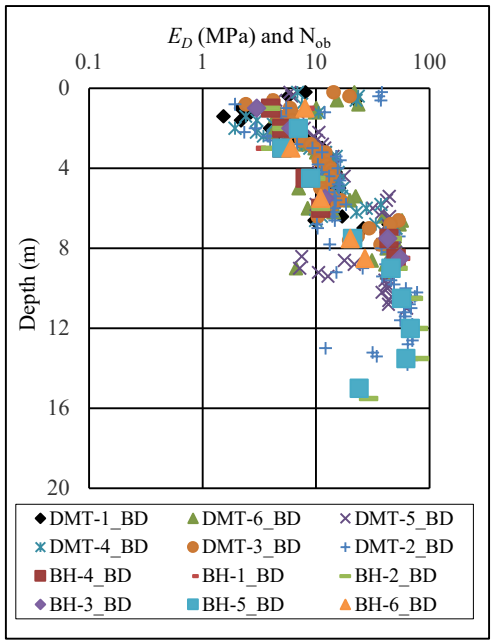

Figure: 6. 9 Variation of E_D (from DMT) and N_{ob} (from BH) along depth for Site-8 (BD)

6.2.3 COMPARATIVE INTERPRETATION OF SPATIAL VARIATION OF M_{DMT} AND N_{OB} WITH DEPTH

In DMT test, vertical drained constrained modulus (M_{DMT}) is estimated by virtue of dilatometer modulus (E_D). Like E_D, the value of M_{DMT} is also dependent on N_{ob}. In this study, M_{DMT} is also compared with the N_{ob} by plotting both the values along depth for each site. In view of this variation, it is depicted that for cohesive sub-soil, the depth wise variation of the value of M_{DMT} is well tallying with the N_{ob}. For cohesionless soil or in presence of decomposed wood, the depth wise variation of M_{DMT} is somewhat scattered. The variations are shown in Figure 6.10 to Figure 6.17.

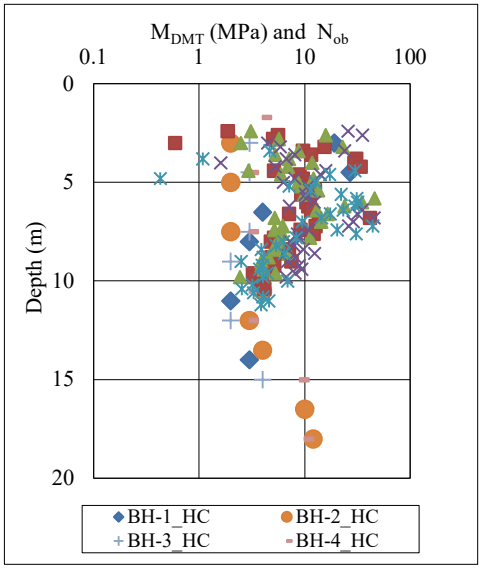

Figure: 6. 10 Variation of M_{DMT} (from DMT) and N_{ob} (from BH) along depth for Site-1 (HC)

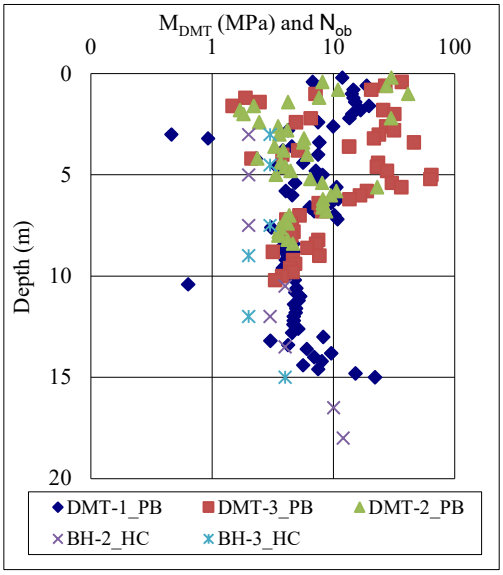

Figure: 6. 11 Variation of M_{DMT} (from DMT) and N_{ob} (from BH) along depth for Site-2 (PB)

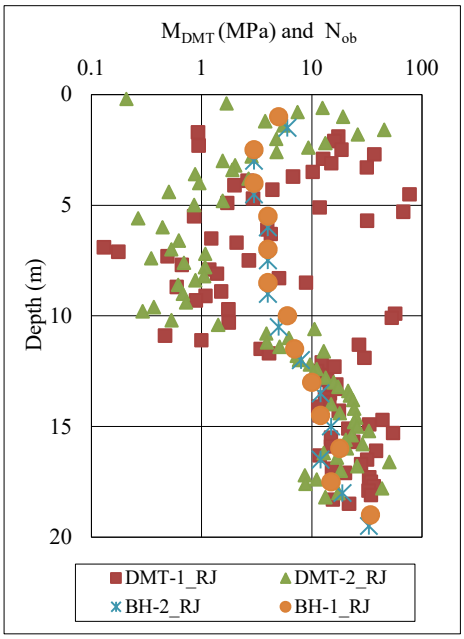

Figure: 6. 12 Variation of M_{DMT} (from DMT) and N_{ob} (from BH) along depth for Site-3 (RJ)

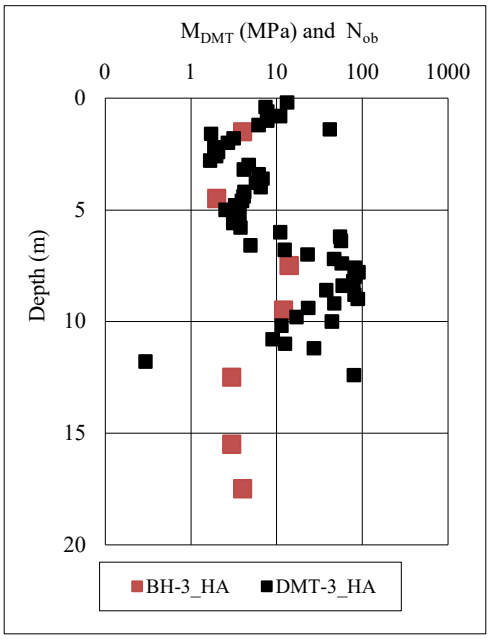

Figure: 6. 13 Variation of M_{DMT} (from DMT) and N_{ob} (from BH) along depth for Site-4 (HA)

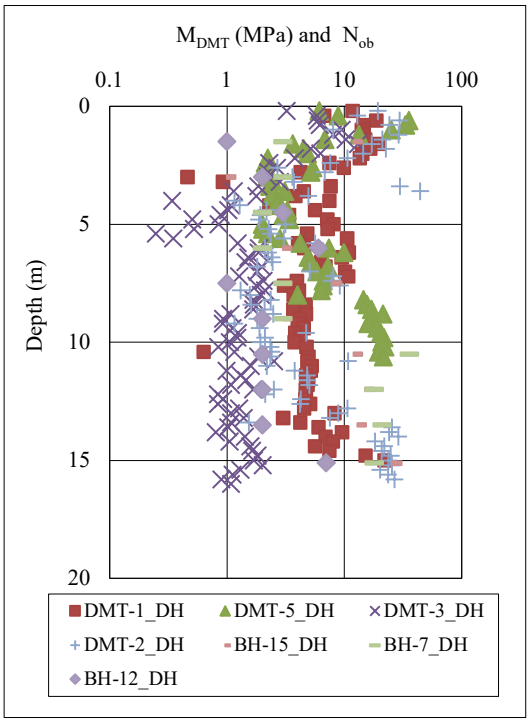

Figure: 6. 14 Variation of M_{DMT} (from DMT) and N_{ob} (from BH) along depth for Site-5 (DH)

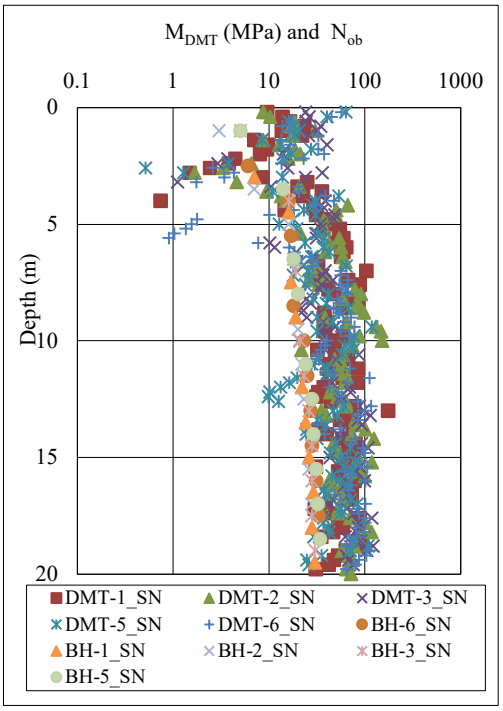

Figure: 6. 15 Variation of M_{DMT} (from DMT) and N_{ob} (from BH) along depth for Site-6 (SN)

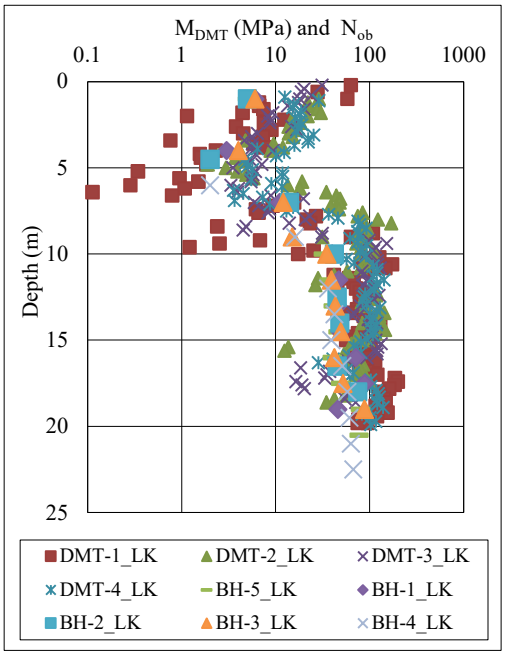

Figure: 6. 16 Variation of M_{DMT} (from DMT) and N_{ob} (from BH) along depth for Site-7 (LK)

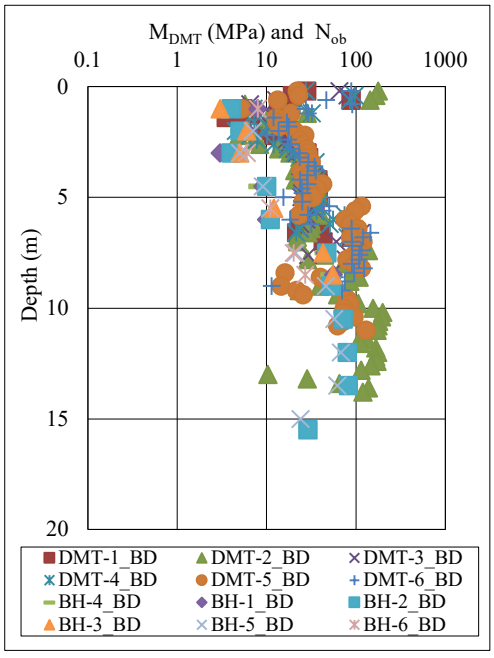

Figure: 6. 17 Variation of M_{DMT} (from DMT) and N_{ob} (from BH) along depth for Site-8 (BD)

6.2.4 RELATION OF E_D AND M_{DMT} WITH N_{OB} AND PLASTIC LIMIT AS WELL AS PLASTICITY INDEX

In view of the nature of the variation of N_{ob}, E_D and M_{DMT} along depth, it is observed that E_D and M_{DMT} very much depends on the consistency of cohesive soil. Therefore, the value of E_D and M_{DMT} are related with N_{ob}, so that the SPT based consistency of such soil may be predicted from the specific range of these parameters. Besides, the value of E_D and M_{DMT} are also compared with the plastic limit and plasticity index of such soil (Appendix A), so that liquid limit, plastic limit and plasticity index may be predicted from the value of E_D and M_{DMT} empirically.

It is observed from both conventional boreholes and DMT estimated material index (I_D), that the sub-soil mostly comprises silty clay / clayey silt soil at all project sites. Therefore, in this study focus is given on the cohesive part of the sub-soil.

In arriving at the interrelationship, the DMT test result corresponding to cohesive soils are considered. The average value of E_D and M_{DMT} are estimated corresponding to the depth at which the undisturbed cohesive soil samples are collected from adjacent boreholes. Also, SPT N values (N_{ob}) (conducted in adjacent boreholes) are considered corresponding to the same depth. The site-wise comparative results are tabulated in Appendix A.

6.2.4.1 RELATION OF N_{OB} WITH E_D

In arriving at the interrelation between N_{ob} values and E_D for cohesive soil, the average value of E_D is estimated corresponding to the depth at which the undisturbed soil samples are collected from adjacent borehole. Also, SPT N value (conducted in adjacent borehole) is considered corresponding to the same depth. The SPT N values

(N_{ob}) and (E_D) are then kept as abscissa and as ordinate respectively. The relationship is presented in Equation 6.1 and shown in Figure 6.18.

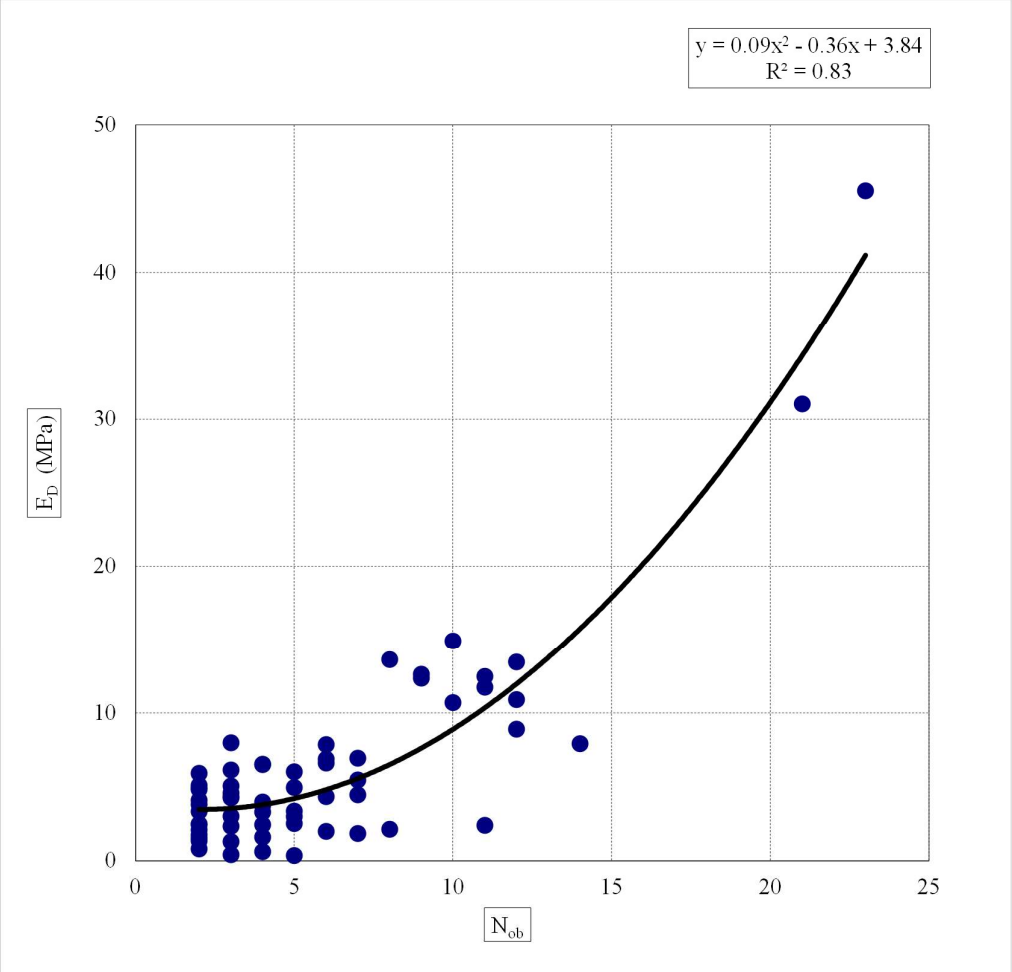

Figure: 6. 18 Relation between E_D with observed SPT N value (N_{ob})

$$\mathbf{E_D = 0.09 \times (N_{ob})^2 - 0.36 \times (N_{ob}) + 3.84} \quad (6.1)$$

6.2.4.2 RELATION OF N_{OB} WITH M_{DMT}

In determining the relation between N_{ob} and M_{DMT}, the average value of E_D is estimated corresponding to the depth at which the undisturbed soil samples are collected from adjacent borehole. Also, SPT N value (N_{ob}) (conducted in adjacent borehole) is considered corresponding to the same depth. The N_{ob} and M_{DMT} values are kept as

abscissa and as ordinate respectively. The relation is presented in Equation 6.2 and shown in Figure 6.19.

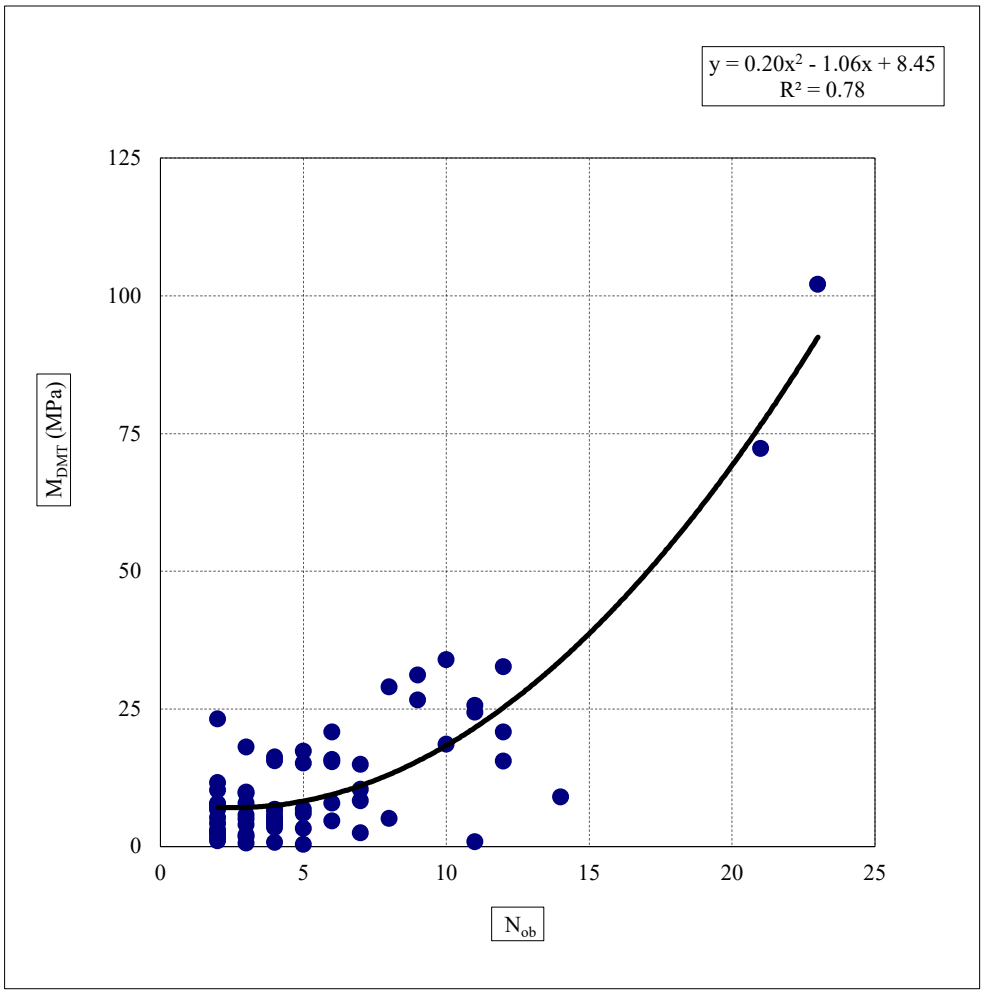

Figure: 6. 19 Relation between M_{DMT} with observed SPT N value (N_{ob})

$$\mathbf{M_{DMT}} = \mathbf{0.20} \times (\mathbf{N_{ob}})^{\mathbf{2}} - \mathbf{1.06} \times (\mathbf{N_{ob}}) + \mathbf{8.45} \qquad (6.2)$$

6.2.4.3 RELATION OF E_D AND M_{DMT} WITH PLASTIC LIMIT AND PLASTICITY INDEX

Vertical drained constrained modulus (M_{DMT}) depends on the value of E_D and a factor R_M. This factor R_M depends on the material type and stress history of soil (Marchetti 1980; Marchetti et al. 2001). Besides, plasticity index (PI) of soil indirectly portrays the sub-soil type and the compressibility characteristics of the cohesive soil (Tomlinson

and Boorman 2001). Therefore, a focus is given to establish a relationship between E_D and M_{DMT} with the plasticity index (PI) and plastic limit (W_P). The value of PI and W_P are taken from the laboratory test results (conducted on collected undisturbed/ disturbed samples from the different depth of adjacent boreholes) for each site. Subsequently, the average value of E_D and M_{DMT} are estimated corresponding to the same depth (Appendix A). Site-wise the value of E_D/PI and E_D/W_P are estimated for all site. The ratio of E_D/PI and E_D/W_P are separately plotted against M_{DMT} by keeping it as ordinate. The relations are presented in Equation 6.3 and Equation 6.4 corresponding to Figure 6.20 and Figure 6.21 respectively.

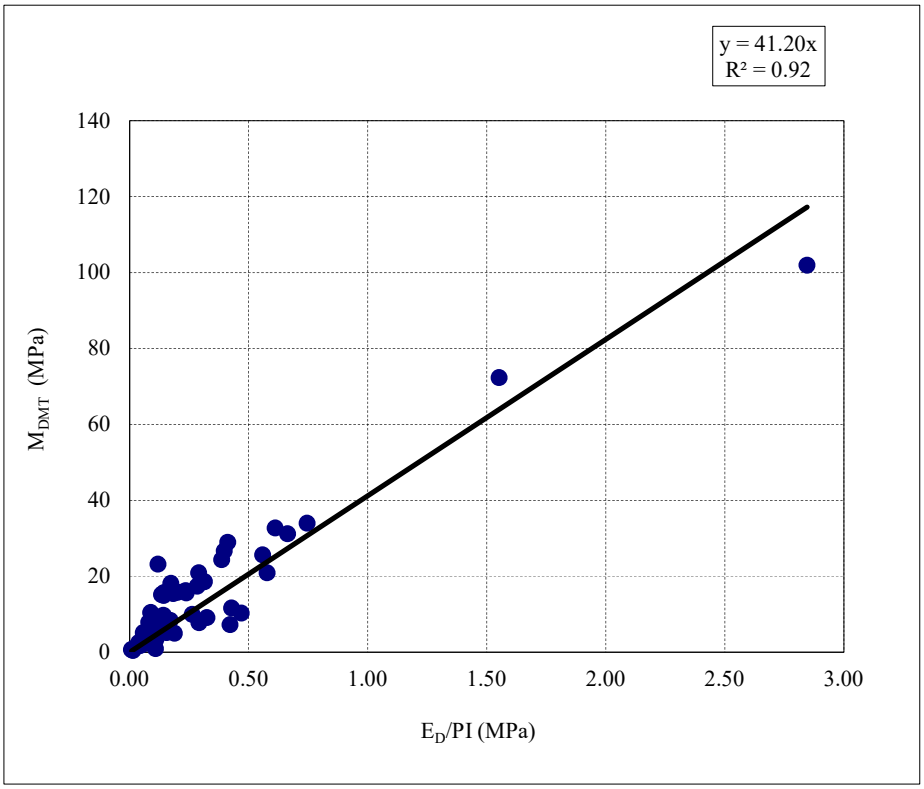

Figure: 6. 20 Relation between (E_D/PI) and M_{DMT}

$$\mathbf{M_{DMT}} = \mathbf{41.20} \times (\frac{\mathbf{E_D}}{\mathbf{PI}}) \quad (6.3)$$

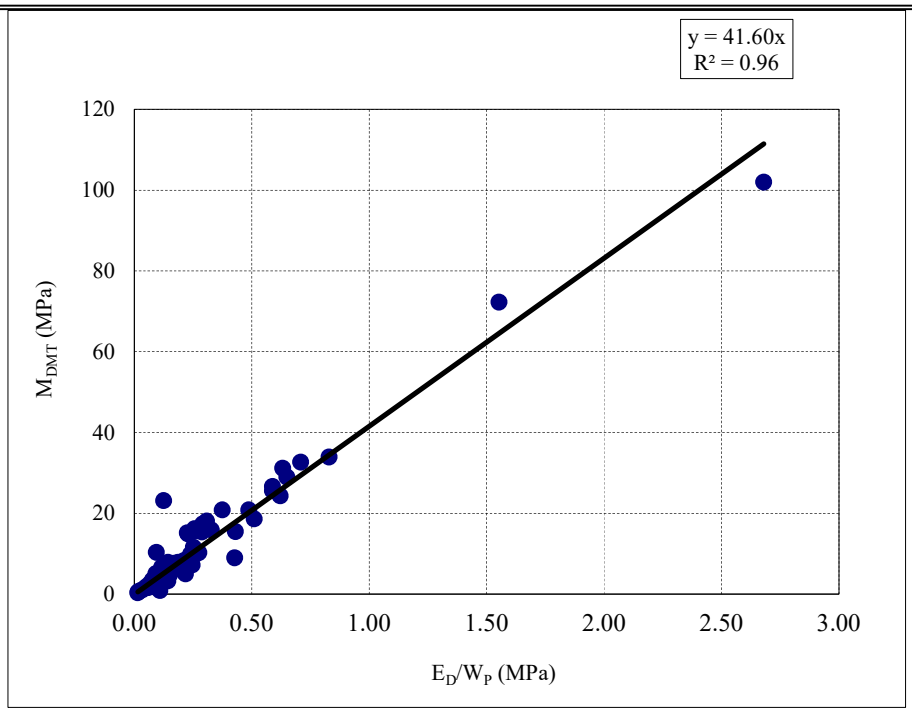

Figure: 6. 21 Relation between (E_D/W_P) and M_{DMT}

$$\mathbf{M_{DMT}} = \mathbf{41.59} \times (\frac{\mathbf{E_D}}{\mathbf{W_P}}) \quad (6.4)$$

6.2.5 DISCUSSION ON THE PREDICTED RELATION

At all project sites, the sub-soil mostly comprises cohesive soil, observed from conventional boreholes. Therefore, in this study focus is given on the cohesive part of the sub-soil. Also, it is observed that the presence of decomposed wood (observed from the adjacent borehole) in the sub soil, largely affects the DMT test results. Therefore, to establish the relationship, good quality data (by eliminating most scattered values) is considered for the calculation purpose. In addition to that, on validation purpose the estimated values (from the established relations) are compared with the laboratory tested values and present at subsequent sections

Based on the proposed relation, it is observed that for the soft soil (N_{ob} lies between 2 to 4) E_D varies between 3.46 MPa to 3.78 MPa, M_{DMT} varies between 7.02 to 7.44 MPa. For firm soil (N_{ob} is in between 4 to 8) E_D varies between 3.78 MPa to 6.72 MPa, M_{DMT}

varies in between 7.44 to 12.77 MPa. For stiff soil (N_{ob} is in between 8 to 16) E_D varies between 6.72 MPa to 21.12 MPa, M_{DMT} varies in between 12.77 to 42.69 MPa. For very stiff soil (N_{ob} lies between 16 to 32) E_D varies between 21.12 MPa to 84.48 MPa, M_{DMT} varies in between 42.69 to 179.33 MPa. The summarised values are presented in Table 6.1.

Table: 6. 1 Value of E_D and M_{DMT} for different observed SPT N values (N_{ob})

N_{ob}	SPT based Consistency	E_D (MPa)	M_{DMT} (MPa)
2 to 4	Soft	3.46 to 3.78	7.02 to 7.44
4 to 8	Firm	3.78 to 6.72	7.44 to 12.77
8 to 16	Stiff	6.72 to 21.12	12.77 to 42.69
16 to 32	Very stiff	21.12 to 84.48	42.69 to 179.33

Additionally, an alternative method is developed to predict the liquid limit (W_L) and plastic limit (W_P) directly from the DMT test results by virtue of E_D and $M_{DMT.}$ Based on these relations (Equation 6.3 and Equation 6.4), it is observed that when the E_D falls within the range of 3.5 MPa to 3.8 MPa and M_{DMT} between 7.1 MPa to 7.4 MPa, the W_P varies between 20.5% to 21.2% and PI ranging from 20.3% to 21.0%. Similarly, for E_D values ranging from 4.2 MPa to 6.4 MPa and M_{DMT} between 8.2 MPa to 12.8 MPa, the W_P and PI are found to be in the range of 21.3% to 20.9%, and 21.1% to 20.7% respectively. Subsequently, in case when E_D value varies from 7.5 MPa to 17.7 MPa and M_{DMT} between 15.1 MPa to 37.6 MPa, the range of W_P and PI is found to be in the range from 20.7% to 19.6% and 20.5% to 19.5% respectively. Finally, for E_D values between 20.1 MPa to 34.2 MPa and M_{DMT} between 42.7 MPa to 74.4 MPa, W_P and PI are ranging from 19.5% to 19.1%, and 19.4% to 19.0% respectively. The summarised values are presented in Table 6.2.

Table: 6. 2 Predicted value of Liquid Limit (W_L), Plastic Limit (W_P) and Plasticity Index (PI) from E_D and M_{DMT}

E_D (MPa)	M_{DMT} (MPa)	E_D/PI (MPa)	E_D/W_P (MPa)	W_L (%)	W_P (%)	PI (%)
3.5	7.1	0.17	0.17	40.7	20.5	20.2
3.8	7.4	0.18	0.18	42.3	21.2	21.1
4.2	8.2	0.20	0.20	42.5	21.3	21.2
6.4	12.8	0.31	0.31	41.6	20.9	20.7
7.5	15.1	0.37	0.36	41.2	20.7	20.5
17.7	37.6	0.91	0.90	39.1	19.6	19.5
20.1	42.7	1.04	1.03	38.9	19.5	19.4
34.2	74.4	1.81	1.79	38.1	19.1	19.0

To validate these proposed relations, Chi-square test is conducted. In this test, the (Greenwood and Nikulin 1996; Shiuly 2018; Shiuly et al. 2020; Shiuly and Roy 2021; Deng 2022)confidence level of the proposed relation is determined. The test is performed as follows (Equation 6.5):

$$\chi 2 = \sum_{i=1}^{n} \frac{(A_i - P_i)^2}{P_i} \quad (6.5)$$

where, χ^2 is denoted the Chi-square value. A_i is denoted as the observed / actual values, and P_i is the estimated / predicted values. After evaluating the Chi-square value, for the relation, the degrees of freedom are evaluated. Which are the number of categories minus the number of parameters of the fitted distribution. The calculated Chi-square value is then compared with the critical value from the Chi-square distribution table for the specific degree of freedom and confidence level.

In this study, the chi-square value is estimated using ten numbers (10) relevant observed data from two different locations outside the study area and the predicted values estimated from the proposed relationships (Table 6.3 and Table 6.4). The graphical presentation of the chi-square distribution for the respective relationship is presented in Figure 6.22 and Figure 6.23.

At null hypothesis (H_0), there is no relation exist whereas for alternate hypothesis, the relation exists (Shiuly 2018; Shiuly et al. 2020; Shiuly and Roy 2021). In this study, the

degree of freedom is calculated as 9. For this degree of freedom, critical value of Chi-square is 16.919 (i.e., $\chi^2_{critical} = 16.919$) at significance level (α) of 0.05. Besides, the calculated value of Chi-square is 6.828 (i.e., $\chi^2_{calculated} = 6.828$) for the relation between E_D with N_{ob}. Hence, for this particular relation, critical value of Chi- square is greater than the calculated value of Chi- square (i.e., $\chi^2_{critical} > \chi^2_{calculated}$), thus, null hypothesis is rejected and the alternate hypothesis at significance level 0.05 is accepted. It signifies that, at a 0.05 significance level, relation between E_D with N_{ob} predicts well for the observed data. Similarly, it is found that the calculated values of Chi-square of all the proposed relations are less than the critical value for the 0.05 significance level (i.e., $\chi^2_{critical}$ 16.919).

Table:6. 3 Comparison of observed value of E_D and M_{DMT} with the estimated value from proposed relation

Depth (m)	Observed SPT values (N_{ob})	Observed E_D (MPa)	Observed M_{DMT} (MPa)	Estimated E_D (MPa)	Estimated M_{DMT} (MPa)
1.0	6	6.0	17.4	4.8	9.5
4.0	5	4.0	6.8	4.2	8.3
7.0	4	3.8	5.1	3.8	7.4
10.0	4	6.9	10.4	3.8	7.4
13.0	7	9.2	12.1	6.1	11.1
16.0	13	14.9	27.3	13.8	29.1
2.0	7	5.0	9.1	5.6	11.1
11.0	4	3.6	5.3	3.8	7.4
14.0	7	7.5	13.2	5.6	11.1
17.0	12	9.2	16.9	12.0	25.1

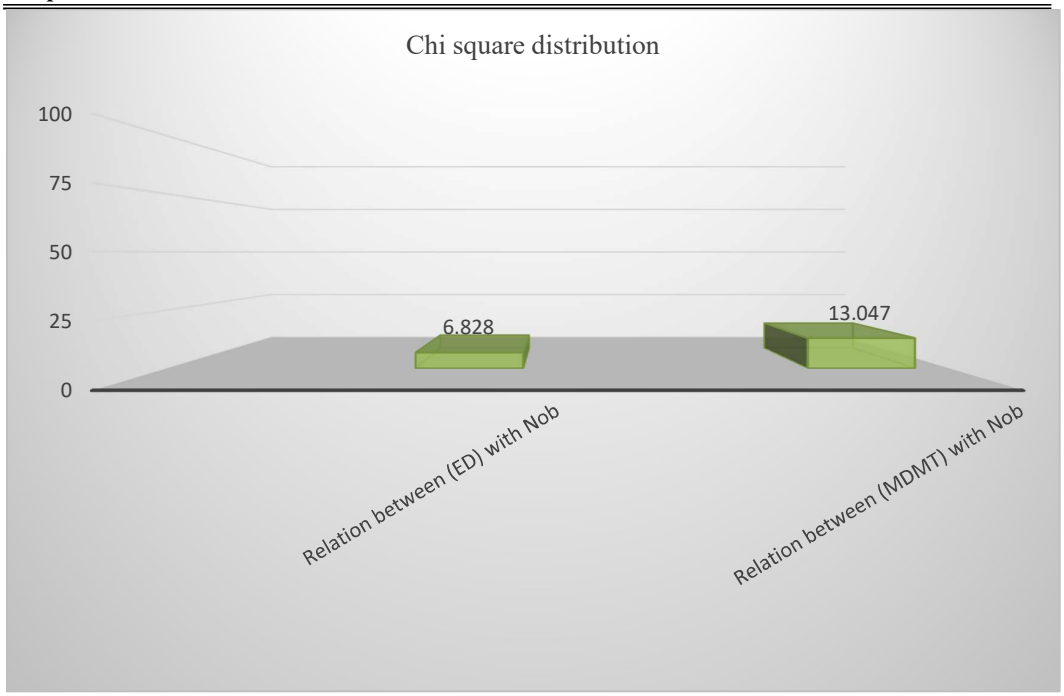

Figure: 6. 22 Chi-square distribution for the proposed relations

Table: 6. 4 Comparison of Laboratory estimated Liquid Limit (W_L), Plastic Limit (W_P) and Plasticity Index (PI) with the predicted value from E_D and M_{DMT}

Depth (m)	Laboratory obtained W_L	Laboratory obtained W_P	Laboratory obtained PI	Estimated W_L	Estimated W_P	Estimated PI
1.0	42.0	21.1	20.9	28.7	14.4	14.3
4.0	53.6	26.5	27.1	48.8	24.5	24.4
7.0	70.7	42.7	28.0	62.3	31.2	31.1
10.0	50.3	25.9	24.4	55.2	27.7	27.6
13.0	59.4	19.4	40.0	63.4	31.7	31.6
16.0	51.1	20.6	30.5	45.2	22.6	22.6
2.0	46.8	20.2	26.6	45.3	22.7	22.6
11.0	51.6	25.5	26.1	56.6	28.4	28.3
14.0	53.9	19.7	34.2	47.4	23.7	23.6
17.0	41.3	22.4	18.9	45.1	22.6	22.5

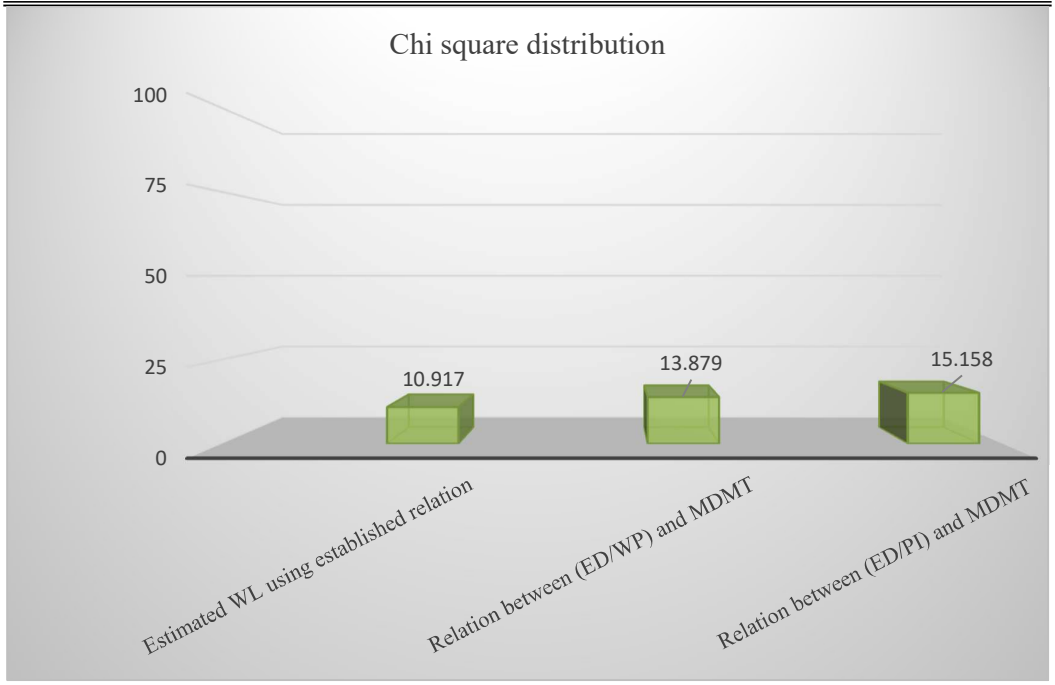

Figure: 6. 23 Chi-square distribution for the proposed relations

6.3 CPT TEST

CPT tests were conducted at eight numbers of sites. From these tests, three numbers of basic parameters (i.e., q_c, f_s, M_{CPT}) are considered for the comparison purpose. In CPT tests, cone penetration resistance (q_c) and the sleeve friction resistance (f_s), indirectly resembles the resistance imparted by the sub-soil (Robertson and Cabal 2015) . Also, the observed (field) SPT N value (N_{ob}) represents the soil resistance (Terzaghi 1943; Terzaghi et al. 1996; Bowles 2001). Hence, at each site, q_c and f_s are compared with the conventional SPT blow count (N_{ob}), conducted in the adjacent borehole. Both the results are then plotted along depth to find out the nature of the variation.

Besides, vertical drained constrained modulus (M_{CPT}) is one of the important parameters in geotechnical design field. The compressibility characteristics and modulus of elasticity can be predicted from this parameter. Hence, site-wise, the estimated value of M_{CPT} has been compared with the N_{ob} by plotting along depth.

6.3.1 CPT ESTIMATED BULK UNIT WEIGHT

At each test location, bulk unit weight (γ) of sub soil (estimated from both the laboratory test and CPT test), is compared. In arriving at the comparison, laboratory measured bulk unit weight is kept as abscissa and CPT estimated bulk unit weight (Robertson and Cabal 2010) (Rocscience Inc. 2016) (Sakleshpur et al. 2022)is kept as ordinate (Figure 6.24). In view of the comparison, it is evident that the bulk unit weight estimated from CPT is more or less at par with the laboratory tested value.

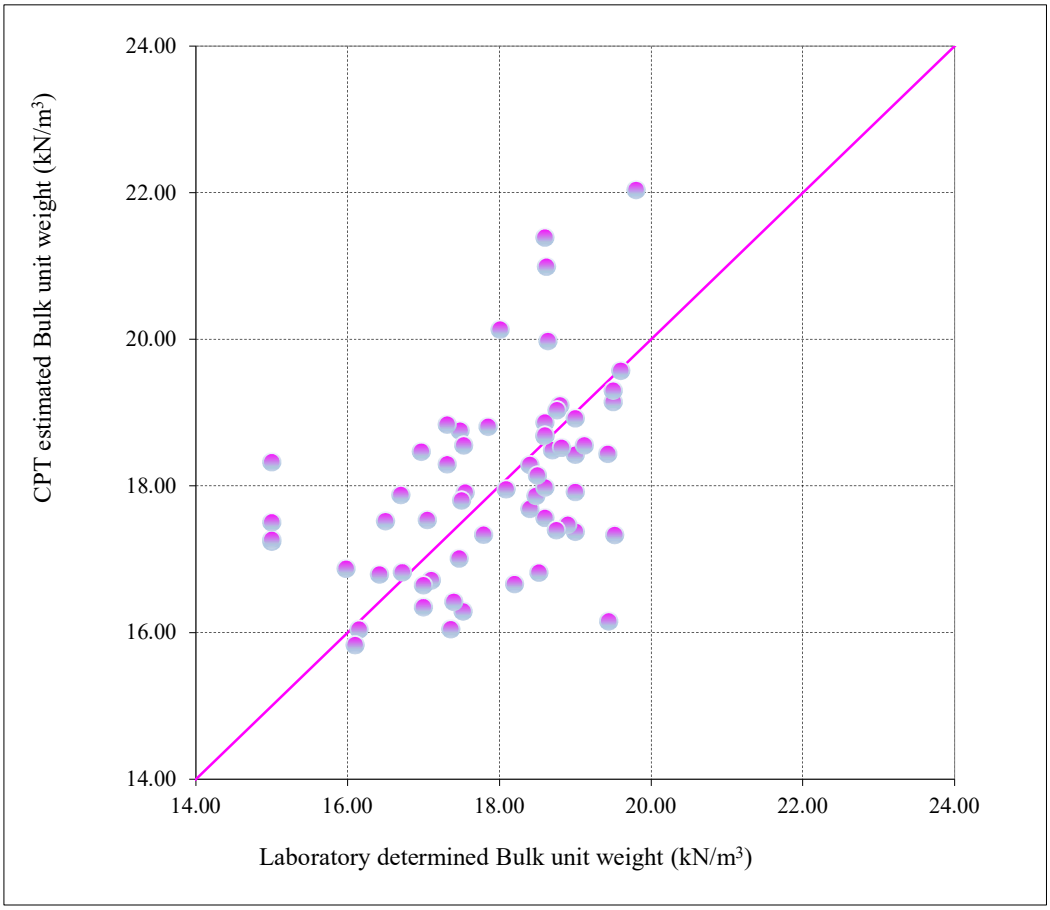

Figure: 6. 24 comparison of laboratory determined bulk unit weight with CPT estimated bulk unit weight

6.3.2 COMPARATIVE INTERPRETATION OF SPATIAL VARIATION OF q_c AND N_{ob} WITH DEPTH

The variation of q_c and observed (field) SPT N value (N_{ob}) are plotted together along depth for each site. From this variation, it is observed that in cohesive soil (silty clay / clayey silt), depth-wise variation of the value of q_c is similar in nature with N_{ob}. Presence of cohesionless soil (sandy silt/ silty sand) and cohesive soil (in some cases) consisting of decomposed wood particles, causes deviation from the normal trend of the variation of q_c along depth. The depth wise variation of q_c is presented in Figure 6.25 to Figure 6.32.

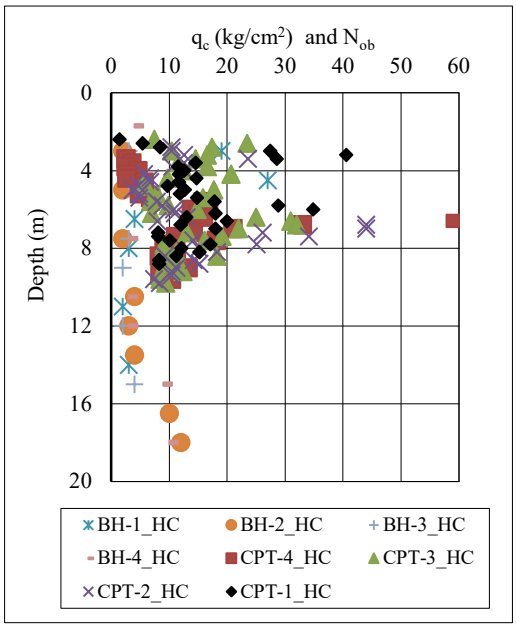

Figure: 6. 25 Variation of q_c (from CPT) and N_{ob} (from BH) along depth for Site-1 (HC)

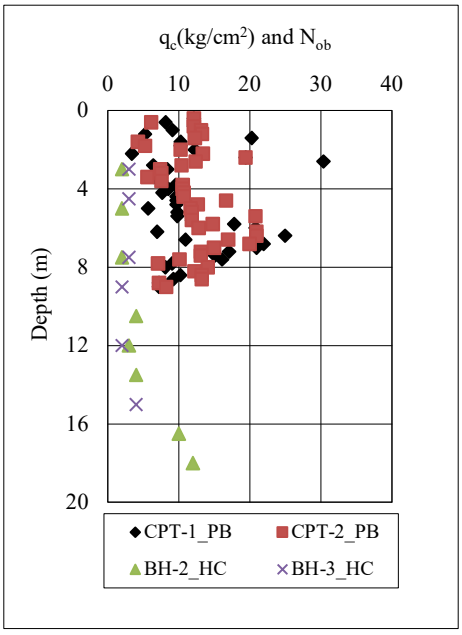

Figure: 6. 26 Variation of q_c (from CPT) and N_{ob} (from BH) along depth for Site-2 (PB)

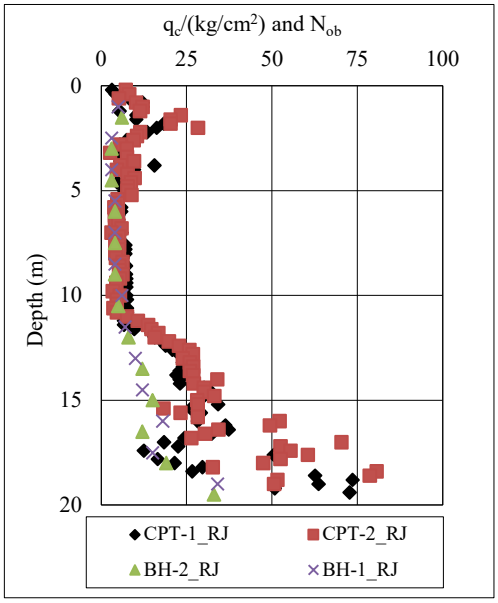

Figure: 6. 27 Variation of q_c (from CPT) and N_{ob} (from BH) along depth for Site-3 (RJ)

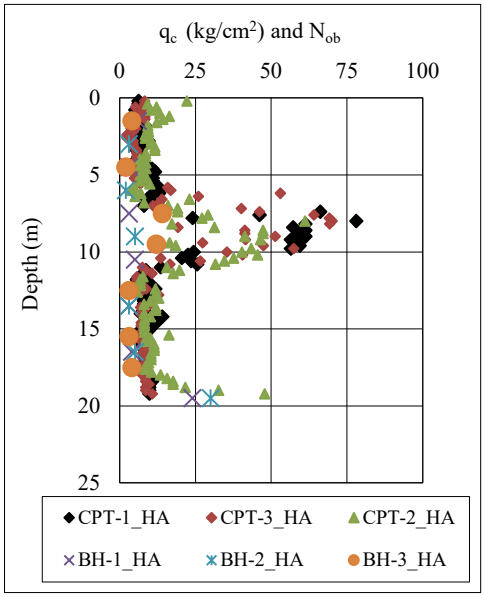

Figure: 6. 28 Variation of q_c (from CPT) and N_{ob} (from BH) along depth for Site-4 (HA)

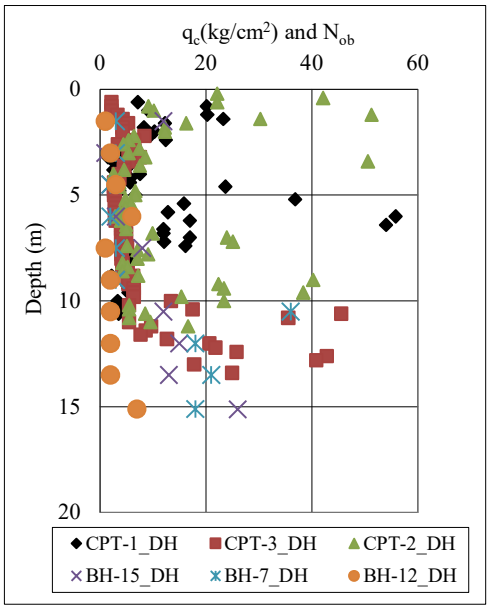

Figure: 6. 29 Variation of q_c (from CPT) and N_{ob} (from BH) along depth for Site-5 (DH)

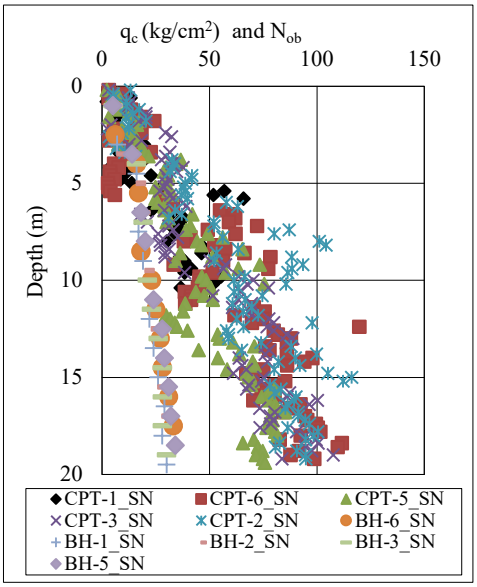

Figure: 6. 30 Variation of q_c (from CPT) and N_{ob} (from BH) along depth for Site-6 (SN)

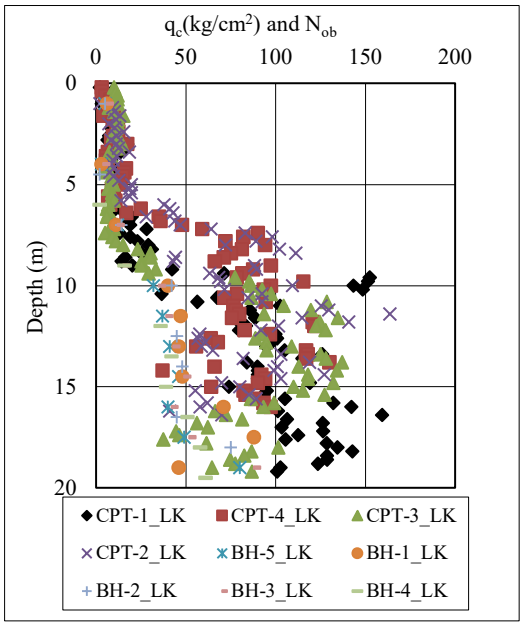

Figure: 6. 31 Variation of q_c (from CPT) and N_{ob} (from BH) along depth for Site-7 (LK)

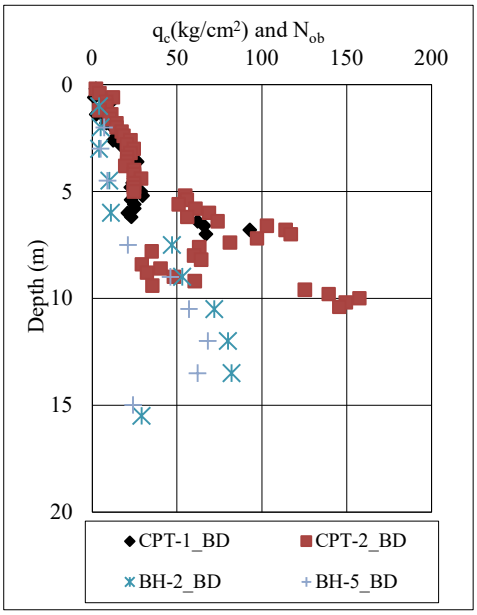

Figure: 6. 32 Variation of q_c (from CPT) and N_{ob} (from BH) along depth for Site-8 (BD)

6.3.3 COMPARATIVE INTERPRETATION OF SPATIAL VARIATION OF f_s AND N_{OB} WITH DEPTH

The variation of f_s and N_{ob} are plotted together along depth for each site. From this variation it has been observed that in cohesive soil (mainly silty clay/ clayey silt), the depth-wise variation of the value of f_s is similar in nature with the N_{ob}. Presence of cohesionless soil (sandy silt/ silty sand) and cohesive soil (in some cases) consisting of decomposed wood particles, causes deviation from the normal trend of the variation of f_s along depth. The variations are shown in Figure 6.33 to Figure 6.40.

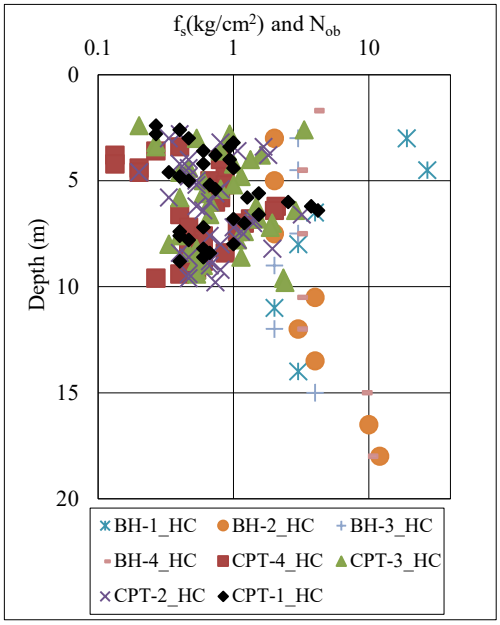

Figure: 6. 33 Variation of f_s (from CPT) and N_{ob} (from BH) along depth for Site-1 (HC)

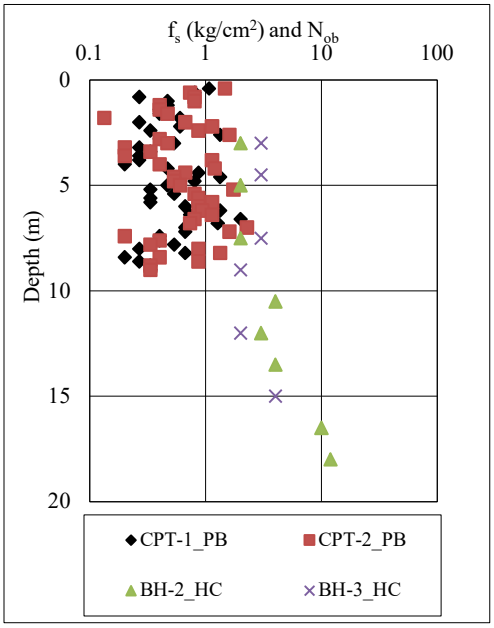

Figure: 6. 34 Variation of f_s (from CPT) and N_{ob} (from BH) along depth for Site-2 (PB)

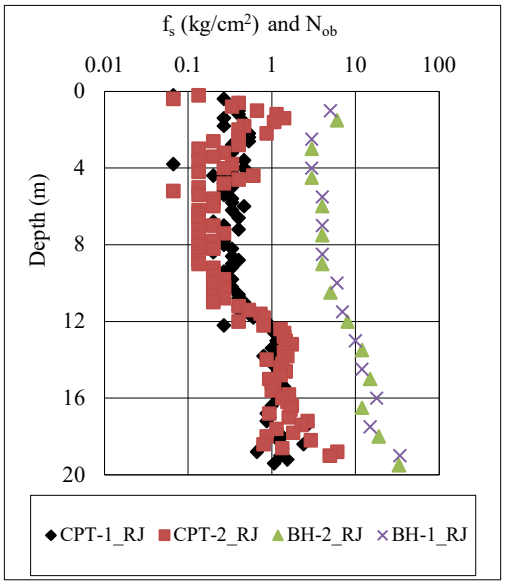

Figure: 6. 35 Variation of f_s (from CPT) and N_{ob} (from BH) along depth for Site-3 (RJ)

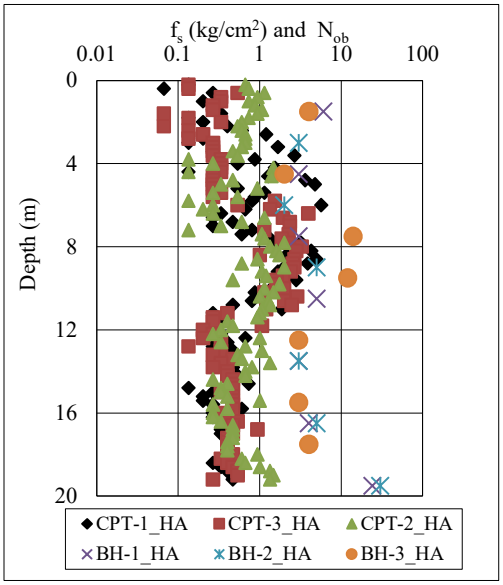

Figure: 6. 36 Variation of f_s (from CPT) and N_{ob} (from BH) along depth for Site-4 (HA)

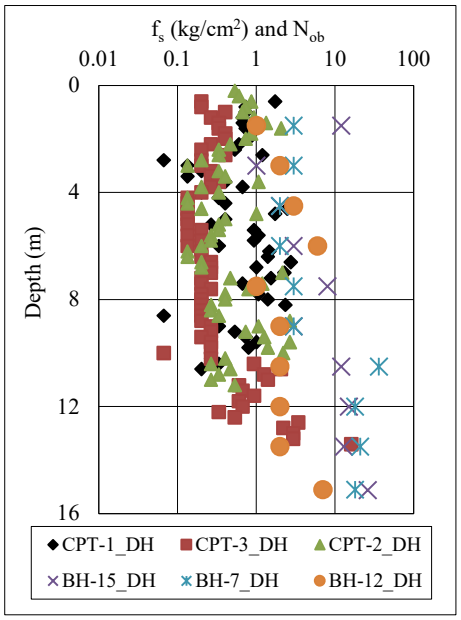

Figure: 6. 37 Variation of f_s (from CPT) and N_{ob} (from BH) along depth for Site-5 (DH)

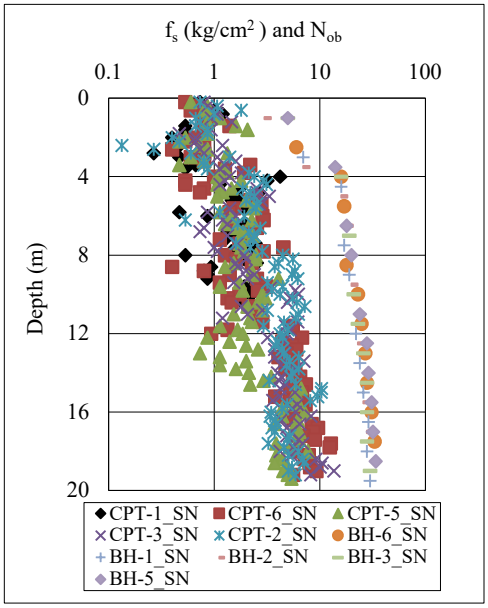

Figure: 6. 38 Variation of f_s (from CPT) and N_{ob} (from BH) along depth for Site-6 (SN)

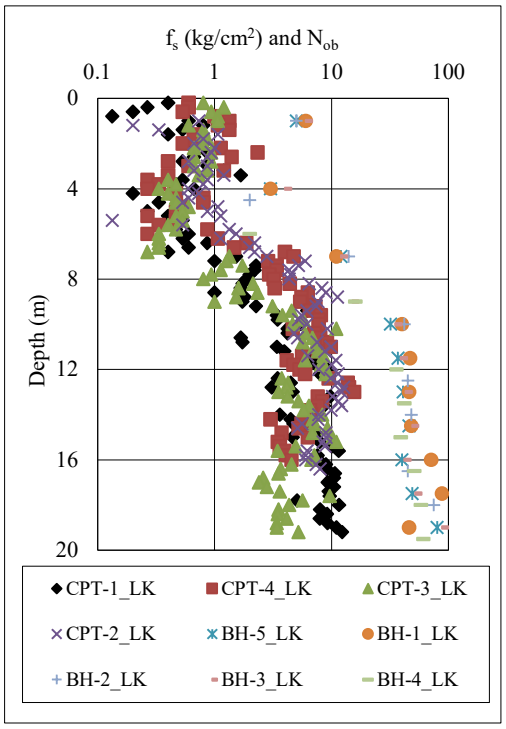

Figure: 6. 39 Variation of f_s (from CPT) and N_{ob} (from BH) along depth for Site-7 (LK)

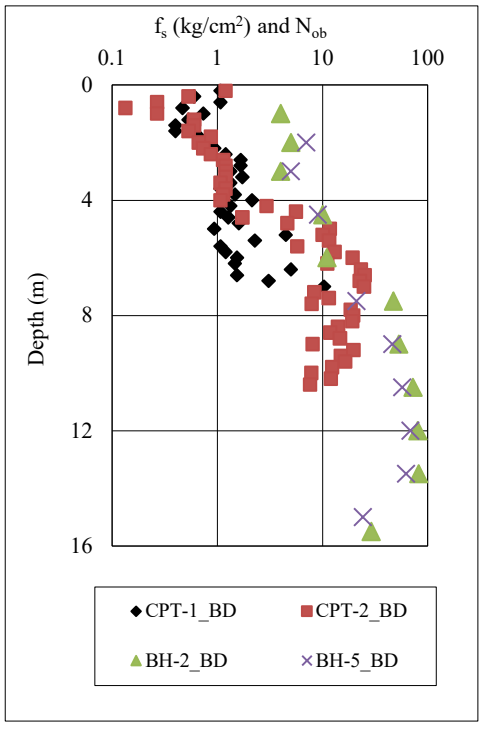

Figure: 6. 40 Variation of f_s (from CPT) and N_{ob} (from BH) along depth for Site-8 (BD)

6.3.4 COMPARATIVE INTERPRETATION OF SPATIAL VARIATION OF M_{CPT} AND N_{ob} WITH DEPTH

The vertical drained constrained modulus (M_{CPT}) mainly depends on the value of cone penetration resistance (q_c) (Rocscience Inc. 2016; Dagger et al. 2018). Therefore, M_{CPT} has also been compared with the N_{ob} by observing the variation along depth. The variation of M_{CPT} and N_{ob} has been plotted together along depth for each site. From this variation it is observed that in cohesive soil (silty clay/ clayey silt) the depth- wise variation of the value of M_{CPT} is similar in nature with N_{ob}. However, in some cases M_{CPT} is found to be scattered. This is mainly observed in cohesionless soil (sandy silt to silty sand) and in some cases where the presence of decomposed wood particles is observed. The variations are shown in Figure 6.41 to Figure 6.48.

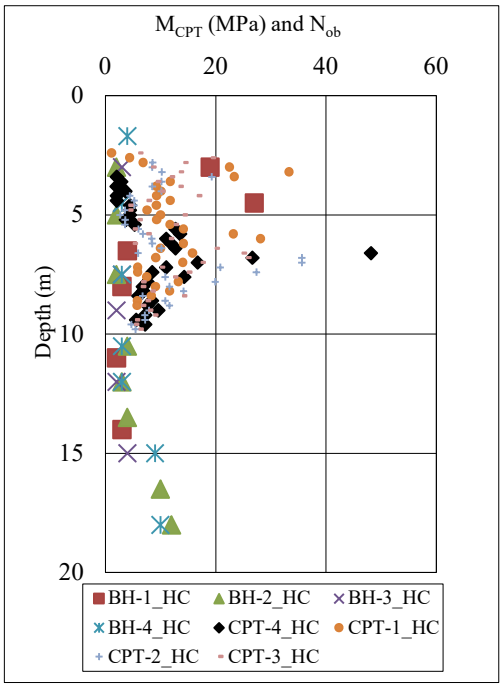

Figure: 6. 41 Variation of M_{CPT} (from CPT) and N_{ob} (from BH) along depth for Site-1 (HC)

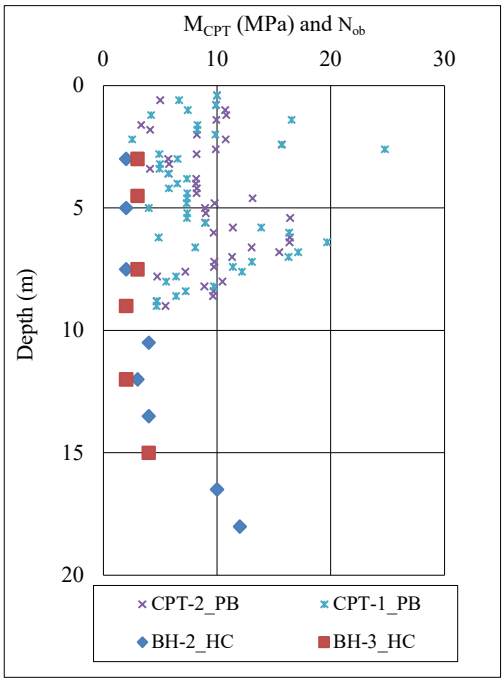

Figure: 6. 42 Variation of M_{CPT} (from CPT) and N_{ob} (from BH) along depth for Site-2 (PB)

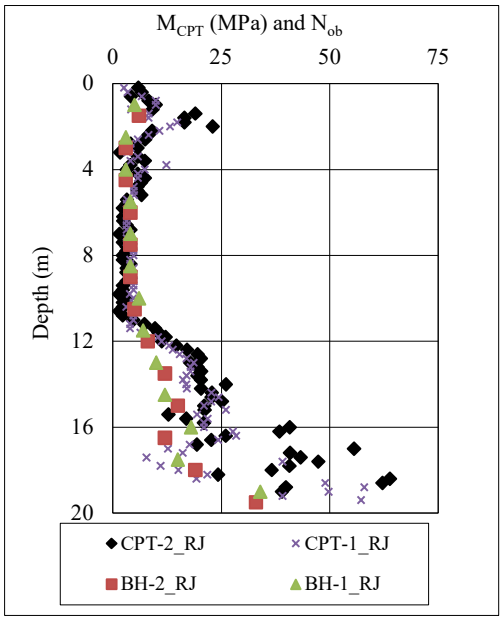

Figure: 6. 43 Variation of M_{CPT} (from CPT) and N_{ob} (from BH) along depth for Site-3 (RJ)

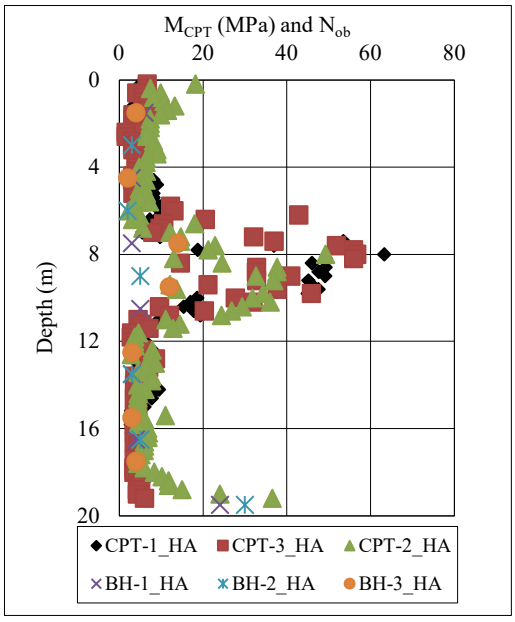

Figure: 6. 44 Variation of M_{CPT} (from CPT) and N_{ob} (from BH) along depth for Site-4 (HA)

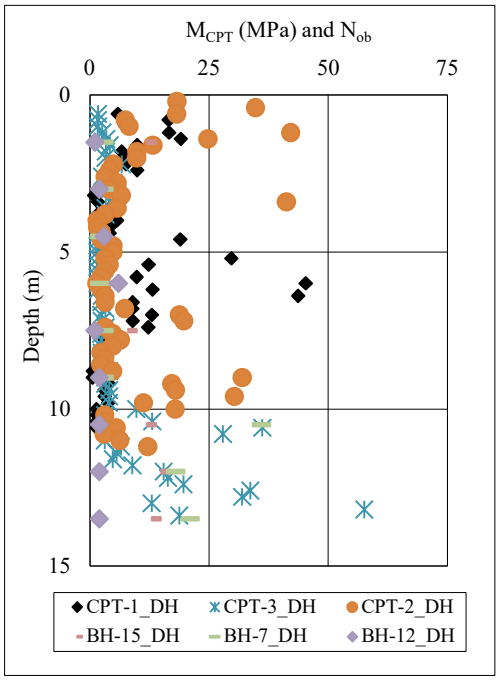

Figure: 6. 45 Variation of M_{CPT} (from CPT) and N_{ob} (from BH) along depth for Site-5 (DH)

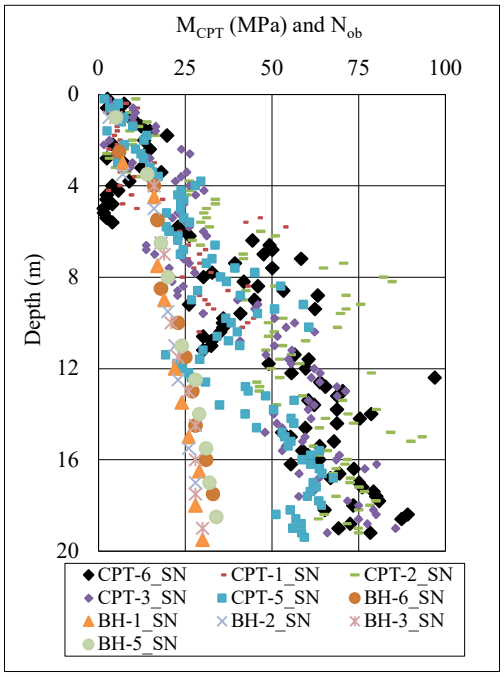

Figure: 6. 46 Variation of M_{CPT} (from CPT) and N_{ob} (from BH) along depth for Site-6 (SN)

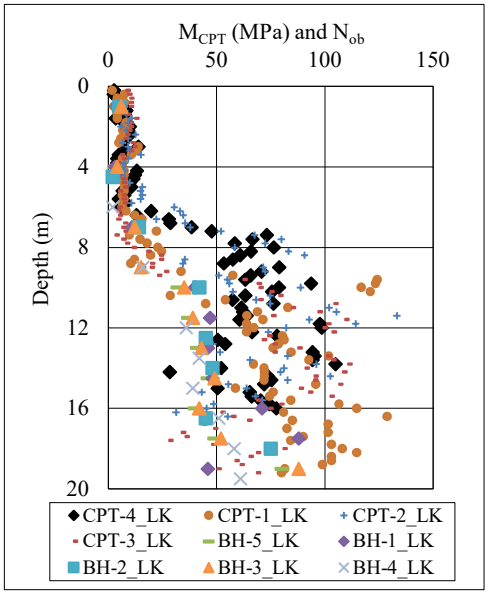

Figure: 6. 47 Variation of M_{CPT} (from CPT) and N_{ob} (from BH) along depth for Site-7 (LK)

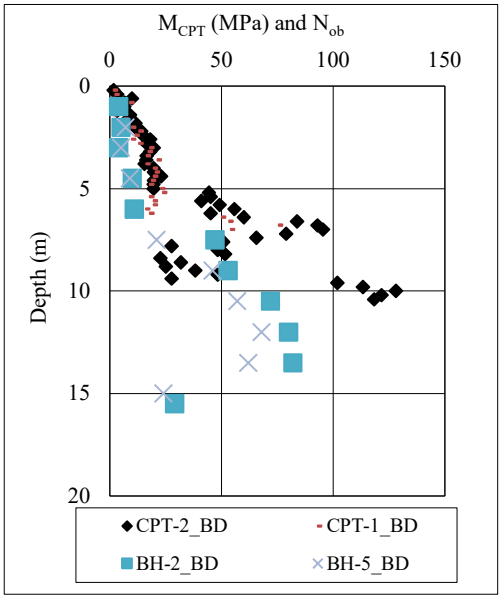

Figure: 6. 48 Variation of M_{CPT} (from CPT) and N_{ob} (from BH) along depth for Site-8 (BD)

6.3.5 RELATION OF q_c, f_s AND M_{CPT} WITH N_{OB} AND PLASTIC LIMIT AS WELL AS PLASTICITY INDEX

In view of the variation of q_c, f_s and M_{CPT} along depth, it has been observed that the value of q_c, f_s and M_{CPT} are very much dependent on the consistency of cohesive soil. Therefore, the values of q_c, f_s and M_{CPT} are related with the N_{ob}, so that the SPT based consistency of soil is predicted from the specific range of these parameters. Besides, another attempt has been made to establish a relationship between M_{CPT} with q_c/PI and q_c/W_P for the prediction of liquid limit and plastic limit empirically from the CPT test results.

It is observed from both conventional boreholes and CPT estimated I_C, that the sub-soil mostly consists of cohesive silty clay/ clayey silt soil at all project sites. Therefore, in this study focus is given on the cohesive part of the sub-soil.

In arriving at the relation, the CPT test result corresponding to cohesive soils are considered. The average value of q_c, f_s and M_{CPT} are estimated corresponding to the depth at which the undisturbed cohesive soil samples are collected from adjacent boreholes. Also, N_{ob} (conducted in adjacent boreholes) are considered corresponding to the same depth. The site-wise comparative results are tabulated in Appendix B.

6.3.5.1 RELATION OF N_{ob} WITH q_c AND f_s

In arriving at the relation, the average value of N_{ob}, q_c and f_s are calculated corresponding to the depth at which undisturbed samples were collected from the adjacent boreholes. It is found that the variation of f_s, q_c and N_{ob} is similar in nature for all the test locations. It is also observed that the value of I_C lies within the range of 2.65 to 3.87 (Robertson and Cabal 2015) (Lunne et al. 2002b)(Robertson and Campanella 1983a, b) (Rocscience Inc. 2016), which indicates the presence of silty clay/ clayey silt soil. Therefore, two numbers of separate graphs (Figure 6.49 and Figure 6.50) are plotted corresponding to the value of average N_{ob} (as abscissa) with q_c (as ordinate) and N_{ob} (as abscissa) with f_s (as ordinate) considering the results from all the tests. Also, it is observed that the graph corresponding to N_{ob} with q_c is best fitted compared to the earlier established relations (Figure 6.49). Based on these two plots, two separate relations are derived and presented in Equation 6.6 and Equation 6.7 respectively.

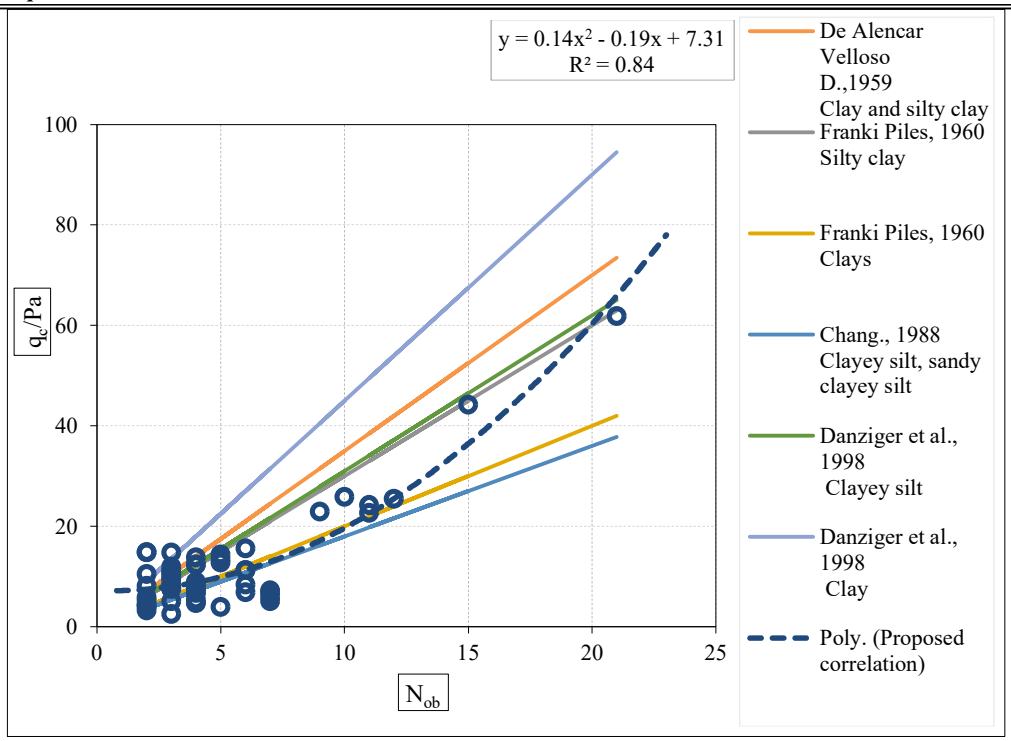

Figure: 6. 49 Relation between (q_c/Pa) with N_{ob}

$$(\mathbf{q_c/Pa}) = \mathbf{0.14} \times (\mathbf{N_{ob}})^{\mathbf{2}} - \mathbf{0.19} \times (\mathbf{N_{ob}}) + \mathbf{7.31} \qquad (6.6)$$

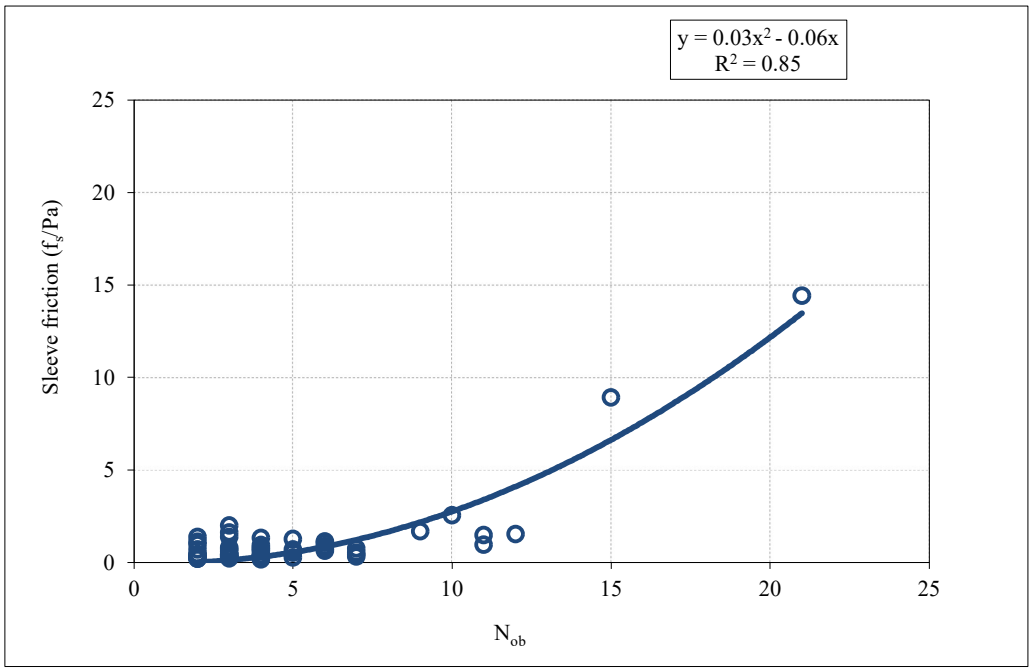

Figure: 6. 50 Relation between f_s with N_{ob}

$$(\mathbf{f_s/Pa}) = \mathbf{0.03} \times (\mathbf{N_{ob}})^{\mathbf{2}} - \mathbf{0.06} \times (\mathbf{N_{ob}}) \qquad (6.7)$$

6.3.5.2 RELATION OF N_{ob} WITH M_{CPT}

In arriving at the relation between N_{ob} and M_{CPT}, the average value of M_{CPT} is estimated corresponding to the depth at which the undisturbed soil samples are collected from adjacent borehole. Also, N_{ob} (conducted in adjacent borehole) is considered corresponding to the same depth. The N_{ob} and M_{CPT} value are kept as abscissa and as ordinate respectively.

The relation is presented in Equation 6.8 and shown in Figure 6.51

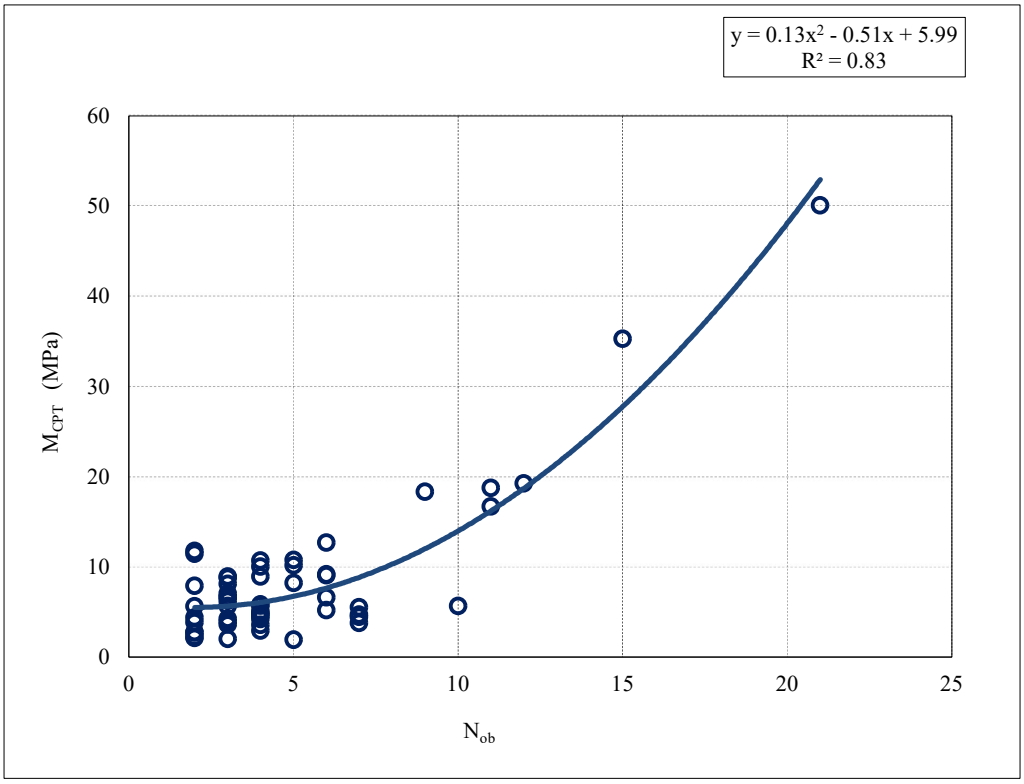

Figure: 6. 51 Relation between M_{CPT} with (N_{ob})

$$\mathbf{M_{CPT}} = \mathbf{0.13} \times (\mathbf{N_{ob}})^{\mathbf{2}} - \mathbf{0.51} \times (\mathbf{N_{ob}}) + \mathbf{5.99} \qquad (6.8)$$

6.3.5.3 RELATION OF q_c AND M_{CPT} WITH PLASTIC LIMIT AND PLASTICITY INDEX

Vertical drained constrained modulus (M_{CPT}) depends on the value of q_c and a factor α_M. This factor depends on the material type and stress history of soil (Senneset et al. 1982; Mayne 2001; Robertson and Cabal 2015; Rocscience Inc. 2016) . Besides, plasticity index (PI) of soil indirectly portrays the sub-soil type and the compressibility characteristics of the cohesive soil (Tomlinson and Boorman 2001). Therefore, an attempt is made to establish a relation between the q_c and M_{CPT} with the plastic limit (W_P) and plasticity index (PI). The value of PI and W_P are taken from the laboratory test results (conducted on collected undisturbed/ disturbed samples from the different depth of adjacent boreholes) for each site. Subsequently, the average value of q_c and M_{CPT} are estimated corresponding to the same depth (Appendix B). Site-wise the normalized value of $(q_c/Pa)/PI$ and $(q_c/Pa)/W_P$ (Pa is atmospheric pressure i.e., 0.1 MPa) are estimated for all sites. The ratio of $(q_c/Pa)/PI$ and $(q_c/Pa)/W_P$ are separately plotted against M_{CPT} by keeping it as ordinate. The relation is presented in Equation 6.9 and Equation 6.10 and shown in Figure 6.52 and Figure 6.53.

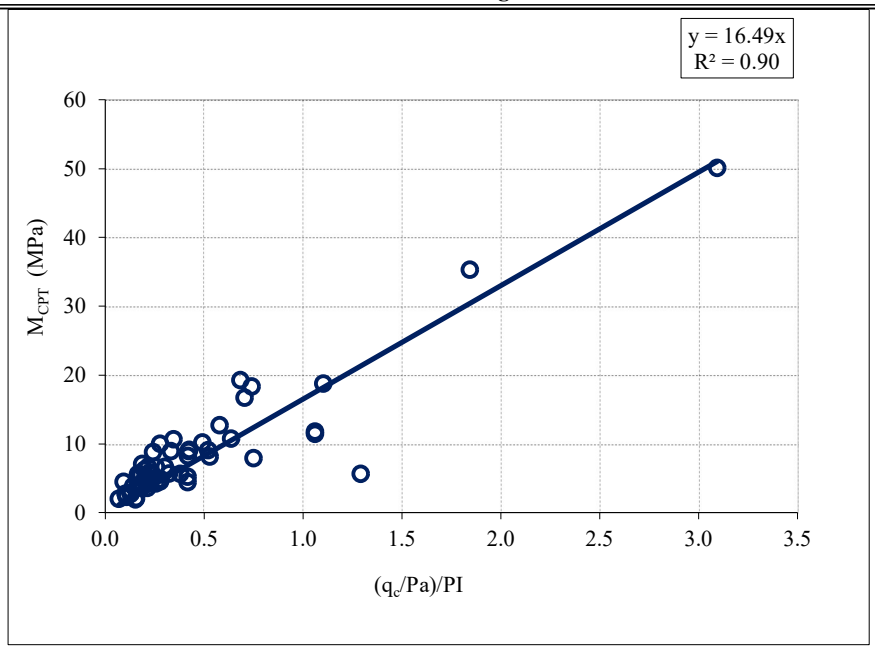

Figure: 6. 52 Relation between M_{CPT} with $(q_c/Pa)/PI$

$$\mathbf{M_{CPT}} = \mathbf{16.49}\,(\frac{\mathbf{q_c}}{\mathbf{Pa}})\mathbf{/PI} \qquad (6.9)$$

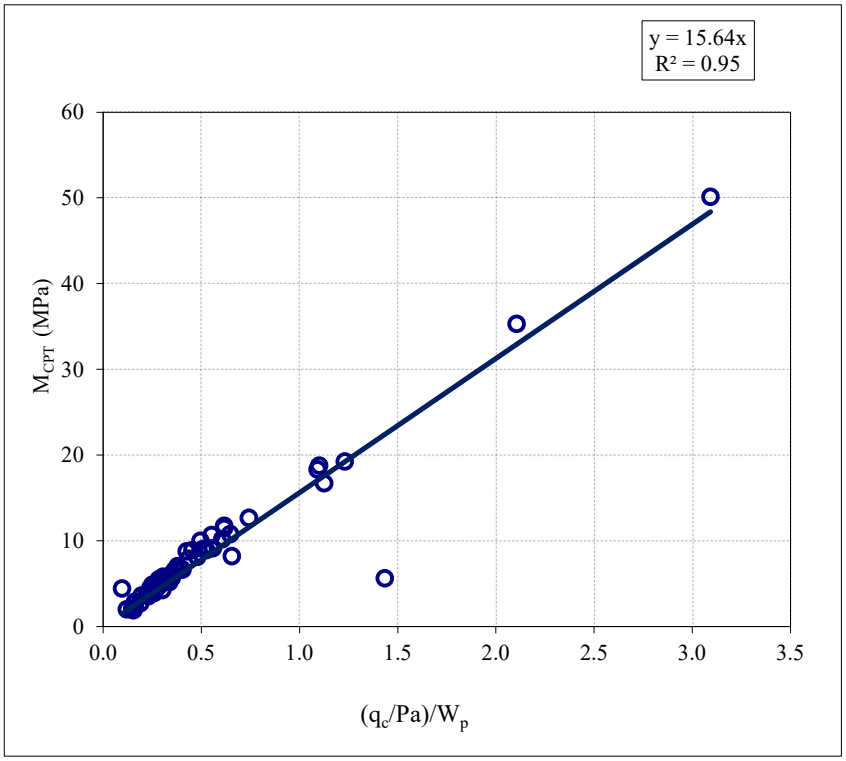

Figure: 6. 53 Relation between M_{CPT} with $(q_c/Pa)/W_P$

$$\mathbf{M_{CPT}} = \mathbf{15.64}(\frac{\mathbf{q_c}}{\mathbf{Pa}})\mathbf{/W_P} \qquad (6.10)$$

6.3.6 DISCUSSION ON THE PREDICTED RELATION

At all project sites, the sub-soil mostly consists of cohesive silty clay/ clayey silt soil, observed from conventional boreholes. Therefore, in this study focus is given on the cohesive part of the sub-soil. Also, it is observed that the presence of decomposed wood (observed from the adjacent borehole) in the sub soil, largely affects the CPT test results. Therefore, to establish the relations, good quality data (by eliminating most scattered values) is considered for the calculation purpose.

Based on the established relations, it is observed that for the soft soil (N_{ob}) between 2 to 4, q_c varies between 7.5 kg/cm^2 to 8.8 kg/cm^2, M_{CPT} varies in between 5.5 to 6.0 MPa and f_s varies in between 0.02 kg/cm^2 to 0.3 kg/cm^2. For firm soil (N_{ob} between 4 to 8) q_c varies between 8.8 kg/cm^2 to 14.8 kg/cm^2, M_{CPT} varies in between 6.0 to 10.3 MPa and f_s varies in between 0.3 kg/cm^2 to 1.7 kg/cm^2. For stiff soil (N_{ob} between 8 to 16) q_c varies between 14.8 kg/cm^2 to 40.6 kg/cm^2, M_{CPT} varies in between 10.3 to 31.3 MPa and f_s varies in between 1.7 kg/cm^2 to 7.6 kg/cm^2. For very stiff soil (N_{ob} between 16 to 21) q_c varies between 40.6 kg/cm^2 to 65.1 kg/cm^2, M_{CPT} varies in between 31.3 to 52.9 MPa and f_s varies in between 7.6 kg/cm^2 to 13.5 kg/cm^2. The summarised values are presented in Table 6.5.

Table:6. 5 Range of q_c, f_s and M_{CPT} for different N_{ob}

N_{ob}	SPT based Consistency	q_c (kg/cm^2)	M_{CPT} (MPa)	f_s (kg/cm^2)
2 to 4	Soft	7.5 to 8.8	5.5 to 6.0	0.02 to 0.3
4 to 8	Firm	8.8 to 14.8	6.0 to 10.3	0.3 to 1.7
8 to 16	Stiff	14.8 to 40.6	10.3 to 31.3	1.7 to 7.6
16 to 21	Very stiff	40.6 to 65.1	31.3 to 52.9	7.6 to 13.5

Further, a relation has been developed to predict the range of liquid limit (W_L) and plastic limit (W_P) using the values of q_c and M_{CPT} obtained from the CPT test. Based

on this relation, it is found that, when q_c ranging from 7.5 kg/cm² to 8.8 kg/cm² and M_{CPT} lies between 5.5 MPa to 6.0 MPa, the plastic limit (W_P) varies in between of 21.2% and 22.8%, and plasticity index (PI) ranges from 22.4% to 24.0%. Similarly, for the value of q_c from 9.9 kg/cm² to 14.9 kg/cm² and M_{CPT} from 6.7 MPa to 10.3 MPa, the values of plastic limit (W_P) and plasticity index (PI) are found to be in between of 23.1% to 22.7%, and 24.4% to 23.9% respectively. Subsequently, in case of q_c ranging from 17.1 kg/cm² to 36.4 kg/cm² and M_{CPT} from 12.0 MPa to 27.8 MPa, the plastic limit (W_P) and plasticity index (PI) varies in between of 22.4% and 20.5% and 23.5% to 21.7% respectively. Further, when the value of q_c ranging from 40.6 to 65.1 and M_{CPT} lies between 31.3 to 52.9, the plastic limit (W_P) and plasticity index (PI) varies in between of 20.3 to 19.5 and 21.4 to 20.5 respectively. The summarised values are presented in Table 6.6. In addition to that, on validation purpose the estimated values (from the established relations) are compared with the laboratory tested values and present at subsequent section.

Table:6. 6 Predicted Value of Liquid Limit (W_L), Plastic Limit (W_P) and Plasticity Index (PI) from q_c and M_{CPT}

q_c (kg/cm^2)	M_{CPT} (MPa)	q_c/PI (kg/cm^2)	q_c/W_P (kg/cm^2)	W_L (%)	W_P (%)	PI (%)
7.5	5.5	0.33	0.35	43.6	21.2	22.4
8.8	6.0	0.37	0.39	46.8	22.8	24.0
9.9	6.7	0.41	0.43	47.5	23.1	24.4
14.9	10.3	0.62	0.66	46.6	22.7	23.9
17.1	12.0	0.73	0.77	45.9	22.4	23.5
36.4	27.8	1.68	1.77	42.2	20.5	21.7
40.6	31.3	1.90	2.00	41.7	20.3	21.4
65.1	52.9	3.21	3.38	40.0	19.5	20.5

To validate these proposed relations, Chi-square test is conducted. In this test, the (Greenwood and Nikulin 1996; Shiuly 2018; Shiuly et al. 2020; Shiuly and Roy 2021; Deng 2022), confidence level of the proposed relation is determined. The test is performed as follows (Equation 6.11):

$$\chi 2 = \sum_{i=1}^{n} \frac{(A_i - P_i)^2}{P_i} \quad (6.11)$$

where, χ^2 is denoted the Chi-square value. A_i is denoted as the observed / actual values, and P_i is the estimated / predicted values. After evaluating the Chi-square value, for the relation, the degrees of freedom are evaluated. Which are the number of categories minus the number of parameters of the fitted distribution. The calculated Chi-square value is then compared with the critical value from the Chi-square distribution table for the specific degree of freedom and confidence level.

In this study, the chi-square value is estimated using ten numbers (10) relevant observed data from two different locations outside the study area and the predicted values estimated from the proposed relationships (Table 6.7 and Table 6.8). The graphical presentation of the chi-square distribution for the respective relationship is presented in Figure 6.54 and Figure 6.55.

At null hypothesis (H_0), there is no relation exist whereas for alternate hypothesis, the relation exist (Shiuly 2018; Shiuly et al. 2020; Shiuly and Roy 2021). In this study, the degree of freedom is calculated as 9. For this degree of freedom, critical value of Chi-square is 16.919 (i.e., $\chi^2_{critical} = 16.919$) at significance level (α) of 0.05. Besides, the calculated value of Chi-square is 12.104 (i.e., $\chi^2_{calculated} = 12.104$) for the relation between M_{CPT} with $(q_c/Pa)/PI$. Hence, for this particular relation, critical value of Chi-square is greater than the calculated value of Chi- square (i.e., $\chi^2_{critical} > \chi^2_{calculated}$), thus, null hypothesis is rejected and the alternate hypothesis at significance level 0.05 is accepted. It signifies that, at a 0.05 significance level, relation between M_{CPT} with $(q_c/Pa)/PI$ predicts well for the observed data. Similarly, it is found that the calculated values of Chi-square of all the proposed relations are less than the critical value for the 0.05 significance level (i.e., $\chi^2_{critical} = 16.919$).

Table:6. 7 Comparison of observed value of q_c/pa, M_{CPT} and f_s with the estimated value from proposed relation

Depth (m)	Observed SPT values (N_{ob})	Observed q_c/pa	Observed M_{CPT} (MPa)	Observed f_s (kg/cm^2)	Estimated q_c/pa	Estimated M_{CPT} (MPa)	Estimated f_s (kg/cm^2)
1.0	6	8.61	6.90	0.45	11.30	7.64	0.85
4.0	5	6.69	4.91	0.27	9.91	6.71	0.54
10.0	4	6.85	4.21	0.33	8.81	6.05	0.30
16.0	13	35.34	26.80	1.05	28.88	21.46	4.87
2.0	7	10.41	8.24	0.48	12.96	8.83	1.22
5.0	5	6.16	4.33	0.13	9.91	6.71	0.54
8.0	4	5.24	3.18	0.15	8.81	6.05	0.30
11.0	4	12.98	9.16	0.56	8.81	6.05	0.30
14.0	7	14.72	10.13	1.36	12.96	8.83	1.22
17.0	12	26.33	19.33	0.93	25.52	18.70	4.09

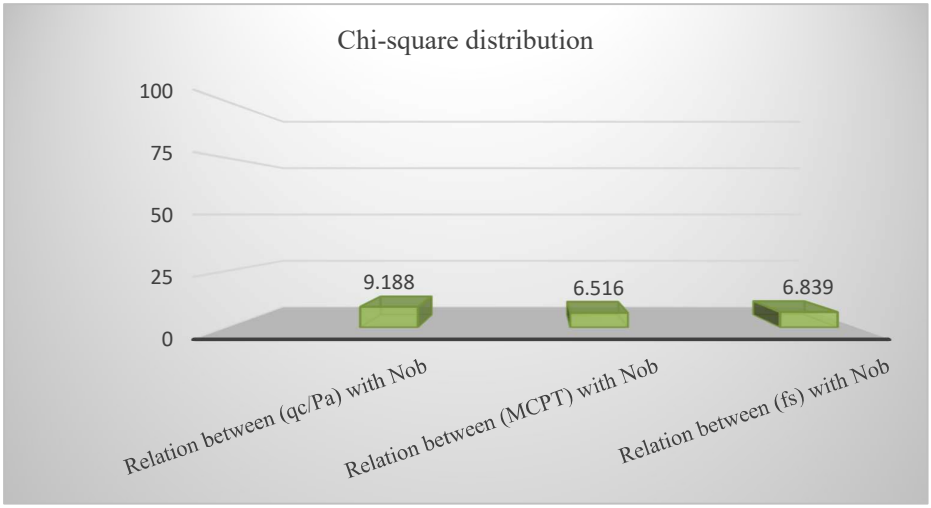

Figure: 6. 54 Chi-square distribution for the proposed relations

Table: 6. 8 Comparison of Laboratory estimated Liquid Limit (W_L), Plastic Limit (W_P) and Plasticity Index (PI) with the predicted value from q_c and M_{CPT}

Depth (m)	Laboratory obtained W_L	Laboratory obtained W_P	Laboratory obtained PI	Predicted W_L	Predicted W_P	Predicted PI
1.0	42.0	21.1	20.9	40.1	19.5	20.6
4.0	53.6	26.5	27.1	43.8	21.3	22.5
10.0	50.3	25.9	24.4	52.3	25.4	26.8
16.0	51.1	20.6	30.5	42.4	20.6	21.7
2.0	48.1	21.3	26.8	40.6	19.8	20.8
5.0	50.3	24.6	25.7	45.7	22.3	23.5
8.0	52.0	26.4	25.6	53.0	25.8	27.2
11.0	53.2	26.6	26.6	45.5	22.2	23.4

Depth (m)	Laboratory obtained W_L	Laboratory obtained W_P	Laboratory obtained PI	Predicted W_L	Predicted W_P	Predicted PI
14.0	53.9	19.7	34.2	46.7	22.7	24.0
17.0	41.3	22.4	18.9	43.8	21.3	22.5

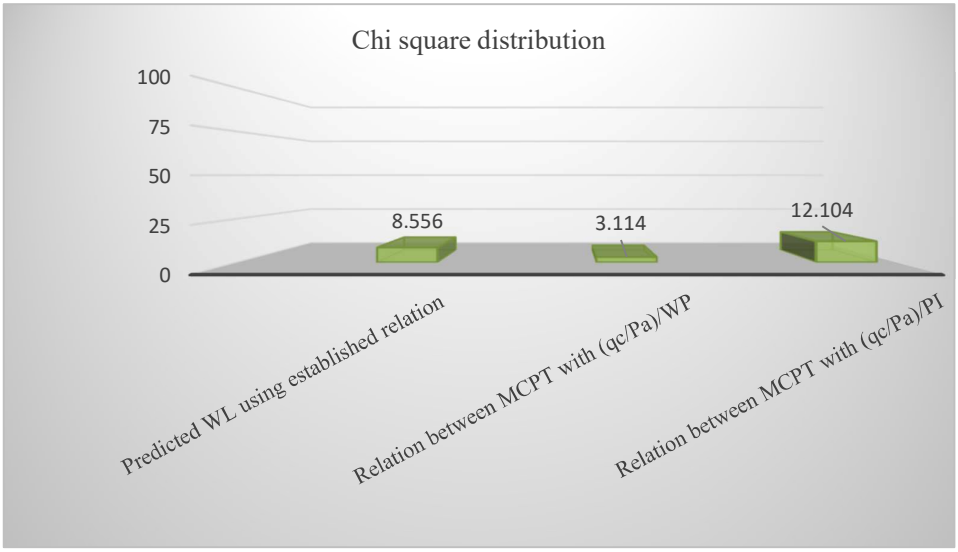

Figure: 6. 55 Chi-square distribution for the proposed relations

6.4 PMT TEST

Pressuremeter tests were conducted in three numbers of sites. In this test, two numbers of basic parameters (i.e., P_L and E_{PMT}) were considered for the comparison purpose. In PMT tests, limit pressure (P_L) indirectly resembles the resistance (in horizontal direction) imparted by the sub-soil. Also, the N_{ob} represents the soil resistance. As such, at each site, P_L has been compared with the N_{ob} (conducted in the adjacent borehole) and both the results are then plotted along depth to find out the nature of the variation. On the other hand, Pressuremeter Modulus (E_{PMT}) is one of the important parameters in geotechnical design field. Indirectly, the pressuremeter modulus resembles the modulus of elasticity of sub-soil. Also, the modulus of elasticity can be predicted from the conventional N_{ob}. Hence, site wise, the estimated value of E_{PMT} has been compared with the N_{ob} by plotting along depth.

6.4.1 COMPARATIVE INTERPRETATION OF SPATIAL VARIATION OF P_L AND N_{OB} WITH DEPTH

The variation of limit pressure (P_L) and N_{ob} are plotted along depth for each site. From this variation it is observed that the depth-wise variation of P_L is similar in nature with the N_{ob} values for all test locations. The variations are shown in Figure 6.56 to Figure 6.58.

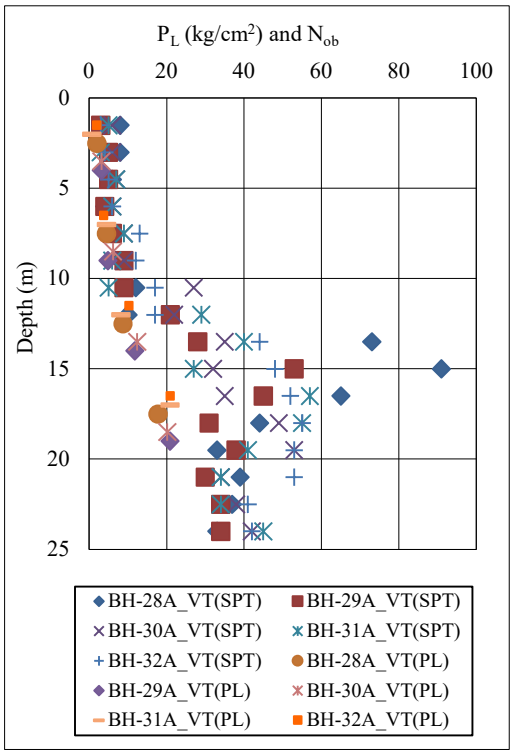

Figure: 6. 56 Variation of Limit Pressure (P_L) and N_{ob} with depth for the Site-9 (VT)

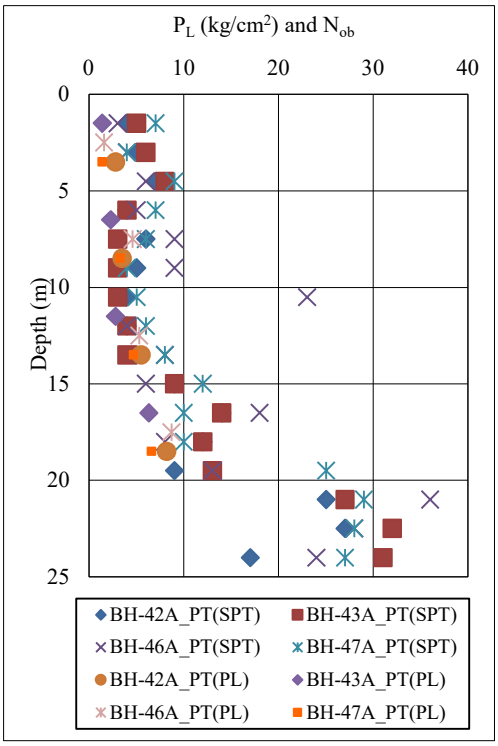

Figure: 6. 57 Variation of Limit Pressure (P_L) and N_{ob} with depth for the Site-10 (PT)

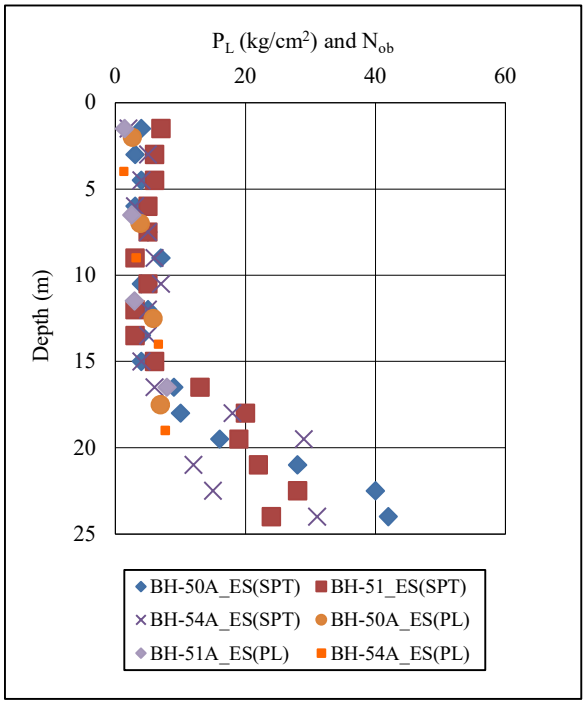

Figure: 6. 58 Variation of Limit Pressure (P_L) and N_{ob} with depth for the Site-11 (ES)

6.4.2 COMPARATIVE INTERPRETATION OF SPATIAL VARIATION OF E_{PMT} AND N_{OB} WITH DEPTH

The variation of E_{PMT} and N_{ob} have been plotted along depth for each study area. From this variation it has been observed that the depth-wise variation of E_{PMT} is similar in nature with the N_{ob} for all tests locations. The variations are shown in Figure 6.59 to Figure 6.61.

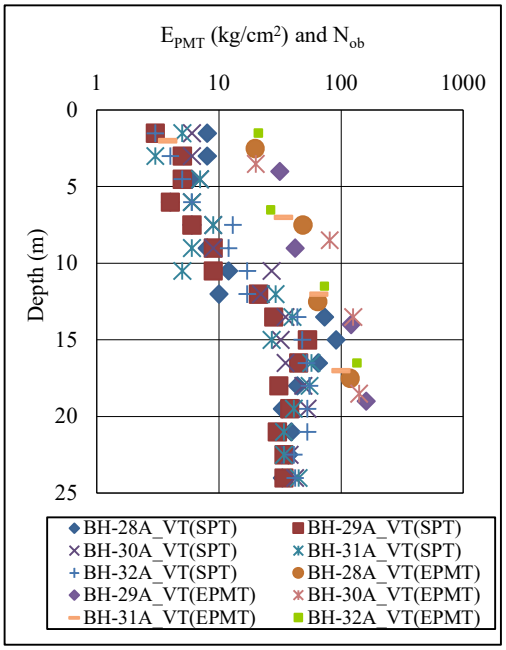

Figure: 6. 59 Variation of E_{PMT} and N_{ob} with depth for the Site-09 (VT)

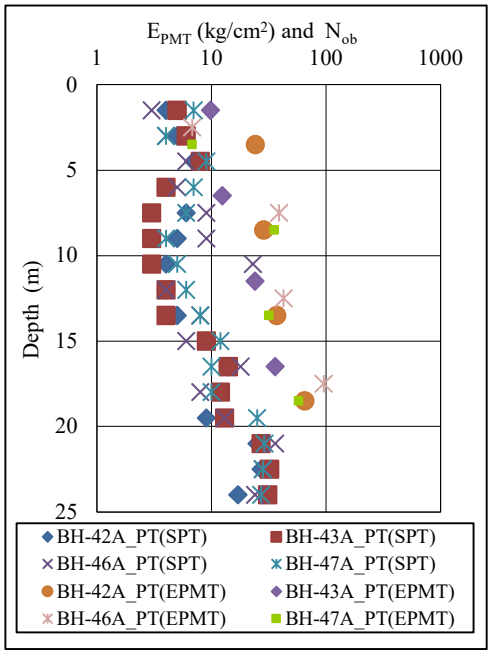

Figure: 6. 60 Variation of E_{PMT} and N_{ob} with depth for the Site-10 (PT)

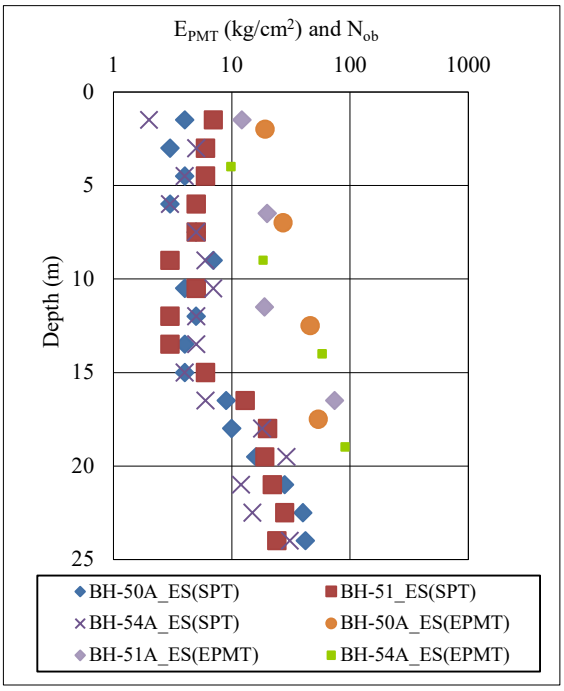

Figure: 6. 61 Variation of E_{PMT} and N_{ob} with depth for the Site-11 (ES)

6.4.3 RELATION OF P_L, E_{PMT} WITH N_{OB} AND LIQUIDITY INDEX (I_L)

In view of the variation of P_L and E_{PMT} along depth, it is observed that the values of P_L and E_{PMT} very much depends on the consistency of cohesive soil. Hence, the value of P_L and E_{PMT} is related with the N_{ob} value, so that a reference value of P_L and E_{PMT} can be predicted for the different consistency or vice versa. Besides, in most of the cases, it is observed that the ratio of E_{PMT}/P_L is well comparable with I_L. Therefore, another relation between the ratio of E_{PMT} and P_L (E_{PMT}/P_L) with liquidity index (I_L) is established.

In this regard, at all tests locations, natural moisture content (w_n), liquid limit (W_L) and plastic limit (W_P) of sub soil (estimated from laboratory tests results corresponding to collected undisturbed sample of soil) are considered adjacent to the depth at which pressuremeter tests were conducted. Also, N_{ob} (adjacent to pressuremeter test depth), are considered for the analysis purpose. The site-wise elaborative results are given in Appendix C.

6.4.3.1 RELATION BETWEEN N_{OB} WITH P_L AND E_{PMT}

In arriving at the relation between N_{ob} with P_L and E_{PMT} , the PMT test results i.e., P_L and E_{PMT} (considering three sites) corresponding to cohesive soils (silty clay/clayey silt) are considered. The value of N_{ob} value is taken for the same depth at which pressuremeter tests were conducted. For the relationship purpose, two numbers of separate graphs are plotted corresponding P_L/Pa with N_{ob} and E_{PMT}/Pa with N_{ob} (where Pa is atmospheric pressure ≈ 0.1 MPa), keeping N_{ob} as abscissae. The relationship is presented in Equation 6.12 (Figure 6.62) and Equation 6.13 (Figure 6.63) respectively.

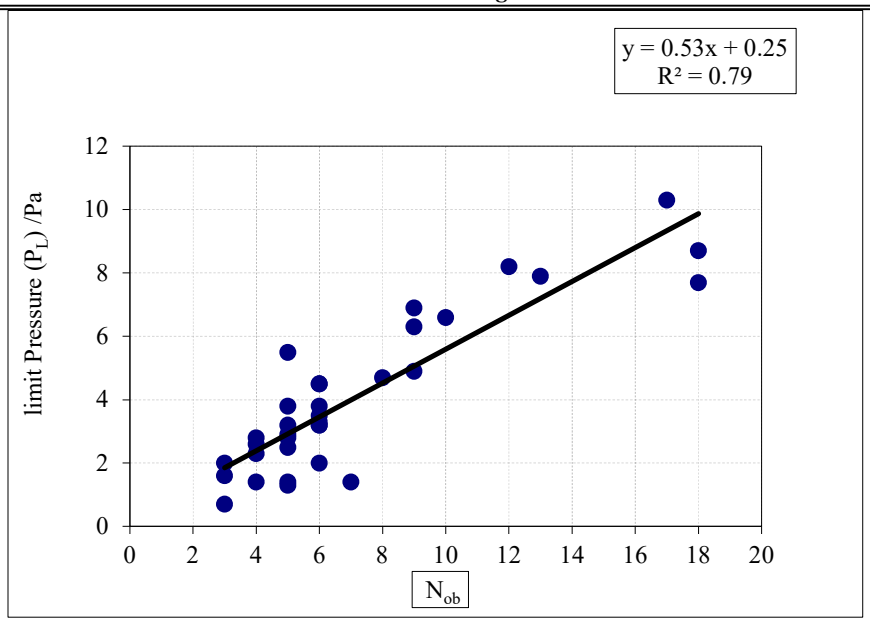

Figure: 6. 62 Relationship between P_L/Pa with N_{ob}

$$(\mathbf{P_L/Pa}) = \mathbf{0.53} \times (\mathbf{N_{ob}}) + \mathbf{0.25} \quad (6.12)$$

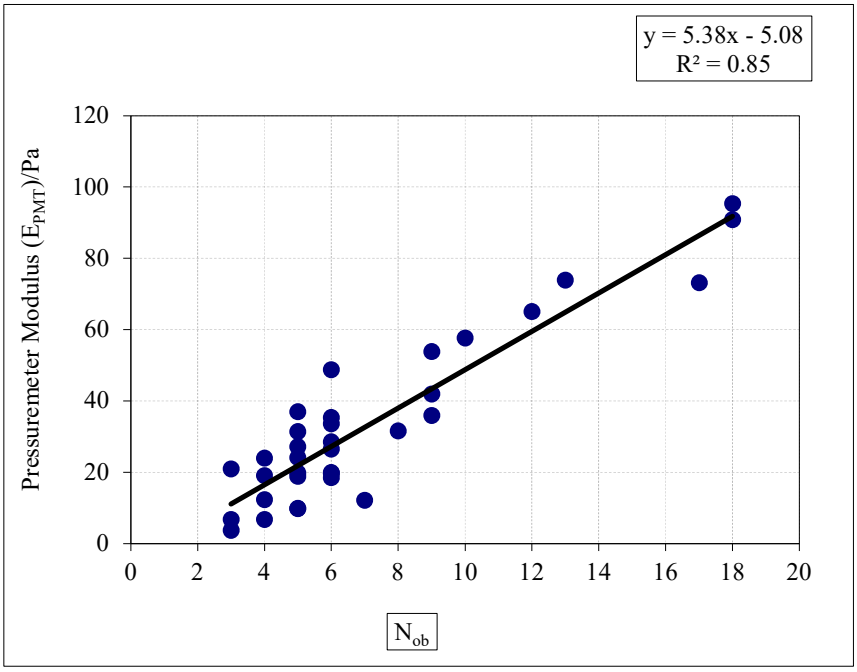

Figure: 6. 63 Relationship between E_{PMT} with N_{ob}

$$(\mathbf{E_{PMT}/Pa}) = \mathbf{5.38} \times (\mathbf{N_{ob}}) - \mathbf{5.08} \quad (6.13)$$

6.4.3.2 RELATION OF E_{PMT}/P_L WITH LIQUIDITY INDEX (I_L)

If the soil is identified by other method (such as by laboratory tests conducted on collected samples), the condition of the sub-soil can be predicted from pressuremeter test results. In this regard, the ratio between E_{PMT} and P_L is useful information and the consistency can be predicted from this value (Briaud 1992, 2019a; Clarke 1994). It is to be noted that the ratio between E_{PMT} and P_L is an important tool to predict the settlement of shallow foundation (Baguelin et al. 1978; Amar et al. 1991; Clarke 1994; Cestari Ferrucio 2012). Besides, liquidity index (I_L) is also an important parameter to characterize the sub-soil in terms of its consistency and compressibility behavior (Carter and Bentley 1991). However, there is no such relation between the E_{PMT}/P_L and I_L. Hence, a relation between E_{PMT}/P_L with liquidity index (I_L) is established. In arriving at the relationship, a graph between E_{PMT}/P_L and I_L is plotted by ignoring some scattered values. For this relationship purpose, I_L is kept as abscissa and E_{PMT}/P_L is kept as ordinate. The relationship is presented in Equation 6.14 (Figure 6.64).

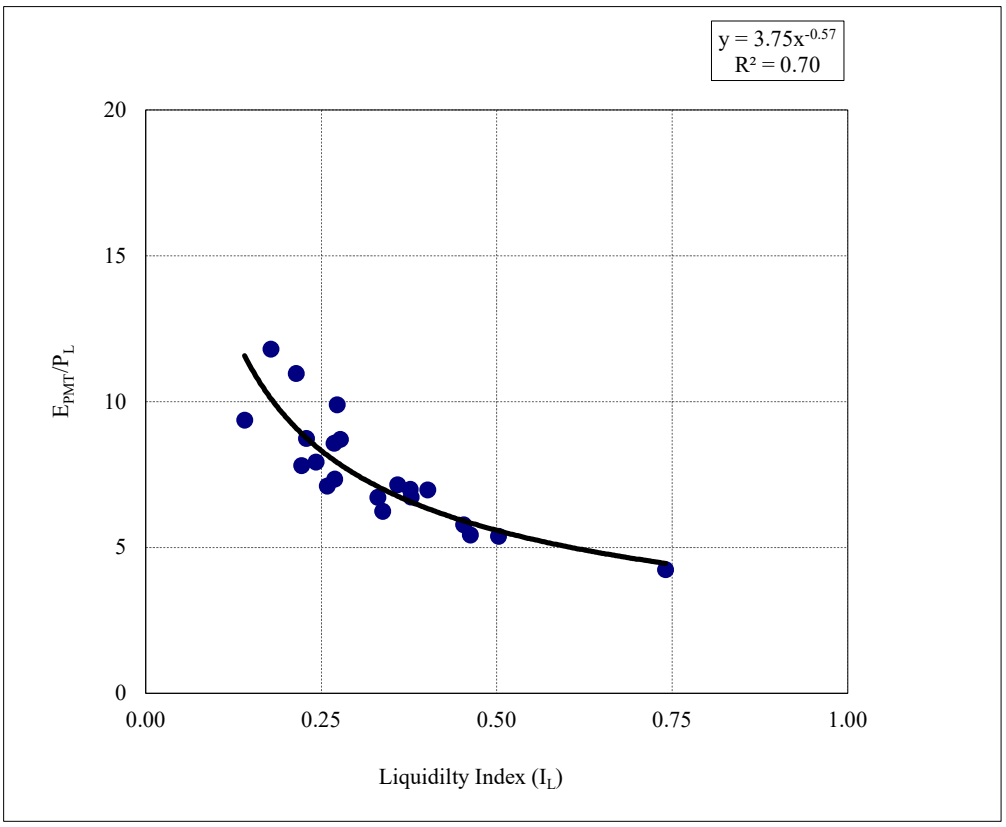

Figure: 6. 64 Relationship between E_{PMT}/P_L with Liquidity Index

$$\mathbf{E_{PMT}/P_L = 3.75 \times I_L^{-0.57}} \quad (6.14)$$

6.4.4 DISCUSSION ON THE PREDICTED RELATIONSHIP

The sub-soil profiles (in most of the cases) are found to be cohesive by nature for all the PMT test locations. This is why to establish the relationship, only the tests results for the cohesive soil, are considered. It is also observed that the presence of decomposed wood (observed during the visual inspection of the excavated soil for the PMT test and also from disturbed samples collected during collection of samples from bore holes) in the sub soil, largely affects the PMT test results. Therefore, to establish the relations, good quality data (by ignoring some scattered values) is considered for the calculation purpose.

In this study, it is observed that P_L and E_{PMT} linearly related with the N_{ob} for the cohesive soil. Based on the new established relations (N_{ob} with P_L and E_{PMT}), it is found that P_L varies between 0.19 MPa to 0.24 MPa and E_{PMT} varies between 1.11 to 1.65MPa for the soft soil (N_{ob} between 3 to 4). For firm soil (N_{ob} between 5 to 8) P_L varies between 0.29 MPa to 0.45 MPa and E_{PMT} varies between 2.18 to 3.80 MPa. For stiff soil (N_{ob} between 9 to 15) P_L varies between 0.51MPa to 0.83MPa and E_{PMT} varies in between 4.34 to 7.57 MPa. For very stiff soil (N_{ob} between16 to 18) P_L varies between 0.88 MPa to 0.99 MPa and E_{PMT} varies in between 9.21 to 9.31 MPa. The summary of all these values is presented in Table 6.9.

Table:6. 9 Value of E_{PMT}, P_L for different observed (field) SPT N values (N_{ob})

N_{ob}	Consistency	Predicted E_{PMT} (MPa)	Predicted P_L (MPa)	Predicted E_{PMT}/P_L
3 to 4	Soft	1.11-1.65	0.19-0.24	5.97-6.89
5 to 8	Firm	2.18-3.80	0.29-0.45	7.47-8.39
9 to 15	Stiff	4.34-7.57	0.51-0.83	8.57-9.16
16 to 18	Very stiff	8.11-9.18	0.88-0.99	9.21-9.31

Besides, the ratio of E_{PMT} and P_L (i.e., E_{PMT}/P_L) varies inversely with the value of liquidity index (I_L) of soil. Based on the established relation between E_{PMT}/P_L with the liquidity index (I_L), it is observed that the value of E_{PMT}/P_L, for soft soil varies in between of 4.4 to 5.6. For firm soil E_{PMT}/P_L lies between of 5.6 to 8.3. For stiff soil E_{PMT}/P_L lies above 8.3. The summary of all these values is presented in Table 6.10.

Table: 6. 10 value of E_{PMT}/P_L for different Liquidity Index

Liquidity index (I_L)	Consistency	Predicted E_{PMT}/P_L
0.75	Soft	4.4
0.50	Firm	5.6
0.25	Stiff	8.3

6.5 SUMMARY

For individual in-situ test (i.e., DMT, CPT and PMT tests), separate relationship has been established by comparing the test results (estimated from DMT, CPT and PMT tests) with the results obtained from the adjacent boreholes. In majority of the cases, the sub-soil profiles were found to be cohesive by nature. Therefore, to establish the relationship, only the test results corresponding to the cohesive sub-soil have been considered. Also, in arriving at the relation, good quality data (by eliminating most scattered value) have been taken in the calculation. The major findings from this investigation are summarised below.

- In DMT test, for the silty clay/ clayey silt soil, the value of E_D and M_{DMT} highly depends on the soil consistency.
- Presence of decomposed wood particles badly affects the test results obtained from DMT, CPT and PMT tests
- It is also observed that the ratio of M_{DMT}/E_D linearly relates with the plastic limit and plasticity index for the silty clay/clayey silt soil.
- In CPT test, the values of q_c, M_{CPT} and f_s highly depend on the consistency of cohesive soil.
- Also, it is observed that the ratio of q_c/PI and q_c/W_P linearly relates with the M_{CPT}.

- In both DMT and CPT tests, the calculated values of Chi-square for all the predicted relations fall well within the critical values at the 0.05 significance level.
- In PMT test, it is observed that P_L and E_{PMT} linearly relates with the observed (field) SPT N values (N_{ob}) whereas the ratio of E_{PMT}/P_L decreases with the increase of liquidity index (I_L), conforming to a 'power-law' behavior.

Chapter# 7
CPT-BASED PREDICTIVE MODEL FOR SHALLOW FOUNDATION SETTLEMENT ON COHESIVE SOIL

7.1 GENERAL

In this chapter focus is given to estimate settlement of shallow foundation (placed on cohesive soil) based on average CPT cone resistance and compare with the other method. The settlement analysis has been carried out based on the average cone resistance (C_{KD}) by using an empirical equation, M_{DMT} from DMT tests and by using conventional Mohr Coulomb model in PLAXIS 2D (ver. 2016) software. Indian standard suggested an empirical equation for carrying out settlement analysis based on CPT cone resistance. It is recommended for cohesionless soil only. In this study, as no other code is available for Indian condition, same empirical equation is tried to predict the settlement of shallow foundation (placed on cohesive soil) based on CPT test as per (Bandyopadhyay et al. 2022). The estimated values are then compared with the estimated settlement by other methods (i.e., using M_{DMT} from DMT settlement software and two-dimensional model created by using PLAXIS 2D software), based on the conventional bore holes results, CPT test results and DMT test results. Finally, efficacy of use of this formula for cohesive soil is judged. For this study purpose, based on the cohesive sub-soil formation, among eight number of test locations (at which CPT and DMT tests were carried out) four numbers of test locations had been selected. On these locations the settlement of shallow foundation had been calculated. Typical calculation for selected sites is given in Appendix D.

7.2 SETTLEMENT ANALYSIS

7.2.1 SITE-1 (HC)

At site-1 (HC), the depth of foundation was at 1.9 m below the existing ground level. The shape of the foundation was found to be 'strip footing' with an approximate width of 2.13 m. Total design load intensity on the footing was 200 kPa. The comparison is shown in Table 7.1.

Table: 7. 1 Comparison of estimated settlement

Location	Size of foundation	Depth of foundation	Load	Settlement value					
				DMT Settlement software	PLAXIS 2D (DMT)	PLAXIS 2D (CPT)	PLAXIS 2D (BH)	CPT Empirical equation	Observed settlement
	(m x m)	(m)	(kPa)	(mm)	(mm)	(mm)	(mm)	(mm)	(mm)
CPT1_HC/ DMT1_HC/ BH2_HC	2.13x 21.3	1.9	200	169.4	158.3	127.6	172.2	151.7	234.91
CPT2_HC/ DMT2_HC/ BH2_HC				118.3	121.7	132.3	172.2	103.2	101.63
CPT3_HC/ DMT3_HC/ BH3_HC				72.4	76.3	123.3	151.8	130.4	78.55
CPT4_HC/ DMT4_HC/ BH1_HC				155.7	197.4	168.3	150.4	167.0	153.42

From the above table it is observed that the settlement estimated from DMT settlement software, PLAXIS 2D, and average cone resistance (C_{KD}) are well tallying with each other. To observe the actual settlement, at this site, six numbers of settlement sensors were installed (Bandyopadhyay et al. 2020, 2022). Therefore, on comparing with the observed values, the estimated settlement is found to be in good agreement.

7.2.2 SITE-3 (RJ)

At Rajarhat test site, the foundation was placed at 1.5 m below the existing ground level. The foundation had been assumed to be isolated footing with varying length and

breadth, i.e. 2.0 m x 2.0 m, 3.0 m x 3.0 m, 1.5 m x 15.0 m, Total design load intensity on the footing was assumed as 40 kPa. The comparison is shown in Table 7.3.

Table: 7. 2 Comparison of estimated settlement.

Location	Size of foundation	Depth of foundation	Load	Settlement value				
				DMT Settlement software	PLAXIS 2D (DMT)	PLAXIS 2D (CPT)	PLAXIS 2D (BH)	CPT Empirical equation
	(m x m)	(m)	(kPa)	(mm)	(mm)	(mm)	(mm)	(mm)
CPT1_RJ/ DMT1_RJ /BH1_RJ	2.0 x 2.0	1.5	40	23.4	29	39	20	30.0
CPT2_RJ/ DMT2_RJ /BH2_RJ	3.0 x 3.0	1.5	40	36.3	45	39	22	39.7
CPT2_RJ/ DMT2_RJ /BH2_RJ	1.5 x 15	1.5	40	38.4	33	28	28	42.5

From the above table, it is observed that the estimated settlement obtained from DMT settlement software and PLAXIS 2D are more or less same. However, in some cases settlement obtained from PLAXIS 2D based on CPT parameters are on lower side as the undrained cohesion obtained from CPT was on higher side. Besides, in all the cases, estimated settlement obtained from average cone resistance (C_{KD}), are found to be a little bit higher.

7.2.3 SITE-4 (HA)

At Haldia test site, the foundation was assumed to be placed at 2.0 m and 6.0 m below the existing ground level. The foundation was considered as isolated footings with varying length and breadth, i.e. 1.5 m x 15.0 m, 6.0 m x 7.0 m, and 10.0 m x 12.0 m. Total design load intensity on the footing was taken as 81 kPa for 1.5 m x 15.0 m, 84 kPa for 6.0 m x 7.0 m, 37 kPa for 10.0 m x 12.0 m at CPT3_HA/DMT3_HA/BH3_HA test points. The comparison is shown in Table 7.4.

Table: 7. 3 Comparison of estimated settlement

Location	Size of foundation	Depth of foundation	Load	Settlement Values				
				DMT Settlement software	PLAXIS 2D (DMT)	PLAXIS 2D (CPT)	PLAXIS 2D (BH)	CPT Empirical equation
	(m x m)	(m)	(kPa)	(mm)	(mm)	(mm)	(mm)	(mm)
CPT3_HA/DMT3_HA/BH3_HA	1.5 x 15.0	2.0	81	28.9	22.2	19.3	23.0	36.4
CPT3_HA/DMT3_HA/BH3_HA	6.0 x 7.0	6.0	84	15.4	16.7	15.2	20.1	17.2
CPT3_HA/DMT3_HA/BH3_HA	10.0x 12.0	6.0	37	9.0	8.8	7.3	13.2	12.0

From the above table, it is observed that settlement values obtained from DMT settlement software, PLAXIS 2D, and average cone resistance (C_{KD}) of CPT, are more or less similar in nature.

7.2.4 SITE-5 (DH)

At Dhamra test site, the foundation was assumed to be placed at 2.0 m and 6.0 m below the existing ground level. The foundation was considered as isolated footings with varying length and breadth, i.e. 2.0 m x 2.0 m, 3.0 m x 3.0 m, 1.5 m x 15.0 m, 2.5 m x 25.0 m, 6.0 m x 7.0 m, and 10.0 m x 12.0 m. Total design load intensity on the footing was considered as 39 kPa for 3.0 m x 3.0 m, 32 kPa for 6.0 m x 7.0 m, 19 kPa for 10.0 m x 12.0 m at CPT1_DH/DMT1_DH/BH12_DH test points, 48 kPa for 2.0 m x 2.0 m, 45 kPa for 3.0 m x 3.0 m, 39 kPa for 1.5 m x 15.0 m, 36 kPa for 2.5 m x 25.0 m at CPT3_DH/DMT3_DH/BH7_DH test points and 32 kPa for 2.5 m x 25.0 m, 52 kPa for 6.0 m x 7.0 m, 38 kPa for 10.0 m x 12.0 m at CPT2_DH/DMT2_DH/BH15_DH test points. The comparison is shown in Table 7.5.

Table: 7. 4 Comparison of estimated settlement

Location	Size of foundation	Depth of foundation	Load	Settlement Values				
				DMT Settlement software	PLAXIS 2D (DMT)	PLAXIS 2D (CPT)	PLAXIS 2D (BH)	CPT Empirical equation
	(m x m)	(m)	(kPa)	(mm)	(mm)	(mm)	(mm)	(mm)
CPT1_DH/DMT1_DH/BH12_DH	3.0 x 3.0	6	39	13.61	14.59	8.59	11.59	19.4
	6.0 x 7.0		32	17.34	14.56	12.56	15.58	19.79
	10.0x 12.0		19	13.74	21.63	19.63	21.78	20.83
CPT2_DH/DMT2_DH/BH15_DH	2.5 x 25.0	6	32	20.48	25.08	15.08	16.23	26.91
	6.0 x 7.0		52	47.91	32.21	33.21	35	54.16
	10.0 x 12.0		38	43.74	35.21	15.21	22.43	45.83
CPT3_DH/DMT3_DH/BH7_DH	2.0 x 2.0	2	48	28.84	22.73	18.73	22.82	34.27
	3.0 x 3.0		45	43.60	38.73	35.73	32.85	49.50
	1.5 x 15.0		39	40.56	45.24	42.24	45	42.86
	2.5 x 25.0		36	58.36	50.8	41.8	47.76	60.85

From the above table, it is observed that settlement values obtained from DMT settlement software, PLAXIS 2D, and average cone resistance (C_{KD}) of CPT, are more or less similar in nature However, in some cases settlement obtained from PLAXIS 2D based on CPT parameters are on lower side as the undrained cohesion obtained from CPT is on higher side.

7.3 SUMMARY

- Settlement analysis was performed utilizing an empirical equation based on average cone resistance (C_{KD}). Although the Indian standard typically suggests this empirical correlation solely for cohesionless soil, due to the lack of alternative codes for Indian conditions, settlement analysis on cohesive soil was carried out by using the same equation. After comparative evaluation with other methods, it is observed that this correlation may be suitable for cohesive soil as well

- In most cases, it is observed that the predicted settlement (foundations placed on cohesive soil) from the average cone resistance (C_{KD}), is well tallying with M_{DMT} based settlement (calculated by using DMT Settlement software).
- In general, it is observed that the value of settlement (estimated by using numerical model through PLAXIS 2D software) lies on lower side compared to other methods.
- Besides, in some cases it is also observed that the settlement of the footing predicted from the PLAXIS 2D software (for the numerical model created by using the CPT based shear strength parameters) depicts lower values. This is due to the comparatively higher values of undrained cohesion estimated from CPT tests.

Chapter # 8
SUMMARY AND CONCLUSIONS

8.1 GENERAL

In India, the geotechnical investigation works are carried out by conventional boring approach, but it is an age-old technique and time consuming. Hence, a transformation from this technique to the new method is very much needed in this field. In this context, an attempt has been made to ascertain some in-situ test parameters which can be related with the basic geotechnical parameters and the prediction of sub-soil profile may be defined. This study has been conducted in two parts: In the first part, three types of in-situ tests (i.e., DMT, CPT and PMT) have been carried out to the adjacent conventional boreholes, at different locations with different geological formation to predict the sub-soil formation. The basic parameters obtained from these in-situ tests are then compared with the conventional SPT N values (N_{ob}) and shear strength parameters (estimated from laboratory tests). The depth wise estimated in-situ test results (i.e., E_D, M_{DMT}, q_c, M_{CPT}, f_s, P_L and E_{PMT}) are then accumulated for all sites, and compared with the observed (field) SPT N values (N_{ob}), plastic limit, plasticity index to establish relation. In the second part, settlement analysis of shallow foundation (placed on cohesive soils), has been carried out based on the results obtained from DMT, CPT and Laboratory tests and tallied. Finally, relations have been proposed for the prediction of consistency, liquid limit, plastic limit and plasticity index of cohesive soils from DMT and CPT tests. Besides, the range of limit pressure and pressuremeter modulus has been proposed for different consistency of sub-soil and the range of the ratio of E_{PMT}/P_L with liquidity index, has been suggested.

8.2 CONCLUSIONS

This study highlights the efficacy of advanced in-situ tests like DMT, CPT, and PMT, and suitability of these results in comparison with in-situ tests with traditional SPT and laboratory experiments. This study also reveals the reliable relations for predicting the sub-soil profiles in terms of its consistency and compressibility characteristics. It also explains about the accurate prediction of settlement from these in-situ tests. Moreover, implementation these advanced techniques can significantly enhance the accuracy and efficiency of geotechnical investigations, leading to improved foundation design and soil characterisation. The major conclusions made from the present study are as follows

1) From the present investigation, for eight numbers of test locations, it is observed that the sub-soil profile predicted from Dilatometer and Cone Penetration tests are more or less similar in nature compared to the sub-soil profile exhibited through the conventional soil exploration by digging bore hole.

2) Secondly, it is noticed that the undrained cohesion obtained from DMT tests shows better parity with the values obtained from laboratory triaxial (UU) test. On other hand, in most of the cases estimated undrained cohesion from CPT tests are on the higher side. Though the influence zone of CPT cone is higher than DMT blade, the cone factor (N_{kt}) played a vital role on the undrained cohesion. As such more research on better prediction of cone factor for cohesive soil deposits is very much needed.

3) The variation of M_{CPT} (which depends on cone resistance q_c) and M_{DMT} along depth is found to be similar in nature for all the cases. Hence from both the tests, compressibility characteristics of sub-soil may be predicted in an accurate manner by estimating these parameters.

4) It is observed that the variation of dilatometer modulus (E_D) along depth is highly dependent on the type of sub-soil formation. In cohesive sub-soil (silty clay/clayey silt), the value of E_D clearly depends on the consistency of sub-soil and it follows a uniform variation with depth. However, in a few cases, the variation is found to be scattered due to the presence of decomposed wood particles (exhibited in the adjacent boreholes). Besides, in silty sand/ sandy silt, the value of E_D is on the higher side.

5) It is also observed that the variation of dilatometer modulus (E_D) and vertical drained constrained modulus (M_{DMT}) along depth is well tallying with N_{ob}.

6) From the established relation (between N_{ob} with DMT estimated E_D and M_{DMT}), SPT based consistency of the cohesive sub-soil (comprising silty clay/ clayey silt) may be predicted by virtue of E_D and $M_{DMT.}$

7) This study also reveals the feasibility of predicting liquid limit, plastic limit and plasticity index based on the established relation (between M_{DMT} with E_D/PI and M_{DMT} with E_D/W_P value) for similar or competent subsoil.

8) Besides, the uniformity in the variation of q_c with depth is noticeably influenced upon consistency/compactness and type of sub-soil. In most of the cases, it is observed that the variation shows uniformity for silty clay / clayey silt soil. But the value of cone resistance is found to be scattered in some cases due to the presence of decomposed wood particles (exhibited in the adjacent boreholes). It is also noticed that, in silty sand/ sandy silt, the value of q_c is on the higher side.

9) It is observed that the variation of cone penetration resistance (q_c), sleeve friction (f_s) and vertical drained constrained modulus (M_{CPT}) with depth is well

tallying with the SPT N values for silty clay/clayey silt soil. Therefore, for similar or comparable sub soil, the SPT based consistency may be predicted by virtue of these parameters. It is also found that the predicted relation is well tallying with other previous relations.

10) Furthermore, it is to be mentioned that the ratio between M_{CPT} and q_c effectively represents the value of plastic limit (W_P) and plasticity index (PI). Therefore, it is possible to predict liquid limit, plastic limit and plasticity index by virtue of M_{CPT} and q_c for similar or comparable sub-soil.

11) Moreover, Chi-square values calculated for all predicted relationships (in both DMT and CPT tests) are significantly within the critical values at the 0.05 significance level.

12) For PMT test, it is observed that the value of limit pressure (P_L) and pressuremeter modulus (E_{PMT}) is high for silty sand/ sandy silt soil compared to cohesive silty clay/ clayey silt soil. Also, these parameters are very much influenced by the amount of decomposed wood particles present in the sub-soil.

13) It is noticed that the variation of limit pressure and pressuremeter modulus with depth is nearly comparable with the SPT N value (N_{ob}), for the cohesive (silty clay/ clayey silt) sub-soil. Therefore, at particular depth in cohesive sub-soil (silty clay/ clayey silt), the limit pressure and pressuremeter modulus may be predicted from the estimated SPT N values (N_{ob}) or vice versa.

14) On the other hand, the ratio of E_{PMT} to P_L (i.e., E_{PMT}/ P_L) can be used to predict liquidity index (I_L) for cohesive (silty clay/clayey silt) sub-soil or vice versa.

15) In this study, it reveals that the values of predicted settlement by using the average cone resistance (C_{KD}) are nearly same as the settlement calculated by using the M_{DMT}.

16) Also, it may be concluded that the estimated settlement by using M_{DMT} values and average cone resistance (C_{KD}) for foundations placed on cohesive soil are more conservative in nature than those obtained from PLAXIS2D.

17) Last but not the least, use of the empirical equation based on the average cone resistance gives well comparable values with other conventional methods for finding settlement of shallow foundation placed on cohesive soil.

8.3 LIMITATIONS OF THE PRESENT STUDY

The limitations of the present study are as follows:

1) The proposed relations in this study are valid for the coastal east zone cohesive (silty clay/ clayey silt) soil.
2) The soil exploration data from 29 numbers of DMT tests, have been incorporated in the study. The value of material index (I_D) of the soil mostly lies between 0.15 to 0.75 which indicates the presence of silty clay / clayey silt sub-soil. It is obvious that more DMT test data with wide range of I_D will be more effective for similar study.
3) In arriving at the relation, it is found that the SPT blow counts are ranging from 2 to 23. Presumably, the proposed relation for the prediction of SPT based consistency from DMT test is valid within this range.
4) The test data used for this study are mostly obtained for sub- soil having plasticity index ranging from 18% to 45% and plastic limit varying between

20% to 29%. Studies with wide variation of plasticity index and plastic limit may be more useful for similar study.

5) Also, it may be noted that the proposed relation for the prediction of liquid limit, plastic limit and plasticity index from DMT test, is valid for the sub soil having similar or comparable properties i.e., coastal east zone cohesive soil.

6) Besides, soil exploration data from 25 numbers of CPT tests have been considered for this study purpose. It is observed that most of the values of I_C lie between 2.6 to 3.6, indicating the presence of silty clay / clayey silt soil. It is obvious that more CPT tests with wide range of I_C may be more effective for similar study.

7) In arriving at the relation to predict the SPT based consistency from CPT test, SPT blow counts ranging from 2 to 21 are considered. Therefore, the proposed relation is valid within this range of SPT blow count.

8) To establish the relation for predicting W_L, W_P, and PI from CPT tests, data from sub-soil having plasticity index ranging from 14% to 50% and plastic limit mostly in between of 18% to 31% are considered. It is obvious that the broad range of plasticity index and plastic limit will enhance the effectiveness of the study.

9) This study utilised data from 48 PMT tests conducted in 12 boreholes. It is evident that a larger dataset of PMT tests would be more beneficial for this study.

10) Moreover, the majority of the PMT test points belonged to cohesive soil profile. Therefore, the analysis focused on using the cohesive soil (silty clay/clayey silt) data to establish relations. It is also to be mentioned that range of I_L varies between 0.18 to 0.75 and the SPT N values lies between

3 to 18 in the present study. Further studies with other I_L and SPT N values may be conducted

11) Further, it is important to note that, all the relations may be used for same or competent deposit having similar geomorphological characteristics. Though, it is to be noted that the DMT, CPT and PMT test results are highly affected by the presence of decomposed wood, one may use these relations with prior knowledge of the presence of decomposed wood in the sub-soil.

12) In numerical model (created in PLAXIS 2D ver. 2016) based on the CPT test results, the cohesion values from CPT test (generally which is on higher side) is used for the settlement analysis. It is obvious, that more comparable value of undrained cohesion estimated from CPT tests, may be more useful for the study.

13) In majority of study locations, CPT based settlement has not been compared with the observed settlement due to the scarcity of data. It is obvious that comparing the estimated settlements (from all methods) with the observed settlement will make the study more accurate.

8.4 RECOMMENDATION FOR FURTHER STUDY

The recommendation for further study as follows:

1) It recommended to carry out more numbers of DMT, CPT and PMT tests at different locations within this region.

2) The value of cone factor (N_{kt}) in CPT tests for estimating the undrained cohesion needs to be reaffirmed for the cohesive sub-soil within this study area.

3) The range of limit pressure and pressuremeter modulus needs to be developed for the silty sand/sandy silty deposits for the Kolkata region.

4) More case studies need to be done for the comparison of the settlement of shallow foundation (placed on cohesive soil) predicted from CPT and DMT tests, with the observed one.

REFERENCES

Aas G (1986) Use of in situ tests for foundation design on clay. In: Proceedings of the ASCE Specialty Conference In Situ'86, Use of In Situ tests in Geotechnical Engineering

Agaiby SS, Mayne PW (2015) Relationship between undrained shear strength and shear wave velocity for clays. In: 6th Symp. on Deformation Characteristics of Geomaterials. IOS Press, Argentina, pp 358–365

Ahmadi MM, Robertson PK (2005) Thin-layer effects on the CPT q_c measurement. Canadian Geotechnical Journal 42:1302–1317. https://doi.org/10.1139/t05-036

Akca N (2003) Correlation of SPT–CPT data from the United Arab Emirates. Eng Geol 67:219–231. https://doi.org/10.1016/S0013-7952(02)00181-3

Aladag CH, Kayabasi A, Gokceoglu C (2013) Estimation of pressuremeter modulus and limit pressure of clayey soils by various artificial neural network models. Neural Comput Appl 23:333–339. https://doi.org/10.1007/s00521-012-0900-y

Amar S, Clarke BG, Gambin M,, Orr TL (1991) The Application of Pressuremeter Test Results to Foundation Design in Europe

Ameratunga J, Sivakugan N, Das BM (2016) Pressuremeter Test. pp 159–181

Amoroso S, Lehane BM, Fahey M (2013a) Determining G-γ decay curves in sand from a Seismic Dilatometer Test (SDMT). In: Geotechnical and Geophysical Site Characterization: Proceedings of the 4th International Conference on Site Characterization ISC-4. Taylor & Francis Books Ltd, pp 447–452

Amoroso S, Monaco P, Lehane BM, Marchetti D (2014) Examination of the potential of the seismic dilatometer (SDMT) to estimate in situ stiffness decay curves in various soil types. Soils and Rocks 37:177–194

Amoroso S, Monaco P, Marchetti D (2013b) Use of the Seismic Dilatometer (SDMT) to estimate in situ G-γ decay curves in various soil types. In: Geotechnical and Geophysical Site Characterization: Proceedings of the 4th International Conference on Site Characterization ISC-4. Taylor & Francis Books Ltd, pp 489–497

Anwar MB (2018) Correlation between PMT and SPT results for calcareous soil. HBRC Journal 14:50–55. https://doi.org/10.1016/j.hbrcj.2016.03.001

Arifuzzaman, Anisuzzaman Md (2022) An initiative to correlate the SPT and CPT data for an alluvial deposit of Dhaka city. International Journal of Geo-Engineering 13:5. https://doi.org/10.1186/s40703-021-00170-3

ASTM International (2007) ASTM Standard D6635-01: Standard Test Method for Performing the Flat Dilatometer. West Conshohocken, Pa

ASTM International (1986) Suggested method for performing the flat dilatometer test. ASTM International

ASTM International (2000a) ASTM Standard D3441-98: Standard Test Method for Mechanical Cone Penetration Tests of Soil. West Conshohocken, Pa

ASTM International (2000b) ASTM Standard D4719-00: Standard Test Method for Prebored Pressuremeter Testing in Soils. West Conshohocken, Pa

ASTM Standard (2007) ASTM Standard D5778-07:Standard Test Method for Electronic Friction Cone and Piezocone Penetration Testing of Soils. West Conshohocken, Pa

Aversa S, Evangelista A (1993) Thermal expansion of Neapolitan yellow tuff. Rock Mech Rock Eng 26:281–306

Aykin K, Akcakal O, Durgunoglu HT (2010) Comparison of soil modeling using CPT and DMT- a case study. In: 2nd International Symposium on Cone Penetration Testing , . Volume 2&3, Paper No. 45, Huntington Beach, CA, USA, pp 487–494

Baguelin F, Jézéquel JF, Shields DH (1978) The Pressuremeter and Foundation Engineering. Trans Tech Publications

Balachandran K, Liu J, Cao L, Peaker SM (2015) Statistical correlations between pressuremeter modulus and SPT- N value for glacial tills

Balachandran K, Liu J, Cao L, Peaker SM (2017) Statistical Correlations between undrained shear strength (C U) and both SPT-N value and net limit pressure (P L) for cohesive glacial tills

Baldi G, Bellotti R, Ghionna V, et al (1986) FLAT DILATOMETER TESTS IN CALIBRATION CHAMBERS. In: Use of In Situ Tests in Geotechnical Engineering, Proceedings of In Situ'86. ASCE

Baldi G, Bellotti R, Ghionna VN, et al (1989) Modulus of sands from CPT's and DMT's. In: Congrès international de mécanique des sols et des travaux de fondations. 12. pp 165–170

Baligh MM (1985) Strain path method. Journal of Geotechnical Engineering 111:1108–1136

Baligh MM, Scott RF (1975) Quasi-static deep penetration in clays. Journal of the Geotechnical Engineering Division 101:1119–1133

Bandyopadhyay K, Das K, Nandi S, Halder A (2022) Dilatometer—an in Situ Soil Exploration Tool for Problematic Ground Conditions vis-à-vis for Economizing Construction Activities. Indian Geotechnical Journal 52:1155–1170. https://doi.org/10.1007/s40098-022-00655-7

Bandyopadhyay K, Nandi S, Scholer P, et al (2020) Prediction of settlement of high court building, kolkata using flat dilatometer-a case study. In: Tamás Huszák AM and EK (ed) 6th International Conference on Geotechnical and Geophysical Site Characterization. ISSMGE, Budapest, Hungary

Been K, Quiñonez A, Sancio RB (2010) Interpretation of the CPT in engineering practice . In: 2nd International Symposium on Cone Penetration Testing, Huntington Beach, CA, USA, CPT 10. CPT 10, Huntington Beach, CA, USA

Begemann HKS (1953) Improved method of determining resistance to adhesion by sounding through a loose sleeve placed behind the cone. In: Proceedings of the 3rd International Conference on Soil Mechanics and Foundation Engineering, ICSMFE, August. pp 16–27

Bellotti R (1986) Deformation characteristics of cohesionless soils from in situ tests. Proc of In situ'86 47–73

Bellotti R, Fretti C, Jamiolkowski M, Tanizawa F (1994) Flat dilatometer tests in Toyoura sand. In: International conference on soil mechanics and foundation engineering. pp 1779–1782

Benoît J, Lutenegger AJ (1992) Determining lateral stress in soft clays. In: Predictive soil mechanics: Proceedings of the Wroth Memorial Symposium held at St Catherine's College, Oxford, 27-29 July 1992. Thomas Telford Publishing, pp 135–155

Bihs A, Long M, Marchetti D, Ward D (2010) Interpretation of CPTU and SDMT in organic, Irish soils. In: 2nd International Symposium on Cone Penetration Testing. Huntington Beach. pp 257–264

Boghrat A (1987) Dilatometer testing in highly overconsolidated soils. Journal of geotechnical engineering 113:516–519

Bogossian F, Muxfeldt AS, Dutra AMB (1989) Some results of flat dilatometer tests in brazilian soils. In: Congrès international de mécanique des sols et des travaux de fondations. 12. pp 187–190

Borden RH (1991) Boundary displacement induced by DMT penetration. In: Proceedings of First International Symposium on Calibration Chamber Testing. Citeseer, pp 101–118

Borden RH, Saliba RE, Lowder WM (1986) Compressibility of Compacted Fills Evaluated by the Dilatometer

Bowles JE (2001) Foundation Analysis and Design, 5th edn. The McGraw-Hill Companies, Inc, Peoria, Illinois

Bozbey I, Togrol E (2010) Correlation of standard penetration test and pressuremeter data: a case study from Istanbul, Turkey. Bulletin of Engineering Geology and the Environment 69:505–515. https://doi.org/10.1007/s10064-009-0248-4

Briaud JL (1992) The Pressuremeter. A.A. Balkema, Rotterdam, Netherlands

Briaud J-L (2019a) The pressuremeter. Routledge

Briaud J-L (2019b) Design of shallow foundations. In: The Pressuremeter. Routledge, p 75

Briaud J.L (2013) Ménard Lecture - The pressuremeter test: Expanding its use. In: 18th International Conference on Soil Mechanics and Geotechnical Engineering (Paris). ISSMGE

Briaud J-L, Jordan G (1983) Pressuremeter design of shallow foundations. Texas Transportation Institute, Texas A & M University System

British Standard (1997) Eurocode 7—Geotechnical design—part 2: ground investigation and testing. British Standard Institution, BS EN 2:2007

Burghignoli A, Cavalera L, Chieppa V, et al (1991) Geotechnical characterisation of Fucino clay. In: X European Conf. on Soil Mech. and Found. Eng. pp 27–40

Campanella RG, Robertson PK (1991) Use and interpretation of a research dilatometer. Canadian Geotechnical Journal 28:113–126

Campanella RG, Robertson PK (1983) Flat plate dilatometer testing: research and development. Department of Civil Engineering, University of British Columbia

Campanella RG, Robertson PK, Gillespie D (1983) Cone penetration testing in deltaic soils. Canadian Geotechnical Journal 20:23–35. https://doi.org/10.1139/t83-003

Campanella RG, Robertson PK, Gillespie D, Grieg J (1985) Recent developments in in-situ testings of soils. In: International conference on soil mechanics and foundation engineering. 11. pp 849–854

Campbell DB, Hudson WR (1969) The determination of soil properties In Situ. Center for Highway Research

Carter M, Bentley SP (1991) Correlations of Soil Properties. Pentech Press

Cassan M (1988) Les essais in situ en mécanique des sols. Eyrolles

Cestari Ferrucio (2012) In situ geotechnical Tests. Pàtroneditore

Chang MF (1991a) Interpretation of overconsolidation ratio from in situ tests in recent clay deposits in Singapore and Malaysia. Canadian Geotechnical Journal 28:210–225

Chang MF (1987) The flat dilatometer test and its role in site investigation. In: Southeast Asian geotechnical conference. 9. pp 93–108

Chang MF (1986) The flat dilatometer test and its application to two Singapore clays. In: 4th International Seminar on Field Instrumentation and In-Situ Measurements, Singapore. pp 81–85

Chang MF (1991b) Flat dilatometer tests in clay deposits of Singapore. In: Proceedings of the 9th Asian Regional Conference on Soil Mechanics and Foundation Engineering, Bangkok, Thailand. pp 23–28

Chang MF, Choa V, Cao LF, Myint Win B (1999) Overconsolidation ratio of a seabed clay from in-situ tests. In: International Conference on Soil Mechanics and FOundation Engineering. pp 453–456

Chatterjee K, Choudhury D (2013) Variations in shear wave velocity and soil site class in Kolkata city using regression and sensitivity analysis. Natural Hazards 69:2057–2082. https://doi.org/10.1007/s11069-013-0795-7

Cheshomi A, Ghodrati M (2015) Estimating Menard pressuremeter modulus and limit pressure from SPT in silty sand and silty clay soils. A case study in Mashhad, Iran. Geomechanics and Geoengineering 10:194–202. https://doi.org/10.1080/17486025.2014.933894

CLARKE BG (1996) PRESSUREMETER TESTING IN GROUND INVESTIGATION. PART 1 - SITE OPERATIONS. Proceedings of the Institution of Civil Engineers - Geotechnical Engineering 119:96–108. https://doi.org/10.1680/igeng.1996.28169

Clarke BG (1996) PRESSUREMETER TESTING IN GROUND INVESTIGATION. PART 1 - SITE OPERATIONS. Proceedings of the Institution of Civil Engineers - Geotechnical Engineering 119:96–108. https://doi.org/10.1680/igeng.1996.28169

Clarke BG (2022) Pressuremeters in geotechnical design. CRC Press

Clarke BG (1994) Pressuremeters in Geotechnical Design. CRC Press

Clarke BG, Wroth CP (1989) Comparison between results from flat dilatometer and self-boring pressuremeter tests. In: Penetration testing in the UK: Proceedings of the geotechnology conference organized by the Institution of Civil Engineers and held in Birmingham on 6–8 July 1988. Thomas Telford Publishing, pp 295–298

Costa YD, Cunha ES, Costa CL, Pereira AC (2016) Correlations between the CPT and the SPT for some Brazilian soils. In: Acosta-Martínez, Kelly (eds) Geotechnical and Geophysical Site Characterisation 5-Lehane. Australian Geomechanics Society, ISBN 978-0-9946261-1-0, Sydney, Australia, pp 407–412

Coutinho RQ, Mayne PW (2012) Geotechnical and geophysical site characterization 4. CRC Press

Cruz N, Viana da Fonseca A, Coelho P, Lemos JL (1999) Evaluation of geotechnical parameters by DMT in Portuguese soils. In: International Conference on Soil Mechanics and FOundation Engineering. pp 77–80

D. B. Campbell (1972) The determination of soil properties in situ. J Terramech 8:109. https://doi.org/10.1016/0022-4898(72)90111-5

da Fonseca AV, Mayne PW (2004) Geotechnical and Geophysical Site Characterization. Millpress

Dagger R, Saftner D, Mayne P (2018) Cone penetration test design guide for state geotechnical engineers

Danziger BR, Velloso DA (1995) Correlations between the CPT and the SPT for some Brazilian soils. Proceedings CPT 95:155–160

Das BM (2019) Advanced soil mechanics. CRC press

Das BM, Sivakugan N (2018) Principles of foundation engineering. Cengage learning

Das K, Nandi S, Chattaraj S, et al (2022) Estimation of subsoil parameters and settlement of foundation for a project in Kolkata based on CPT, DMT. J Phys Conf Ser 2286:012026. https://doi.org/10.1088/1742-6596/2286/1/012026

Davidson JL, Boghrat A (1983) Flat dilatometer testing in Florida, USA

De Beer EE (1965) Bearing capacity and settlement of shallow foundations on sand. In: Proc. Symp. Bearing capacity and settlement of foundations. Duke University, pp 15–34

de Ruiter J (1971) Electric penetrometer for site investigations. Journal of the Soil Mechanics and Foundations Division 97:457–472

Deng J (2022) Probabilistic characterization of soil properties based on the maximum entropy method from fractional moments: Model development, case study, and application. Reliab Eng Syst Saf 219:108218. https://doi.org/10.1016/j.ress.2021.108218

Fabius M (1985) Experience with the Dilatometer in Routine Geotechnical Design. In: Proceedings 38th Canadian Geotechnical Conference, Edmonton. pp 163–169

Fahey M, Carter JP (1993) A finite element study of the pressuremeter test in sand using a nonlinear elastic plastic model. Canadian Geotechnical Journal 30:348–362. https://doi.org/10.1139/t93-029

Failmezger RA, Rom D, Ziegler SB (1999) SPT?—A Better Approach to Site Characterization of Residual Soils Using Other In-Situ Tests. In: Behavioral Characteristics of Residual Soils. ASCE, pp 158–175

(Fear) Wride CE, Robertson PK, Biggar KW, et al (2000) Interpretation of in situ test results from the CANLEX sites. Canadian Geotechnical Journal 37:505–529. https://doi.org/10.1139/t00-044

Feda Aral I, Gunes E (2017) Correlation of Standard and Cone Penetration Tests: Case Study from Tekirdag (Turkey). IOP Conf Ser Mater Sci Eng 245:032028. https://doi.org/10.1088/1757-899X/245/3/032028

Finno RJ (1993) Analytical interpretation of dilatometer penetration through saturated cohesive soils. Geotechnique 43:241–254

Firuzi M, Asghari-Kaljahi E, Akgün H (2019) Correlations of SPT, CPT and pressuremeter test data in alluvial soils. Case study: Tabriz Metro Line 2, Iran. Bulletin of Engineering Geology and the Environment 78:5067–5086. https://doi.org/10.1007/s10064-018-01456-0

Fonseca da VA (2010) Regional Report for Southern Europe. In: 2nd International Symposium on Cone Penetration Testing, CPT10. geoengineer, Huntington Beach, CA, USA

Gabr M, Lunne T, Mokkelbost KH, POWELL JJM (1992) Dilatometer soil parameters for analysis of piles in clay. Publikasjon-Norges Geotekniske Institutt 186:

Gabr MA, Borden RH (1988) Analysis of load deflection response of laterally loaded piers using DMT. In: International Symposium on penetration testing; ISOPT-1. 1. pp 513–520

Gravesen S (1960) Elastic semi-infinite medium bounded by a rigid wall with a circular hole. Laboratoriet for Bygningsteknik

Greenwood PE, Nikulin MS (1996) A Guide to Chi-Squared Testing. Wiley

Greig JW, Campanella RG, Robertson PK (1988) Comparison of field vane results with other in-situ test results. Vane Shear Strength Testing in Soils: Field and Laboratory Studies 247–263

Hamouche KK, Leroueil S, Roy M, Lutenegger AJ (1995) In situ evaluation of K 0 in eastern Canada clays. Canadian Geotechnical Journal 32:677–688

Hasancebi N, Ulusay R (2007) Empirical correlations between shear wave velocity and penetration resistance for ground shaking assessments. Bulletin of Engineering Geology and the Environment 66:203–213. https://doi.org/10.1007/s10064-006-0063-0

Hayes JA (1986) Comparison of flat dilatometer in-situ test results with observed settlement of structures and earthwork. In: Proceedings 39th Geotechnical Conference, Ottawa, Ontario, Canada

Hepton P (1989) Shear wave velocity measurements during penetration testing. In: Penetration testing in the UK: Proceedings of the geotechnology conference organized by the Institution of Civil Engineers and held in Birmingham on 6–8 July 1988. Thomas Telford Publishing, pp 275–278

Hobbs NB, Dixon JG (1969) In-situ testing for bridge foundations in the Devonian Marl

Holtrigter M (2010) A Comparison Between the Flat Dilatometer and the Cone Penetrometer Test with the Aid of Artificial Neural Networks". MASTER OF ENGINEERING, The University of Auckland

Huang A-B, Haefele KC (1990) Lateral Earth Pressure Measurements in a Marine Clay. Transp Res Rec

Hughes JMO, Robertson PK (1985) Full-displacement pressuremeter testing in sand. Canadian Geotechnical Journal 22:298–307

Hughes JMO, Wroth CP, Windle D (1977) Pressuremeter tests in sands. Geotechnique 27:455–477

IS 1892 (1979) IS 1892: Code of Practice for Sub Surface Investigations. Indian Standard (IS 1892)

IS 2131 (2002) Method of standard penetration tests for soils. Indian Standard (IS 2131)

IS 2132 (2002) IS 2132: Code of practice for thin-walled tube sampling of soils. . Indian Standard (IS 2132)

IS 4968 (Part-III) (1976) IS: 4968 (Part-III) Method for Subsurface Sounding for Soils. Static Cone Penetration Test (First Revision). Indian Standard (IS 4968: Part-III)

IS 8009 Part-1 (1985) IS:8009 (Part-1) Indian standard code of practice for calculation of settlements of foundations. shallow foundations subjected to symmetrical static vertical loads. Indian Standards (IS 8009: Part 1)

Iwasaki K, Tsuchiya H, Saka Y (1991) Applicability of the Marchetti dilatometer test to soft ground in Japan

Jamiolkowski M, Ghionna VN, Lancellotta R, Pasqualini E (1988) New correlations of penetration tests for design practice. In: Proc. ISOPT-1,Vol. 1. AA Balkema, Orlando F.L, pp 263–296

Janbu N, Senneset K (1974) Effective stress interpretation of in situ static penetration tests. In: Proceedings of the 1st European symposium on penetration testing. pp 181–194

Jefferies MG, Davies MP (1993) Use of CPTU to estimate equivalent SPT N 60. Geotechnical Testing Journal 16:458–468

Johnston IW (1983) Why in situ testing?

Kalteziotis NA, Pachakis MD, Zervogiannis HS (1991) Applications of the flat dilatometer test (DMT) in cohesive soils. Proc X ECSMFE, Florence 1:125–128

Kamei T, Iwasaki K (1995) Evaluation of undrained shear strength of cohesive soils using a flat dilatometer. Soils and Foundations 35:111–116

Kaplan N, Cakan G, Erol AO (2004) Plastik killerde ödometrik deformasyon modülünün CPT uç direncinden tahmini. Zemin Mekaniği ve Temel Mühendisliği Onuncu Ulusal Kongresi, Istanbul Teknik Üniversitesi, Istanbul

Kara O, Gündüz Z (2010) Correlation between CPT and SPT in Adapazari, Turkey. In: 2nd International Symposium on Cone Penetration Testing, Huntington Beach, CA, USA, CPT 10. CPT 10, Huntington Beach, CA, USA

Karlsrud K, Lunne T, Kort DA, Strandvik S (2005) CPTU correlations for clays. In: Proceedings of the 16th international conference on soil mechanics and geotechnical engineering. IOS Press, pp 693–702

Kates GL (1996) Development and implementation of a seismic flat dilatometer test for small-and high-strain soil properties . (Doctoral dissertation, Directed by Paul W. Mayne, Georgia Institute of Technology .

Kayabasi A (2012) Prediction of pressuremeter modulus and limit pressure of clayey soils by simple and non-linear multiple regression techniques: a case study from Mersin, Turkey. Environ Earth Sci 66:2171–2183. https://doi.org/10.1007/s12665-011-1439-4

Kayabaşı A (2015) Some emprical equations for predicting standard penetration test blow counts in clayey soils: a case study in Mersin, Turkey. Arabian Journal of Geosciences 8:7643–7654. https://doi.org/10.1007/s12517-014-1694-2

Keaveny JM, Mitchell JK (1988) Strength of fine-grained soils using the piezocone. Publikasjon-Norges Geotekniske Institutt 1–9

Kim D-S, Lee SR, Kim SI, et al (1997) Characterization of In-situ Properties of Korean Marine Clays using CPTU and PMT. In: ISSMFE. pp 519–522

Konrad J-M (1988) Interpretation of flat plate dilatometer tests in sands in terms of the state parameter. Geotechnique 38:263–277

Ku T, Mayne PW (2013) Evaluating the In Situ Lateral Stress Coefficient (K0) of Soils via Paired Shear Wave Velocity Modes. Journal of Geotechnical and Geoenvironmental Engineering 139:775–787. https://doi.org/10.1061/(asce)gt.1943-5606.0000756

Kulhawy FH, Mayne PW (1990) Manual on estimating soil properties for foundation design (No. EPRI-EL-6800). Palo Alto, CA (USA)

Lacasse S (1986) In situ site investigation techniques and interpretation for offshore practice. Norwegian Geotechnical Institute, Report 40019 28:

Lacasse S (1988) Calibration of dilatometer correlations. In: Proc. lst International Symposium on Penetration Testing. pp 539–548

Lacasse S, Lunne T (1988) Dilatometer tests in sand. Publikasjon-Norges Geotekniske Institutt 1–8

Ladd CC, Foott R, Ishihara K, Schlosser F (1977) Stress-deformation and strength characteristics.

Lambe TW, Whitman R V (1991) Soil mechanics. John Wiley & Sons

Lanzano G, Luzi L, D'Amico V, et al (2020) Ground motion models for the new seismic hazard model of Italy (MPS19): selection for active shallow crustal regions and subduction zones. Bulletin of Earthquake Engineering 18:3487–3516. https://doi.org/10.1007/s10518-020-00850-y

Lawter Jr RS, Borden RH (1990) Determination of Horizontal Stress in Normally Consolidated Sands by Using the Dilatometer Test: A Calibration Chamber Study. Transp Res Rec

Leonards GA, Frost JD (1988) Settlement of shallow foundations on granular soils. Journal of Geotechnical Engineering 114:791–809

Lukas RG (2013) Pressuremeter Testing in Stiff to Hard Cohesive Soils. In: Seventh International Conference on Case Histories in Geotechnical Engineering. 3. Missouri University of Science and Technology, Missouri

Lunne T (1997) Sample disturbance effects in soft low plastic Norwegian clay. In: Proc. of the Conf. on Recent Developments in Soil and Pavement Mechanics, Rio de Janeiro, 1997. pp 81–102

Lunne T, Christoffersen HP, Tjelta TI (1986) Engineering use of piezocone data in North Sea clays. Publikasjon-Norges Geotekniske Institutt

Lunne T, Lacasse S, Rad NS, Décourt L (1990a) SPT, CPT, pressuremeter testing and recent developments on in situ testing. Publikasjon-Norges Geotekniske Institutt 179:

Lunne T, Powell J, Robertson P (2002a) Cone Penetration Testing in Geotechnical Practice

Lunne T, Powell JJM, Hauge EA, et al (1990b) Correlation of dilatometer readings with lateral stress in clays. Transp Res Rec

Lunne T, Powell JJM, Robertson PK (2002b) Cone Penetration Testing in Geotechnical Practice. CRC Press

Lutenegger AJ (1990a) Current status of the Marchetti dilatometer test. In: International Journal of Rock Mechanics and Mining Sciences and Geomechanics Abstracts. Elsevier Science, pp A90–A91

Lutenegger AJ (1990b) Determination of in situ lateral stresses in a dense glacial till. Transp Res Rec

Lutenegger AJ, Timian DA (1986) Flat plate penetrometer tests in marine clays. In: Proceedings 39 th Canadian Geotechnical Conference, Ottawa. pp 301–309

Marchetti S (2006) Origin of the flat dilatometer. In: The second international flat dilatometer conference. Washington, DC, United States

Marchetti S (1975) A New In Situ Test for the Measurement of Horizontal Soil Deformity. In: In Situ Measurement of Soil Properties. ASCE, pp 255–259

Marchetti S. (1997) The Flat Dilatometer: Design Applications. . In: Proc. Third International Geotechnical Engineering Conference, Keynote lecture, Cairo University, . pp 421–448

Marchetti S (1985) On the field determination of K_0 in sand. Discussion Session No 2A, Proc XI ICSMFE, S Francisco, 1985 5:2667–2673

Marchetti S (1979) The in Situ Determination of an" Extended" Overconsolidation Ratio. Proc 7th ECSMFE, Brighton 2:239–244

Marchetti S (1980) In situ tests by flat dilatometer. Journal of the geotechnical engineering division 106:299–321

Marchetti S (2015) Some 2015 updates to the TC16 DMT report 2001. In: The 3rd International Conference on the Flat Dilatometer. pp 43–65

Marchetti S (2010) Sensitivity of CPT and DMT to stress history and aging in sands for liquefaction assessment. In: Proc., 2nd Int. Symp. on Cone Penetration Testing (CPT'10). Technical Committee TC-16 of the ISSMGE in collaboration with California …, pp 3–50

Marchetti S, Crapps DK (1981) Flat dilatometer manual. GPE incorporated

Marchetti S, Monaco P (2018) Recent Improvements in the Use, Interpretation, and Applications of DMT and SDMT in Practice. Geotechnical Testing Journal 41:837–850

Marchetti S, Monaco P, Calabrese M, Totani G (2006) Comparison of moduli determined by DMT and backfigured from local strain measurements under a 40 m diameter circular test load in the Venice area. In: Proc. 2nd Int. Conf. on the Flat Dilatometer, Washington DC. pp 220–230

Marchetti S, Monaco P, Totani G, Calabrese M (2001) The flat dilatometer test (DMT) in soil investigations–A report by the ISSMGE committee TC16

Marchetti S, Monaco P, Totani G, Marchetti D (2008a) In situ tests by seismic dilatometer (SDMT). In: From research to practice in geotechnical engineering. pp 292–311

Marchetti S, Monaco P, Totani G, Marchetti D (2008b) In Situ Tests by Seismic Dilatometer (SDMT). ASCE Geotechnical Special Publication honoring Dr John H Schmertmann GSP No. 170:

Marchetti S, Totani G (1989) Ch evaluation from DMTA dissipation curves. In: Congrès international de mécanique des sols et des travaux de fondations. 12. pp 281–286

Marchetti S, Totani G, Calabrese M (1993) Internal report, Istituo di Idraulica. L.Aquila, Italy

Marchetti S, Totani G, Calabrese M, Monaco P (1991) Py curves from DMT data for piles driven in clay. In: Proc. 4th Int. Conf. on Piling and Deep Foundations, DFI, Stresa. pp 263–272

Marchetti S, Totani G, Campanella RG, et al (1986) The DMT-σ h c Method for Piles Driven in Clay. In: Use of In Situ Tests in Geotechnical Engineering. ASCE, pp 765–779

Mayne P (2006a) In situ test calibrations for evaluating soil parameters. . In: Characterization and Engineering Properties of Natural Soils II. Singapore

Mayne PW (1987) Determining preconsolidation stress and penetration pore pressures from DMT contact pressures. Geotechnical Testing Journal 10:146–150

Mayne PW (2015) Peak friction angle of undisturbed sands using DMT. In: Proc. 3rd Int. Conf. on the Flat Dilatometer DMT'15

Mayne PW (2007) In-situ test calibrations for evaluating soil parameters. In Characterization & Engineering Properties of Natural Soils . Taylor & Francis Group London 3:1601–1652

Mayne PW (2006b) Interrelationships of DMT and CPT readings in soft clays. Flat Dilatometer Testing 231–236

Mayne PW (2006c) Interrelationships of DMT and CPT readings in soft clays. Flat Dilatometer Testing 231–236

Mayne PW (2006d) Interrelationships of DMT and CPT readings in soft clays. Flat Dilatometer Testing 231–236

Mayne PW (2001) Stress-strain-strength-flow parameters from enhanced in-situ tests. In: Proc. Int. Conf. on In Situ Measurement of Soil Properties and Case Histories, Bali. pp 27–47

Mayne PW (1995) Profiling yield stresses in clays by in situ tests. Transp Res Rec

Mayne PW, Bachus RC (1989) Penetration pore pressures in clay by CPTu, DMT, and SBP. In: Congrès international de mécanique des sols et des travaux de fondations. 12. pp 291–294

Mayne PW, Brown D, Vinson J, et al (2000) Site characterization of Piedmont residual soils at the NGES, Opelika, Alabama. In: National geotechnical experimentation sites. pp 160–185

Mayne PW, Frost DD (1988) Dilatometer experience in Washington, DC, and vicinity. Transp Res Rec

Mayne PW, Kulhawy FH (1990) Direct and indirect determinations of in situ k sub 0 in clays. Transp Res Rec

Mayne PW, Liao T (2004) CPT-DMT interrelationships in piedmont residuum. Geotechnical & Geophysical Site Characterization (Proc ISC'2, Porto-Portugal) 1:345–350

Mayne PW, Martin GK (1998) Commentary on Marchetti flat dilatometer correlations in soils. Geotechnical Testing Journal 21:222–239

Mayne PW, Rix GJ (1995) Correlations Between Shear Wave Velocity and Cone Tip Resistance in Natural Clays. Soils and Foundations 35:107–110. https://doi.org/10.3208/sandf1972.35.2_107

Mayne PW, Schneider JA, Martin GK (1999) Small-and large-strain soil properties from seismic flat dilatometer tests. In: Proc. 2nd Int. Symp. on Pre-Failure Deformation Characteristics of Geomaterials. pp 419–427

Mayne PW, Stewart HE (1988) Pore Pressure Behavior of K o-Consolidated Clays. Journal of Geotechnical Engineering 114:1340–1346

McGillivray A, Mayne PW (2004) Seismic piezocone and seismic flat dilatometer tests at Treporti. In: Proc. 2nd Int. Conf. on Site Characterization, Porto. pp 1695–1700

McNulty G, Harney MD (2010) Comparison of CPT-and DMT-correlated effective friction angle in clayey and silty sands. In: 2nd international symposium on cone penetration testing, CPT'10, California, USA. pp 2–53

Meigh AC (2013) Cone penetration testing: methods and interpretation. Elsevier

Mello Vieira MVC, Danziger FAB, Almeida MSS, Lopes PCC (1999) Dilatometer tests at Sarapuí soft clay site. In: International Conference on Soil Mechanics and FOundation Engineering. pp 161–162

Mesri G (1975) Discussion of "New design procedure for stability of soft clays." Journal of the Geotechnical Engineering Division 101:409–412

Mesri G, Rokhsar A, Bohor BF (1975) Composition and compressibility of typical samples of Mexico City clay. Geotechnique 25:527–554

Meyerhof GG (1974) Penetration testing outside Europe: General report. In: Proceedings of the European Symposium on Penetration Testing. pp 40–48

Młynarek Z, Gogolik S, Marchetti D (2006) Suitability of the SDMT method to assess geotechnical parameters of post-flotation sediments. In: Proc. 2nd Int. Conf. on the Flat Dilatometer, Washington DC. pp 148–153

Młynarek Z, Wierzbicki J, Stefaniak K (2010) CPTU, DMT, SDMT results for organic and fluvial soils. In: Proceedings 2nd International Symposium on Cone Penetration Testing (CPt'10). Omnipress, Huntington Beach, California. pp 455–462

Moghadari Poor M, Azarafza M, Derakhshani R (2023) A correlation based on pressuremeter, SPT and CPT tests for characterizing of coastal alluvium: A study for phase 14 South Pars, Iran. MethodsX 10:101938. https://doi.org/10.1016/j.mex.2022.101938

Mohammadi A, Eslami A (2016) Drained Soil Shear Strength Parameters from CPT and CPTu Data in Coastal Deposits by an Analytical Approach. In: Geo-Chicago 2016. American Society of Civil Engineers, Reston, VA, pp 497–506

Monaco P, Marchetti S (2004) Evaluation of the coefficient of subgrade reaction for design of multipropped diaphragm walls from DMT moduli. Proceedings International Site Characterization 993–1002

Monaco P, Marchetti S (2007) Evaluating liquefaction potential by seismic dilatometer (SDMT) accounting for aging/stress history. In: Proc. 4th Int. Conf. on Earthquake Geotechnical Engineering

Monaco P, Totani G, Calabrese M (2006a) DMT-predicted vs observed settlements: a review of the available experience. In: Proc. 2nd Int. Conf. on the Flat Dilatometer, Washington DC. pp 244–252

Monaco P, Totani G, Calabrese M (2006b) DMT-predicted vs observed settlements: a review of the available experience. In: Proc. 2nd Int. Conf. on the Flat Dilatometer, Washington DC. pp 244–252

Motaghedi H, Eslami A (2013) Determining soil shear strength parameters from CPT and CPTu data. Scientia Iranica 20:1349–1360

Motan ES, Gabr MA (1984) A Flat-Dilatometer Study of Lateral Soil Response. In: Analysis and Design of Pile Foundations. ASCE, pp 232–248

Motan ES, Khan AQ (1988a) In-situ shear modulus of sands by a flat-plate penetrometer: a laboratory study. Geotechnical Testing Journal 11:257–262

Motan ES, Khan AQ (1988b) In-situ shear modulus of sands by a flat-plate penetrometer: a laboratory study. Geotechnical Testing Journal 11:257–262

Nandi S, Bandyopadhyay K, Basu D, Shiuly A (2024) Correlation of Pressuremeter Test Results with SPT N Values and Liquidity Index for Cohesive Soil of Normal Calcutta Deposit. Indian Geotechnical Journal 1–15. https://doi.org/https://doi.org/10.1007/s40098-023-00842-0

Nandi S, Bandyopadhyay K., Halder A., Basu D. (2022) Equivalent CPT Method for estimation of shear strength parameters for a project site in Kolkata using combination of SPT, DMT and CPT- a case study. In: Rahman, Jaksa (eds) Proceedings of the 20th International Conference on Soil Mechanics and Geotechnical Engineering . © 2022 Australian Geomechanics Society, ISBN 978-0-9946261-4-1, Sydney, Australia, , pp 483–487

Narimani S, Chakeri H, Davarpanah SM (2018) Simple and Non-Linear Regression Techniques Used in Sandy-Clayey Soils to Predict the Pressuremeter Modulus and Limit Pressure: A Case Study of Tabriz Subway. Periodica Polytechnica Civil Engineering. https://doi.org/10.3311/PPci.12063

Naseem A, Jamil SM (2016) Development of Correlation Between Standard Penetration Test and Pressuremeter Test for Clayey Sand and Sandy Soil. Soil Mechanics and Foundation Engineering 53:98–102. https://doi.org/10.1007/s11204-016-9371-y

Nash DFT, Powell JJM, Lloyd IM (1992) Initial investigations of the soft clay test site at Bothkennar. Géotechnique 42:163–181

Nayak N V (2001) Foundation design manual for practicing engineers. Dhanpat Rai Publication, New Delhi

Nayak N V (1979) Foundation Design Manual for Practising Engineers and Civil Engineering Students. Dhanpat Rai

Nuno Cruz, Marcelo J. Devincenzi, António Viana da Fonseca (2006) DMT experience in Iberian transported soils. In: proceedings from the Second International Flat Dilatometer Conference. Washington, D.C

Ohya S, Imai T, Matsubara M (2021) Relationships between N-value by SPT and LLT measurement results. In: Penetration Testing, volume 1. Routledge, pp 125–130

Onal FO, Özmen G (2015) Using Combination of SPT, DMT and CPT to Estimate Geotechnical Model for a Special Project in Turkey. In: 3rd International Conference on the Flat Dilatometer

Önal M, Ceylan Ç (2020) Correlations Between SPT, PMT and MASW on Quaternary Alluvial - Fluvial Sediments in Battalgazi, Malatya, Turkey. NATURENGS MTU Journal of Engineering and Natural Sciences, Malatya Turgut Ozal University 1:39–53. https://doi.org/10.46572/nat.2020.15

Özvan A, Akkaya İ, Tapan M (2018) An approach for determining the relationship between the parameters of pressuremeter and SPT in different consistency clays in Eastern Turkey. Bulletin of Engineering Geology and the Environment 77:1145–1154. https://doi.org/10.1007/s10064-017-1020-9

Pagani Geotechnical Equipment (manual) (2014) Original instructions for self-propelled penetrometer TG63-100 TG63-150, Revision: 10. Pagani Geotechnical Equipment, Via Campogrande 29010 – Calendasco (Piacenza) – Italia , Località Santimento, 44, – Italia

Peck RB, Hanson WE, Thornburn TH (1991) Foundation engineering. John Wiley & Sons

Penna A (2006) Some recent experience obtained with DMT in Brazilian soils. In: Proc., 2nd Int. Conf. on the Flat Dilatometer. In-Situ Soil Virginia, pp 170–177

Phoon K-K, Kulhawy FH (1999) Evaluation of geotechnical property variability. Canadian Geotechnical Journal 36:625–639. https://doi.org/10.1139/t99-039

Poenaru A (2016) Correlations between Cone Penetration Test and Seismic Dilatometer Marchetti Test with Common Laboratory Investigations. Energy Procedia 85:399–407. https://doi.org/10.1016/j.egypro.2015.12.219

Powell JJM, Uglow IM (1988) Marchetti dilatometer testing in UK soils. In: International Symposium on penetration testing; ISOPT-1. 1. pp 555–562

Powell JJM, Uglow IM (1989) The interpretation of the Marchetti dilatometer test in UK clays. In: Penetration testing in the UK: Proceedings of the geotechnology conference organized by the Institution of Civil Engineers and held in Birmingham on 6–8 July 1988. Thomas Telford Publishing, pp 269–273

Powell JJM, Uglow IM (1986) Dilatometer testing in stiff overconsolidated clays. In: Proc. 39th Canadian Geotech. Conf., In Situ Testing and Field Behaviour. pp 317–326

Presti LD, Meisina C (2019) CPT Hand Book "Use of cone penetration tests for soil profiling and design of shallow and deep foundations". Pagani Geotechnical Equipment , Località Campogrande- Comune di Calendasco - 29010 Piacenza - Italia , Piacenza

Prof. Marchetti S.r.l. Studio SDMT e lab processing software. In: Marchetti DMT home page (https://www.marchetti-dmt.it/instruments/software/)

Ramaswamy SD, Daulah IU, Hasan Z (2021) Pressuremeter correlations with standard penetration and cone penetration tests. In: Penetration Testing, volume 1. Routledge, pp 137–142

Ramdane B, Nassim A, Ouarda B (2013) Interpretation of a pressuremeter test in cohesive soils. In: Proceedings of the international conference on geotechnical engineering, Tunisia

Ramkrishnan R, Sreevalsa K, Sitharam TG (2022) Strong Motion Data Based Regional Ground Motion Prediction Equations for North East India Based on Non-Linear Regression Models. Journal of Earthquake Engineering 26:2927–2947. https://doi.org/10.1080/13632469.2020.1778586

Redel C, BIECHMAN D, Feferbaum S (1999) Flat dilatometer testing in Israel. In: International Conference on Soil Mechanics and FOundation Engineering. pp 581–584

Rindertsma J, Karreman WJ, Engels SPJ, Gavin KG (2018) CPT based settlement prediction of shallow footings on granular soils. In: Michael A. Hicks, Federico Pisanò, Joek Peuchen (eds) INTERNATIONAL SYMPOSIUM ON CONE PENETRATION TESTING (CPT'18), DELFT, THE NETHERLANDS, ISBN 978-1-138-58449-5. CRC press, Delft University of Technology

Robbins D (2013) Initial Elastic Modulus Degradation Using Pressuremeter and Initial Elastic Modulus Degradation Using Pressuremeter and Standard Penetration Test Results at Two Sites Standard Penetration Test Results at Two Sites. https://doi.org/10.34917/4478297

Robertson PK (1988) Excess pore pressures and the flat dilatometer test. In: Proceedings of the First International Symposium on Penetration Testing, 1988

Robertson PK (1986a) In situ testing and its application to foundation engineering. Canadian Geotechnical Journal 23:573–594. https://doi.org/10.1139/t86-086

Robertson PK (2009) Interpretation of cone penetration tests — a unified approach. Canadian Geotechnical Journal 46:1337–1355. https://doi.org/10.1139/T09-065

Robertson PK (1990) Soil classification using the cone penetration test. Canadian geotechnical journal 27:151–158

Robertson PK (1986b) Use of Piezoeter Cone Data. In: Proc. of Insitu'86, Speciality Conference. ASCE

Robertson PK (2016) Cone penetration test (CPT)-based soil behaviour type (SBT) classification system — an update. Canadian Geotechnical Journal 53:1910–1927. https://doi.org/10.1139/cgj-2016-0044

Robertson PK, Cabal KL (2010) Estimating soil unit weight from CPT . In: 2nd International Symposium on Cone Penetration Testing, Huntington Beach, CA, USA, CPT 10. CPT 10, Huntington Beach, CA, USA

Robertson PK, Cabal KL (2015) Guide to Cone Penetration Testing for Geotechnical Engineering. Signal Hill, CA: Gregg Drilling & Testing

Robertson PK, Campanella RG (1983a) Interpretation of cone penetration tests. Part II: Clay. Canadian Geotechnical Journal 20:734–745. https://doi.org/10.1139/t83-079

Robertson PK, Campanella RG (1983b) Interpretation of cone penetration tests. Part I: Sand. Canadian Geotechnical Journal 20:718–733. https://doi.org/10.1139/t83-078

Robertson PK, (Fear) Wride CE, List BR, et al (2000) The Canadian Liquefaction Experiment: an overview. Canadian Geotechnical Journal 37:499–504. https://doi.org/10.1139/t00-043

Rocscience Inc. (2016) CPT Data Interpretation Theory Manual . Rocscience Inc.

Roque R, JANBU N, SENNESET K (1988) Basic interpretation procedures of flat dilatometer tests. In: International Symposium on penetration testing; ISOPT-1. 1. pp 577–587

Sakleshpur VA, Prezzi M, Salgado R, Zaheer M (2022) CPT-Based Geotechnical Design Manual, Volume 2: CPT-Based Design of Foundations—Methods. West Lafayette, IN

Salgado R (2006) The Engineering of Foundations, 1st edition. McGraw-Hill Education;

Sanglerat G (2012) The penetrometer and soil exploration. Elsevier

Sargand SM, Masada T, Abdalla B (2003) Evaluation of cone penetration test-based settlement prediction methods for shallow foundations on cohesionless soils at highway bridge construction sites. Journal of geotechnical and geoenvironmental engineering 129:900–908

Schmertmann J, Marchetti S (1981) In Situ Test by Flat Dilatometer

Schmertmann JH (1983) Revised Procedure for Calculating Ko and OCR From DMT's With ID> 1.2 and Which Incorporate the Penetration Force Measurement to Permit Calculating the Plane Strain Friction Angle. DMT digest 1:

Schmertmann JH (1986a) Some Developments in Dilatometer Testing and Analysis. In: Proceedings, Innovations in Geotechnical Engineering. Pennsylvania Department of Transportation, Harrisburg, p 14

Schmertmann JH (1988a) Report No. FHWA-PA-024+84-24, Vol. III (of IV) Guidelines for Using the CPT, CPTU, and Marchetti DMT for Geotechnical Design, DMT Test Methods and Data Reduction, prepared by Schmertmann & Crapps. Gainesville, Florida,

Schmertmann JH (1988b) DMT Digest No. 10. GPE, Inc., 28

Schmertmann JH (1989) DMT Digest No. 11. GPE, Inc. 18

Schmertmann JH (1991) DMT Digest No. 12 . GPE, Inc., 4509 NW 23rd Avenue, Suite19, 22

Schmertmann JH (1982) A method for determining the friction angle in sands from the Marchetti dilatometer test (DMT). In: Proc. 2nd European Symp. on Penetration Testing. pp 853–861

Schmertmann JH (1986b) Dilatometer to compute foundation settlement. Use of insitu tests in geotechnical engineering, Geotechnical Special Publication 303–321

Schmertmann JH (1988c) Dilatometers settle in. Civil Engineering 58:68

Schnaid F (2008) In situ testing in geomechanics: the main tests. CRC Press

Sedran G, Failmezger RA, Drevininkas A (2013) Relationship between Menard EM and Young's E moduli for cohesionless soils. In: Proceeding of the 18th

International conference on soil mechanics and geotechnical engineering, Paris 2013

Senneset K, Janbu N, Svanø G (1982) Strength and deformation parameters from cone penetration tests

Senneset K, Sandven R, Janbu N (1989) Evaluation of soil parameters from piezocone tests. Transp Res Rec

Shiuly A (2018) Global attenuation relationship for estimating peak ground acceleration. Journal of the Geological Society of India 92:54–58

Shiuly A, Roy N (2018) A generalized VS–N correlation using various regression analysis and genetic algorithm. Acta Geodaetica et Geophysica 53:479–502. https://doi.org/10.1007/s40328-018-0220-5

Shiuly A, Roy N, Sahu RB (2020) Prediction of peak ground acceleration for Himalayan region using artificial neural network and genetic algorithm. Arabian Journal of Geosciences 13:1–10

Shiuly A, Roy S (2021) Study on Settlement Behaviour of Annular Raft Foundation using Finite Element–Boundary Element Method. Iranian Journal of Science and Technology, Transactions of Civil Engineering 45:1705–1721

Shiuly A, Sahu RB, Mandal S, Roy N (2018) Local Site Effect Due to Past Earthquakes in Kolkata. Journal of the Geological Society of India 91:400–410. https://doi.org/10.1007/s12594-018-0872-3

Singh A (1981) Soil Engineering in theory and Practice . Asia Publishing House (P.) Ltd., New Delhi

Skiles DL, Townsend FC (1994) Predicting Shallow Foundation Settlement in Sands from DMT. In: Vertical and Horizontal Deformations of Foundations and Embankments. ASCE, pp 132–142

Smith MG, Houlsby GT (1995) Interpretation of the Marchetti dilatometer in clay. In: Proc., 11th European Conf. on Soil Mechanics and Foundation Engineering. pp 1–247

Su PC, Chen YC, Sun CY, Wang GS (1993) The Flat Dilatometer Tests in Clay. In: Proceedings, 11th Southeast Asian Geotechnical Conference. pp 205–210

Sundaram R, Gupta S, Gupta S (2023) Advances in the State-of-Practice of Geotechnical Investigation in India. Indian Geotechnical Journal. https://doi.org/10.1007/s40098-023-00750-3

Tanaka H, Tanaka M (1998) Characterization of sandy soils using CPT and DMT. Soils and Foundations 38:55–65

Teh CI, Houlsby GT (1991) An analytical study of the cone penetration test in clay. Geotechnique 41:17–34

Terzaghi K (1943) Theoretical soil mechanics

Terzaghi K, Peck RB, Mesri G (1996) Soil mechanics in engineering practice. John wiley & sons

Tomlinson MJ, Boorman R (2001) Foundation design and construction. Pearson education

Totani G, Calabrese M, Marchetti S, Monaco P (1999) Use of in-situ flat dilatometer (DMT) for ground characterization in the stability analysis of slopes. In:

International Conference on Soil Mechanics and FOundation Engineering. pp 607–610

Totani G, Marchetti S, Monaco P, Calabrese M (2001) Use of the Flat Dilatometer Test (DMT) in geotechnical design. In Situ Measurement of Soil Properties

Üzeler V (2013) Compressibility of clays determined from in-situ tests. M.S. - Master of Science, Middle East Technical University

Vermeiden J (1948) Improved sounding apparatus as developed in Holland since 1936. In: Proc. 2nd Int. Conf. on Soil Mech. and Found. Eng., Rotterdam. pp 280–287

Verruijt A (2021) Penetration Testing, volume 1: Proceedings of the second European symposium on penetration testing, Amsterdam, 24-27 May 1982. Routledge

Winter E (1986) The pressuremeter in geotechnical practice. Transp Res Rec 1089:11

Wong JTF, Wong MF, Kassim K (1993) Comparison between dilatometer and other in situ and laboratory tests in Malaysian alluvial clay. In: Proceedings of the 11th Southeast Asian Geotechnical Conference, Singapore. pp 275–279

Yagiz S, Akyol E, Sen G (2008) Relationship between the standard penetration test and the pressuremeter test on sandy silty clays: a case study from Denizli. Bulletin of Engineering Geology and the Environment 67:405–410. https://doi.org/10.1007/s10064-008-0153-2

Yildiz Ö (2021) CORRELATION BETWEEN SPT AND PMT RESULTS FOR SANDY AND CLAYEY SOILS. Eskişehir Technical University Journal of Science and Technology A - Applied Sciences and Engineering 22:175–188. https://doi.org/10.18038/estubtda.896491

Yu H-S (2004) James K. Mitchell Lecture. In situ soil testing: from mechanics to interpretation. Geotechnical & Geophysical Site Characterization 1:3–38

Yu HS, Carter JP, Booker JR (1992) Analysis of the dilatometer test in undrained clay. In: Predictive soil mechanics: Proceedings of the Wroth Memorial Symposium held at St Catherine's College, Oxford, 27-29 July 1992. Thomas Telford Publishing, pp 783–795

APPENDIX

APPENDIX A

Table: Appendix A: 1 DMT Comparison: Comparison of DMT tests parameters with conventional Borehole

Site identification	Samples Depth	Undrained cohesion (C_u) from laboratory Test	Depth wise undrained (C_u) cohesion from DMT	Natural Moisture Content (w_n)	Liquid Limit (W_L)	Plastic Limit (W_P)	Plasticity Index (PI)	Bulk density (γ_t) (Undisturbed soil)	Average Bulk density (γ_t) predicted from DMT	Average M_{DMT}	Average E_D	Observed (field) SPT N value	I_D
	(m)	(kPa)	(kPa)	(%)	(%)	(%)	(%)	(gm/cc)	(gm/cc)	(MPa)	kg/cm^2		
Site-1_HC	5.00	42.0	40.6	31.7	47.0	22.0	25.0	1.850	1.570	6.75	25.69	4	0.29
Site-1_HC	5.50	36.0	27.7	29.4	38.0	24.0	14.0	1.860	1.668	10.27	65.70	2	0.90
Site-1_HC	5.50	36.0	41.0	29.4	38.0	24.0	14.0	1.860	1.668	11.63	60.11	2	0.60
Site-1_HC	6.00	32.0	43.6	30.2	42.0	22.0	20.0	1.840	1.668	9.95	52.56	3	0.49
Site-1_HC	9.00	20.0	44.3	48.2	64.0	27.0	37.0	1.500	1.668	5.85	35.14	4	0.31
Site-1_HC	9.00	20.0	46.8	48.2	64.0	27.0	37.0	1.500	1.668	4.12	24.16	4	0.20
Site-1_HC	9.50	20.0	49.0	50.2	63.0	25.0	38.0	1.650	1.668	4.06	23.22	3	0.19
Site-2_PB	2.00	32.0	14.1	29.8	46.0	20.0	26.0	1.870	1.570	5.71	43.34	3	1.09
Site-2_PB	5.50	36.0	32.5	29.4	38.0	24.0	14.0	1.860	1.619	7.73	40.94	2	0.52
Site-2_PB	5.50	36.0	26.5	29.4	38.0	24.0	14.0	1.860	1.668	7.26	59.11	2	0.73

Site identification	Samples Depth	Undrained cohesion (C_u) from laboratory Test	Depth wise undrained (C_u) cohesion from DMT	Natural Moisture Content (w_n)	Liquid Limit (W_L)	Plastic Limit (W_P)	Plasticity Index (PI)	Bulk density (γ_t) (Undisturbed soil)	Average Bulk density (γ_t) predicted from DMT	Average M_{DMT}	Average E_D	Observed (field) SPT N value	I_D
	(m)	(kPa)	(kPa)	(%)	(%)	(%)	(%)	(gm/cc)	(gm/cc)	(MPa)	kg/cm^2		
Site-2_PB	6.00	32.0	31.6	30.2	42.0	22.0	20.0	1.840	1.668	12.56	85.27	3	0.98
Site-2_PB	9.00	20.0	40.4	48.2	64.0	27.0	37.0	1.500	1.668	4.31	24.50	4	0.24
Site-2_PB	15.00	60.0	63.9	29.5	55.0	21.0	34.0	1.880	1.766	18.62	107.07	10	0.66
Site-3_RJ	1.00	33.0	26.5	26.2	46.8	20.2	26.6	1.870	1.570	4.67	19.91	6	0.34
Site-3_RJ	2.00	28.0	35.8	26.3	41.8	20.7	21.1	1.840	1.667	17.38	60.22	5	0.89
Site-3_RJ	4.00	16.0	24.7	44.3	53.8	25.7	28.1	1.700	1.521	1.81	12.91	3	0.19
Site-3_RJ	5.00	18.0	28.8	43.6	50.9	26.8	24.1	1.710	1.570	6.75	39.78	4	0.52
Site-3_RJ	7.00	15.0	27.3	53.7	64.5	28.6	35.9	1.610	1.422	0.81	6.23	4	0.08
Site-3_RJ	8.00	17.0	29.9	44.6	52.7	28.1	24.6	1.710	1.602	5.11	38.42	4	0.46
Site-3_RJ	10.00	20.0	25.8	38.8	51.6	25.5	26.1	1.740	1.373	0.41	3.64	5	0.05
Site-3_RJ	11.00	13.0	25.5	129.5	57.3	31.6	25.7	1.330	1.602	10.41	69.41	7	0.65
Site-3_RJ	13.00	62.0	71.9	26.4	58.1	20.7	37.4	1.950	1.766	15.54	89.05	12	0.48
Site-3_RJ	14.00	51.0	88.5	28.3	52.3	20.1	32.2	1.912	1.815	24.41	124.78	11	0.57
Site-3_RJ	16.00	59.0	103.4	26.3	41.3	22.4	18.9	1.950	1.815	20.87	109.14	12	0.43
Site-4_HA	3.00	23.0	30.8	32.3	43.7	20.9	22.8	1.852	1.540	3.51	15.97	4	0.30
Site-4_HA	6.00	23.0	89.2	31.2	40.9	20.1	20.8	1.864	1.570	23.20	24.93	2	0.40
Site-4_HA	11.00	20.0	49.3	39.9	53.3	25.5	27.8	1.750	1.670	16.25	65.36	4	0.90
Site-5_DH	1.00	20.0	23.5	40.5	58.0	20.9	37.1	1.752	1.570	7.90	30.07	3	0.63
Site-5_DH	4.00	10.0	15.6	37.7	42.9	22.0	20.9	1.736	1.504	2.47	17.62	2	0.40
Site-5_DH	4.00	10.0	13.8	54.6	62.9	24.4	38.5	1.615	1.472	1.07	8.07	2	0.22

Site identification	Samples Depth	Undrained cohesion (C_u) from laboratory Test	Depth wise undrained (C_u) cohesion from DMT	Natural Moisture Content (w_n)	Liquid Limit (W_L)	Plastic Limit (W_P)	Plasticity Index (PI)	Bulk density (γ_t) (Undisturbed soil)	Average Bulk density (γ_t) predicted from DMT	Average M_{DMT}	Average E_D	Observed (field) SPT N value	I_D
	(m)	(kPa)	(kPa)	(%)	(%)	(%)	(%)	(gm/cc)	(gm/cc)	(MPa)	kg/cm^2		
Site-5_DH	4.00	10.0	18.5	54.6	62.9	24.4	38.5	1.615	1.570	2.59	15.52	2	0.33
Site-5_DH	4.00	11.0	13.4	48.5	60.8	23.6	37.2	1.672	1.570	3.07	21.04	2	0.58
Site-5_DH	7.00	-	20.1	35.7	42.2	19.6	22.6	1.755	1.602	4.99	42.70	3	0.74
Site-5_DH	7.00	10.0	16.0	47.1	57.0	22.9	34.1	1.700	1.537	1.69	13.62	2	0.30
Site-5_DH	7.00	10.0	22.6	47.1	57.0	22.9	34.1	1.700	1.602	6.78	49.14	2	0.80
Site-5_DH	10.00	17.0	18.9	47.8	66.4	24.2	42.2	1.697	1.570	2.13	23.45	3	0.41
Site-5_DH	10.00	12.0	42.7	56.4	68.1	27.2	40.9	1.598	1.668	4.26	24.63	2	0.23
Site-5_DH	10.00	56.0	15.5	24.0	40.6	19.5	21.1	1.944	1.504	1.05	10.93	-	0.23
Site-5_DH	10.00	56.0	74.8	24.0	40.6	19.5	21.1	1.944	1.766	21.63	100.81	-	0.59
Site-5_DH	13.00	14.0	45.0	48.3	61.2	22.8	38.4	1.652	1.668	5.28	33.52	2	0.28
Site-5_DH	13.00	70.0	29.3	24.5	43.0	18.6	24.4	1.945	1.668	9.05	79.27	14	0.92
Site-6_SN	1.50	33.0	22.3	28.0	47.0	21.0	26.0	1.900	1.570	8.37	44.62	7	0.82
Site-6_SN	1.50	34.0	42.1	28.0	48.0	21.0	27.0	1.900	1.700	20.87	78.64	6	0.91
Site-6_SN	2.50	34.0	16.3	29.0	48.0	21.0	27.0	1.890	1.570	2.49	18.53	7	0.40
Site-6_SN	2.50	35.0	11.6	28.0	48.0	21.0	27.0	1.900	1.570	3.30	29.92	5	0.87
Site-6_SN	2.50	34.0	26.0	28.0	47.0	21.0	26.0	1.900	1.570	6.06	25.25	5	0.39
Site-7_LK	2.50	33.1	31.3	30.7	62.0	23.0	39.0	1.848	1.635	7.89	43.42	6	0.58
Site-7_LK	2.50	25.1	41.4	35.6	70.0	25.0	45.0	1.731	1.668	15.63	65.07	4	0.74
Site-7_LK	2.50	25.1	39.3	35.7	72.0	26.0	46.0	1.731	1.668	18.14	79.78	3	0.92
Site-7_LK	5.50	26.1	23.3	36.5	76.0	25.0	51.0	1.779	1.373	0.64	4.23	3	0.07

Site identification	Samples Depth	Undrained cohesion (C_u) from laboratory Test	Depth wise undrained (C_u) cohesion from DMT	Natural Moisture Content (w_n)	Liquid Limit (W_L)	Plastic Limit (W_P)	Plasticity Index (PI)	Bulk density (γ_t) (Undisturbed soil)	Average Bulk density (γ_t) predicted from DMT	Average M_{DMT}	Average E_D	Observed (field) SPT N value	I_D
	(m)	(kPa)	(kPa)	(%)	(%)	(%)	(%)	(gm/cc)	(gm/cc)	(MPa)	kg/cm^2		
Site-7_LK	5.50	24.3	18.8	36.5	65.0	25.0	40.0	1.748	1.570	4.86	37.49	4	0.70
Site-7_LK	5.50	24.5	27.4	36.6	67.0	24.0	43.0	1.747	1.635	9.73	61.33	3	0.85
Site-7_LK	7.50	20.1	39.0	37.4	75.0	26.0	49.0	1.753	1.668	7.84	48.37	2	0.47
Site-7_LK	8.50	65.1	26.3	28.3	44.0	22.0	22.0	1.876	1.373	0.95	24.05	11	0.09
Site-8_BD	1.00	33.0	39.3	31.0	62.0	24.0	38.0	1.820	1.635	14.96	54.62	7	0.71
Site-8_BD	1.50	36.0	33.7	29.0	60.0	23.0	37.0	1.850	1.570	5.13	21.32	8	0.29
Site-8_BD	1.50	34.0	52.2	30.0	59.0	22.0	37.0	1.840	1.700	15.18	49.65	5	0.48
Site-8_BD	2.50	35.0	99.9	28.0	56.5	22.0	34.5	1.860	1.635	6.81	33.54	5	0.36
Site-8_BD	2.50	35.0	51.8	28.0	55.0	21.0	34.0	1.850	1.700	15.85	68.87	6	0.60
Site-8_BD	2.50	37.0	59.4	28.0	59.0	23.0	36.0	1.870	1.700	15.44	66.03	6	0.51
Site-8_BD	4.00	54.0	106.2	24.0	39.0	20.0	19.0	1.950	1.815	31.19	126.14	9	0.56
Site-8_BD	4.00	44.0	73.1	25.0	54.0	21.0	33.0	1.910	1.766	29.01	136.25	8	0.82
Site-8_BD	4.00	41.0	81.2	27.0	52.0	21.0	31.0	1.880	1.766	26.66	123.51	9	0.68
Site-8_BD	4.50	50.0	108.3	24.0	41.0	19.0	22.0	1.950	1.799	32.73	134.60	12	0.58
Site-8_BD	4.50	56.0	81.4	24.0	41.0	20.0	21.0	1.930	1.766	25.65	117.48	11	0.63
Site-8_BD	5.00	63.0	177.3	23.0	38.0	18.0	20.0	1.960	1.815	33.96	149.08	10	0.70
Site-8_BD	6.00	103.0	107.9	21.0	40.0	20.0	20.0	1.980	1.876	72.31	310.34	21	1.26
Site-8_BD	7.5 and 8.5	-	-	-	33.0	17.0	16.0	-	1.913	101.99	455.40	23	1.72

APPENDIX B

Table: Appendix B: 1: CPT Comparison: Comparison of CPT tests parameters with conventional Borehole

Site identification	Samples Depth	Undrained cohesion (C_u) from laboratory Test	Depth wise undrained cohesion (C_u) from CPT	Natural Moisture Content (w_n)	Liquid Limit (W_L)	Plastic Limit (W_P)	Plasticity Index (PI)	Bulk density (γ_t) (Undisturbed soil)	Average Bulk density (γ_t) predicted from CPT	M_{CPT}	Average f_s	Average q_c	Observed (field) SPT N value	Ic
	(m)	(kPa)	(kPa)	(%)	(%)	(%)	(%)	(gm/cc)	(gm/cc)	(MPa)	kg/cm^2	kg/cm^2		
Site-1_HC	5.0	42.0	36.4	31.67	47.0	22.0	25.0	1.850	1.815	4.20	0.80	5.40	4	3.0
Site-1_HC	5.5	36.0	101.8	29.39	38.0	24.0	14.0	1.860	1.870	11.75	0.97	14.83	2	2.8
Site-1_HC	5.5	36.0	38.0	29.39	38.0	24.0	14.0	1.860	1.798	4.39	0.69	5.83	2	3.2
Site-1_HC	6.0	32.0	70.3	30.15	42.0	22.0	20.0	1.840	1.829	8.12	0.81	10.54	3	3.0
Site-1_HC	9.0	20.0	50.2	48.20	64.0	27.0	37.0	1.500	1.751	5.79	0.40	8.24	4	3.1
Site-1_HC	9.0	20.0	77.1	48.20	64.0	27.0	37.0	1.500	1.833	8.90	0.71	12.28	4	3.2
Site-1_HC	9.5	20.0	57.6	50.24	63.0	25.0	38.0	1.650	1.753	6.65	0.40	9.71	3	3.4
Site-2_PB	4.0	16.0	31.3	44.30	53.8	25.7	28.1	1.700	1.665	3.62	0.30	5.05	3	3.3
Site-2_PB	5.0	18.0	42.1	43.60	50.9	26.8	24.1	1.710	1.672	4.86	0.29	6.73	4	3.2
Site-2_PB	5.5	36.0	68.3	29.39	38.0	24.0	14.0	1.860	1.757	7.89	0.40	10.49	2	3.0
Site-2_PB	5.5	36.0	99.2	29.39	38.0	24.0	14.0	1.860	1.887	11.46	1.11	14.83	2	3.1
Site-2_PB	7.0	15.0	25.1	53.70	64.5	28.6	35.9	1.610	1.584	2.90	0.15	4.67	4	3.4
Site-2_PB	8.0	17.0	39.1	44.60	52.7	28.1	24.6	1.710	1.672	4.51	0.29	6.81	4	3.3
Site-2_PB	9.0	20.0	40.6	48.20	64.0	27.0	37.0	1.500	1.725	4.69	0.33	7.24	4	3.4
Site-2_PB	9.0	20.0	44.0	48.20	64.0	27.0	37.0	1.500	1.727	5.08	0.33	7.74	4	3.3

Site identification	Samples Depth	Undrained cohesion (C_u) from laboratory Test	Depth wise undrained cohesion (C_u) from CPT	Natural Moisture Content (w_n)	Liquid Limit (W_L)	Plastic Limit (W_P)	Plasticity Index (PI)	Bulk density (γ_t) (Undisturbed soil)	Average Bulk density (γ_t) predicted from CPT	M_{CPT}	Average f_s	Average q_c	Observed (field) SPT N value	Ic
	(m)	(kPa)	(kPa)	(%)	(%)	(%)	(%)	(gm/cc)	(gm/cc)	(MPa)	kg/cm^2	kg/cm^2		
Site-2_PB	10.0	20.0	69.6	38.80	51.6	25.5	26.1	1.740	1.642	1.90	0.27	3.94	5	3.9
Site-3_RJ	1.0	33.0	79.1	26.20	46.8	20.2	26.6	1.870	1.850	9.13	1.13	11.28	6	2.82
Site-3_RJ	2.0	28.0	93.1	26.30	41.8	20.7	21.1	1.840	1.769	10.76	0.53	13.41	5	2.7
Site-3_RJ	11.0	13.0	38.4	129.50	57.3	31.6	25.7	1.330	1.719	4.44	0.42	7.23	7	3.5
Site-3_RJ	13.0	62.0	166.6	26.40	58.1	20.7	37.4	1.950	1.915	19.24	1.53	25.50	12	3.0
Site-3_RJ	14.0	51.0	144.6	28.30	52.3	20.1	32.2	1.912	1.856	16.70	0.95	22.64	11	3.0
Site-3_RJ	16.0	59.0	289.3	26.30	41.3	22.4	18.9	1.950	1.931	33.41	1.49	43.24	12	2.7
Site-3_RJ	16.0	-	201.0	-	37.3	20.6	16.7	-	1.906	23.22	1.34	30.91	18	2.9
Site-4_HA	1.5	32.0	78.3	30.20	43.8	22.1	21.7	1.882	1.853	9.05	0.87	11.28	6	2.7
Site-4_HA	3.0	34.0	45.0	30.80	36.6	20.2	16.4	1.875	1.740	5.19	0.63	6.84	6	2.9
Site-4_HA	3.0	23.0	30.8	32.30	43.7	20.9	22.8	1.852	1.682	3.56	0.27	4.84	4	3.0
Site-4_HA	4.5	22.0	48.7	35.80	43.9	23.6	20.3	1.809	1.796	5.63	0.72	7.69	3	3.1
Site-4_HA	6.0	21.0	77.2	37.60	51.0	22.7	28.3	1.785	1.882	8.92	1.99	11.92	3	3.1
Site-4_HA	6.0	23.0	117.9	31.20	40.9	20.1	20.8	1.864	1.999	13.61	2.77	17.63	2	3.2
Site-4_HA	9.0	22.0	404.6	36.70	52.2	20.5	31.7	1.801	2.014	46.73	1.98	58.33	5	2.4
Site-4_HA	11.0	20.0	49.3	39.90	53.3	25.5	27.8	1.750	1.781	5.69	0.59	8.94	4	3.4
Site-4_HA	14.0	18.0	36.6	45.60	55.5	25.4	30.1	1.705	1.754	4.23	0.42	7.68	3	3.5
Site-4_HA	15.0	17.0	33.8	52.00	72.9	28.7	44.2	1.642	1.680	3.90	0.22	7.49	3	3.5
Site-4_HA	15.0	17.0	57.5	47.60	62.8	26.8	36.0	1.670	1.788	6.64	0.59	10.82	3	3.4
Site-4_HA	18.0	76.0	44.9	26.20	44.8	20.8	24.0	1.952	1.734	5.18	0.34	9.57	24	3.5

Site identification	Samples Depth	Undrained cohesion (C_u) from laboratory Test	Depth wise undrained cohesion (C_u) from CPT	Natural Moisture Content (w_n)	Liquid Limit (W_L)	Plastic Limit (W_P)	Plasticity Index (PI)	Bulk density (γ_t) (Undisturbed soil)	Average Bulk density (γ_t) predicted from CPT	M_{CPT}	Average f_s	Average q_c	Observed (field) SPT N value	Ic
	(m)	(kPa)	(kPa)	(%)	(%)	(%)	(%)	(gm/cc)	(gm/cc)	(MPa)	kg/cm^2	kg/cm^2		
Site-4_HA	18.0	60.0	87.6	26.70	43.1	21.4	21.7	1.943	1.845	10.12	0.74	15.57	30	3.3
Site-5_DH	1.0	20.0	17.3	40.50	58.0	20.9	37.1	1.752	1.629	2.00	0.29	2.52	3	2.9
Site-5_DH	4.0	10.0	18.3	37.70	42.9	22.0	20.9	1.736	1.605	2.11	0.21	3.26	2	3.5
Site-5_DH	4.0	10.0	27.5	54.60	62.9	24.4	38.5	1.615	1.605	2.75	0.20	3.93	2	3.1
Site-5_DH	4.0	11.0	33.1	48.50	60.8	23.6	37.2	1.672	1.683	3.83	0.38	5.26	2	3.2
Site-5_DH	7.0	-	132.0	35.70	42.2	19.6	22.6	1.755	1.792	15.24	0.90	19.68	3	2.7
Site-5_DH	7.0	10.0	23.4	47.10	57.0	22.9	34.1	1.700	1.635	2.70	0.24	4.34	2	3.3
Site-5_DH	10.0	17.0	92.9	47.80	66.4	24.2	42.2	1.697	1.847	10.73	1.38	14.75	3	3.3
Site-5_DH	10.0	12.0	19.5	56.40	68.1	27.2	40.9	1.598	1.688	2.25	0.46	4.42	2	3.8
Site-5_DH	10.0	56.0	49.0	24.00	40.6	19.5	21.1	1.944	1.616	5.66	0.24	8.42	-	3.0
Site-6_SN	1.5	33.0	40.4	28.00	47.0	21.0	26.0	1.900	1.738	4.67	0.53	5.94	7	3.1
Site-6_SN	1.5	34.0	109.7	28.00	48.0	21.0	27.0	1.900	1.843	12.67	1.07	15.61	6	2.6
Site-6_SN	2.5	34.0	32.7	29.00	48.0	21.0	27.0	1.890	1.748	3.78	0.75	5.08	7	3.4
Site-6_SN	2.5	35.0	207.0	28.00	48.0	21.0	27.0	1.900	1.893	23.91	0.91	26.75	5	2.5
Site-6_SN	2.5	34.0	87.9	28.00	47.0	21.0	26.0	1.900	1.792	10.16	0.69	12.75	5	2.8
Site-7_LK	2.5	33.1	57.1	30.70	62.0	23.0	39.0	1.850	1.787	6.60	0.73	8.41	6	3.1
Site-7_LK	2.5	25.1	86.6	35.60	70.0	25.0	45.0	1.730	1.830	10.01	0.93	12.41	4	2.8
Site-7_LK	2.5	25.1	76.0	35.65	72.0	26.0	46.0	1.731	1.884	8.78	1.61	11.08	3	3.2
Site-7_LK	5.5	26.1	61.1	36.54	76.0	25.0	51.0	1.779	1.734	7.05	0.44	9.49	3	3.0
Site-7_LK	5.5	24.3	92.4	36.52	65.0	25.0	40.0	1.748	1.876	10.67	1.33	13.83	4	3.1

Site identification	Samples Depth	Undrained cohesion (C_u) from laboratory Test	Depth wise undrained cohesion (C_u) from CPT	Natural Moisture Content (w_n)	Liquid Limit (W_L)	Plastic Limit (W_P)	Plasticity Index (PI)	Bulk density (γ_t) (Undisturbed soil)	Average Bulk density (γ_t) predicted from CPT	M_{CPT}	Average f_s	Average q_c	Observed (field) SPT N value	Ic
	(m)	(kPa)	(kPa)	(%)	(%)	(%)	(%)	(gm/cc)	(gm/cc)	(MPa)	kg/cm^2	kg/cm^2		
Site-7_LK	5.5	24.5	53.8	36.57	67.0	24.0	43.0	1.747	1.702	6.22	0.36	8.49	3	3.1
Site-7_LK	7.5	20.1	48.5	37.36	75.0	26.0	49.0	1.753	1.856	5.60	1.37	8.10	2	3.6
Site-7_LK	8.5	65.1	162.4	28.32	44.0	22.0	22.0	1.876	1.904	18.76	1.48	24.24	11	2.9
Site-7_LK	8.5	70.2	305.5	25.68	45.0	21.0	24.0	1.860	2.139	35.28	8.93	44.24	15	3.1
Site-7_LK	8.5	70.3	461.5	25.65	46.0	22.0	24.0	1.862	2.100	53.30	5.53	66.24	12	2.7
Site-8_BD	1.0	33.0	47.7	31.00	62.0	24.0	38.0	1.820	1.667	5.51	0.31	6.85	7	2.7
Site-8_BD	2.5	35.0	99.9	28.00	56.5	22.0	34.5	1.860	1.868	8.20	1.25	14.41	5	2.9
Site-8_BD	4.0	41.0	158.6	27.00	52.0	21.0	31.0	1.880	1.911	18.32	1.68	22.93	9	2.9
Site-8_BD	5.0	63.0	177.3	23.00	38.0	18.0	20.0	1.960	1.958	5.63	2.55	25.83	10	3.0
Site-8_BD	6.0	103.0	433.8	21.00	40.0	20.0	20.0	1.980	2.204	50.10	14.42	61.87	21	3.1

APPENDIX C

Table: Appendix C: 1:PMT Comparison: Comparison of PMT tests parameters with conventional Borehole

Site Identification	Sample Depth	Natural Moisture Content (w_n)	Bulk density (γ_t) (Undisturbed soil)	Dry Density (γ_d)	Liquid Limit (W_L)	Plastic Limit (W_P)	Plasticity Index (PI)	Undrained cohesion (C_u) from laboratory Test	Liquidity Index (I_L)	Limit Pressure (P_L)	Presssuremeter Modulus (E_{PMT})	Observed (field) SPT N value
	(m)	(%)	(gm/cc)	(gm/cc)	(%)	(%)	(%)	(kPa)		kg/cm^2	kg/cm^2	
Site-9_VT	1.50	32.40	1.802	1.361	45.8	18.8	27.0	21.0	0.50	2.0	21.0	3
Site-9_VT	2.00	28.40	1.868	1.455	37.7	20.4	17.3	31.0	0.46	0.7	3.8	3
Site-9_VT	2.50	28.40	1.868	1.455	46.8	21.5	25.3	33.0	0.27	2.0	19.8	6
Site-9_VT	3.50	27.90	1.879	1.469	45.9	18.7	27.2	36.0	0.34	3.2	20.0	6
Site-9_VT	4.00	29.20	1.862	1.441	47.6	22.5	25.1	30.0	0.27	3.2	31.4	5
Site-9_VT	6.50	30.40	1.848	1.417	47.3	19.1	28.2	28.0	0.40	3.8	26.5	6
Site-9_VT	7.00	28.80	1.860	1.444	38.1	20.3	17.8	29.0	0.48	4.5	33.6	6
Site-9_VT	7.50	28.80	1.862	1.446	38.8	20.8	18.0	28.0	0.44	4.5	48.8	6
Site-9_VT	8.50	24.50	1.921	1.543	30.3	22.9	7.4	36.0	0.22	6.2	80.7	9
Site-9_VT	9.00	26.20	1.898	1.504	35.2	22.9	12.3	38.0	0.27	4.9	42.0	9
Site-9_VT	11.50	24.60	1.951	1.566	32.9	21.7	11.2	67.0	0.26	10.3	73.2	17
Site-9_VT	12.50	-	-	-	29.5	20.3	9.2	-	-	8.8	64.2	10
Site-10_PT	1.50	28.10	1.854	1.447	41.2	20.2	21.0	28.0	0.38	1.4	9.8	5
Site-10_PT	2.50	32.10	1.801	1.363	36.6	19.3	17.3	16.0	0.74	1.6	6.8	3
Site-10_PT	3.50	28.30	1.852	1.443	42.7	18.9	23.8	25.0	0.39	2.8	24.2	5
Site-10_PT	3.50	32.20	1.830	1.384	53.4	21.6	31.8	23.0	0.33	1.4	6.8	4
Site-10_PT	6.50	30.60	1.835	1.405	40.8	20.3	20.5	20.0	0.50	2.3	12.4	4
Site-10_PT	8.50	-	-	-	32.3	21.5	10.8	-	-	3.3	35.4	6

Site Identification	Sample Depth	Natural Moisture Content (w_n)	Bulk density (γ_t) (Undisturbed soil)	Dry Density (γ_d)	Liquid Limit (W_L)	Plastic Limit (W_P)	Plasticity Index (PI)	Undrained cohesion (C_u) from laboratory Test	Liquidity Index (I_L)	Limit Pressure (P_L)	Presssuremeter Modulus (E_{PMT})	Observed (field) SPT N value
	(m)	(%)	(gm/cc)	(gm/cc)	(%)	(%)	(%)	(kPa)		kg/cm^2	kg/cm^2	
Site-10_PT	8.50	68.70	1.497	0.887	90.1	43.3	46.8	15.0	0.54	3.5	28.6	6
Site-10_PT	11.50	86.00	1.427	0.767	115.8	56.5	59.3	17.0	0.50	2.8	24.0	4
Site-10_PT	12.50	-	-	-	130.0	66.0	64.0	-	-	5.3	42.6	4
Site-10_PT	13.50	51.60	1.670	1.102	78.7	35.1	43.6	21.0	0.38	5.5	37.0	5
Site-10_PT	13.50	64.00	1.563	0.953	97.4	47.5	49.9	19.0	0.33	4.7	31.6	8
Site-10_PT	16.50	27.10	1.928	1.517	55.7	18.0	37.7	51.0	0.24	6.3	36.0	9
Site-10_PT	17.50	26.10	1.965	1.558	53.6	18.6	35.0	79.0	0.21	8.7	95.4	18
Site-10_PT	18.50	27.50	1.918	1.504	59.3	18.1	41.2	52.0	0.23	6.6	57.7	10
Site-10_PT	18.50	25.20	1.927	1.539	42.8	19.6	23.2	50.0	0.24	8.2	65.1	12
Site-11_ES	1.50	25.90	1.870	1.485	44.2	18.9	25.3	30.0	0.28	1.4	12.2	7
Site-11_ES	2.00	30.10	1.826	1.404	53.1	21.6	31.5	20.0	0.27	2.6	19.1	4
Site-11_ES	4.00	28.00	1.861	1.454	33.5	23.0	10.5	26.0	0.48	1.3	9.9	5
Site-11_ES	6.50	56.00	1.619	1.038	73.4	43.1	30.3	20.0	0.42	2.5	19.9	5
Site-11_ES	7.00	64.00	1.567	0.955	99.3	44.3	55.0	17.0	0.36	3.8	27.2	5
Site-11_ES	9.00	36.80	1.785	1.305	50.2	25.7	24.5	27.0	0.45	3.2	18.5	6
Site-11_ES	11.50	40.80	1.740	1.236	52.4	26.8	25.6	23.0	0.55	2.9	18.9	5
Site-11_ES	12.50	43.20	1.682	1.175	57.8	25.9	31.9	20.0	0.54	5.8	46.0	5
Site-11_ES	14.00	40.00	1.749	1.249	52.1	26.8	25.3	25.0	0.52	6.6	58.1	5
Site-11_ES	16.50	26.90	1.938	1.527	64.1	20.8	43.3	65.0	0.14	7.9	74.0	13
Site-11_ES	17.50	25.60	1.962	1.562	51.0	18.4	32.6	73.0	0.22	6.9	53.9	9
Site-11_ES	19.00	26.10	1.951	1.547	60.8	18.6	42.2	65.0	0.18	7.7	90.9	18

APPENDIX D

SAMPLE CALCULATION FOR THE PREDICTION OF SETTLEMENT

SITE-1 (HC)

2.13m X 21.3 m Strip footing (depth of foundation 1.9 m, design load 200 kPa)

LOCATION CPT1_HC, DMT1_HC, BH2_HC

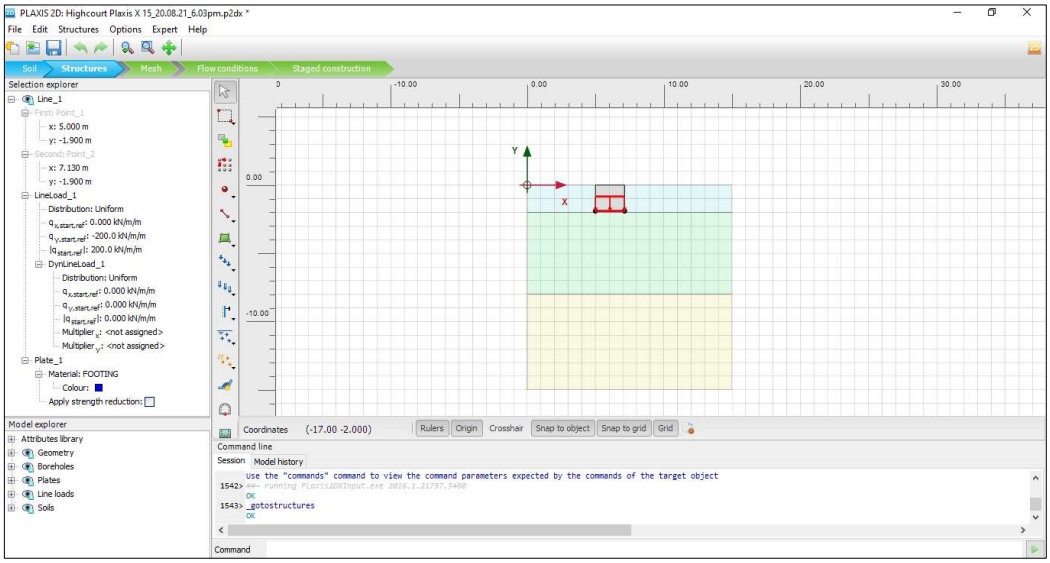

Figure: Appendix-D: 1 : Input parameters in Plaxis 2D for modelling based on conventional Borehole

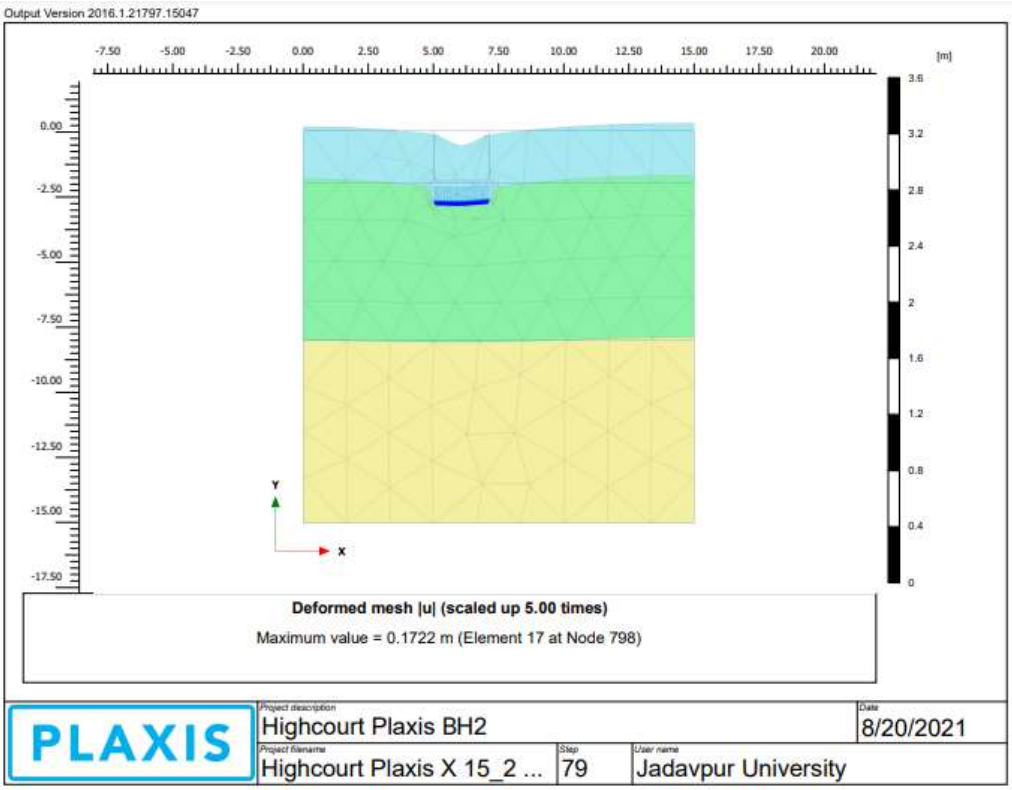

Figure: Appendix-D: 2 : Output in Plaxis 2D for modelling based on conventional Borehole

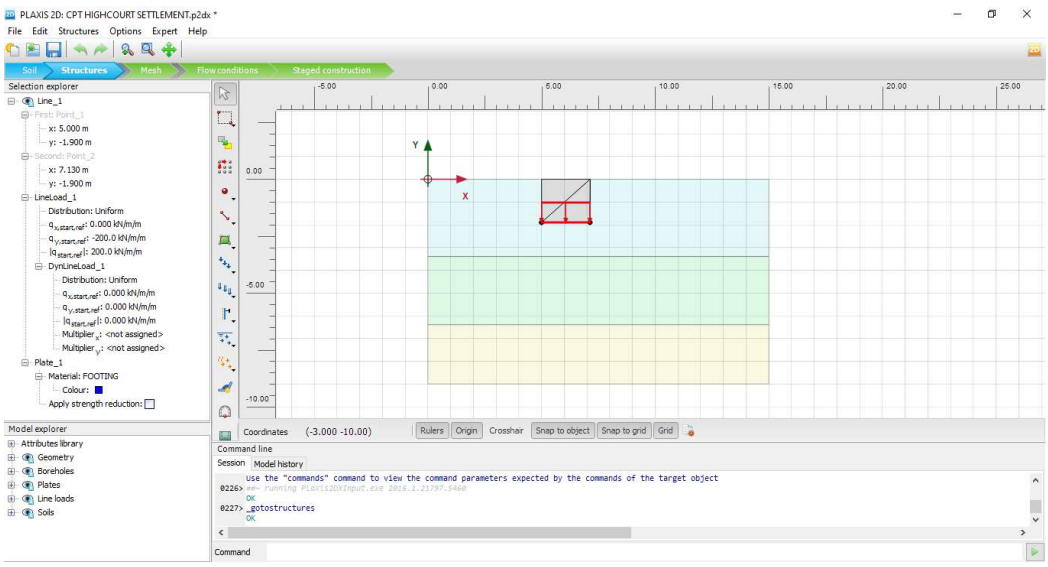

Figure: Appendix-D: 3 : Input parameters in Plaxis 2D for modelling based on CPT predicted sub-soil profile

Figure: Appendix-D: 4 : Output in Plaxis 2D for modelling based on CPT predicted sub-soil profile

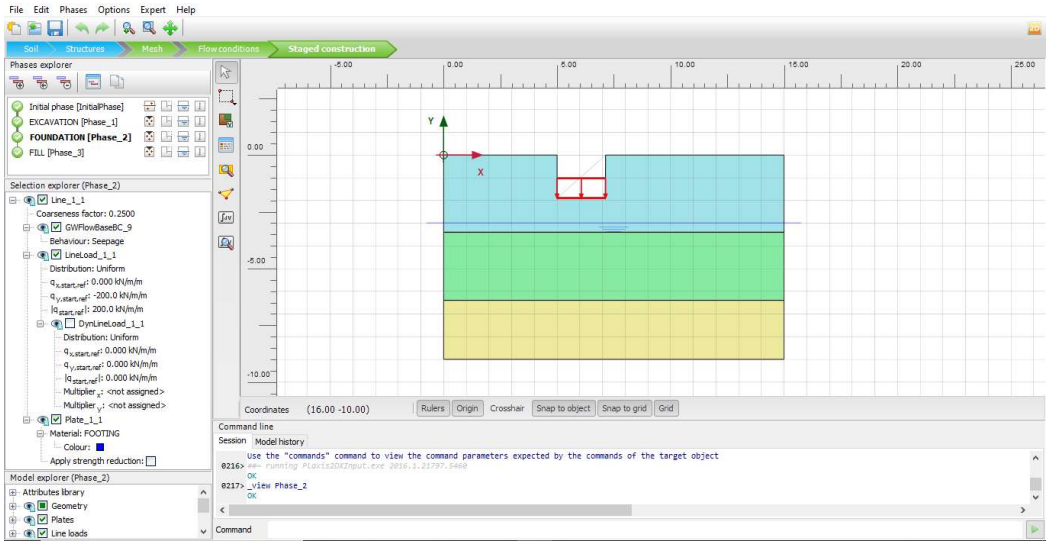

Figure: Appendix-D: 5 : Input parameters in Plaxis 2D for modelling based on DMT predicted sub-soil profile

Figure: Appendix-D: 6: Output in Plaxis 2D for modelling based on DMT predicted sub-soil profile

Table: Appendix D: 1 Settlement Calculation using empirical equation

CPT-1_HC							
Vertical stress increments (Δp)	Depth below ground level	Cone Resistance (q_c)	C_{KD}	In-situ effective stress (σ')	Compressibility (c)	Settlement (ΔS_t)	Total Settlement (S_t)
(kPa)	m	(kPa)	(kPa)	(kPa)	(kPa)	(m)	(m)
192.84	2.5	163.15	310	3.27	69.0	0.0291	0.0291
183.9	2.7	563.15		6.74			
172.68	2.9	863.15		10.15			
160.62	3.1	2763.15		13.78			
148.73	3.3	4076.9	1170	15.62	57.7	0.085	0.114
137.55	3.5	2876.9		17.42			
127.33	3.7	1476.9		19.06			
118.13	3.9	1176.9		20.73			
109.89	4.1	1276.9		22.46			
102.54	4.3	1190.65		24.09			
95.97	4.5	1490.65		25.85			
90.09	4.7	1190.65		27.34			
84.81	4.9	990.65		28.85			
80.06	5.1	1290.65		30.42			
75.76	5.3	1204.4		32.07			
71.86	5.5	1504.4		33.76			
68.3	5.7	1804.4		35.64			
65.06	5.9	2904.4		37.51			
62.08	6.1	3504.4		39.56			
59.33	6.3	1818.15		41.65			
56.8	6.5	1318.15		43.73			
54.45	6.7	2018.15		45.62			
52.27	6.9	1218.15		47.37			
50.24	7.1	1818.15		49.19			
48.34	7.3	831.9	890	50.78	23.4	0.0376	0.1517
46.56	7.5	831.9		52.28			
44.89	7.7	1031.9		53.8			
43.32	7.9	1731.9		55.4			
41.84	8.1	1231.9		57.14			
40.45	8.3	1545.65		58.79			
39.13	8.5	1145.65		60.43			
37.88	8.7	845.65		62.03			
36.69	8.9	845.65		63.53			
					Total Settlement		0.1517

SETTLEMENT CALCULATION FROM M_{DMT} BY USING DMT SETTLEMENT SOFTWARE

DMT-1_HC

SITE-1 (HC)

LOAD DESCRIPTION

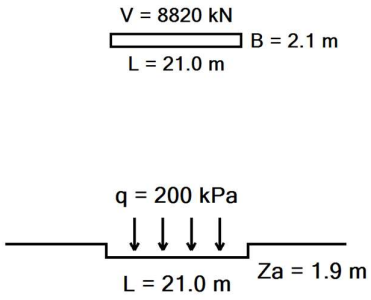

CONSTRAINED MODULUS M (MPa)

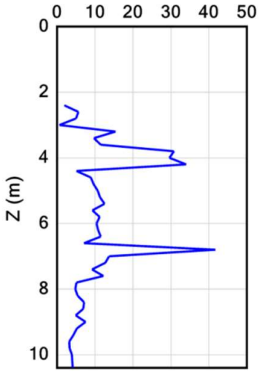

CALCULATION OPTIONS

Lower limit of Constrained Modulus assigned in the calculation	0.60 MPa
Thickness of calculation layer	0.20 m
End of Calculation	Z = 9.00 m

SETTLEMENTS CALCULATION

(one-dimensional conventional method)

$$S = \sum \frac{\Delta\sigma_v}{M} \Delta z$$

Calculation Point	Settlements	Z Stop
	[mm]	[m]
below the center	169.4	8.90
below the corner	52.4	8.90
below the median point of short side	84.9	8.90
below the median point of long side	104.5	8.90

Settlements [mm]

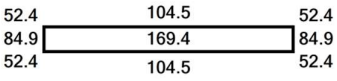

The calculated settlements are obtained using the interpretation formulae and the calculation method recommended in the TC16 DMT Report(2001). It is the designer's responsability to use alternative procedures if considered preferable.

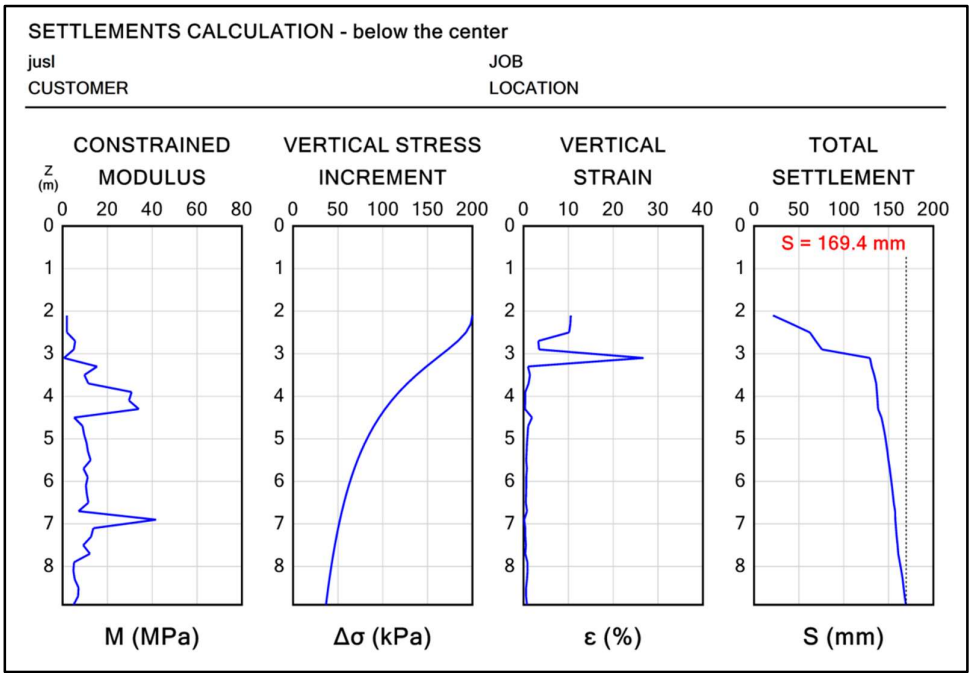

Figure: Appendix-D: 7: Output in DMT settlement software based on M_{DMT}

Table: Appendix D: 2 Settlement below the center of the footing

Z [m]	M [MPa]	σ'v [kPa]	Δσ [kPa]	ε [%]	ΔS [mm]	S [mm]
2.10	1.9	3	199.93	10.523	21.05	21.0
2.30	1.9	3	198.20	10.431	20.86	41.9
2.50	1.9	3	192.84	10.149	20.30	62.2
2.70	5.6	6	183.90	3.284	6.57	68.8
2.90	5.0	9	172.68	3.454	6.91	75.7
3.10	0.6	13	160.62	26.770	53.54	129.2
3.30	15.4	16	148.73	0.966	1.93	131.2
3.50	9.7	19	137.55	1.418	2.84	134.0
3.70	11.5	22	127.33	1.107	2.21	136.2
3.90	30.8	25	118.13	0.384	0.77	137.0
4.10	29.6	29	109.89	0.371	0.74	137.7
4.30	34.0	32	102.54	0.302	0.60	138.3
4.50	5.1	36	95.97	1.882	3.76	142.1
4.70	8.9	39	90.09	1.012	2.02	144.1
4.90	9.6	42	84.81	0.883	1.77	145.9
5.10	10.7	45	80.06	0.748	1.50	147.4
5.30	11.3	49	75.76	0.670	1.34	148.7
5.50	12.5	50	71.86	0.575	1.15	149.9
5.70	9.3	51	68.30	0.734	1.47	151.3
5.90	11.2	53	65.06	0.581	1.16	152.5
6.10	10.4	54	62.08	0.597	1.19	153.7
6.30	10.8	56	59.33	0.549	1.10	154.8
6.50	11.5	57	56.80	0.494	0.99	155.8
6.70	7.1	58	54.45	0.767	1.53	157.3

Z [m]	M [MPa]	σ'v [kPa]	Δσ [kPa]	ε [%]	ΔS [mm]	S [mm]
6.90	41.7	60	52.27	0.125	0.25	157.6
7.10	13.7	61	50.24	0.367	0.73	158.3
7.30	12.7	63	48.34	0.381	0.76	159.0
7.50	9.2	64	46.56	0.506	1.01	160.1
7.70	12.2	66	44.89	0.368	0.74	160.8
7.90	5.1	67	43.32	0.849	1.70	162.5
8.10	4.8	68	41.84	0.872	1.74	164.2
8.30	5.4	70	40.45	0.749	1.50	165.7
8.50	7.1	71	39.13	0.551	1.10	166.8
8.70	6.9	72	37.88	0.549	1.10	167.9
8.90	4.9	74	36.69	0.749	1.50	169.4

Kaushik Bandyopadhyay

Dipanjan Basu